THÈSE

En vue de l'obtention du
DOCTORAT DE L'UNIVERSITÉ DE TOULOUSE

Délivré par l'Université Toulouse 3 - Paul Sabatier

Présentée et soutenue par
Somprasong THONGKHAM

Le 24 octobre 2019

Synthèse de lactones fonctionnalisées par réaction de thiol-ène et leur application à la préparation de polymères biodégradables de propriétés modulables

Ecole doctorale : **SDM - SCIENCES DE LA MATIERE - Toulouse**

Spécialité : **Chimie Organométallique et de Coordination**

Unité de recherche :
LHFA - Laboratoire Hétérochimie Fondamentale et Appliquée

Thèse dirigée par
Didier BOURISSOU et Blanca MARTIN-VACA

Jury

M. Yohann GUILLANEUF, Rapporteur
M. Haritz SARDON, Rapporteur
M. Khamphee PHOMPHRAI, Examinateur
M. Yves GENISSON, Examinateur
Mme Blanca MARTIN-VACA, Directrice de thèse
M. Didier BOURISSOU, Directeur de thèse

To my parents: Chaleaw and Boonsong THONGKHAM

Acknowledgement

Foremost, I would like to express my deep sense of thank to Assistant Professor Julien Monot, Professor Blanca Martin-Vaca, and Dr. Didier Bourissou for their supportive and helpful in my research journey as well as their assistance, guidance, and understanding throughout my academic graduate program at LHFA, Paul Sabatier university, Toulouse, France. I am extremely grateful for pushing me to complete this PhD work. Without their supervision, this work would not be succeeded. Besides my advisors, I would like to thank the rest of my thesis committee for their kind to contribute to the success in my PhD thesis: Dr. Yohann Guillaneuf, Professor Haritz Sardon, Professor Khamphee Phomphrai, and Dr. Yves Genisson.

I also appreciate valuable suggestions and useful academic discussions as well as kindly help from Olivier Thillaye du Boullay, Dr. Omar Sadek, Dr. Miquel Navarro, and Dr. Enrico Marelli. I got a very lucky to know them along with my journey. Thanks a lot guys, I will miss you time to time.

This thesis cannot be succeeded without true support, great academic discussions and enjoyable place to work in from my lovely LBPB group members as well as my colleagues in LHFA. I would also like to thank CAMPUS France for the Franco-Thai scholarship, Centre National de la Recherche Scientifique, the Université de Toulouse and the Agence Nationale de la Recherche (ANR CE6-CYCLOOP) for financial support.

Didier: You are my idol and my hero. I still remember the first time we had a talk (interview) by video Skype. Thanks for offer me the best opportunity I ever had in my life. I have been my pleasure to know you and work with you. I love every single time we had a discussions and a life talking as well. I hope we can have a collaboration in the future. Finally, I hope one day we can join the marathon somewhere. Cheers!!!

Blanca: I could not have imagined having a better advisor for my whole time in this PhD program. Your guidance helped me a lot in all the time of research and writing of this thesis as well as my life in France. I never had any bad feeling for my three years working

with you. The first time we met at the airport, it was a very good moment and very impressive for me. I still remember when you said that "we are here to be a part of your family in France, we are not your boss. We are the team" I appreciate everything you have done for me, both academic and life. If I did something wrong for you, I am so sorry for that. I will keep your guidance, and I will find the way to have a collaboration with you as well. See you soon in Thailand ☺

Julien: Thanks god, I have finally found my brother hahaha. I enjoy every single day working with you, Boss. Thanks for your kind help for solving many problems of my life and my research in France. Without your precious support, it would not be possible to conduct this research as well as live in France. Thanks for being a very very perfect brother, as you are always there beside me no matter what it goes wrong….Thanks Boss. I hope to see you again in Thailand (Or somewhere in this world). As we do know, you are the best hahahah. See you!!!

Rinoi: I appreciated everything you did for me. I enjoy every time we had a party at your house, with your family. I still remember the first time we cooked Thai dishes together, it was so fun and memorable. Thanks once again for your kind and support during my journey in France.

Frank: It have been my pleasure to meet you bro. Thanks for help me a lot. I enjoy the time we spent together: playing football, eating out, cooking Thai-French dishes, and talking about our polymer chemistry. Hope to see you somewhere again, especially in Thailand. Cheers!!!!

Richard: Thanks for you kind help Richard. It was my pleasure to meet you. I enjoy all the time we hang out together, even it did not long but enough to be my good memory. See you someday man, Cheers.

Chaliew: It was hard to say goodbye to you at that moment you were leaving from the team. Indeed, it have been my pleasure to know you bro. I am happy for all the parties we went, all the games we played, all the concerts/activities we joined, and every time we

got drunk together hahahahaha. Thanks for your kind help Chacha. As we know, you are the best….always. Hope we will meet again in Thailand or elsewhere. Take care and enjoy your life bros!!!

Paul & Abdallah: To my beloved smoker hahaha, I am glad to meet you guys. Thanks for every kind help you did for me bros. Hope to see you guys again one day. And please let me know if you plan to visit Thailand. Be safe guys!!! Take care your lungs hehehe!!!

Enrico: Nice to meet you Enrico, it have been my pleasure to spend my last 2 year in France with you. We got a lot of funs together. We had a lot of academic discussions, very very helpful for me. Thanks for being a very good friend, I still remember a lot of things that we did together; we enjoyed playing FIFA and Dark souls, cooking Italian and Thai food, drinking wine/beers like a jar of water hahaha, and having fun for our talks ☺. It was fun, isn't it? Hope to see you again bro. Please let me know, if you are coming to Thailand. You are always very very welcome. Good luck

Miguel: Ohhh my lovely mom in France hahaha. Well, I miss you sometimes, but not always hehehe. Thanks god that sent you to meet me, it have been my pleasure to know you bro. Thanks for your kind help and support me, life and thesis. I very enjoyed all the talks we had, all the parties we went, all the games we played, and all the times we spent together ☺. Hope to see you again, and wish you have a good luck for your position in Spain. Thanks once again for coming in my life, cheers.

Omar: Who are you??? Hahaha, just kidding :p. I am very very glad to meet you. I would personally like to say that you are incredible, so kind so nice all the time we had spent together. I loved every time we had discussions in both academic and life topics. Thanks once again for your kind help, truly smile, and strong support for my thesis as well as my life outside the lab. Miss you man and Hope to see you someday elsewhere ☺ Take care and Good luck for your work & life.

Max: Coca or Cola??? Of course, I choose you Maxime BJ Pierre Cola hahaha (sound like in Pokémon animation). I never knew that I could find a very good French friend like

you buddy. It is indeed my truly pleasure to meet you who is a very nice and funny guy. Thanks for being beside me no matter what it happens. Thanks for your kind help dude. And Thanks for fulfill my life in Toulouse, France…It was so fun for every party we went out together, wasn't it? Take care yourself and Good luck for your future in USA. Hope to see you again, my lovely buddy. Miss you man.

Cyril: The smartest guy in the world I have met hahahah. I thank my fellow labmates for the stimulating discussions, for the sleepless nights we were working together before deadlines, and for all the fun we have had in the last three years. Good luck bro, see you one day elsewhere.

Mathilde: The kindest girl, for non-permanent people, in LHFA as well as in France that I have ever met. I would like to express my deep sense of thank to you and Adrian. Thanks for your help and support me for almost three years at LHFA. With your mentally sharp that make you have good decisions, I am sure that you will succeed for whatever you want to make it happens. It has been my pleasure to meet you, my friend. I am looking forward to being invited as a guest for your wedding in the future hahahaha. Let's see then when it would be ☺ Good luck for your work and take care…Hope to see you and Adrian again.

Maryne and Aymeric: So BBQ or Raclette for tonight??? Haahaha I am very happy for every times we went out and all the dinner and parties we had at your nice place. It was indeed my pleasure to meet both of you. Wishing both of you the very best for all the new ventures, that life has in store for you all ☺ Hope to see you again. Take care and invite me for your wedding as well hahaaha.

Arnald: Wowwww biker!!! I want to show my deep sense of thanks to you and your girlfriend for a lot of good times we had spent together. It has been my pleasure to meet both of you. I love the dinner time we had at your house, it was so awesome. Good luck and tons of best wishes to you, to your girlfriend, and to your family. See you a very nice couple ☺

Jessica: Hola Jess!!! It has been my pleasure to meet you, Jess. Thank you so much for your kind help and for being a very good friend in the lab. I very love your Spanish food that you brought me once from your hometown. Hope you have a great happiness for your future. Wish you have a ton of luck and success with a good health ☺ See you Jess!!!

Yuri: It has been my pleasure to meet you, bro. Thanks for your kind help. It was a good time for me to have academic discussions and chit chat with you. I wish you have the best of luck and success in your work as well as your future. All the success, and happiness for you family as well.

Jean: I still want to have a glass of whisky with you, dude. Oh yeah, may be more than one glass hahah. A lot of fun that we had together, I will keep it in my mind ☺ Do not forget to practice some Thai words…like a fat boy hahha. It was my pleasure to know such a very nice guy like you, bro. Thanks for everything you did for me. I wish you the best of luck, all the success, and happiness for you work and life in the future. Hope we will meet again…somewhere we will see.

Julien P.: Think about Juju think about a lovely guy in France that you cannot find someone look like him hahaha. So poor guy. Well, I will try to be polite with you man haah. Thanks for everything you have done for me, I got a lot of your helps and supports. It has been my pleasure to know you. I wish you will have a great time in the future and a good luck for your work. See you somewhere bro….I hope ☺

Sukaina: I hope you will take care my washing machine like I do hahahaha. Well, every party must come to the end: however, we can keep our friendship as long as we want (I hope it is not too long hahah). Thanks for being "too" kind for me and Thanks for your food that save my life…sometimes. Good luck for your future and Have a nice day for every single day of your life. My pleasure to meet you and hope to see you one day, my friend.

In the end, I would like to thank my beloved family: my parents Chaleaw THONGKHAM and Boonsong THONGKHAM for supporting me and also for their love, and being there no matter what.

Somprasong Thongkham

Table of Contents

List of Abbreviations

2-chloro-ε-CL	2-chloro-ε-caprolactone
4-amino-TEMPO	4-amino-2,2,6,6-tetramethylpiperidine-1-oxyl
AIBN	Azobisisobutyronitrile
Al(O^{i}Pr)$_3$	Aluminium(III) isopropoxide
ASTM	American Society for Testing and Materials
ATRP	Atom transfer radical polymerization
α-acrylate-ε-CL	α-acrylate-ε-caprolactone
α-PL	α-propiolactone
α-Propargyl-ε-CL	α-propargyl-ε-caprolactone
β-BL	β-butyrolactone
BCL	Benzyloxycarbonylmethyl-ε-functionalized-ε-CL
β-PL	β-propiolactone
BMD	3-(S)-[(benzyloxycarbonyl)methyl]-l,4-dioxane-2,5-dione
β-Me-δ-VL	β-methyl-δ-valerolactone
βMe-ε-^{i}Pr-ε-CL	Carvomenthide
BnNH$_2$	Benzyl amine
BnOH	Benzyl alcohol
BnSH	Benzyl thiol
BPO	Benzoyl peroxide
BV	Baeyer–Villiger oxidation
BzCH$_2$SH	Benzyl 2-mercaptoacetate (benzyl ester thiol)
CALB	*Candida antarctica* Lipase B
C$_6$D$_6$	Deuterated benzene

CEN/TR	European committee for standardization/Technical report
CDCl$_3$	Deuterated chloroform
CO$_2$	Carbon dioxide
C$_6$H$_5$CHO	Benzaldehyde
CuAAC	Copper(I) catalyzed azide-alkyne cycloaddition
CuI	Copper(I) iodide
D	Rate of water diffusion into the bulk polymer
Đ	Polydispersity index
DBU	1,8-diazabicyclo[5.4.0]undec-7-ene
DCM	Dichloromethane
DMA	Dynamic mechanical analysis
DMAP	4-dimethylaminopyridine
DMBA	3,5-dimethoxybenzyl alcohol
DMF	Dimethylformamide
DMPA	2,2-dimethoxy-2-phenylacetophenone
DP	Degree of polymerization
DPP	Diphenyl phosphate
DSC	Differential scanning calorimetry
δ-VL	δ-valerolactone
δ-DL	δ-decalactone
δ-Me-δ-VL	δ-methyl-δ-valerolactone
EtOH	Ethanol
EtOAc	Ethyl acetate
ε-CL	ε-caprolactone
ε-DL	ε-decalactone

γ-BL	γ-butyrolactone
GC–MS	Gas chromatography–mass spectrometry
HEMA	Hydroxyethyl methacrylate
HPLC–MS	High-performance liquid chromatography–mass spectrometry
InCl$_3$	Indium(III) chloride
IUPAC	International Union of Pure and Applied Chemistry
λ'	Rate of hydrolysis
L	Thickness of the specimen
L$_{crit}$	Critical thickness
LA	Lactide
LDA	Lithium diisopropylamide
L-LA	*L*-lactide
MALDI-TOF	Matrix-Assisted Laser Desorption/Ionization- Time-of-Flight
*m*CPBA	*m*-Chloroperoxybenzoic acid
MeI	Methyl iodide
MMA	Methyl methacrylate
MS	Mass Spectrometry
*M*n	Number average molecular weight
*M*w	Weight average molecular weight
NaN$_3$	Sodium azide
N	number of specimens
n	Average number of monomer per polymer chain
NEt$_3$	Triethylamine
NHC	N-heterocyclic carbenes
NHO	N-heterocyclic olefins

NMR	Nuclear Magnetic Resonance
HOBnOH	1,4-benzenedimethanol
PBBL	Poly (β-butyrolactone)
PBS	Phosphate-buffered saline solutions
PCL	Poly (ε-caprolactone)
PCC	Pyridinium chlorochromate
Pd/C	Palladium on carbon
PDL	Poly (ε-decalactone)
PDVL	Poly (δ-valerolactone)
PEO	Poly (ethylene oxide)
PEG	Poly (ethylene glycol)
PHA	Poly (3-hydroxyalkanoate),
PLA	Poly (lactide)
PLGA	Poly (lactic acid-co-glycolic acid)
Poly OPD	Poly (2-oxepane-1,5-dione)
PSAs	Pressure-sensitive adhesives
RCOCl	Acyl chloride
RcoOP	Ring-opening copolymerization
ROP	Ring-opening polymerization
ROS	Reactive oxygen species
SAXS	Small-angle X-ray scattering
SEC	Size-exclusion chromatography
TBD	Triazabicyclodecene
T_c	Crystallization temperature
T_d	Degradation temperature

TGA	Thermal gravimetric analysis
T_g	Glass transition temperature
THF	Tetrahydrofuran
T_m	Melt temperature
TMP	2,2,6,6-tetramethylpiperidine
TrtS–LA	3-methyl-6-(tritylthiomethyl)-1,4-dioxane-2,5-dione
W_0	Initial weight of the material
W_t	Weight of the remaining material
$W(R)_t$	Weight of the released product from degradation
$ZnEt_2$	Diethyl zinc
ΔH_p^0	Enthalpy
ΔS_p^0	Entropy

Materials and Instruments

All reactions were performed under an inert atmosphere of argon using quartz vessel for thiol-ene reactions and standard Schlenk techniques. Ethanol, Dichloromethane, Tetrahydrofuran, and Toluene (> 99.9%) were dried with a Braun solvent-purifier system and degassed by Freeze-pump-thaw process prior to use. Chloroform, $CDCl_3$, and C_6D_6 were dried prior to use by distillation over molecular sieves. 2,2-Dimethoxy-2-phenylacetophenone was purchased from Acros and used as received. Indium(III) chloride (99.999%, Alfa Aesar) was used as received and stored in a glovebox. Benzyl mercaptan, Thioglycolic acid, and Mesitylene were purchased from Aldrich. The alcohols, benzyl amine, triethyl amine and PEG-NH_2 were purchased from Aldrich, dried and stored under argon prior to use. All initiators were dried either under vacuum in the presence of P_2O_5 or over molecular sieves and then filtrated prior to use. ε-DL (99%, Aldrich) ε-CL (98%, Aldrich) were purified by distillation over CaH_2 and stored under argon. Triethylamine (99% Fluorochem) was dried over molecular sieves and then filtrated prior to use.

SEC Analyses. The number-average, weight-average molar masses (M_n and M_w, respectively) and molar mass distributions ($Đ$) of the polymer samples were determined by size exclusion chromatography (SEC) at 35 °C with a Waters 712 WISP high-speed liquid chromatograph equipped with a R410 refractometer detector. Tetrahydrofuran (THF) was used as the eluent, and the flow rate was set up at 1.0 mL/min. A SHODEX precolumn (polystyrene AT806M/S M_w = 50000000 g/mol) and two STYRAGEL columns (HR1, 100–5000 g/mol, and HR 4E, 50–100000 g/mol) were used. Calibrations were performed using polystyrene standards (400–100000 g/mol).

NMR Analyses. NMR spectra were recorded in $CDCl_3$ on BRUKER Avance 300 MHz spectrometers at room temperature, and chemical shifts are reported in ppm relative to Me_4Si as an external standard. [1]H measurements were used for determination of the monomer conversion, the degree of polymerization (DP_{NMR}), and the end-group analysis for copolymers architectures. In ε-DL polymerizations the conversion was assessed by comparing the peak area integral of $-O-CH(C_4H_9)-$ (proton attached to ε-carbon; δ = 4.22 ppm) of ε-DL to the integral of the same peak within the PDL polymer (PDL; δ = 4.84 ppm) in the ^{1}H NMR spectrum. In ε-CL based reactions the integral intensity of $-O-CH_2-$ (δ = 4.14 ppm) for the ε-CL monomer was compared to the intensity of the same peak for PCL polymer (δ = 4.08 ppm). DP_{NMR} was determined from the relative intensities of the OCH signals for polymer (multiplet at δ = 4.84 and 4.08 ppm respectively for PDL and PCL) and the signal of initiator used as

reference. Copolymers architectures were confirmed by the end-group analysis from ^{1}H measurements and ^{13}C measurements. 2D COSY NMR was used for determination of one polymer chain growth at N atom of benzyl amine. For copolymerization of new monomers with ε-DL, the conversion of monomers were determined from the relative intensities of the OCH signals for the monomer (ε-DL = multiplet at δ = 4.22 ppm, **1** = multiplet at δ = 4.02 ppm, and **2** = multiplet at δ = 4.40 ppm) and copolymers (PDL multiplet at δ = 4.84 ppm, **P2** = multiplet at δ = 4.96 ppm, and **P3** = multiplet at δ = 4.99 ppm). DP$_{NMR}$ was determined from the relative intensities of the OCH signals of copolymers and the ^{1}H signal of initiator used as reference; DMBA = 6H, the -(OCH_3)$_2$ signal (singlet at δ = 3.75 ppm) and BnOH = 2H, the C$_6$H$_5$-CH_2-O signal (singlet at 5.10 ppm). Copolymers architectures were confirmed by ^{13}C measurements.

MALDI-TOF MS analyses. MALDI-TOF-MS analyses were performed on a MALDI MicroMX from Waters equipped with a 337 nm nitrogen laser. An accelerating voltage of 20 kV was applied. Mass spectra of 1000 shots were accumulated. The polymer sample was dissolved in THF at a concentration of 1 mg mL^{-1}. The cationization agent used was NaI dissolved in THF at a concentration of 1 mg mL^{-1}. The matrix used was dithranol and was dissolved in THF at a concentration of 10 mg mL^{-1}. Solutions of matrix, salt, and polymer were mixed in a volume ratio of 10 : 1 : 1 respectively. The mixed solution was hand-spotted on a stainless steel MALDI target and left to dry. The spectrum was recorded in the reflectron mode. Baseline corrections and data analyses were performed using MassLynx version 4.1.

GC-MS analyses. The analyses of new monomers were performed on a MS Perkin Elmer Clarus MS560, GC PerkinElmer Clarus 500 and Agilent HP6890.

HPLC-MS analyses. The degraded products were analyzed by HPLC using Autopurification Waters with a Photodiode Array Detector, and a C18 column (X bridge C18 5μm 100 mm × 2.1 mm). Acetic acid in water and Acetic acid in methanol were employed as the eluents with a flow rate of 0.3 mL/min. The elution was followed by UV detection at 254 nm. The sample was dissolved in water at a concentration of 10 mg mL^{-1}. The spectra were recorded in the negative mode. Baseline corrections and data analyses were performed using MS TIC neg.

Differential Scanning Calorimetry. The thermal properties of the copolymers were measured on a NETZCH DSC 204 system under a nitrogen atmosphere at heating and cooling rates of

20 and 10 °C min^{-1}, respectively. The T_{g} and T_{m} values were extracted from the second heating curves.

Thermal Gravimetric Analysis. The thermal stability of the copolymers was measured on a PerkinElmer DIAMOND TG/TDA thermobalance, under air from 30 to 650 °C at a heating rate of 10 °C/min. The degradation temperatures correspond to the temperature from which the curves switched off the baseline.

General introduction

Nowadays, plastics are ubiquitous materials, so that life without plastics is difficult to imagine.[1] The worldwide production of plastics is currently exceeding up to 150 million tons per year corresponding to an exponential growth of industrial factory.[1a] However, using such high amount of plastics is associated with serious environmental problems. The interest on renewable, biodegradable and biocompatible materials as alternatives to non-degradable plastics has thus been increasing. Environmentally-friendly polymers are used more and more in daily (packaging and agriculture…) and specific (biomedical materials, engineering of tissue scaffolds…) applications.[1b] An increasing amount of polymers that can be decomposed in nature is being investigated.[1c] Among biodegradable polymers, we can differentiate those derived from nature (i.e. starch) and those synthetically made. The synthetic polymers are mostly based on hydrolytic or enzymatic sensitive linkages such as esters and amides (e.g., polyesters, polyamides, polycarbonates, and polyanhydrides).[2] Among these degradable polymers, polyesters have been attracting much interest because of their balanced sensitivity to hydrolytic degradation.[1a,1b] In addition, aliphatic polyesters, synthesized from lactones or diesters, are of special interest, as the degradation of polymer chains can generate small molecules that can be directly eliminated or metabolized by the body. They are thus biocompatible.

Up to date, Polylactide (PLA), derived from lactic acid, is the most used biodegradable polyester. It is a commercially renewable polymer. PLA can be synthesized by the ROP of lactide (LA), which is derived from biomass such as corn or wheat. Among industrial polymers, the production of PLA has currently increased to a ton scale constituting 24 % of the global biodegradable plastics production, and the price has decreased from ≈ 1,000 to ≈ 6 US $ per kg (a price level similar to that of polystyrene, ≈ 1.6 US $ per kg).[3] Besides PLA, other biodegradable polyesters such as polyhydroxyalkanoates (PHAs) and poly(butylene succinate) (PBS) are also produced on an industrial scale (Figure 1).[4]
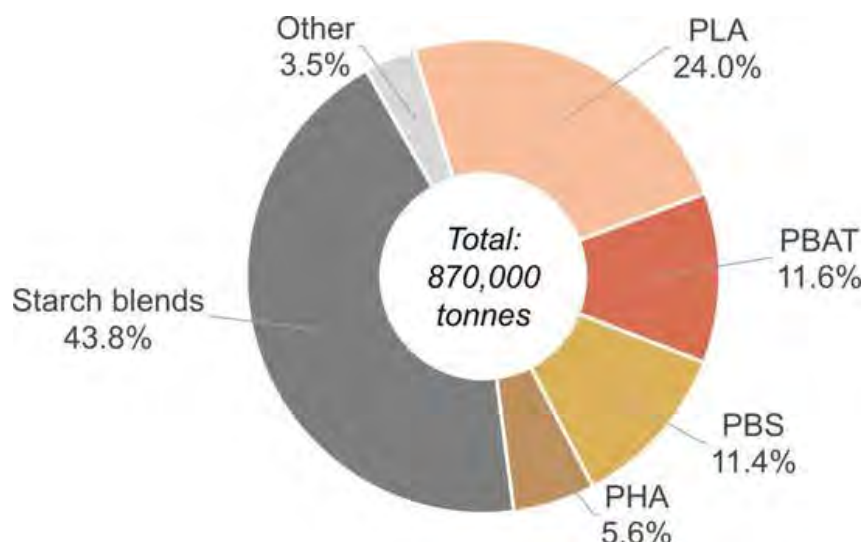
Figure 1 Global production capacities of biodegradable plastics in 2017.[4]

PLA has high potential in mechanical and thermal properties, making it suitable for many applications.[1a,1c] The hydrolysis of PLA is predominantly associated with a metabolite in the carboxylic acid cycle leading to the formation of lactic acid which is then transformed into CO_2 and H_2O via the Krebs cycle (Figure 2).[5]
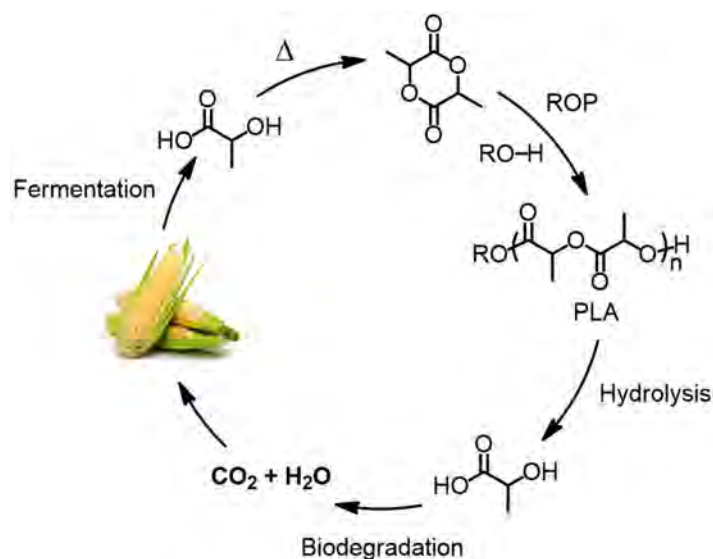
Figure 2 PLA life cycle associated with a metabolite in the carboxylic acid cycle.[5]

The applications of PLA are exponentially increasing, thanks to its ability to be degraded as well as its compatibility with biomedical fields (e.g., for the use in dental implants, vascular grafts, bone screws, and a vector for drug delivery).[6] However, PLA has some drawbacks that hamper its use for some applications: for example, its brittleness from high crystallinity and low thermal stability ($T_m \approx 160$ °C, $T_g \approx 60$ °C, and $T_d \leq 280$ °C), its hydrophobic character, and its low functionalization degree.

The properties of PLA can be modulated by the combination or the replacement with other polyesters, such as polycaprolactone (PCL). PCL is a semi-crystalline polymer with a T_m of around 60 °C and a T_g of about –60 °C (both T_m and T_g are lower than PLA).[7] In fact, PCL is also considered as a biodegradable polymer, although its hydrolytic degradation is slower (2-3 years) than that of semi-crystalline PLA (1-2 years).[8] This semi-crystalline polyester has been widely used in biomedical applications such as in nanoparticles for targeted drug delivery systems and in the engineering of tissue scaffolds.[7a] However, PCL has the important drawback of not being renewable, as it is prepared by ROP of ε-CL, a petroleum-based lactone (it has to be noted that a recent synthesis starting from sugar has been reported).[7b] ε-Decalactone (ε-DL), which is derived from biomass is another 7-membered ring lactone monomer of choice, as it is close to ε-CL. Being environmentally friendly, ε-DL attracts increasing attention as an alternative renewable monomer. However, the pendant butyl group at ε-position has a large impact not only on the polymerization rates but also on the polymer properties and especially on the degradation rates. Note that the polymerization rates of polydecalactone (PDL) is slower than that of PCL, while the degradation rates of PDL is faster than that of PCL but still slower than the one of PLLA (see chapter III for more detail). One possibility to modulate and/or improve further the properties of PDL and develop its use is to introduce functional lateral groups using modified ε-caprolactones. Therefore, it is very desirable to develop the access to reactive functionalized monomers of close structure to ε-DL to ensure similar behavior in ROP and to devise a reliable method for their controlled (co)polymerization.

The most used strategies for the preparation of 6- to 9-membered ring lactones can be separated in three different methods, as follows:

(1) Cyclization or lactonization is similar to the lactide preparation.[9] The ring formation is basically performed by activation of either the acid or the alcohol. However, the functionalized lactones prepared by this method are often obtained in moderate to low yields due to the competition with the intermolecular reaction which leads to the formation of undesired products (i.e., oligomers).[10]

(2) Alkylation at α-position of already existing lactones is a well-known method in organic chemistry to prepare specifically α-functionalized lactones using a strong base.[11] α-Propargyl-ε-caprolactone is one of the monomers prepared by this method. The propargyl pendant group can be subsequently modified by "click" chemistry as a post-polymerization

modification.[12] However, this approach has some drawbacks: it is a multi-step reaction and is accompanied by side products due to transesterification reactions and anionic polymerization of caprolactone.

(3) Baeyer−Villiger oxidation of (functionalized) cyclic ketones is probably the most widely applied approach to produce (functionalized) lactones, e.g., ε-caprolactone from cyclohexanone.[13] The most important issue in Baeyer−Villiger oxidation is related to the lack of regioselectivity in the case of dissymmetric lactones.[14] As a result, very few examples of ε-functionalized-ε-caprolactone have been reported.

Here, we propose an alternative and selective approach for the preparation of ε-functionalized-ε-CL (Scheme 1) and their application as a biodegradable polymer. Based on our developed strategy, the functionalized lactone precursor, ε-alkylidene-ε-lactone, is easily prepared by the cycloisomerization of the corresponding alkynoic acid.[15] This precursor will be further modified by a simple and selective thiol-ene functionalization prior to copolymerize with ε-DL yielding functionalized copolymers. Note that both cycloisomerization and thiol-ene functionalization are fully atom-economic reactions.
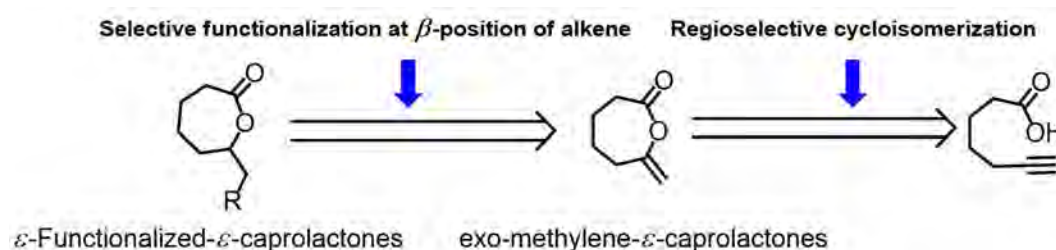
**Scheme 1.** Proposed alternative approach for ε-functionalized-ε-caprolactones

Post-modification reactions of the resulting copolymers will be achieved by two steps, acetylation and hydrogenolysis, which will lead to the copolymers featuring pendant carboxyl groups. These carboxyl functional groups may have an impact on the polymer properties, especially the degradation rates. To probe the degradability of these functionalized copolymers, their degradation will be investigated in hydrolytic and enzymatic conditions. The influence of our new monomer (in deprotected form) on PDL backbone will be presented based on the results from degradation tests.

This manuscript thus deals with the synthesis of functional lactones, including the investigation of dual catalysts for ROP of ε-DL. The works aims at using a new functional

monomer for the preparation of biodegradable polyesters featuring pendant functional groups (Scheme 2). The manuscript is composed of four chapters, as illustrated hereafter:
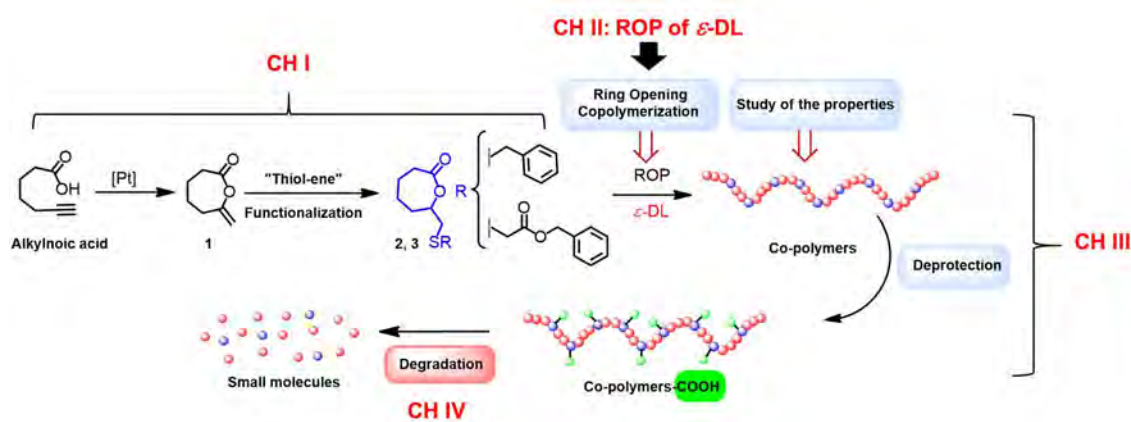
Scheme 2. Overview of the project represents the functional monomer preparation, RcoOP and their copolymers architecture, the study of copolymers properties, and the degradation study.

In Chapter I, we will focus on the synthesis of the ε-functionalized-ε-CL. These new functionalized monomers present a close structure to ε-DL to ensure similar behavior in ROP. First, an alternative approach for the synthesis of ε-functionalized lactone monomers will be described. They are easily prepared from a γ-alkynoic acid by a sequence of cycloisomerization and thiol-ene reaction developed in our group. The optimization of the thiol-ene reaction and the structure analysis of these new monomers will be presented.

In Chapter II, an alternative catalyst for the ROP of ε-DL will be presented. To date, $Sn(Oct)_2$ and TBD have been the most used catalysts to polymerize ε-DL. The polymerizations are mainly in bulk conditions at high temperature (110 °C to 150 °C) and enable relatively good control of M_n and Đ. Even though the polymerizations could be performed up to high monomer loading with these catalysts, the major problem lies in the harsh conditions and the catalyst traces remaining in polymer. We thus aimed to find an alternative catalyst that could promote the ROP of ε-DL under milder conditions, and could be removed easily. As far as we know, this is the first time the $InCl_3/NEt_3$ dual catalyst is applied to the ROP of ε-DL. The optimization of polymerization conditions for well-controlled M_n and Đ, the kinetic studies, the investigation of various initiators (alcohols, amines, and macro initiators) and the copolymerization with ε-CL will be presented, as well as the confirmation of living and controlled character of the polymerization and the analysis of the copolymer architectures.

In **Chapter III**, copolymerization of ε-functionalized-ε-CL with ε-DL will be investigated using the InCl$_3$/NEt$_3$ dual catalyst. First, the optimization of copolymerization conditions will be presented. Then, the kinetics of the copolymerization and the structure of the obtained copolymers will be thoroughly discussed. Finally, the removal of the protecting groups installed on the functionalized monomer using conditions that respect the integrity of the polymer backbone will be presented.

The last chapter, **Chapter IV**, will probe the impact of the carboxylic acid pendant groups on the degradation rates of the copolymers, compared with PDL. In this chapter, the preparation of polymer films will be presented as well as the results of hydrolytic and enzymatic degradation tests.

Finally, the general conclusion will summarize the work and highlight the advantages of our approach based on ε-functionalized-ε-CL. The possibility of using these functionalized monomers in some applications will also be discussed.

References

1   (a) Williams, C. K. *Chem. Soc. Rev.* **2007**, *36*, 1573. (b) Bednarek, M. *Prog. Polym. Sci.* **2016**, *58*, 27. (c) Vert, M. *Biomacromolecules*, **2005**, *6*, 538.

2   Laycock, B.; Nikolić, M.; Colwell, J. M.; Gauthier, E.; Halley, P.; Bottle, S.; George, G. *Prog. Polym. Sci.* **2017**, *71*, 144.

3   Schneiderman, D. K.; Hillmyer, M. A. *Macromolecules*, **2017**, *50*, 3733.

4   Bioplastics market data 2017, European Bioplastics, https://www.european-bioplastics.org/market/. 21.06.2018.

5   Ragauskas, A. J.; Williams, C. K.; Davison, B. H.; Britovsek, G.; Cairney, J.; Eckert, C. A.; Fredrick Jr.,W. J.; Hallett, J. P.; Leak, D. J.; Liotta, C. L.; Mielenz, J. R.; Murphy, R.; Templer, R.; Tschaplinski, T. *Science*, **2006**, *311*, 484.

6   Albertsson, A.-C.; Varma, I. K. *Biomacromolecules*, **2003**, *4*, 1466.

7   (a) Abedalwafa, M.; Wang, F.; Wang, L.; Li, C. *Rev. Adv. Mater. Sci.* **2013**, *34*, 123. (b) Buntara, T.; Noel, S.; Phua, P. H.; Melián-Cabrera, I.; de Vries, J. G.; Heeres, H. J. *Angew. Chem. Int. Ed.* **2011**, *50*, 7083.

8   Almeida, B. C.; Figueiredo, P.; Carvalho, A. T. P. *ACS Omega*. **2019**, *4*, 6769.

9   Parenty, A.; Moreau, X.; Campagne, J. M. *Chem. Rev.* **2006**, *106*, 911.

10   Galli, C.; Mandolini, L. *J. Chem. Soc., Chem. Commun.* **1982**, 251.

11   (a) Herrmann, J. L.; Schlessinger, R. H. *J. Chem. Soc., Chem. Commun.* **1973**, 711. (b) Habnouni, S. E.; Darcos, V.; Coudane, J. *Macromol. Rapid Commun.* **2009**, *30*, 165.

12   Darcos, V.; El Habnouni, S.; Nottelet, B.; El Ghzaoui, A.; Coudane, J. *Polym. Chem.* **2010**, *1*, 280.

13   ten Brink, G. J.; Arends, I. W. C. E.; Sheldon, R. A. *Chem. Rev.* **2004**, *104*, 4105.

14   Itoh, Y.; Yamanaka, M.; Mikami, K. *J. Org. Chem.* **2013**, *78*, 146.

15   Ke, D.; Espinosa-Jalapa, N. Á; Mallet-Ladeira, S.; Monot, J.; Martin-Vaca, B.; Bourissou, D. *Adv. Synth. Catal.* **2016**, *358*, 2324.

16   Felpin, F. -X. and Fouquet, E. *Chem. Eur. J.* **2010**, *16*, 12440.

Chapter I: The preparation of a functionalized analogue of ε-DL

1.1 Functionalized equivalents of CL-based monomer for the preparation of functional aliphatic polyesters

Aliphatic polyesters are known as representatives of synthetic biodegradable polymers, which have been used in a wide range of applications including bio-based packaging materials, agriculture, and in the biomedical field, due to their high biocompatibility and degradability.[1-7] Thanks to the benign products formed after decomposition, aliphatic polyesters offer a sustainable alternative to petroleum-based polymers (i.e., polyolefin).[8] Ring opening polymerization (ROP) of lactones or diesters (e.g., lactide or gylcolide) is a reliable method to synthesize a broad range of aliphatic polyesters tuning the polymer properties. ROP surpasses polycondensation and step polymerization, since it can promote living and controlled polymerization enabling to finely control the molecular weights (M_n), molar distributions ($Đ$) and chain-ends (Figure 1.1).
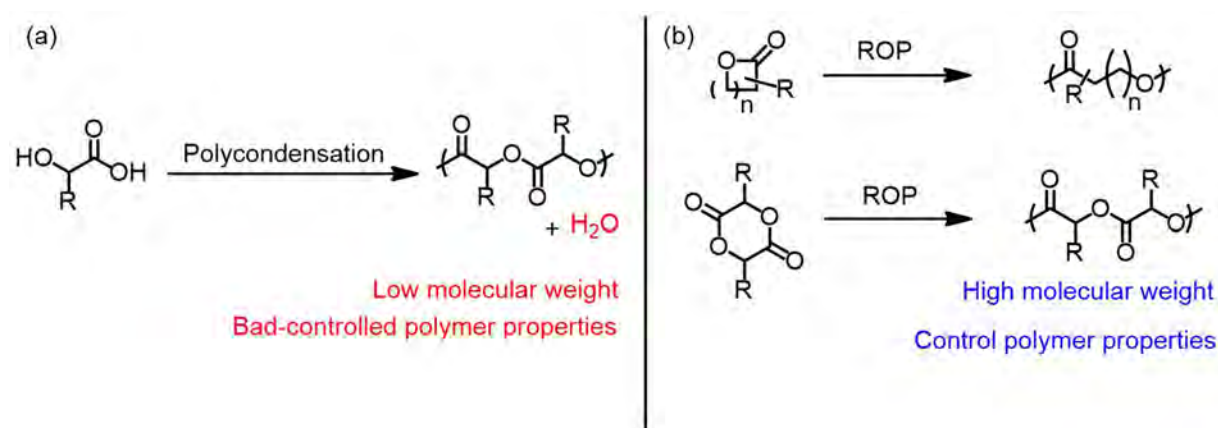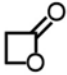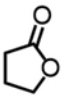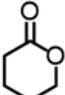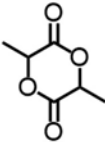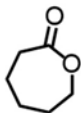

Figure 1.1 (a) Polycondensation of lactic acid. (b) ROP of lactones and diesters.

Aliphatic polyesters prepared by this method enlarge thus the scope of available biodegradable polymers through chain-growth polymerization of lactones with different ring sizes (Table 1), e.g., ε-caprolactone (ε-CL), δ-valerolactone (δ-VL), γ-butyrolactone (γ-BL), β-butyrolactone (β-BL), α-propiolactone (α-PL), and β-propiolactone (β-PL).[9,12] However, the variety of functional groups in known lactone monomers is limited, leading to a narrow range of polymer properties. Therefore, the introduction of functionalities onto the monomer or polymer is essentially important as the functionalized monomer/polymer can expand the scope of polymer properties (e.g., varying the T_g or degradation rates) and thereby of applications.

Access to functionalized aliphatic polyesters *via* an available synthetic method is thus attracting increasing attention, so that well-defined functionalized materials can be prepared. Moreover, the functionalized aliphatic polyesters will permit to access new materials that can be further used in many applications, from packaging and plastics applications to biomedical studies.[10] Before going to the discussion of the possible synthetic strategies for the preparation of functionalized aliphatic polyesters, it is worth introducing briefly the thermodynamic and kinetic polymerizability of lactone monomers. When investigating the polymerization behavior of a specific monomer, there are two aspects that need to be considered: (1) the influence of monomeric structure on the equilibrium monomer conversion (thermodynamic factor), and (2) the availability of a catalytic system that yields the best control of the rate of polymerization, M_n, and $Đ$ (kinetic factor).[12] Concerning the thermodynamic aspect, the driving force for the ROP is strongly related to the ring strain of the lactone (ΔH_p^0) and to the entropy of the process (ΔS_p^0).[9,12] For small and medium lactones (ring size 4-7), the ring strain ($\Delta H_p^0 < 0$) is favorable to the ring-opening while the entropy is unfavorable ($\Delta S_p^0 < 0$) (Table 1.1). The reverse situation is encountered for macrocycles. For unsubstituted lactones, the ratio between ΔH_p^0 and ΔS_p^0 is significantly more favorable for 4- and 7-membered rings than for 6-membered ring (δ-VL) and even more than for 5-membered ring (γ-BL) (see Table 1). As a result, high conversions are typically observed for β- and ε-lactones.

Table 1.1 Enthalpy (ΔH_p^0) and entropy (ΔS_p^0) of ROP for selected lactones and lactide (298 K)

Ring size					
	β-PL	γ-BL	δ-VL	LA	ε-CL
ΔH_p^0 (kJ mol^{-1})	−82.3	−5.7	−12.2	−22.9	−28.8
ΔS_p^0 (J mol^{-1} K^{-1})	−74.0	−19.3	−28.6	−25.0	−53.9
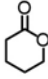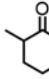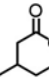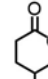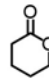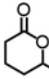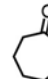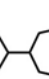
[Monomer] = 1 M, conducted in solution.[9,12]

When dealing with substituted lactones (δ-lactones have been widely studied[12b,c]), two factors should be taken into account: (1) the position of the substituent on the ring, and (2) the length (bulkiness) of the substituent.

(1): The presence of a substituent on δ-lactones results in higher ring strain (more negative ΔH_p^0) whatever the position, the highest impact being the one on δ-position. The substituted δ-lactones also feature lower ΔS_p^0 values, making ring opening less favorable. In particular, the strong decrease of ΔS_p^0 for δ-substituted-δ-VL (δ-CL), from -28.6 Jmol^{-1}K^{-1} for δ-VL to -62 Jmol^{-1}K^{-1} for δ-CL (Table 1.2), explains the less favorable ROP of this monomer (only 90% conversion achieved at 27 °C *vs* 99% conversion at 27 °C for non-substituted and even α- and γ-substituted-δ-VL).

(2): Concerning the length or bulkiness of the substituent, it has been investigated for δ-substituted-δ-lactones, and the results show a very slight impact on the thermodynamics of ring-opening (decrease of ring strain but increase of ΔS_p^0, as they are compensable).[12b,c]

Table 1.2 Enthalpy (ΔH_p^0) and entropy (ΔS_p^0) of ROP for selected lactones (298 K)

Lactone	δ-VL	α-Me δ-VL	β-Me δ-VL	γ-Me δ-VL	δ-CL	δ-DL	ε-CL	CM
ΔH_p^0 (kJ mol⁻¹)	−12.2	−13	−13.8	−15.8	−19.3	−17	−28.8	−18.6
ΔS_p^0 (J mol⁻¹ K⁻¹)	−28.6	−34	−46	−45	−62	−55	−53.9	−33.1

[Monomer] = 1 M, conducted in solution.[9,12]

What about the kinetics of ROP of substituted lactones? Typically, a catalyst is required to promote ROP of lactones.[12d,e] The different way of actions with the activation of either the monomer, the propagating chain-end, or both of them strongly depend on the catalytic system. In addition, the performance of a catalytic system is impacted by the structure of the monomer. For instance, when using diphenyl phosphate (DPP) as a catalyst (note: bifunctional catalyst), ROP of δ-VL and ε-CL is efficiently promoted.[12c, d] ROP of ε-CL is more thermodynamically favorable than δ-VL, but it typically shows lower polymerization rates. Among the methyl-substituted δ-VL monomers, the substitution at β-position (β1 or β-Me-δ-VL) presents very similar polymerization rates to the unsubstituted partner δ-VL (δ0) under the same conditions (Figure 1.2).[12c] In contrast, the substitution at δ-position (δ1 or δ-Me-δ-VL) exhibits the slowest ROP rate over the methyl-substituted and unsubstituted VL monomers. The slowest rate of ROP of δ-Me-δ-VL is very likely caused by the relative low reactivity of the propagating secondary alcohol.[12f, g] Increasing the n-alkyl length at fixed substituent position further decreases the polymerization rate.
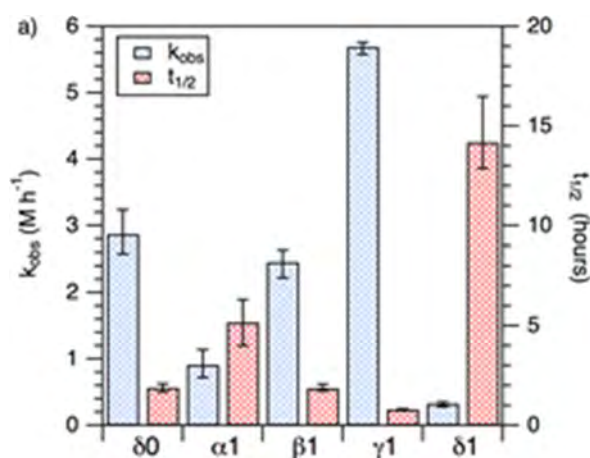

Figure 1.2 Observed rate for the DPP-catalyzed bulk polymerization of poly(n-alkyl-δ-valerolactones). Polymerizations were conducted in the bulk at temperatures of 27 ± 2 °C using initial catalyst and initiator loadings of ([M]₀:[DPP]₀ ≈ 200:1 and [M]₀:[BnOH]₀ ≈ 200:1).

Comparatively to substituted δ-VL, much less studies on substituted ε-CL have been carried out. The reported study on carvomenthide (**CM**, β^iPr-ε-methyl-ε-CL) suggests that the impact of the substituent (at ε-position) is less discriminant from a thermodynamic point of view (Table 2).[12b] Thus, using the appropriate catalyst should overcome the kinetic reluctance even for the ε-substituted one.

Being to one of the most favorable lactones in ROP, ε-CL is then an attractive lactone monomer for the synthesis of aliphatic polyesters including functionalized ones. The functionalized polycaprolactones (PCL) can be prepared by two main approaches: (1) the introduction of the functional groups onto the PCL backbone (typically at α-position) and (2) ROP of functionalized ε-CL monomers (Scheme 1.1).[13, 14] Having five methylene groups –(CH₂)– along with the ring, the approach from ε-CL is thus more versatile. So, it can be functionalized in various positions, mainly at the α-, β- or γ-positions, with a broad range of functional groups.
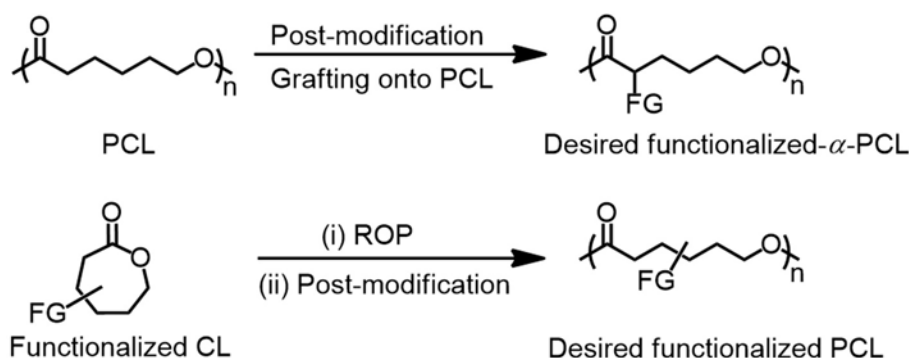
Scheme 1.1 Two main strategies for the preparation of functionalized PCL.[13, 14]

1.1.1 The synthetic approaches for the preparation of functionalized PCL

As mentioned before, two approaches for the synthesis of PCL featuring pendant functional groups have been proposed over the last years.[10, 13-16] The first approach is based on the grafting of functional groups specific at the α-position of the ester from PCL. The second approach (the major one) is based on the synthesis and polymerization of functional lactones substituted mostly in α-, β- or γ-position.

(1) Grafting of functional groups onto PCL chain: This is an interesting method for the functional derivation specific at α-position of the ester in the PCL chains.[14] The functional

group grafting can be achieved by either (i) the post-polymerization modification of functional PCL prepared by commercially available functional CL monomer (i.e., 2-chloro-ε-CL) or (ii) the functional derivatization by an enolate pathway (Scheme 1.2).[15, 16]
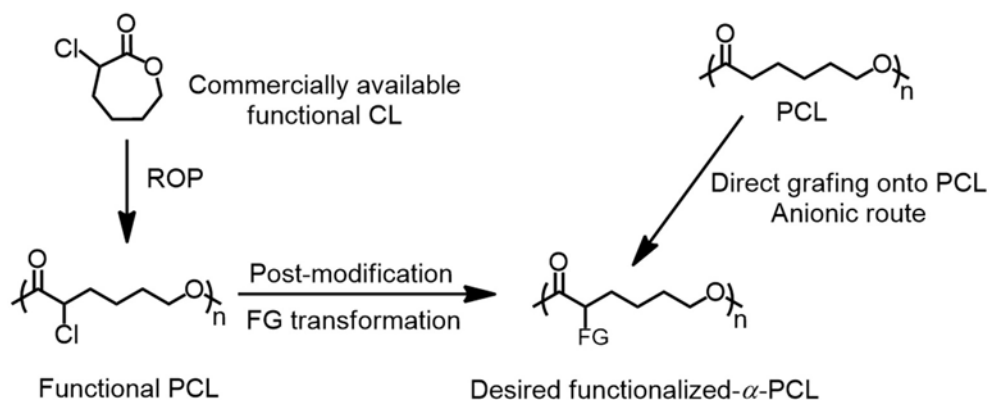
Scheme 1.2 Strategies to prepare the functionalized-α-PCL.[15, 16]

As described before, the combination of ROP and functional group derivatization represents an alternative synthetic pathway to obtain the desired functionalized PCL: for example, the synthesis of chlorinated PCL and subsequent azide substitution for further "click" reactions. In the first step, ε-CL substituted with a chloride is polymerized by ROP yielding the α-chloro substituted PCL as a pre-functional polymer. Then, the corresponding PCL is further substituted with an azide followed by the "click" reaction with alkynes (Scheme 1.3).[17] This method can be applied with a wide range of alkynes bearing different functional groups depending on the desired polymer properties.
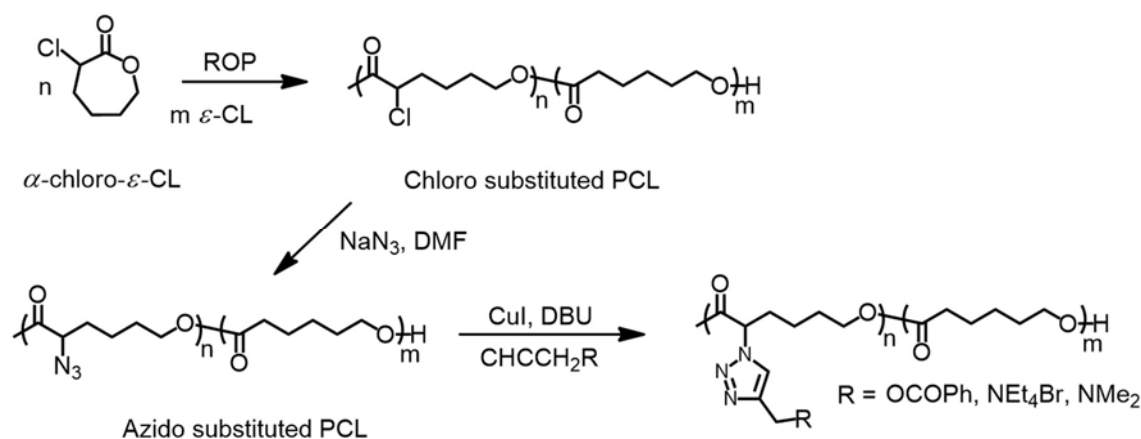
Scheme 1.3 Synthesis of azido substituted PCL and subsequent Click coupling reactions.

However, the major drawback of this strategy is the backbone degradation that was observed during either the chemical transformation or further applied reactions. For example, when a PCL featuring the azido group (M_n, = 18000 g/mol; $Ð$= 1.5) was treated with 0.1 equiv. CuI, 0.1 equiv. DBU and 1.2 equiv. propargyl benzoate at 35 °C in THF for 4 h,[17a] the SEC

trace converted from unimodal to bimodal with a lower M_n (7500 g/mol for the first trace and 1500 kg/mol for the second one), which is the result from the intramolecular transesterification (Figure 1.3 trace b).[17a]
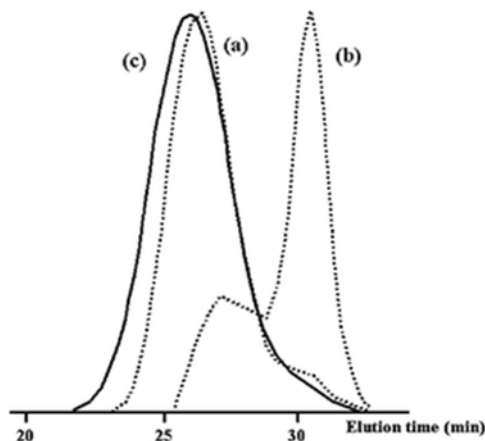
Figure 1.3 SEC traces of PLA copolymers: (a) Poly(αN$_3\varepsilon$CL-co-DL-LA); (b) after "click" reaction with propargyl benzoate and unprotected OH chain-end groups, in the presence of DBU (c) with protected OH chain-end groups, in the presence of NEt$_3$.[17a]

The second strategy for the preparation of functionalized PCL by post-polymerization modification is the introduction of functional groups by an anionic pathway at the α-position of the ester group.[16, 18-19] Several examples of functionalized PCL by this method have been reported, which mainly involve the formation of poly(enolate) anions. The metallation of PCL by lithium diisopropylamide (LDA) leads to the formation of an enolated PCL that can react with a variety of activated electrophiles, e.g., acyl chloride (RCOCl), methyl iodide (MeI), carbon dioxide (CO$_2$), and benzaldehyde (C$_6$H$_5$CHO), (Scheme 1.4). Post-polymerization functionalization by grafting to PCL is generally not very successful. Moreover, the implementation of this method is not widely applicable to a large range of electrophiles due to a problem with backbone scission in competition with chain metallation by LDA. For example, during the reaction to synthesize carboxyl-substituted PCL, the chain degradation was detected leading to a huge change in M_n from 50000 g/mol to 20000 g/mol, and in $Đ$ from 1.48 to 4.1.[18] Note that the very broad $Đ$ of these carboxyl-substituted PCL compared with the starting polymer reveals a physical cross-linking of the polymer by intermolecular hydrogen bonds from carboxylic acid groups.[18] More details about carboxyl-substituted PCL will be discussed later in Chapter III and IV.
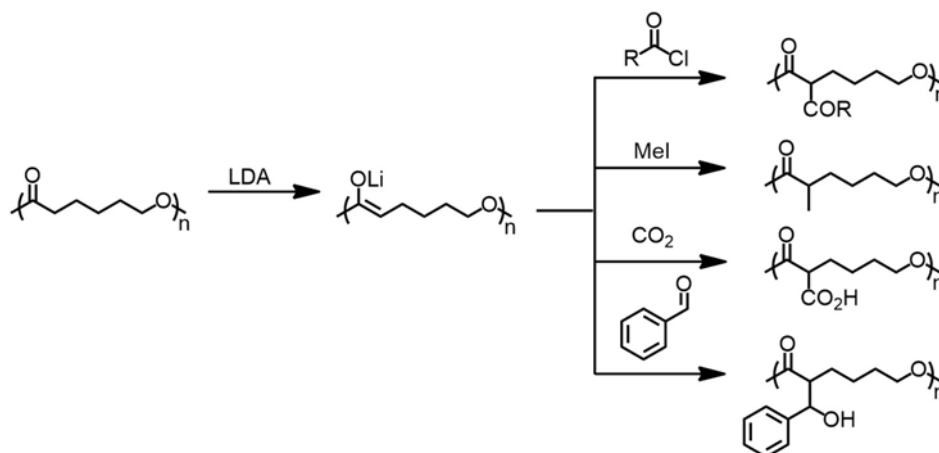
Scheme 1.4 Chemical functionalization of PCL by an anionic route.

(2) The synthesis and polymerization of functionalized CL substituted at α-, β-, or γ-position: This strategy has much more potential for the development of novel functionalized PCL because a variety of functional groups can be introduced not only at α-position but also at β-, or γ-position. Interestingly, very few examples of substituents located at ε-position have been reported, and this fact will be discussed later. In general, functionalized ε-CL monomers with or without a protecting group will be polymerized by ROP to tune the properties of the polymer. These functionalized ε-CL are generally applicable, although they are synthesized in multistep approaches. Another benefit of using functionalized ε-CL is the possibility to purify them prior to the polymerization. Thus, the final polymer is not contaminated by chemicals, as would be the case of functional groups grafting onto the PCL backbone. However, ROP, in principal, only tolerates some functionalities in the monomers. Pendant alcohols, amines or carboxylic acids can act as initiators or terminating agents of the polymerization. Thus, any functional groups that could react with the catalyst need to be protected prior to the polymerization, and then the deprotection is required afterwards. In addition, the selected protecting group also must be considered, because the degradation of PCL backbone can be found, if too stable protecting groups are used.

Eventually, the key success of this approach depends on several required criteria[14]: for example, (i) The preparation of functionalized ε-CL should be as direct as possible (one or two steps), (ii) this functionalized ε-CL should agree with controlled (co)-polymerization, and (iii) the post-polymerization modification, if need, should be carried out under mild conditions without affecting the polymer backbone. For the post-polymerization modification, the method should be also possible to use in quantitative reaction, even if high amounts of functional groups is introduced in the polymer chain.

1.1.2 Synthesis of functionalized caprolactones
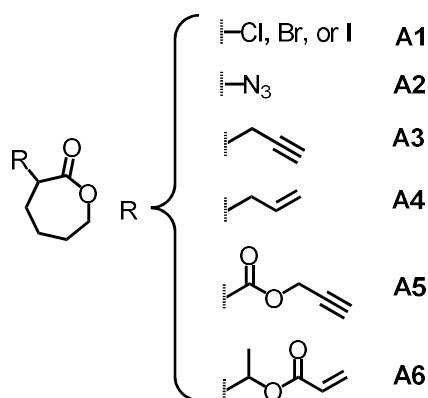
Figure 1.4 α-Substituted-ε-CL for the synthesis of functional PCL.

α-Functionalized-ε-CL: The α-substituted-ε-CL can be prepared by two major strategies (Scheme 1.5): (1) the ring expansion by Baeyer–Villiger oxidation (BV) reaction of functionalized cyclohexanones with meta-chloroperoxybenzoic acid (*m*CPBA) and (2) by the enolate activation of ε-CL monomer with a strong base, LDA, and subsequent nucleophilic substitution reaction.
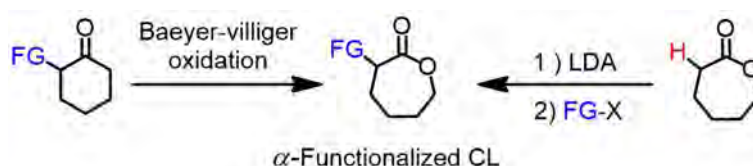
Scheme 1.5 Two major strategies for α-functionalized-ε-CL preparation.

For instance, α-halogenated-ε-caprolactones (**A1**) were prepared by BV reaction of 2-halogenated cyclohexanone with moderated yield of 45–70% (Scheme 1.6a).[20] These α-halogenated-ε-CL were polymerized as homo- or copolymer with ε-CL. The halides were then replaced by azide which can be further reacted with alkynes for the Huisgen 1,3-dipolar cycloaddition reaction, as mentioned previously.[21] In addition, PCL substituted with the chlorides or bromides were also used as a macroinitiator for ATRP of methyl methacrylate (MMA) or hydroxyethyl methacrylate (HEMA).[22] Another way to synthesize the azide-functionalized PCL is the direct polymerization of α-azido-ε-CL (**A2**) monomer. **A2** monomer is synthesized by the substitution of α-halogenated-ε-CL or α-halogenated-ketone with sodium azide (NaN$_3$) (Scheme 1.6b).[17a]
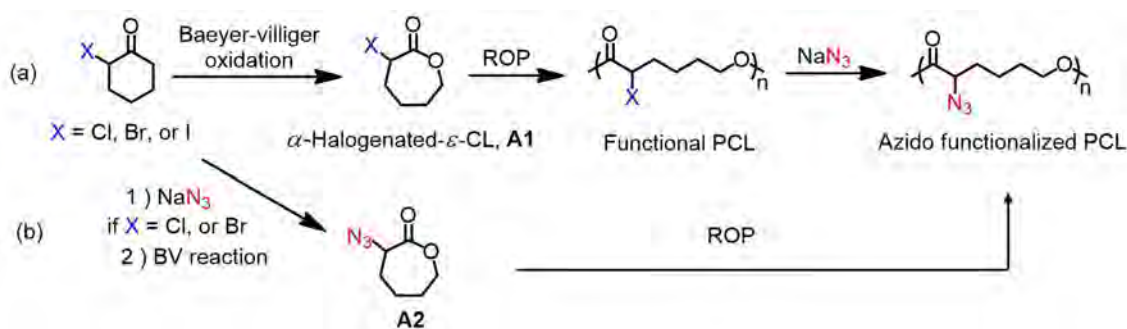
Scheme 1.6 (a) The BV reaction of 2-halogenated cyclohexanone and substitution by N_3 after ROP (b) the preparation of α-azido-ε-CL from α-halogenated-ε-CL.[22, 17a]

Next, the synthesis of α-propargyl-ε-CL (**A3**)[23] was initially performed by the deprotonation of cyclohexanone by LDA and subsequent reaction with propargyl bromide. Then this propargyl cyclohexanone was extended to ε-CL by BV reaction (Scheme 1.7). However, the α-propargyl-ε-CL monomer prepared by this synthetic pathway was obtained in low yield of 14%, as an isomeric mixture of α- and ε-substituted-ε-CL were observed with 30% of α-substituted and 70% of the other.[23] Alkyne-functionalized copolymers of **A3** and ε-CL were further functionalized by the Huisgen-type cycloaddition with mono-(6-azido-6-desoxy)-β-cyclodextrin. The obtained copolymers can be potentially applied in supramolecular chemistry as a drugs or catalyst carriers (Scheme 1.8).[23a]
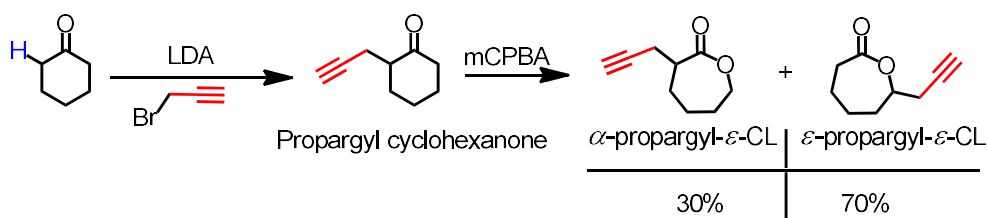
Scheme 1.7 α-Propargyl-ε-CL synthesis and its regioisomer.[23]
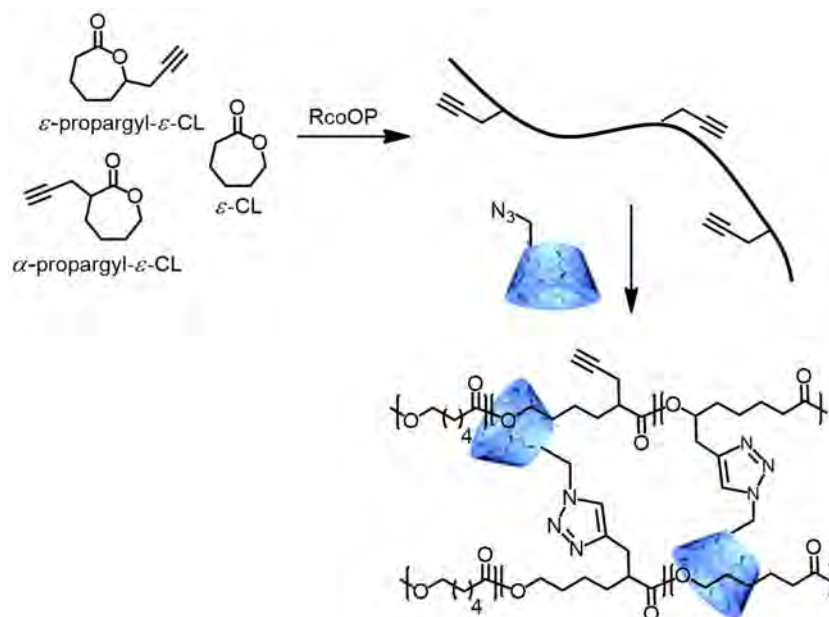
Scheme 1.8 Cyclodextrin-modified PCL as a new drug/catalyst carrier systems.[23]

The second strategy is the direct anionic activation of ε-CL at α-position. Anionic activation of ε-CL can be performed using LDA, non-nucleophilic strong base, to abstract a methylene proton from α-position of the ester carbonyl ($-CH_2-CO$). Subsequently, the generated lithium enolate rapidly reacts with an activated electrophile to obtain α-functionalized-ε-CL (Scheme 1.9).[24-26] However, the main drawback of this strategy is not only the control of reaction temperature (−78 °C approximately) in ε-CL deprotonation step by LDA, but also the formation of side products from transesterification reaction or anionic polymerization of ε-CL.
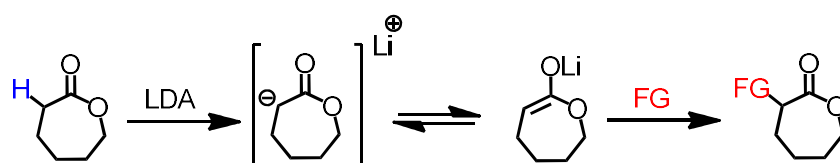
Scheme 1.9 Anionic mechanism for α-substituted-ε-CL monomer synthesis.[24-26]

In general, α-alkene and -alkyne functionalized-ε-CL are synthesized for the aim of further introducing functionalities or bulky molecules, e.g., mono-(6-azido-6-desoxy)-β-cyclodextrin for drug carrier system, or tetraethylene glycol (bis)azide for micelle formation, by thiol–ene and "click" reaction.[23-25] Following the deprotonation of ε-CL by LDA as described above, the deprotonated ε-CL then reacts with allyl bromide, or propargyl chloroformate (Scheme 1.10) to yield α-allyl-ε-CL (**A4**, 50% isolated yield) and α-propargyl carboxylate-ε-CL (**A5**, 49% isolated yield).[24a, 25]
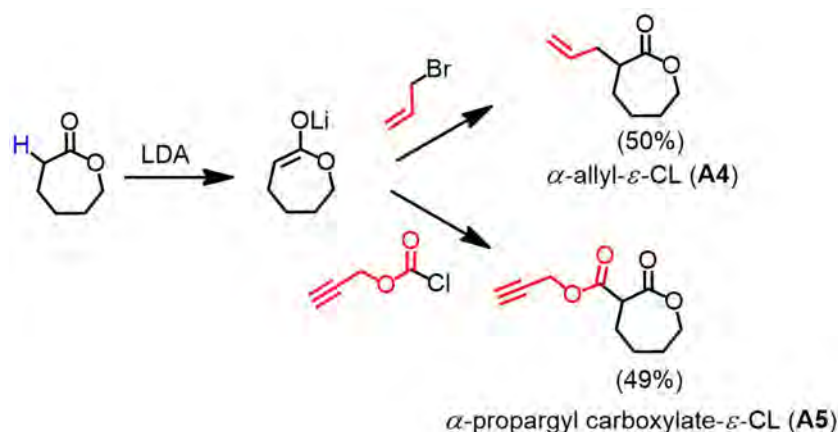
Scheme 1.10 Anionic mechanism for **A4** and **A5** monomer synthesis.[24a, 25]

A4 was copolymerized with ε-CL by Sn(Oct)$_2$, and these copolymers were then attached with amino protecting groups (Boc-protected-amines) by the radical thiol–ene reaction, without observing the polymer backbone degradation (Scheme 1.11).[24b] Then, the cleavage of the Boc protecting groups was done by protonolysis using trifluoroacetic acid. Interestingly, this aminated PCL also displays a water-soluble cationic behaviour, which can be applied as materials for gene delivery.
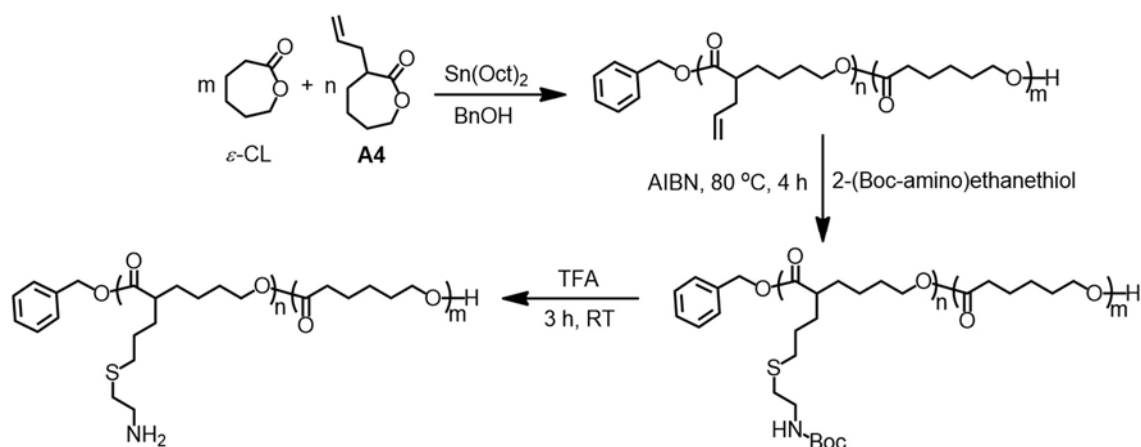
Scheme 1.11 General pathway for the synthesis of aminated PCL.[24b]

A5 was polymerized by Sn(Oct)$_2$ with poly(ethylene oxide), PEO, as a macroinitiator to build the amphiphilic diblock copolymers of PEO-*b*-PPCL featuring pendant propargyl carboxylate groups. The terminal alkynes were then reacted with tetraethylene glycol bis(azide) by "click" reaction (Scheme 1.12).[25] The resulting copolymers represent a cross-linked micelles which can be used as nanodelivery vehicles.
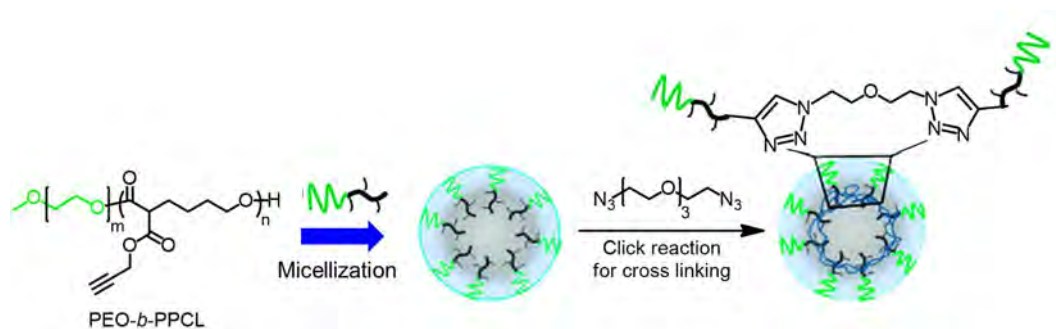
Scheme 1.12 A cross-linked micelles of diblock copolymers of PEO-b-PPCL featuring pendant propargyl carboxylate groups.[25]

The synthesis of α-acrylate-ε-CL (**A6**) was achieved in three steps (Scheme 1.13a).[26] First, trimethylsilylketene acetal is formed by a treatment of the enolate CL with trimethylsilyl chloride. Subsequently, the ketene acetal reacts with acetaldehyde by Mukaiyama aldol reaction to generate hydroxylated-ε-CL. Finally, the esterification of the hydroxylated-ε-CL with acryloyl chloride yields the final functionalized monomer **A6** with a low yield of 36% (global yield). A small amount of **A6** was used as a comonomer in order to prepare a living cyclic PCL macroinitiator by tin dialkoxide catalyzed ROP with ε-CL, and subsequent intramolecular cross-linking reaction (Scheme 1.13b).[26b] After that, the tin dialkoxide containing macrocyclic PCL was applied to initiate the ROP of lactide to form the final tadpole-shaped macrocyclic polyesters.
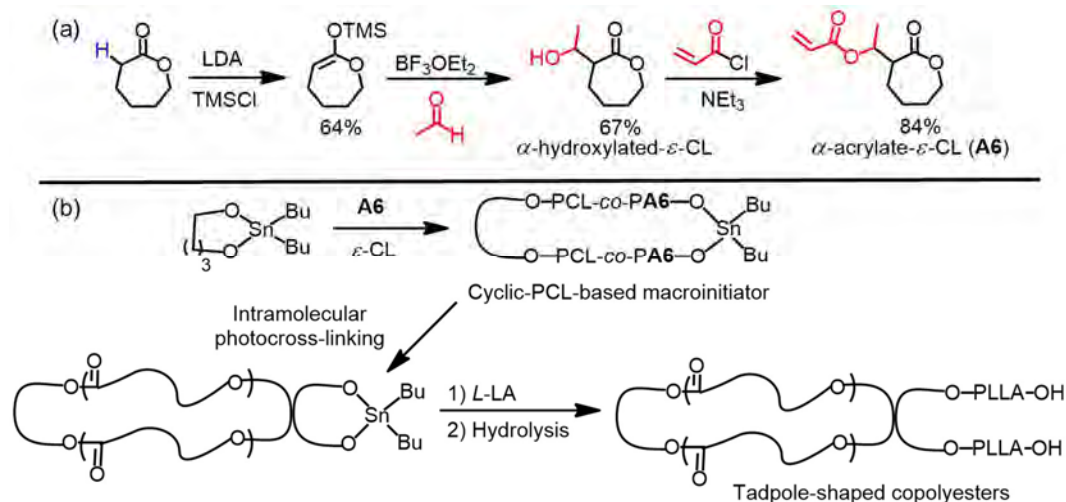
Scheme 1.13 Synthesis of α-acrylate-substituted CL monomer (**A6**), its application for the preparation of tadpole-shaped macrocyclic polyesters.[26]

β-Functionalized-ε-CL: Few examples of ε-CL substituted at β-position have been reported (Figure 1.5).[27, 28a] The first three β-substituted-ε-CL monomers were derived from natural carvone with two steps synthesis (Scheme 1.14).[27]
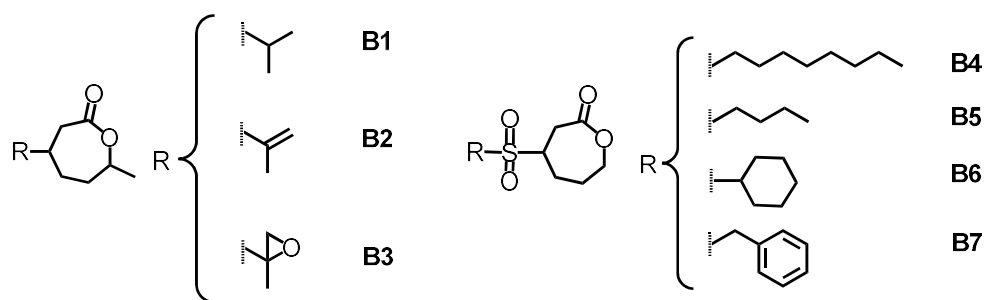
Figure 1.5 *β*-Substituted-*ε*-CL monomers.

First, the carvomenthone and dihydrocarvone were obtained from the hydrogenation of carvone. Carvomenthide (**B1**, 68% global yield) was synthesized by the ring-expansion with *m*CPBA *via* BV reaction without observing any side products, whereas the ring-expansion of dihydrocarvone with Oxone® yielded dihydrocarvide (**B2**, 42% isolated yield, 86 % conversion in ^{1}H NMR) and epoxide side product (10% NMR yield).[27a] Interestingly, using *m*CPBA with dihydrocarvone promoted the epoxidation and ring-expansion resulting in the formation of regioisomeric epoxylactone monomers (25% isolated yield containing **B3** with the regioisomer **B3**' as the ratio 9:1, respectively).[27b]
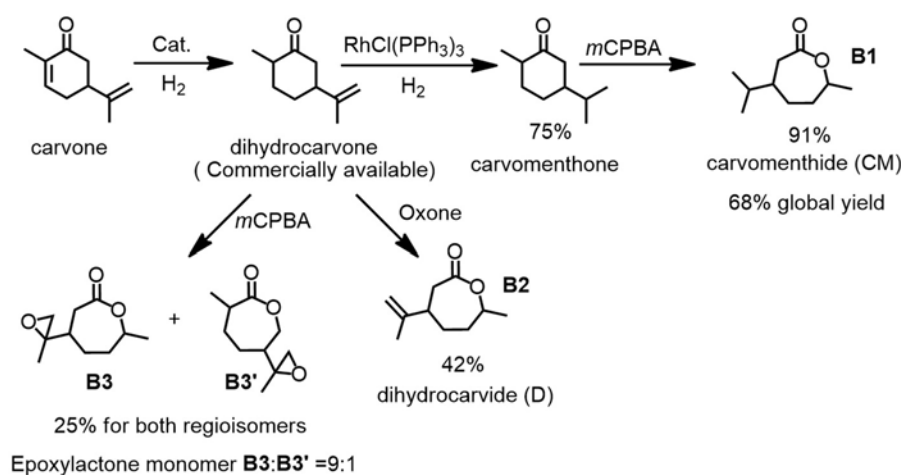
Scheme 1.14 Transformation of carvone into functionalized lactones: **B1**, **B2**, and **B3** (with regioisomer **B3**') monomers.[27]

Homo- and copolymers of **B1** and **B2** were effectively prepared under bulk or solution conditions with diethyl zinc (ZnEt₂) catalyzed ROP and using benzyl alcohol as initiator.[27a] In addition, the corresponding copolymers substituted with alkene pendant groups were also epoxidized or cross-linked to demonstrate the possible post-polymerization modification. **B3** could be used as a multifunctional monomer, from lactone and epoxide, and a cross-linker in ROPs as well. Homo- and copolymerizations of **B3** with *ε*-CL were achieved using either ZnEt₂ (60 °C for 72 h with *Đ* = 2 for homoROP) or Sn(Oct)₂ (120 °C for 24h *Đ* = 2.6 for homoROP

and $Đ$ = 1.6 -1.9 for ROcoP) as catalyst promoting the ring-opening of both lactone and pendant epoxide functional groups.[27b] The resulting copolymers were characterized as a flexible cross-linked material and exhibited perfect shape memory properties. They have high potential for applications in biomedical devices (Figure 1.6).
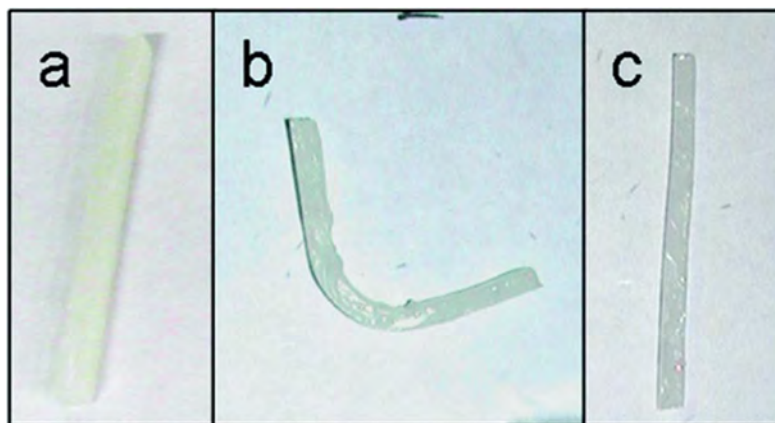
Figure 1.6 Shape memory experiment: (a) original, unbent sample bar of poly(**B3**-co-CL); (b) sample bar after bending to a temporary shape; (c) sample bar after being allowed to recover its original shape following 10 bending cycles.[27b]

Other examples of β-substituted-ε-CL were synthesized in two steps by (1) the thia-Michael addition of cyclohex-2-en-1-one with different thiols and (2) followed by BV reaction to form the ε-CL substituted with sulfonyl groups selectively at β-position (**B4** − **B7**, Scheme 1.15).[28a] During the Baeyer–Villiger oxidation, the sulfide moiety was simultaneously oxidized to the sulfone, so an excess of *m*CPBA was used to obtain full oxidation of both sulfide and ketone.
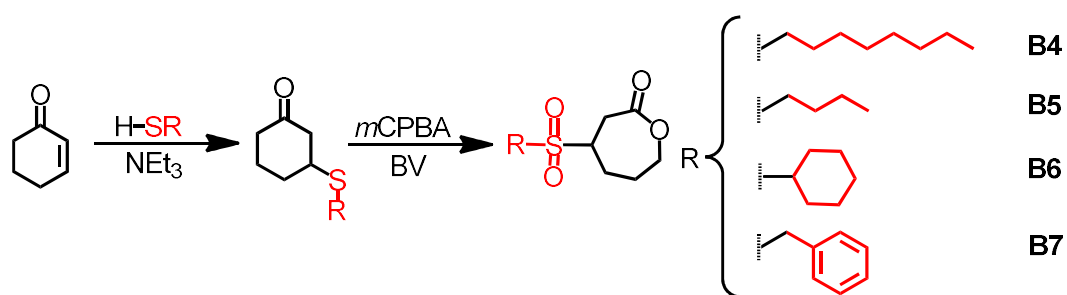
Scheme 1.15 Two synthetic steps of thiol-ene reaction and BV reaction for the preparation of ε-CL substituted with sulfonyl groups.[28a]

HomoROPs of these monomers were done using Sn(Oct)$_2$ at 150 °C in bulk conditions, obtaining low M_ns that differ from the theoretically expected values. According to NMR analysis, the sulfone is stable under the applied polymerization conditions without performing any side reaction, such as elimination. However, the M_ns of the obtained polymer are significantly lower than the targeted ones, although $Đ$s are rather narrow (1.10–1.28).[28b,c,d]

Interestingly, the kinetic studies of homoROP of these monomers showed a well-controlled ROP. In contrast to conventional CL, these functional polymers containing the sulfonyl moieties showed no melt transitions and no thermal degradation up to 180 °C. The steric hindrance from sulfonyl moieties may inhibit the interactions between the polymer chains, thus preventing the formation of crystalline structures.[28a]

γ-Functionalized-ε-CL: Several examples of γ-functionalized-ε-CL have also been reported, and the preparation of these monomers is generally based on the BV reaction of functional cyclohexanones, which are often prepared by multistep synthesis (Figure 1.7). [29, 30, 32, 35, 36, 40, 41]
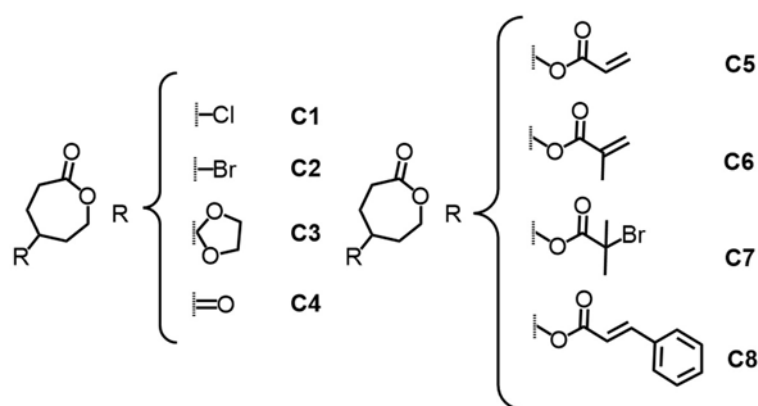
Figure 1.7 The selected examples of γ-functionalized-ε-CL monomers.

γ-Halogenated-ε-CL were synthesized by the oxidation of 4-halogenated-cyclohexanol using pyridinium chlorochromate (PCC) and subsequent ring-expansion with *m*CPBA *via* BV reaction (Scheme 1.16) obtaining γ-chloro-ε-CL (**C1**, ≈ 35% global yield) or γ-bromo-ε-CL (**C2**, 50% global yield).[29, 30] **C1** was polymerized with ε-CL and LA. The pendant chloride groups of the obtained copolymers were replaced by azides, which were subsequently clicked with cholesterol derivatives. Thanks to their properties, the resulting copolymers have a high potential in many applications, especially the use in biocompatible elastomer cell scaffolds and foams.[29]
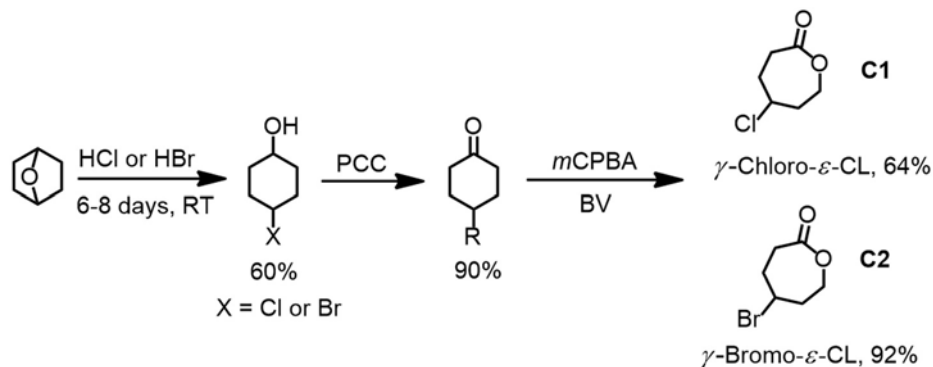
Scheme 1.16 The synthesis of γ-chloro-ε-CL (**C1**) and γ-bromo-ε-CL (**C2**).[29, 30]

The first γ-brominated PCL-based polymer was prepared by ROP of **C2** initiated with Al(O^{i}Pr)$_3$ at 0 °C.[30] Next, random and block copolymerizations of **C2** with ε-CL were also investigated. The results revealed that the living polymerization is consistent with the expected M_n from the monomer to initiator ratio, the narrow Đ, and the good agreement between the comonomers molar fraction in the comonomer feed and the copolymer.[30] Moreover, **C2** was used as a comonomer for the preparation of A$_2$B PCL-based amphiphilic star-shaped copolymers. To obtain the expected star-shaped copolymers, ROP of ε-CL was initiated by an alkyne substituted diol (Scheme 1.17).[31] Then, the alkyne end-group of these prepared PCL was modified by copper(I) catalyzed azide-alkyne cycloaddition (CuAAC) to obtain a hydroxyl group, which was used as an initiator for the copolymerization of **C2** with ε-CL. Finally, the pendant bromide functional groups were substituted by azides and following the click reaction with tertiary amines yielding the pH-sensitive and water-soluble star-shaped polyesters.[31]
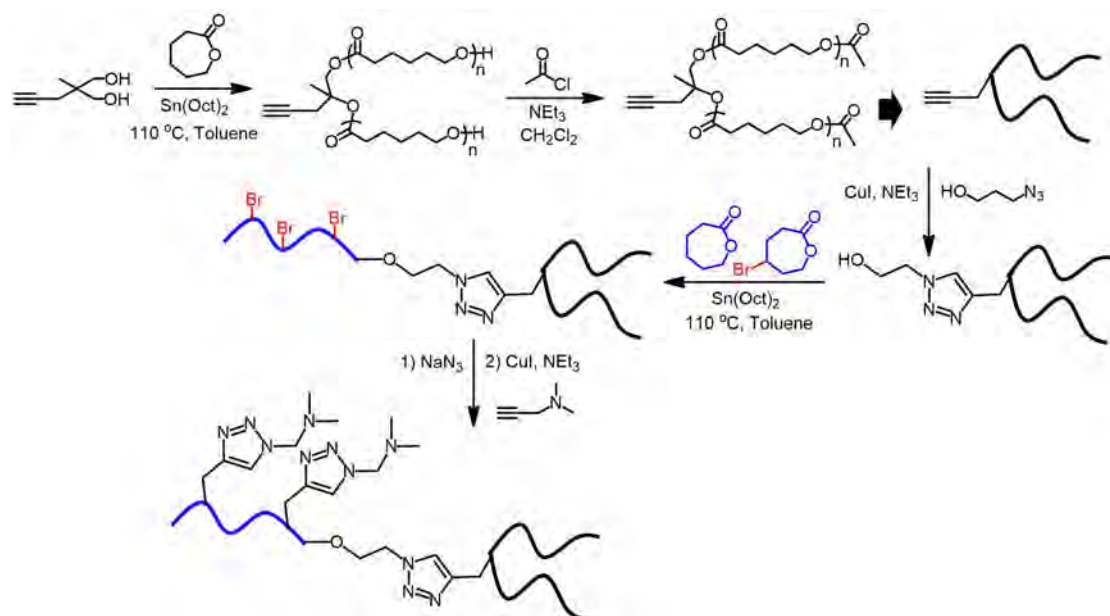
Scheme 1.17 Synthesis of the A$_2$B amphiphilic star-shaped copolymers based on aliphatic polyesters.[31]

γ-Ethylene ketal-ε-caprolactone (**C3**) was synthesized by the BV reaction of the commercially available 1,4-cyclohexanedione monoethylene acetal and was used for the preparation of poly(2-oxepane-1,5-dione), initiated with Al(O^{i}Pr)$_3$ at 25 °C, also known as poly OPD, in which the deprotection of the acetal pendant groups are required after the polymerization (Scheme 1.18a).[32a] Poly OPD has the same structure as PCL, except that the γ-methylene group (–CH$_2$–) in each monomer unit is substituted by a carbonyl functional group.[32] In addition, the keto groups were further conjugated with hydroxyethyl hydrazine and

subsequent coupling reaction with 4-nitrophenyl chloroformate to produce NPC-activated polymers for cell adhesion tests.[33]
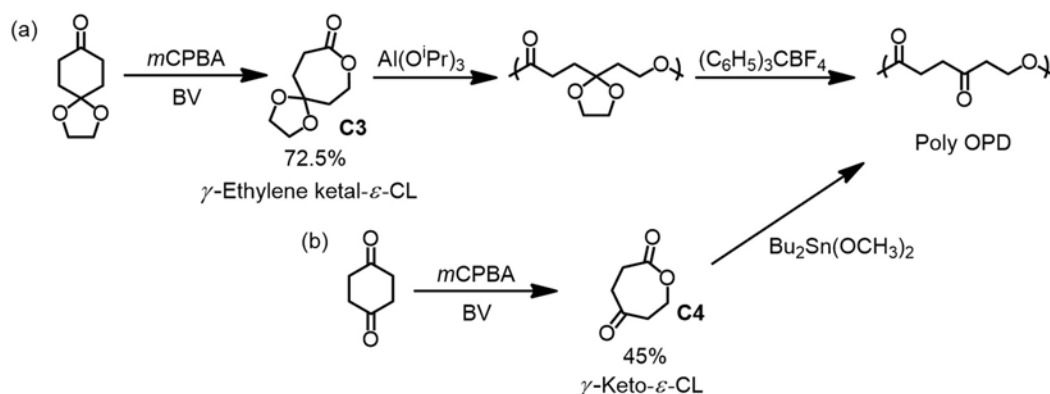
Scheme 1.18 The synthesis of (a) γ-ethylene ketal-ε-caprolactone (**C3**) and (b) γ-keto-ε-caprolactone (**C4**) and their application for the preparation of poly OPD. [32]

γ-Keto-ε-caprolactone (**C4**) is an alternative monomer for the synthesis of poly OPD.[32b] The synthesis of **C4** was described by the ring-expansion of 1,4-cyclohexanedione, and it was used as a monomer for the synthesis of poly OPD, initiated with $Bu_2Sn(OCH_3)_2$ at 150 °C, without requiring any post-polymerization modifications (Scheme 1.18b).[32b] The use of **C4** is potentially attributed to the preparation of comb-type polyester-based biodegradable graft copolymers. After the copolymerization with ε-CL, the keto groups in the copolymer were reduced to hydroxyl groups by sodium borohydride. The resulted copolymers were used as a macroinitiator for building block copolyesters with L-LA (Scheme 1.19).[34]
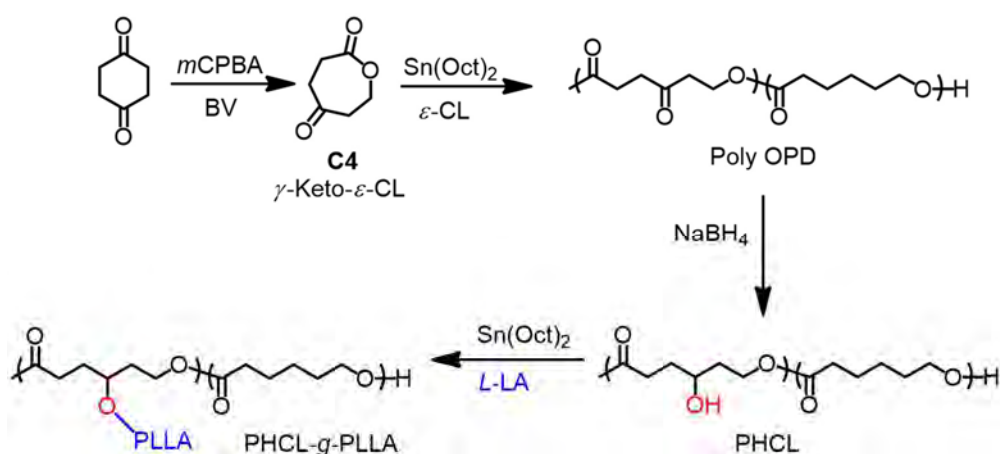
Scheme 1.19 Synthesis of the comb-type PHCL-g-PLA.[34]

It is worth noticing that the introduction of a polarized ketone function on the central methylene group of ε-CL increases the intermolecular interactions, thereby affecting the T_m of polymers from 60 °C up to 110−112 °C. In addition, the thermal and physical properties of

poly OPD synthesized from either **C3** or **C4** are actually identical as both polymers reveal a semi-crystalline phase with a high T_m of 147 °C and a T_g of 37 °C.[32]

Other examples of γ-functionalized-ε-CL monomers consist on the combination of two different functionalities (bifunctional monomer) that, in general, can be selectively polymerized in ROP and radical polymerization (Figure 1.8).[35]
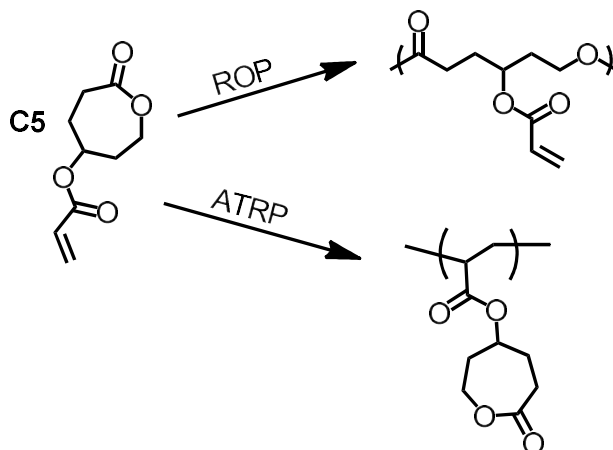
Figure 1.8 An example of difunctional monomer for ROP and radical polymerization.[35]

γ-Acryloyloxy-ε-CL (**C5**) was synthesized in two or three synthetic steps from 1,4-cyclohexanediol (Scheme 1.20a).[35] First, the diol reacted with acryloyl chloride to generate the monoalcohol, which was further oxidized into the ketone using PCC. Then, the ring of the corresponding cyclohexanone featuring pendant acryloyl group was extended, by BV, into the 7-membered ring of CL-based monomer in an overall yield of 36%.[35]
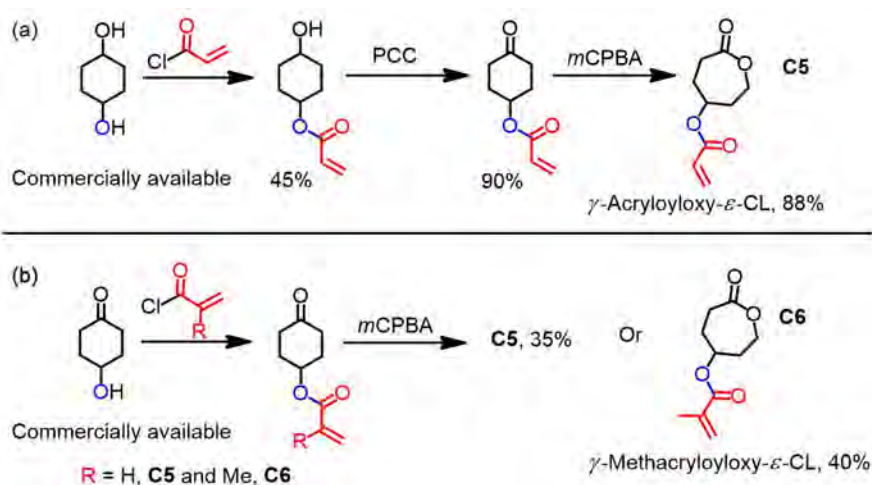
Scheme 1.20 (a) γ-Acryloyloxy-ε-CL (**C5**) synthesis from1,4-cyclohexanediol. (b) Two steps synthesis of **C5** and **C6** monomer by acylation and BV reaction.

C5 was also prepared with another shorter approach (Scheme 1.20b). The synthesis started directly with the reaction of 2-hydroxycyclohexan-1-one with acryloyl chloride followed by the ring-expansion with *m*CPBA *via* BV to yield the final monomer in an overall yield of 24%.[36] Besides using a similar strategy, γ-methacryloyloxy-ε-CL (**C6**) was prepared using methacryloyloxy chloride instead of acryloyl chloride, and the final monomer was obtained in an overall yield of 29%. [36] **C5** was used as a comonomer for RcoOP with ε-CL to prepare the copolymers bearing alkene pendant groups, which could be used for further radical processes. For example, the corresponding copolymers were grafted onto metallic surfaces by a cathodic electrochemical process,[37] cross-linked by UV to form the 2D or 3D microstructured polyester resins,[36] and functionalized with thiol compounds by Michael-addition as well.[38] **C6** and ε-CL were used for the preparation of polyester-based functional resins. These resins were cross-linked to form microparticles for drug delivery systems.[39]

A similar strategy was used for the preparation of γ-(2-bromo-2-methy propionate)-ε-CL (**C7**) and γ-cinnamate-ε-CL (**C8**) (Scheme 1.21). **C7** was used as a radical initiating group in ATRP, whereas **C8** promoted the photoreactions for cis/trans isomerization and [2+2] cycloaddition.[40, 41]
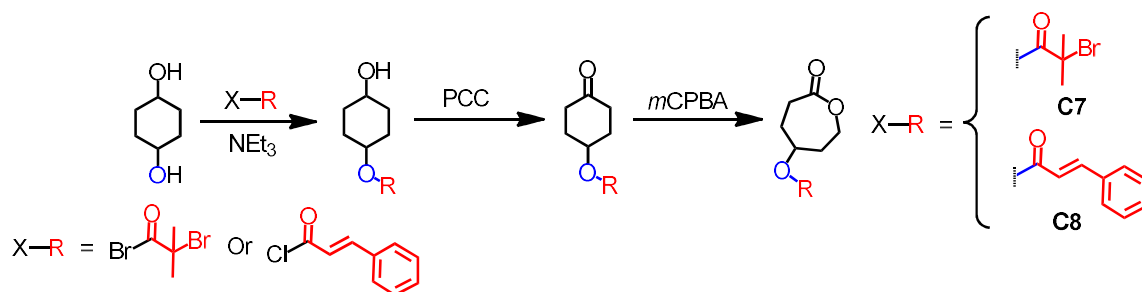
Scheme 1.21 The synthesis of γ-(2-bromo-2-methy propionate)-ε-CL (**C7**) and γ-cinnamate-ε-CL (**C8**).

Based on the reviews described above, the anionic activation strategy that starts from the formation of deprotonated either CL or cyclohexanone is used specifically for substitution at α-position of ε-CL. However, the major drawback of this approach strongly indicates to the loss of starting material caused by transesterification reaction or anionic polymerization of ε-CL. In contrast, most of the functionalized CL at α-, β-, or γ-position are generally prepared by the ring-expansion using BV reaction, in all cases, for the last step.

*So, what about **ε-functionalized-ε-CL** synthesis???* Prior to discuss about the reported examples of ε-functionalized-ε-CL synthesis, it has to be noted that CL-based monomers substituted at α-, β-, or γ-position are appropriate for copolymerization with ε-CL as the

kinetics of ROP of these functionalized ε-CL are quite close to that of ε-CL as they all do propagation through a primary alcohol. In marked contrast, ε-functionalized-ε-CL have different properties for ROP as the poor nucleophilicity of its propagating secondary alcohol can slow down the rate of ROP. The introduction of functional groups at ε-position is interesting, as the functional group can influence the polymer properties like the functional group at chain-end such as the autocatalyzed-hydrolysis of carboxyl group at chain end (more detail will be presented in Chapter III and IV). As mentioned in the general introduction, it is also the opportunity to dispose of monomers capable to copolymerize efficiently with ε-DL.

The use of BV reaction for the preparation of ε-Functionalized-ε-CL synthesis is hampered by the lack of regioselectivity. Depending on the steric and electronic properties of the substituent, the regioisomeric mixture of α- and ε-functionalized-ε-CL are typically obtained: for example, the preparation of **A3**[23] and the BV reaction of α-Me-, -F-, and -CF$_3$-cyclohexanones (Scheme 1.22).[42]
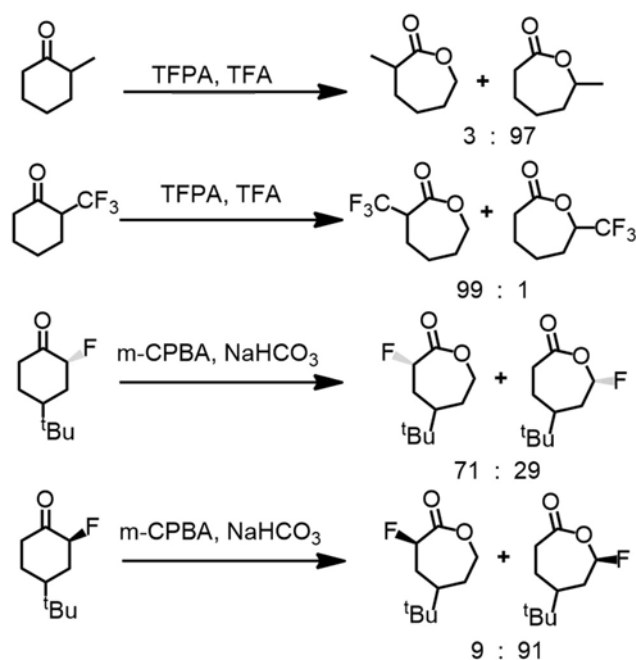
Scheme 1.22 BV reactions of α-Me-, α-F-, and α-CF$_3$-cyclohexanones and their regioisomeric mixture.[42]

As a result, very few examples of ε-functionalized-ε-CL synthesis have been reported.[43] ε-Allyl-ε-CL (**E1**) was prepared by BV reaction from the corresponding ketone (commercially available 2-allyl cyclohexanone) (Scheme 1.23).[43a] However, a side product was detected from the competitive epoxidation of the double bond yielding ε-epoxy-ε-CL (**E2**) with a 35% yield to **E1**. Homo- and copolymers of **E1** with ε-CL or LA were prepared with a catalytic amount of Sn(Oct)$_2$ initiated by either benzyl alcohol or bifunctional alcohol from benzyl ester. In

addition, different chemical transformations, e.g., bromination, epoxidation, and hydrosylilation, were successfully carried out with the bearing pendant allyl groups in copolymers.

Scheme 1.23 The single synthetic step of ε-allyl-ε-CL (**E1**) with the side product ε-epoxy-ε-CL (**E2**).[43a]

ε-Carbamoyl-ε-CL (**E3**) was synthesized and used for the preparation of novel aliphatic polyester bearing pendant N-isopropylamide functional group.[43b] To obtain **E3** monomer (70 % global yield), 2-(N-Isopropyl-2-carbamoylethyl)cyclohexanone was first synthesized by the Michael reaction of N-isopropylacrylamide with cyclohexanone and followed by the BV reaction using mCPBA as oxidant (Scheme 1.24).[43b] HomoROP of **E3** was investigated under bulk conditions with a catalytic amount of Sn(Oct)$_2$ at 130 °C. However, the oligomers were found as a major product including the residue of unpolymerized **E3**. In contrast, copolymerization of **E3** with ε-CL was carried out successfully with similar conditions to that of homoROP. The prepared copolymers containing 9.1 mol% **E3** formed flexible films and revealed its degradability, which is much faster compared with PCL. Note that the hydrolytic degradation was performed in phosphate buffer (pH = 7.4) at 37 °C and was monitored by the weight loss and change of intrinsic viscosity.[43b]

Scheme 1.24 Synthetic route of ε-carbamoyl-ε-CL (**E3**) and its copolymerization with ε-CL.[43b]

The last example of ε-functionalized-ε-CL was selected based on the substitution of carboxyl group onto PCL backbone for its applications in pH-responsive material, as well as

the prospective in biodegradable material.[43c] ε-Benzyloxycarbonylmethly-ε-CL (**E4**) was synthesized in three steps from cyclohexanone as followed by: (1) the activation of cyclohexanone with morpholine forms an enamine intermediate, (2) the corresponding enamine reacts with benzyl bromoacetate *via* the nucleophilic substitution reaction and (3) the ring-expansion of the prepared ketone to benzyloxycarbonylmethyl substituted CL by the BV reaction (Scheme 1.25).[43c] However, the regioisomeric mixture associated with the regioselectivity in BV reaction were obtained containing 90% of **E4** and 10% *α*-benzyloxycarbonylmethyl-ε-CL (**E4'**).
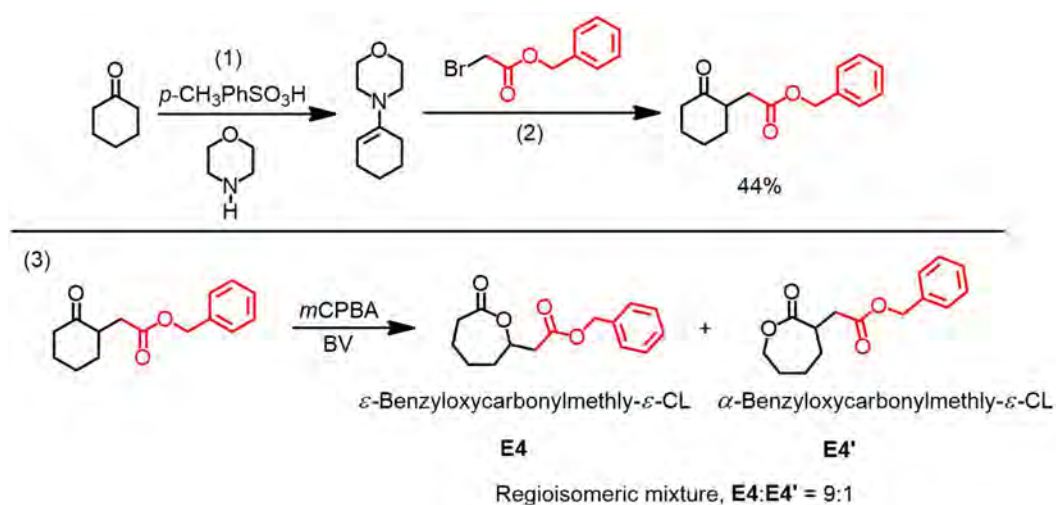
Scheme 1.25 Synthesis of ε-benzyloxycarbonylmethly-ε-CL (**E4**) and its regioisomer **E4'**.[43c]

E4 and its regioisomer were used as monomers for the preparation of amphiphilic PCL-based diblock copolymers, mPEG-*b*-P(**E4**-co-**E4'**) (Scheme 1.26). The copolymers bearing pendant carboxyl groups were obtained after post-polymerization modification using commercially available Pd/C catalyst under H_2 atmosphere. Furthermore, the behaviors of these prepared copolymers in solution were studied by various methods, revealing its rich pH-responsive behavior and the pH-induced micellar formation.[43c]
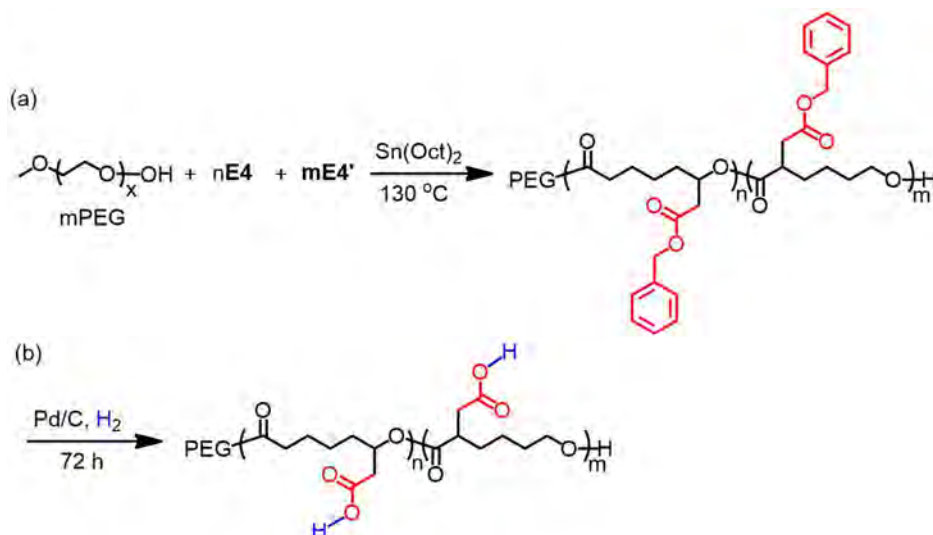
Scheme 1.26 (a) Copolymerization of **E4** and **E4'**with m-PEG, and 2-BCL and (b) their post-polymerization modification for the preparation of carboxylated PCL.[43c]

Accordingly, very few examples of ε-functionalized-ε-CL monomers have been reported. (Note that the regioselectivity of BV reaction can be controlled by biocatalyst.)[43d, 43e, 43f] So, an alternative strategy for the preparation of ε-functionalized-ε-CL within only two synthetic steps is here proposed (Scheme 1.27): (1) transition metal catalyzed cycloisomerization of alkynoic acids and subsequent (2) functionalization with thiols by thiol-ene chemistry.
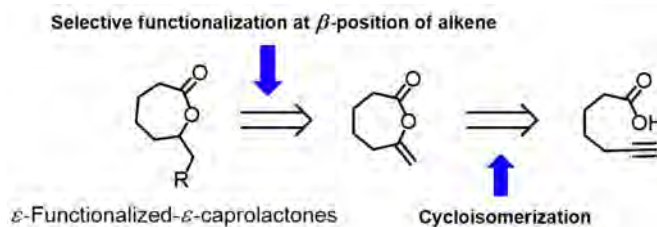
Scheme 1.27 A new proposed strategy for ε-functionalized-ε-CL preparation.

1.1.3 Alkylidene-lactones prepared by Pt-based catalyzed cycloisomerization of alkynoic acids

Over the last few years, the LBPB team has reported original pincer Pd or Pt complexes of type **A** in which two P=S side-arms support in-plane σ-coordination of the central indenediide moiety to the metal center, Pd and Pt (Figure 1.9).[44]
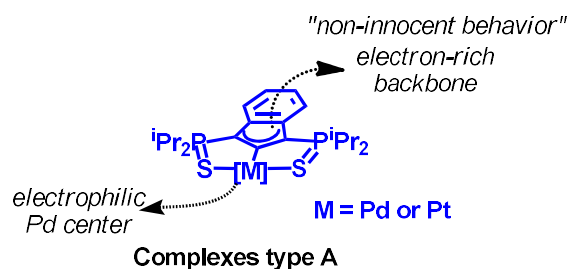
Figure 1.9 Pd or Pt complexes of type A in which the indenediide backbone displays non-innocent behavior.[44]

According to experimental and theoretical studies, these complexes **A** feature an electrophilic Pd center, while the indenediide backbone is electron-rich and displays non-innocent behavior as a base.[45] In particular, complexes of type **A** have been applied in catalytic hydrofunctionalization reactions. A range of alkylidene-lactones with diverse substitution patterns have been efficiently prepared by cycloisomerization of alkynoic acids.[46] In contrast to usual Pd catalysts[47], these Pd and Pt catalysts enables to prepare efficiently 5, 6 and even 7-membered lactones including ε-alkylidene-ε-lactones in excellent yields of >80% (Scheme 1.28).
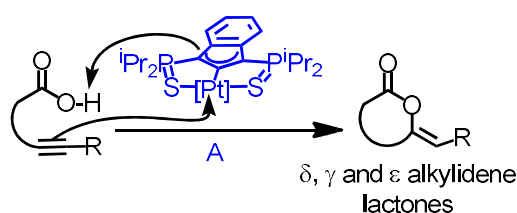
Scheme 1.28 The preparation of δ-, γ-, and ε-alkylidene lactones using Pt complexes of type.[46,47]

In addition, the reaction has a full atom economy, and it takes place under mild conditions with the absence of any base or additives. The cycloisomerization of the alkynoic acids yields an interesting exo-methylene products that can be used as a ε-modified-ε-caprolactone precursor. In particular, the corresponding precursors reveal a unique opportunity to overcome the aforementioned problems of regioselectivity for the preparation of ε-functionalized-ε-lactones with the BV reaction. Based on the results obtained previously[47], ε-alkylidene-ε-lactones derived from 6-heptynoic acid will be prepared in multi-gram scale and will be further modified to the corresponding ε-functionalized-ε-lactones according to the proposed strategy by thiol-ene click chemistry (Scheme 1.29).
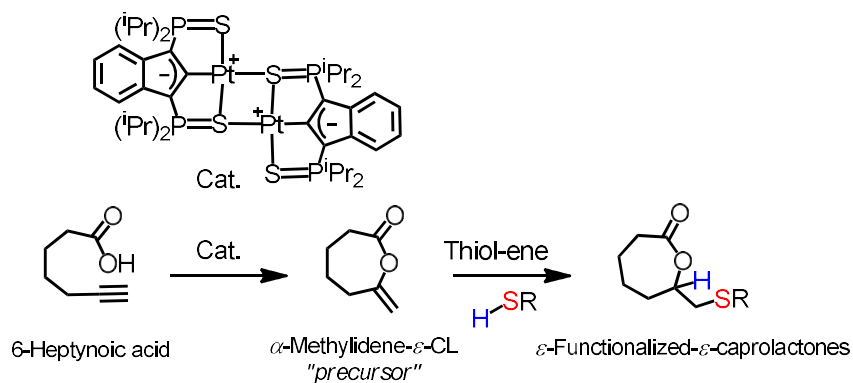
Scheme 1.29 Two synthetic steps for the selective preparation of ε-functionalized-ε-CL.

In regard to thiol-ene reaction, the thiols bearing the desired functional group, in protected form if required, will be used. Due to its good compatibility with the ester moiety, thiol-ene is an efficient and selective reaction that has already been applied in many examples for the functionalization either in post-polymerization modification of functional polyesters or in pre-polymerization modification of functional-ε-CL.[48] In the case of pre-polymerization modification, the targeted functional groups of carboxylic acid, amide or hydroxyl will be introduced in a protected form, which can be removed easily without affecting the polymer backbone.[49]

1.1.4 Functionalization by Thiol-ene chemistry

As mentioned before, the effective and selective functionalization strategy will be described based on the thiol-ene coupling reaction, which is a well-known addition-type organic reaction. Thiol-ene coupling reaction is a hydrothiolation of alkene to form thioether.[50] The reaction is specifically the addition of a S−H bond across a C=C double bond by either a free radical or ionic mechanism (Scheme 1.30). Thiol-ene reaction has high potential in many applications, especially in materials and biomedical sciences, due to its outstanding features as a "click-type" reaction, e.g., full atom economy reaction, highly efficient and selective to anti-Markovnikov product in a high yield, tolerant of various solvents and functional groups, and generally free of side-products from the reactions.[50, 51] In principle, there are two different pathways to carry out the thiol-ene addition: (1) base/nucleophilic-catalyzed Michael addition and (2) free-radical addition.[50-52]

Scheme 1.30 Hydrothiolation of a C=C bond with anti-Markovnikov representation.[50]

1.1.4.1   Thiol-ene reaction conditions

A) Base/Nucleophilic-catalyzed Michael addition:[50,52] Base-catalyzed Michael thiol-ene addition principally requires a catalytic amount of a base, e.g., an amine, to facilitate the specific coupling reaction of an *electron-deficient alkene* with a thiol. This thermodynamically favored reaction represents a special type of conjugate 1,4-addition in which the strong nucleophilic thiol attack on the β-carbon of an electron poor ene to yield selectively the anti-Markovnikov product.[50]
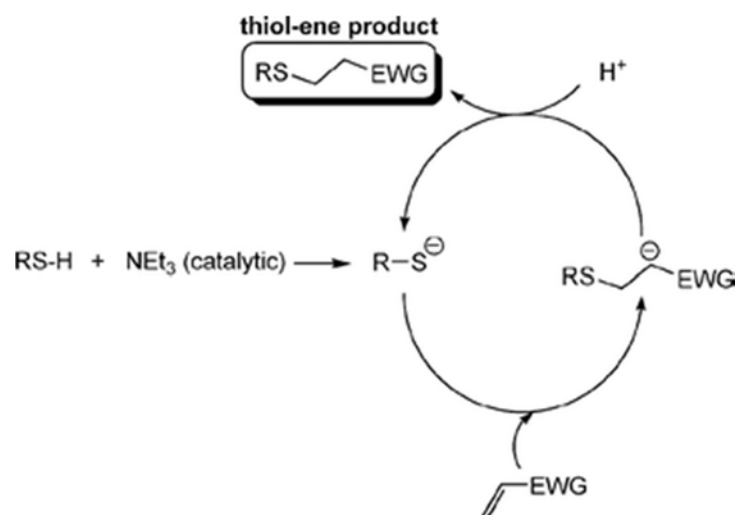
Scheme 1.31 Base-catalyzed mechanism for the hydrothiolation of an activated C=C bond, EWG = ester, amide, or cyano.[50]

In general, this pathway is initiated by a relatively weak base (such as NEt₃), which is used to produce a stronger nucleophile: the thiolate anion. As illustrated in Scheme 1.31, the base-catalyzed pathway is as follows: in the presence of a base (e.g. NEt₃), a proton from the thiol is abstracted generating a thiolate anion along with a conjugate acid, e.g., ammonium cation. Subsequently, the thiolate anion, a strong nucleophile, reacts with an electron-deficient alkene at β-carbon yielding an intermediate carbon-centered anion. This intermediate anion is generally a strong base, which can further abstract a proton either from a thiol or from the conjugate acid to yield the thio-ene product with anti-Markovnikov representation. The base catalyst is then regenerated in the catalytic cycle.

Additionally, several mechanistic studies showed that not only a base can promote the thiol-ene reaction, but a nucleophile, simple primary/secondary amines or phosphines, can also catalyze the thiol-Michael addition reaction.[53, 54] In contrast to the base-catalyzed system, a strong base, thiolate, is formed by a strong nucleophile instead of using a weak base (Scheme 1.32). Nucleophilic addition at the activated alkene forms an enolate intermediate which further

abstracts a proton from thiol to generate the thiolate anion. This thiolate anion is a key intermediate in this nucleophile-mediated pathway, in which the anionic chain process begins the formation of the thiol-ene product once it is generated.[55]
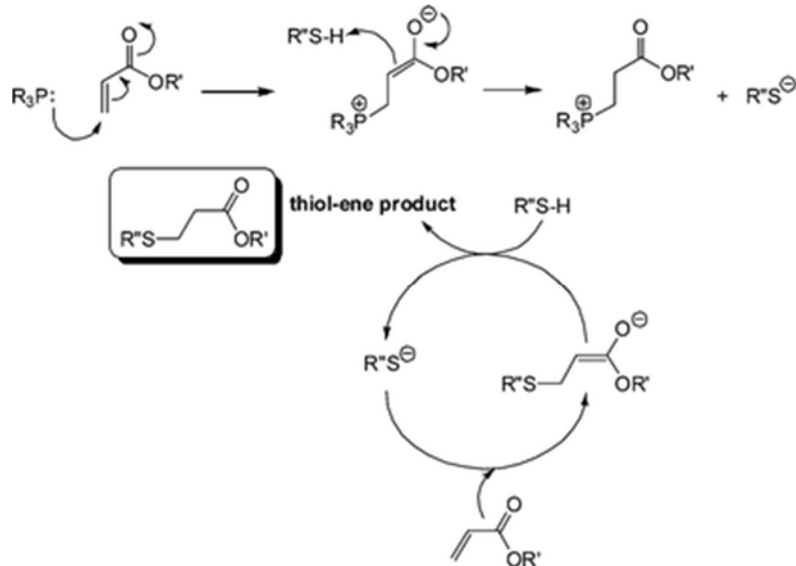
Scheme 1.32 Nucleophile-mediated hydrothiolation of an acrylic C=C bond using phosphine as a catalyst.[50]

B) Radical addition: Aside from the base/nucleophilic-catalyzed thiol-ene Michael addition, thiol-ene coupling can be readily conducted under radical conditions. Free-radical addition could be initiated by photo or thermal radical initiator to form a thiyl radical (Scheme 1.33). This radical further reacts with an alkene functional group *via* an anti-Markovnikov orientation leading to the formation of an intermediate carbon-centered radical. After that, the carbon-centered radical abstracts a hydrogen radical from another thiol molecule generating the thiol-ene coupling product and a new thiyl radical that further initiates the reaction (Figure 1.10).[50, 56] Radical thio-ene reaction is typically encountered with electron rich alkenes.
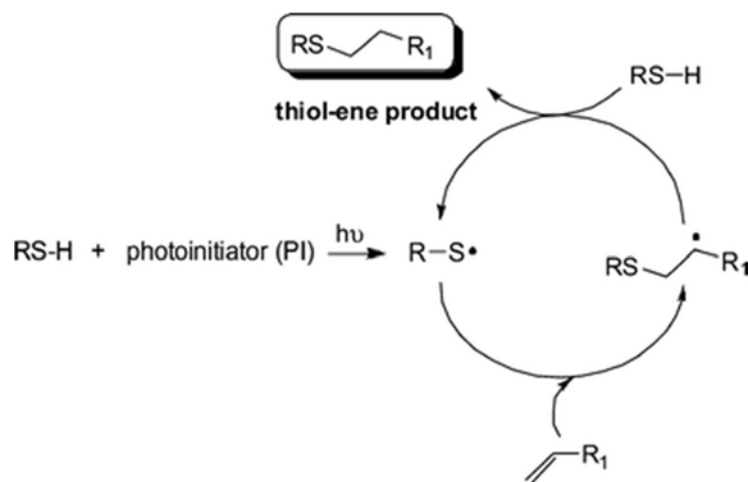
Scheme 1.33 Free radical hydrothiolation of a C=C bond in the presence of a photoinitiator.[50]
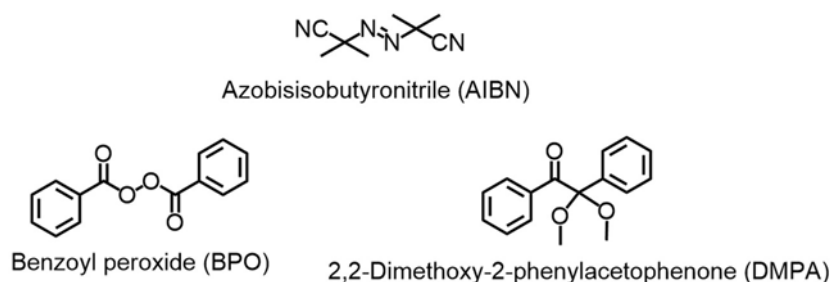
Figure 1.10 Selected radical initiators such as AIBN (thermal), BPO (photo), and DMPA (photo).[50]

The factors that need to be considered, the structure and pKa of thiol affects the rate of hydrogen abstraction from thiol and also the homolytic cleavage of the S–H bond in the free radical thiol-ene reaction.[50]

1.1.4.2   Functionalization of polyesters by thiol-ene chemistry

Typically, there are two major approaches for applying the thiol-ene chemistry to the synthesis of functionalized polyesters (Scheme 1.34).[57] The first strategy is to graft the thiol with functional groups as side groups/chains to the preformed polymer. The other way is to use the monomers bearing thiol pendant groups that are functionalized by thiol-ene reaction prior to polymerizations.
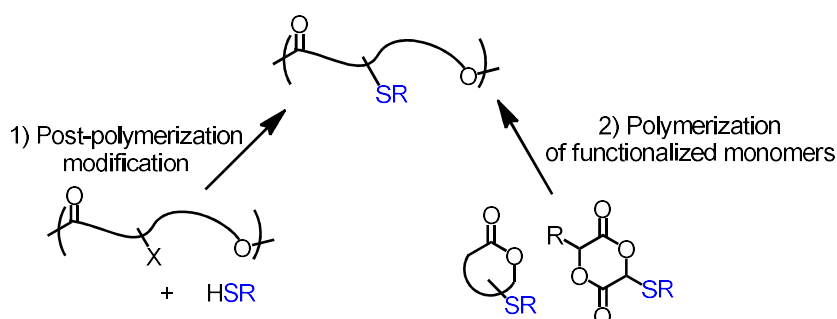
Scheme 1.34 Two main strategies for the preparation of thiol-functionalized polyesters. [57]

Post-polymerization modification: The concept of post-polymerization modification is generally a grafting onto the polymeric chains with thiols bearing functional groups.[57, 58]

Modification of pendant alkene groups: thiol-ene reaction was applied on the unsaturated polyesters bearing alkene pendant groups.[59] For instance, the alkene pendant groups in poly(3-hydroxyalkanoate), PHA, were functionalized with fluorinated and PEG thiols using AIBN as a thermally activated initiator (Scheme 1.35). The number of PEG or fluorinated chains grafted onto the backbone of the obtained functionalized PHA were well-

defined with this strategy, thus proving self-assembly behavior to form a multicompartment micelle.

Scheme 1.35 Synthetic pathway for the preparation of functionalized fluorinated/PEG PHA.
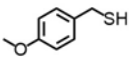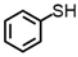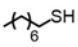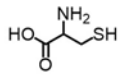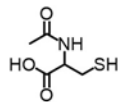
Modification of methylene groups on polyester backbone: Copolylactides with exo double bonds along the polymeric chains were alternatively prepared by ROP of LA (95 mol%) with chloro-substituted lactide (5 mol%).[60] The unsaturated polymer chain with exo-methylene, in the same monomeric unit, was functionalized by either free radical-mediated or base-catalyzed thiol Michael addition with a broad range of thiols under mild conditions (Scheme 1.36).
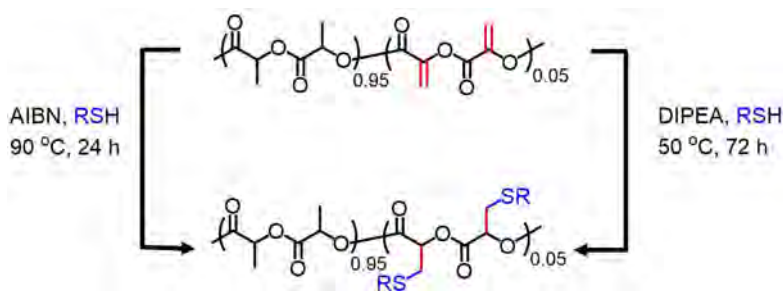
Scheme 1.36 Post-polymerization modification of ene-PL by free radical-mediated or base-catalyzed thiol Michael addition.[60]

However, the functionalization of the unsaturated polymer chain by free radical-mediated thiol-ene reaction was still incomplete. Using a larger excess of thiol (25 equiv.) resulted in only 56% of thiol addition to the alkene units. This could be a result of a competing radical catalyzed cross-linking of the alkene-containing copolymers as well as the reaction of thiol radicals to form disulfides.[60] In contrast, the treatment of the ene-PL by base-catalyzed thiol Michael addition showed a complete conversion of thiol addition to the exo-methylene units. Interestingly, the base-catalyzed thiol-ene reactions of ene-PL with a variety of thiols were achieved without a significant decrease in the M_n of copolymer (Table 1.3).

Table 1.3 Base-Catalyzed conjugate addition of thiols to ene-PL

	% thiol addition	M_{nsec} (kDa)
Chloro-PL	-	15.3
ene-PL	-	14.1
[structure: 4-methoxybenzyl thiol] SH	100	16.6
[structure: benzyl thiol] SH	97.2	15.9
[structure: octanethiol] SH	98	16.1
[structure: cysteine] NH$_2$ HO SH O	100	2.0
[structure: N-acetyl cysteine] NH SH HO O	100	15.8

Modification of endo double bonds in polyester chain: The unsaturated polymers described above generally required a multistep synthetic procedure. Therefore, a more straightforward synthetic route for unsaturated polyesters preparation is required. For example, the ROP of globalide macromonomer, a commercially available endo-methylene macrolactone with 16-membered ring, was catalyzed by CALB (*Candida antarctica* Lipase B (CALB) immobilised on macroporous resin) yielding unsaturated polyesters in a single step.[61] In addition, the feasibility of the thiol-ene click reaction on the internal double bonds (endo-methylene groups) of the linear polymer was also assessed in the presence of three different thiol-bearing molecules (Scheme 1.37).
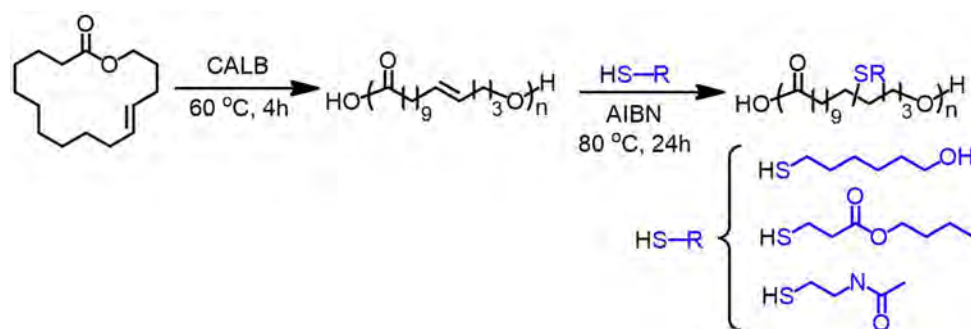
Scheme 1.37 ROP of globalide and post-polymerization modification by thiol-ene reaction.[57, 61]

Monomer functionalization: Another approach is to functionalize the unsaturated monomers by thiol-ene reaction prior to the ROP. For instance, Three β-functionalized-δ-VL monomers with different thioether pendant groups were prepared by Michael addition of thiol-bearing compounds to α, β-unsaturated δ-VL (Scheme 1.38).[62]
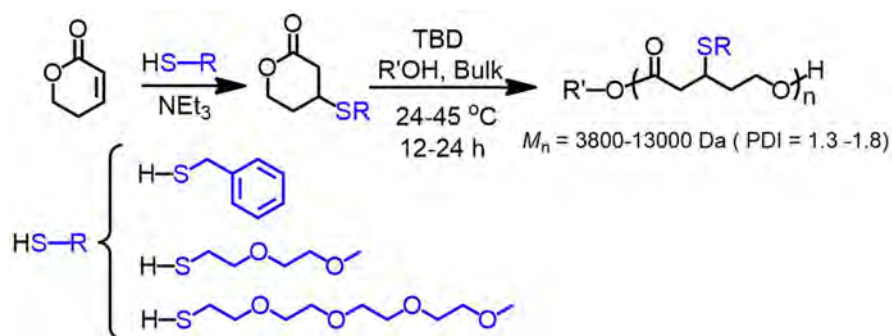
Scheme 1.38 Synthesis and ring-opening polymerization of thioether-substituted δ-valerolactones.

These functionalized monomers displayed their ability to carry out the ROP catalyzed by organocatalyst (TBD). Homo- and co-polymers of these monomers with ε-CL were also prepared with good conversions and molecular weights up to 13,000 g/mol.

Biodegradable PLA-based block copolyesters bearing pendant protected functional groups were prepared by ROP of thiol-functionalized LA with either LA or ε-CL as a comonomer.[63] The synthesis of this functionalized LA was performed in two steps involving the base-catalyzed Michael addition of the exo-methylene LA with triphenylmethanethiol (Scheme 1.39). The building block was easily modified, and the thiol groups, protected as trityl thio-ether, provided the possibilities for the fabrication of functional materials. For example, the pyridyl disulfide group was substituted *via* thiol–disulfide exchange reaction (Scheme 1.40). This bearing pyridyl disulfide group (PDS) was attached with a cysteine-containing peptide by two-step modification, which is a selective route to access polymer–peptide conjugates in mild conditions.
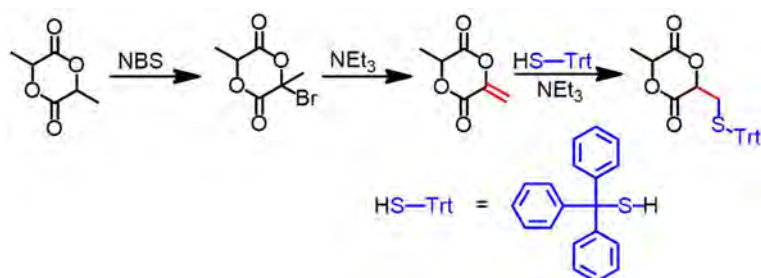
Scheme 1.39 Synthesis of 3-methyl-6-(tritylthiomethyl)-1,4-dioxane-2,5-dione (TrtS–LA) by Modification of l-Lactide.[63]
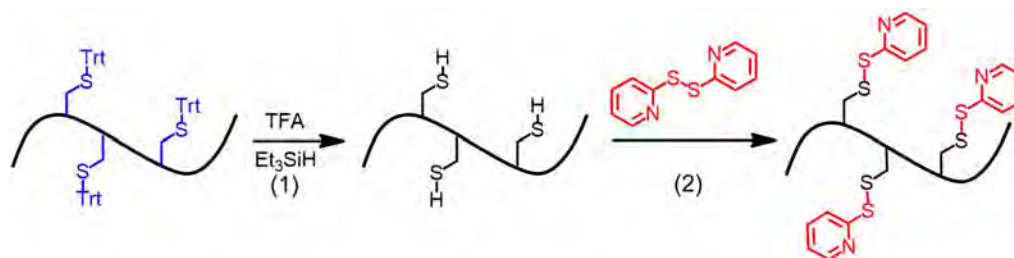
Scheme 1.40 The preparation of block copolyesters featuring pendant pyridyl disulfide group: (1) deprotection of trityl thio-ether (2) thiol–disulfide exchange.[63]

Unless a catalytic amount of base, e.g. methylbenzylamine and NEt_3, was used, the ring-open of LA substituted with exo-methylene group was observed instead of the thiol addition to the bearing methylene group.[48] This limitation led to a new method using catalytic I_2 for the functionalization of methylene LA based on the thiol-addition to an exo-methylene group (Scheme 1.41).[48] The thiol-ene reaction of methylene lactide with 1,3-propanedithiol using I_2 as a catalyst was achieved under mild conditions without the presence of the ring-open form of allylic LA.
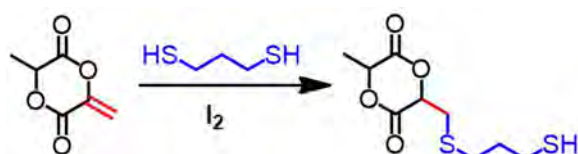
Scheme 1.41 I_2-catalyzed functionalization of allylic LA with dithiol.[48]

In summary, polyesters functionalized with thiol moieties along the polymer chains, can be achieved by two major strategies: (1) post-polymerization modification and (2) ROP of thiol-functionalized monomers. Post-polymerization pathway has a drawback related to efficiency of the addition and the chain scissions, thus possibly decreasing in the molecular weight of the polymer and changing the polymer properties. Alternatively, the ROP of thiol-functionalized monomers is the most attractive route to prepare high molecular weight polymers in a controlled way. Moreover, by doing copolymerization with ε-DL, the ratio of functional group should be easily adjusted, thereby allowing the tuning of the polymer properties. According to a new proposed strategy in Scheme 1.27 (modified version in Scheme 1.42), this synthetic approach displays an implementation for the synthesis of versatile precursor monomers (exo-methylene CL). The corresponding precursor permits the simple and selective functionalization with a broad range of functional groups being a last synthetic step right before the polymerization.
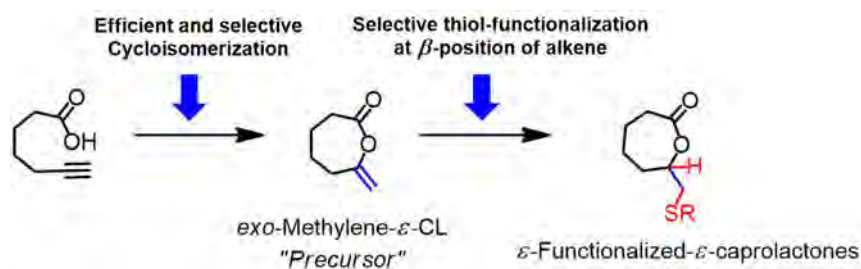
Scheme 1.42 A new proposed strategy for ε-functionalized-ε-CL preparation. The scheme is modified from Scheme 1.27.

For the functionalization, the thiol-ene reaction will be first investigated with a model thiol (BnSH) set the reaction conditions for the introduction of functional groups at ε-position of the lactone. Then, the targeted ε-functionalized ε-lactone monomer in protected form will be prepared with benzyl 2-mercaptoacetate (benzyl ester thiol) following the optimized thiol-ene reaction conditions. Thereafter, the targeted functionalized CL-based monomers will be further polymerized though ROP and/or ROcoP with a close structure monomer like ε-DL to yield the new copolymers featuring pendant benzyl protected groups. Finally, these benzyl-protected groups will be modified to obtain the carboxyl functional groups. Interestingly, copolymers featuring pendant carboxyl groups may feature the hydrophilic/hydrophobic balance and self-assembly behavior as well as the degradation rates of PDL.

1.2 Results and Discussions

1.2.1 Preparation of CL-based precursor by Pt pincer complexes catalyzed cycloisomerization of alkynoic acids

As mentioned in the introduction, our group has described that catalytic cycloisomerization by Pt pincer complexes of more challenging substrates of alkynoic acids and N-tosyl alkynylamides, leading to the preparation of a broad range of exo-methylene lactones/lactams. Interestingly, cycloisomerization catalyzed by Pt pincer complexes enables the highly efficient and selective preparation of exo-methylene-ε-lactone (**1**), which could be further used as a precursor for the preparation of ε-caprolactone functionalized at ε-position. Accordingly, **1** was easily prepared by the cycloisomerization of heptynoic acid catalyzed by Pt pincer complexes featuring an SCS indenediide backbone (1 mol% of [Pt], Scheme 1.43).
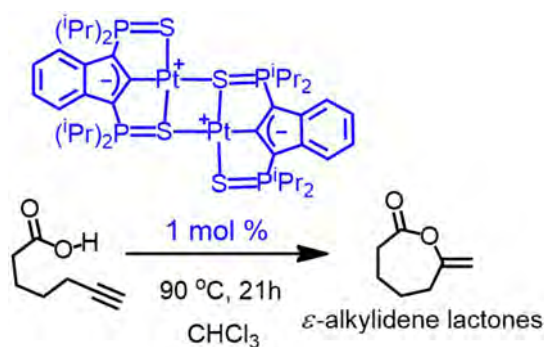
Scheme 1.43 The synthesis of exo-methylene-ε-lactones from heptynoic acid catalyzed by Pt pincer complexes.

The reaction was complete after 21 hours at 90 °C with the absence of any additives or bases. The crude was purified by sublimation to yield a pure form of **1** in good yields (79% for 2.5 grams scale). The structure was confirmed by ^{1}H NMR with the characteristic signals of olefinic (=CH$_2$) functional group at 4.79 and 4.66 ppm corresponding to those reported by our group.[47] As mentioned before, compound **1** is a possible precursor for the preparation of ε-functionalized-ε-caprolactone. Moreover, the reaction can be performed properly in large scale, up to 5 grams scale in a good yield (72%). Thus, a new approach for ε-functionalized-ε-lactones preparation was proposed (Scheme 1.44) by (i) taking the efficiency of cycloisomerization catalyzed by Pt pincer complexes to synthesize compound **1** in high selectivity and good yields, and (ii) followed by the thiol-ene functionalization of methylene functional group at ε-position. Note that both cycloisomerization and thiol-ene reaction are atom economy reactions.
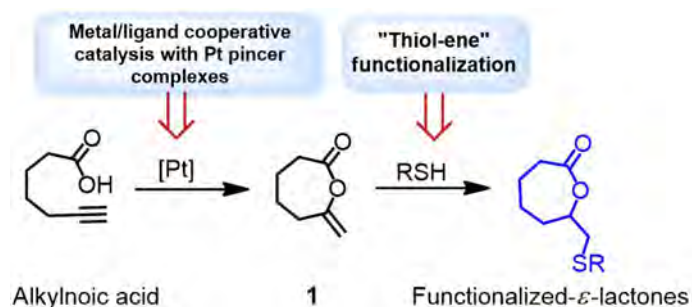
Scheme 1.44 Proposed strategy for the preparation of ε-functional-ε-lactones.

Having an exo-methylene at ε-position of **1**, this functionalized monomer cannot be used as a monomer for ROP due to its tautomerization after the first ring-opening reaction. Therefore, the functionalization of **1** is necessary prior to the ROP. According to the possible facile ring-opening of **1** with nucleophiles, the reactions of lactone containing exo-methylene are expected to be challenging: therefore, the functionalization conditions need to be considered carefully to remain the character of ε-CL.

1.2.2 Screening of the reaction conditions for the thiol-ene reaction: the promoter

As already mentioned about a general route to modify **1**, the character of this thiol-ene reaction that involves the thiol addition at the selective position of the less substituted alkene (β-position) fits to the aim of functionalization of compound **1** (Scheme 1.45).
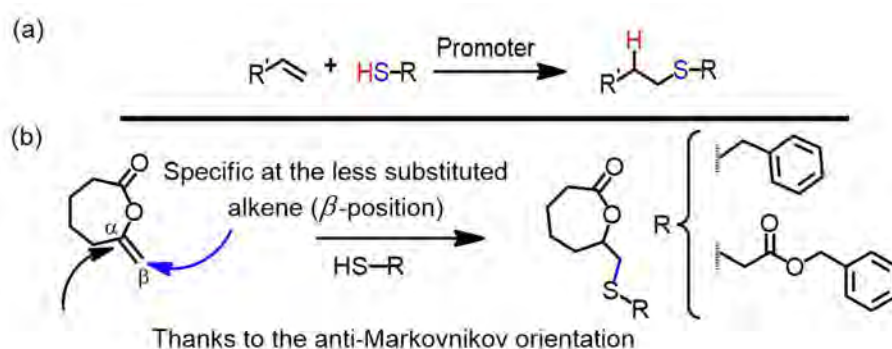
Scheme 1.45 (a) General thiol-ene reaction with anti-Markovnikov product (b) The β-position of compound **1** that aims to be functionalized by thiol-ene reaction.

First, the coupling of compound **1** with benzyl thiol was planned to set the reaction conditions as a model study for the synthesis of a new functionalized lactone modified at ε-position. Several different reaction conditions were investigated to find a good protocol fitting to our thiol-ene process, in which the thiol-ene coupling would be promoted rather than the

ring-opening of **1**. The initial study was based on the promoter screening (Scheme 1.46), e.g., I$_2$, benzoyl peroxide (BPO), and 2,2-dimethoxy-2-phenylacetophenone (DMPA).
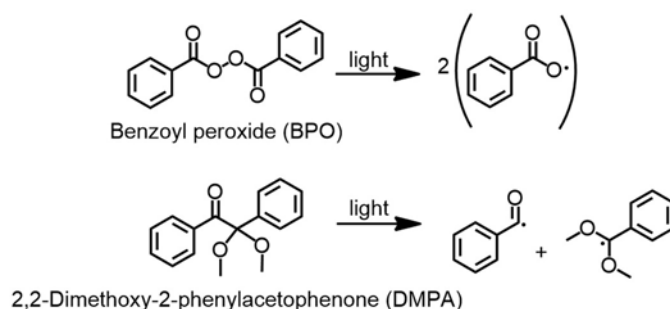
Scheme 1.46 The structure of BPO and DMPA, and their fragments under UV irradiation.

The first study was performed by iodine-catalyzed thiol-ene reaction (5 mol% of I$_2$ as reported for the functionalization of LA)[48] of compound **1** (0.5 M in CDCl$_3$) and benzyl thiol (1.2 equiv.) at 0 °C for 2 hours (Scheme 1.47). Mesitylene (1 equiv. to compound **1**) was added and used as an internal standard (IS) in order to monitor precisely the conversion of **1**.
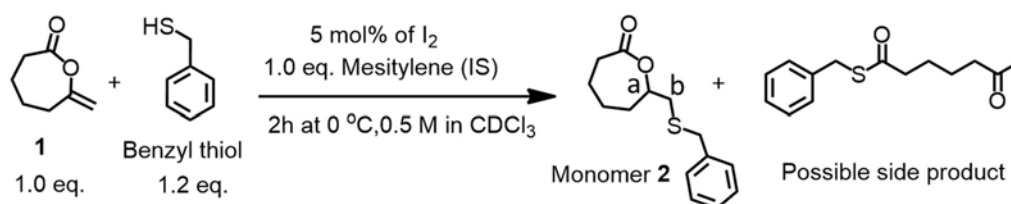
Scheme 1.47 The conditions of Iodine-catalyzed thiol-ene reaction.

After 2 hours of reaction, **1** was completely consumed, as determined by ^{1}H NMR. Then, the crude was analyzed by GC-MS, and a signal at 250.25 m/z was detected. As the theoretical m/z of the desired product (monomer **2**, 250.10 m/z) is similar to the mass of side product (250.10 m/z) resulting from ring opening, this analysis is not likely to be discriminating. So, the crude product was analyzed by ^{1}H NMR. None of the characteristic signals related to monomer **2** was observed, i.e., no signal of –C**H**– (a) from the stereocenter and of its neighboring diastereotopic protons –C**H**$_2$– (b) (see Scheme 1.47), although it showed the disappearance of the olefinic (=CH$_2$) functional group of compound **1**. *"What is the product from the Iodine-catalyzed thiol-ene reaction?"* Looking carefully at the ^{1}H NMR spectrum in Figure 1.11, the signal at 2.12 ppm is attributed to the characteristic signal of a methyl ketone (–CH$_3$), and the signal at 4.11 refers to the two protons of –CH$_2$–S– from benzyl thiol. All signals in ^{1}H NMR spectrum confirm the structure of *S*-benzyl 6-oxoheptanethioate as a ring-opening form of compound **1**.
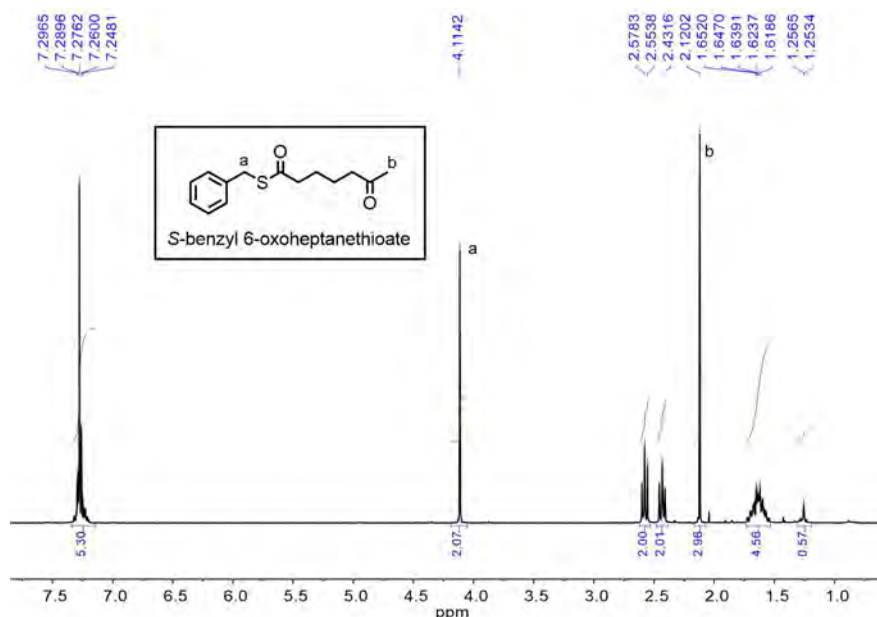
Figure 1.11 ¹H NMR spectrum (CDCl₃, 300 MHz) of *S*-benzyl 6-oxoheptanethioate as a product of ring-opening reaction catalyzed by I₂.

So, how the ring-opening of 1 was formed by Iodine-catalyzed thiol-ene reaction? In the presence of I₂, which acts as a Lewis acid, the C=O from the ester of compound **1** could be activated followed by the nucleophilic attack of benzyl thiol. The intermediate enol is then generated and subsequent keto-enol tautomerization generates the *S*-benzyl 6-oxoheptanethioate (ring-opening of **1**) (Scheme 1.48). To sum up for the first promoter screening, the coupling reaction of compound **1** with benzyl thiol by iodine-catalyzed thiol-ene reaction does not work as expected. The iodine catalyst promotes the ring-opening of **1** instead of the thiol-ene coupling.
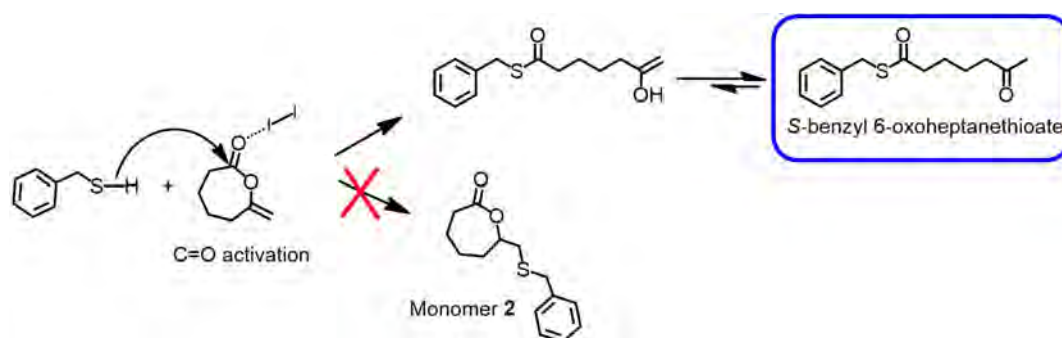
Scheme 1.48 Proposed mechanism for the ring-opening of **1**.

Next, we moved to the free-radical addition pathway using either BPO or DMPA as a radical initiator. Two tests of thiol-ene reaction of compound **1** (0.5 M in CDCl₃) and benzyl thiol (1.2 equiv.) were initially performed using 2 wt% of the radical initiator, either BPO or DMPA, under UV irradiation (365 nm) from UV lamp and at 40 °C (Scheme 1.49). The conversion (%) of compound **1** and the generation (%) of monomer **2** were calculated related

to the reference signal at 6.81 ppm (3H, Ph) from mesitylene (1 equiv. to compound **1**), which was used as an internal standard (IS).
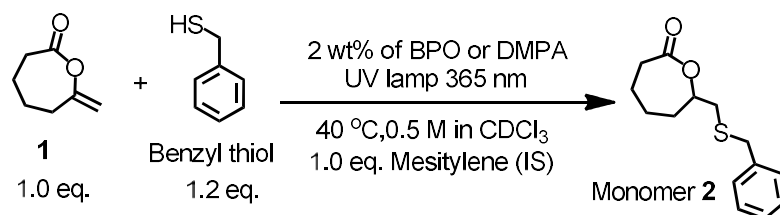
Scheme 1.49 The free radical reaction conditions using either BPO or DMPA.

Free radical thiol-ene reaction was easily followed by ^{1}H NMR (e.g., Figure 1.14 represented the stacked ^{1}H NMR spectra from thiol-ene reaction using DMPA). From the stacked ^{1}H NMR spectra, the decreasing of the characteristic signals of olefinic (=CH$_2$) functional group at 4.79 and 4.66 ppm corresponding to the exo-methylene from **1**, and of the thiol (S–H) at 1.76 ppm can be followed. The growth of new characteristic signals of a proton (–CHO, a) at 4.08 – 3.98 ppm and new signals in the aliphatic region (b and b') at 2.74 and 2.54 ppm were also observed. After 4 days of UV irradiation, the reaction initiated by BPO showed the total consumption of **1** observed by ^{1}H NMR. In contrast, another attempt with DMPA presented better results, **1** was completely consumed after only 24 hours, faster than using BPO.

From the signals in the stacked ^{1}H NMR spectra (Figure 1.12), not only the monomer **2** was detected but side products were also found. All the signals marked with an asterisk (*) in the stacked ^{1}H NMR spectra (Figure 1.12) represented the unknown compounds, which were formed after 12 hours of UV irradiation. The signals around 5.26 ppm are close to the signals of olefinic functional group. These signals could be the proton(s) from another alkene, which is different from the exo-methylene of **1**. Furthermore, the singlet signal at 2.12 ppm cloud be attributed to the methyl ketone (CH$_3$). This signal may correspond to the ring-opening of **1** (see Figure 11 for more details). It is necessary to identify the side products, so that the optimization of reaction conditions can be done to suppress their formation.
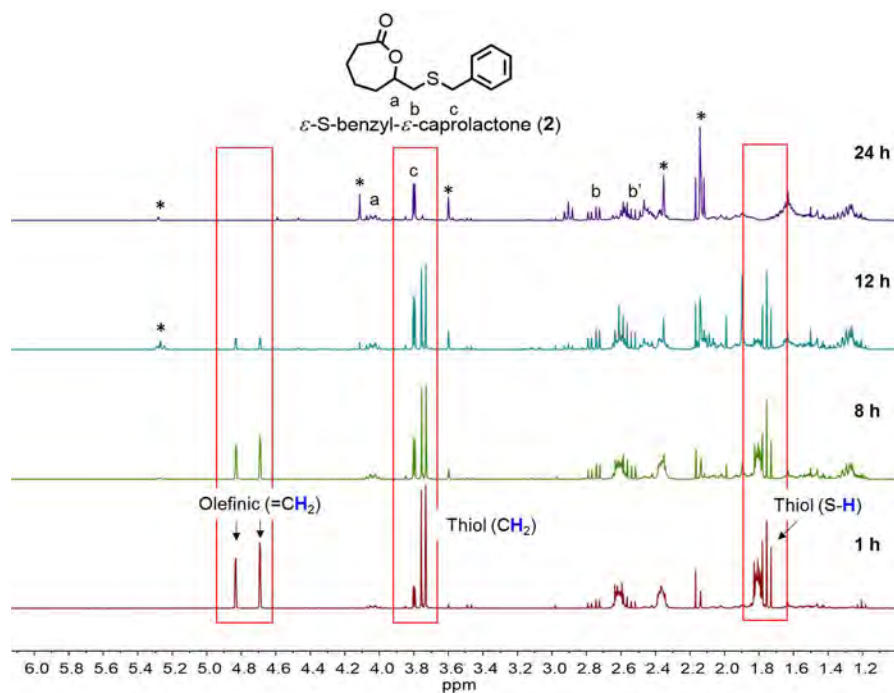
Figure 1.12 Stacked ^{1}H NMR spectra (CDCl$_3$, 300 MHz) of radical thiol-ene reaction of **1** with benzyl thiol using DMPA as an initiator. The sampling from reaction was collected at 1h, 8h, 12h, and 24 h.*side products.

Then, the crude product from both reactions, initiated with either BPO or DMPA, was analyzed by GC-MS. The signal at 250.27 m/z corresponding to the monomer **2** was found in the mass spectra of both reactions. In addition, another signal at 246.26 m/z was also observed from both reactions, which corresponds to the mass of 1,2-dibenzyldisulfane (Calculated = 246.05 m/z).
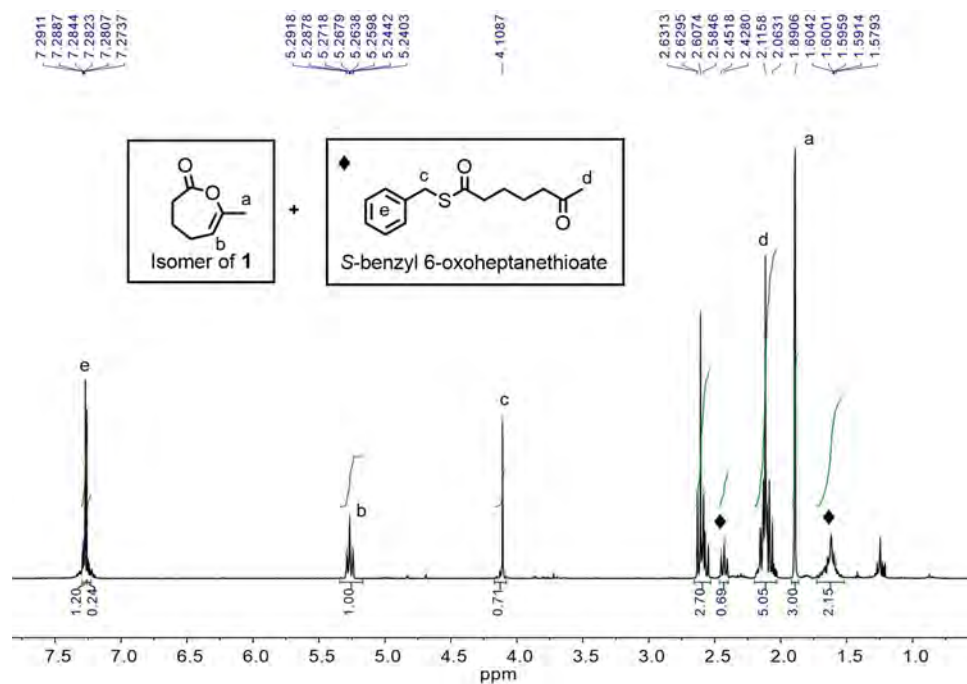
Figure 1.13 ^{1}H NMR spectrum (CDCl$_3$, 300 MHz) of the isomer of **1** and ring-open of **1** (♦), isolated from the crude by column chromatography.

After the analysis by ^{1}H NMR and MS of crude products from both reactions, the monomer **2** was detected in 40% conversion from BPO-initiated thiol-ene reaction and in 55% conversion from the reaction initiated by DMPA. In addition, the isomer of **1** and the ring-opening of **1** were also observed and characterized as side products (Figure 1.13). Finally, the crude product from both reactions were purified by column chromatography. The isomer and impurities were eluted first by 1:9 pentane and ethyl acetate mixture, and the pure form of monomer **2** was collected by 1:4 of pentane and ethyl acetate mixture. ε-S-Benzyl-ε-caprolactone (monomer **2**) was obtained as a yellow oil. The structure of monomer **2** was finally confirmed by 1D NMR (Figure 14) and 2D NMR. ^{1}H NMR spectrum of pure monomer **2** shows the characteristic signals of one proton (a) of –CHO at 4.08 – 3.98 ppm that were changed from α-olefinic functional group of **1**. The signals of diastereotopic protons (b) which are not chemically equivalent of –CH$_2$–S– were also observed at 2.74 and 2.54 ppm with the ABX system, due to being adjacent to a stereocenter (a). In addition, these signals can be used to prove the new C–S bond forming from β-olefinic functional group of **1** with benzyl thiol. The signals of two protons (c) of methylene functional group (-C*H*$_2$-CHO-), which is next to the chiral center (a) were also detected at 3.63–3.55 ppm and 2.42–2.32 ppm. The monomer **2** was also characterized by ^{13}C NMR, and the spectrum showed the characteristic signal of C=O (in ester) at 174 ppm without the observation of C=O in ketone in the chemical shift from 200 – 220 ppm. For 2D NMR, the analysis also showed more information about the correlation of proton and its neighbouring protons for their coupling to each other. The elemental analysis reported that the amount of C and H from measurement is equal to those calculations without any different in significant, thus confirming the high purity of new monomer.
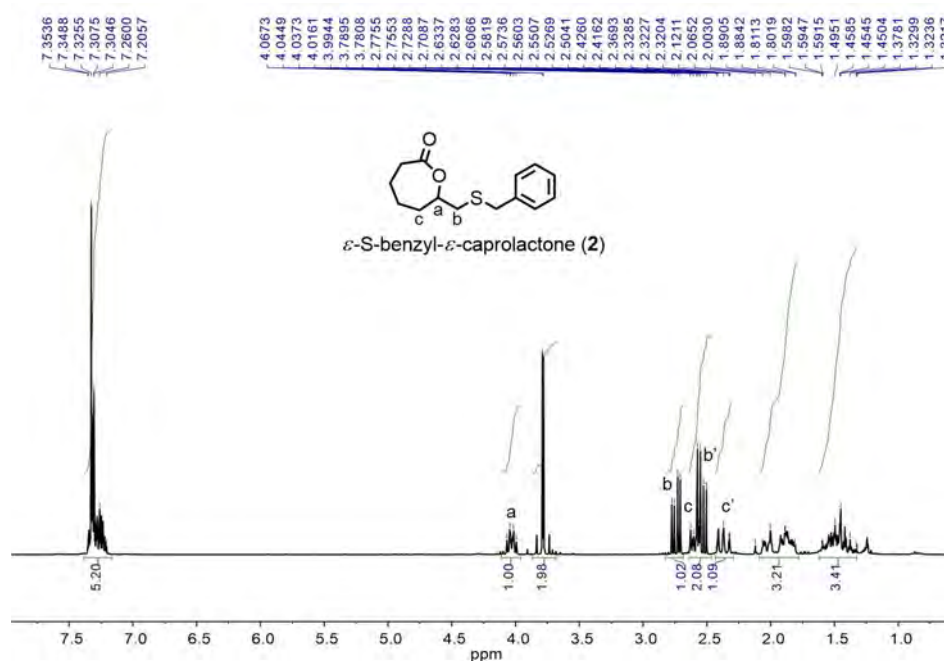
Figure 1.14 ^{1}H NMR spectrum (CDCl$_3$, 300 MHz) of ε-S-benzyl-ε-caprolactone (monomer **2**).

In summary, a new strategy for the preparation of ε-functionalized-ε-caprolactone was initially investigated. Thanks to the catalytic cycloisomerization of alkynoic acid developed in our group, that opened an opportunity to the synthesis of lactone precursor namely exo-methylene lactone (**1**). This lactone precursor was functionalized with benzyl thiol by thiol-ene reaction obtaining a new monomer **2**, ε-S-benzyl-ε-caprolactone. Based on the results of the promoter screening (Table 1.4), thiol-ene reaction initiated by DMPA showed the better results, when compared with I$_2$ and BPO.

Table 1.4 Thiol-ene reaction with different catalysts.

	I$_2$	BPO	DMPA
Reaction time	2 h	4 d	1 d
Thiol-ene coupling product (%)^a	✗	40	55
Thiol dimer	✗	√	√
Ring-open form of **1**	√	√	√
Isomer of **1**	✗	√	√

^{a}determined by ^{1}H NMR

However, the initial attempt with DMPA showed not only the formation of **2** but also the isomerization of **1** and other side reactions (e.g. the formation of thiol dimer and the ring-opening of **1**). The isomerization is obviously a main competitive reaction for this thiol-ene

reaction, due to 40% NMR yield of the isomer was detected against 55% yield of monomer **2**. To increase the thiol-ene coupling efficiency, the optimization of reaction conditions was then planned and pointed out to the general parameters that affect to the thiol-ene free radical addition: (i) light source, (ii) solvent (type/concentration), (iii) the amount of thiol compound, and (iv) the amount of initiator.

1.2.3 Optimization of reaction conditions with DMPA and examples

According to the first study of radical thiol-ene using DMPA as an initiator, several undesired products were observed, especially the isomer of **1**. The isomerization of **1** was detected during the reaction in high yields, so that the thiol-ene coupling efficiency was low. To optimize all parameters that need to be considered for thiol-ene reaction conditions and to avoid the generation of the isomer of **1**, it is, therefore, necessary to visualize thoroughly the free radical addition mechanism (Scheme 1.50).[64-66] Considering the alkene of compound **1** as an electron rich alkene, the benzyl thiyl should act as an electrophilic radical. Additionally, the fragmentation rate of DMPA to generate the primary carbon-centered radicals (I_1I_2*) may significantly impact on the ratio of the addition/transfer rate to the decomposition rate of initiator, thus turning the thiol-ene coupling efficiency.[64-66]
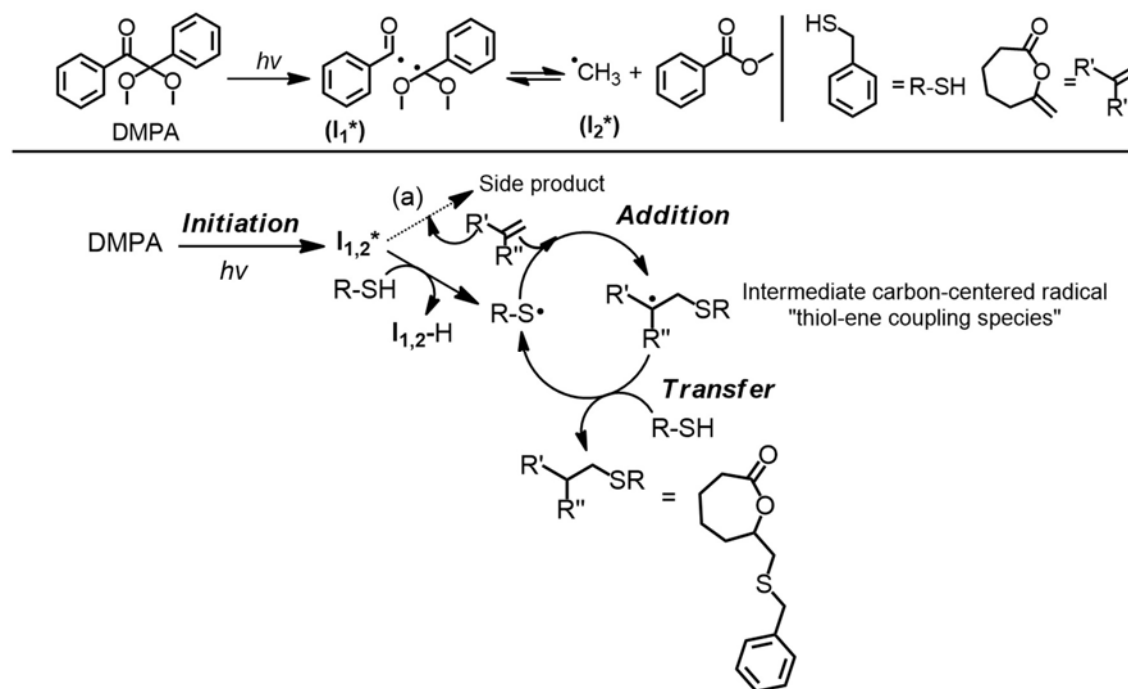
Scheme 1.50 Free radical addition mechanism using DMPA as a radical initiator. (a) Possible side reaction from the rearrangement of **1** (isomerization).[64-66]

In general, the UV-initiated thiol−ene process occurs *via* a chain process consisting of three main steps: initiation, addition, and chain-transfer.[65] Under irradiation, the initiation step occurs *via* the formation of carbon-centered radicals generated by the cleavage of DMPA (I_1I_2*). These carbon-centered radicals then abstract a hydrogen from the thiol (R–SH) yielding the thiyl radicals (RS•). After that, the thiyl radical further reacts directly by addition to the C=C bond of the alkene (CH$_2$=CR'R'') yielding an intermediate carbon-centered radical, thiol-ene coupling species, in the radical addition step. Then, the carbon-centered radical containing thiol-ene coupling species abstracts a hydrogen from another molecule of thiol in the chain transfer step. Finally, the thiol-ene coupling product is formed with anti-Markovnikov orientation, and a new thiyl radical will undergo further thiol-ene reaction, if the alkene compounds still remain. Additionally, termination reactions possibly happen involving the coupling of radical-radical species as side reactions[50], e.g., thiyl−thiyl radical coupling (thiol dimer), and the rearrangement of **1** to generate the more stable isomeric form (isomerization).

To have an idea about the isomerization of compound **1**, the photoreaction of compound **1** was carried out with similar conditions (0.5 M in CDCl$_3$) as the thiol-ene reaction in the absence of thiol and DMPA. After 12 hours of UV irradiation, no reaction was found, as no characteristic signals of isomer and other side products observed by ^{1}H NMR. However, 8% of the isomer of **1** was found after adding 2 wt% of DMPA in the reaction, and the mixture was stirred under UV irradiation for 12 hours longer. That means, the isomerization of **1** could be spotted in the thiol-ene reaction with the presence of DMPA in reaction media. The proposed mechanism for the formation of the isomer of **1** (**1'**) may involve the H• transfer and the H• abstraction (Scheme 1.51). First, the primary radical species ($I_{1,2}$*) from DMPA are generated under the UV irradiation. These radical species ($I_{1,2}$*) may abstract the active allylic H• from compound **1** leading to the formation of a conjugated carbon-centered radical (**1***↔ **1•**). Subsequently, the rearrangement of **1•** takes place following by the H• abstraction, possible from **1** or thiol, to yield the isomer (**1'**). After that, the regenerated **1*** may further react with the new compound **1**.
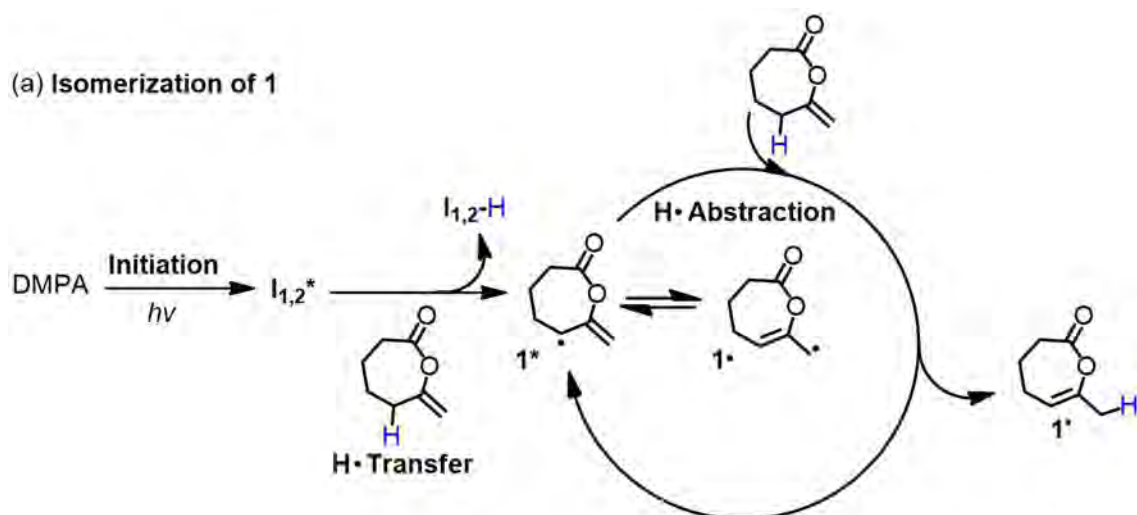
Scheme 1.51 Proposed radical processes for the isomerization of **1** with DMPA.

The principle free radical addition mechanism suggests that the different alkene-containing compounds exhibit different overall reaction orders.[69] In addition, the overall rates mainly depend on the ratio between the addition and the transfer rate coefficient.[69] It clearly showed that the coupling efficiency significantly depends on the chosen reaction conditions related to both characters of thiol and alkene. Consequently, we proposed the parameters for the optimization of reaction conditions as followed by (1) UV irradiation source, (2) the initial concentrations of **1**, (3) the polarity of solvent, (4) the amount of benzyl thiol, and (5) the radical initiator concentration (wt%).

1.2.3.1 UV irradiation source

The initial attempt of thiol-ene reaction initiated by DMPA was performed under a UV lamp with a low intensity of UV light generating a low quality of UV at 365 nm. As mentioned above, the radical initiator species are formed before the initiation step. Fast forming of the initial radical species from DMPA may favor the initiation process, thus increasing the kinetic of thiyl radical generation. So that, either the high intensity (UV laser) or high quality of UV light (UV strip) with specific wavelength at 365 nm may fit to this aspect.

(a) UV laser: The thiol-ene reaction of compound **1** and benzyl thiol was performed using UV laser as a UV light source with high intensity and a specific wavelength at 365 nm. The reaction conditions were similar to those using UV lamp. The thiol-ene reaction was observed approximately 58% of monomer **2** and 40 % of the isomer of **1** after 36 hours of UV laser irradiation, whereas 55% of monomer **2** was formed after 24 hours in case of using UV lamp. The reaction took longer time than that of UV lamp, and the isomer of **1** was still detected

in high yield. The results clearly showed that using UV laser with high intensity and specific wavelength does not improve significantly the thiol-ene coupling efficiency, compared with the initial study using UV lamp. This high intensity probably supports not only the fast-generation of the initial radical species but also favor the isomerization of **1**. With these results, using UV laser for this thiol-ene reaction clearly is less efficient than that of UV lamp.

(b) UV strip light: The UV strip light with 5 UV light (365 nm) dots was then applied on our thiol-ene reaction as another alternative UV light source. The strip light provides high quality of UV light with a specific wavelength at 365 nm. The strip of this UV light can be cut, so that it is flexible to use in any reaction scale (Figure 1.15). Additionally, the strip light can be set up easily with the borosilicate glass vessel, thus using quartz vessel is not necessary. The thiol-ene reaction using the strip of UV light (5 dots) was performed with similar reaction conditions to the UV lamp. Gratifyingly, neither the isomer nor other side products were found in the reaction after 36 hours of the UV light irradiation. However, the thiol-ene coupling product was reached only 39%, and no conversion of **1** was observed afterwards.

Figure 1.15 The set-up of thiol-ene reaction with the strip light, 5 UV light dots (365 nm).

According to the results obtained using different UV light sources (Table 1.5), the UV lamp was chosen for further optimization of thiol-ene reaction conditions as it showed less time-consuming than the others and higher thiol-ene coupling efficiency that that of strip light.

Table 1.5 Thiol-ene reaction with different UV light sources.

	UV laser	Strip light	UV lamp
Reaction time (h)	36	36	24
Thiol-ene coupling product (%)[a]	58	39	55
Isomer of **1** (%)[a]	40	×	40

[a]determined by ^{1}H NMR

1.2.3.2 Other parameters: solvent, initial concentration of 1, initial amount of DMPA, and initial amount of benzyl thiol

Other parameters that affect the coupling efficiency were next investigated (Table 1.6). Deuterated solvents (e.g., $CDCl_3$ and C_6D_6) were used, so that the reaction could be monitored directly by ^1H NMR. Looking at the entry 1 in Table 1.6 as the reference data, the thiol-ene reaction was performed with 0.5 M of **1** in $CDCl_3$ for 36 hours under UV irradiation, and the crude was observed about 58% of monomer **2** including 40% of the isomer of **1**. Changing the initial concentration of **1** from 0.5 M to 0.25 M in $CDCl_3$ (entry 2 in Table 1.6), the reaction was not completed after 36 hours and observed only 60% conversion of **1**. Nevertheless, the formation of monomer **2** reached approximately 50% while the isomerization was mostly suppressed. The isomer of **1** was seen only 3%, which is approximately 13 times lower than that of preparing with 0.5 M. That means, reducing the initial concentrations of **1** drastically affects the rate of the isomerization reaction, thus favoring the thiol-ene coupling reaction.

Table 1.6 Optimization of thiol-ene reaction conditions:

Entry	Solvent	[1]	BnSH (equiv.)	DMPA (wt%)	Reaction time (h)	Conv. of 1 (%)[a]	2 (%)[a]	Isomer (%)[a]
1	$CDCl_3$	0.5	1.2	2	36	>99	58	40
2	$CDCl_3$	0.25	1.2	2	36	60	47	3
3	C_6D_6	0.25	1.2	2	36	42	28	7
4	$CDCl_3$	0.25	1.2	6	36	48	26	22
5	$CDCl_3$	0.25	3	2	16	74	66	1
					36	85	68	5

[a]determined by ^1H NMR

Next, the thiol-ene reaction was optimized by changing the solvent from $CDCl_3$ to C_6D_6 (entry 3 in Table 1.6). The reaction was carried out directly in 0.25 M of **1** according to the result written above. After 36 hours of photoreaction, only 42% of **1** was consumed. The monomer **2** was detected in a low yield of 28%, which is 2 times lower than the case of using $CDCl_3$. Moreover, the isomer of **1** was turn up to 7% which is higher than the result of $CDCl_3$. Based on these results, the polarity of solvent seems to impact the thiol-ene coupling efficiency as the less polar solvent (C_6D_6) might not promote properly the free radical thiol-ene reaction of compound **1** and benzyl thiol. The effect of the solvent polarity on radical reaction rates is in accordance with the study of photo-induced thiol-ene reaction reported in the literature.[67, 68]

According to the results from entry 2 in Table 1.6, the thiol-ene reaction prepared by 0.25 M of **1** in CDCl$_3$ showed a good result providing a moderate yield of monomer **2** and a low yield of the isomer of **1**. Then, the initial concentration of DMPA was considered as the next parameter to optimize the reaction condition (entry 4 in Table 1.6). Instead of 2 wt% of DMPA, the initial DMPA concentration was increased to 6 wt%. The reaction was checked at 36 hours similar to those before, and the conversion of **1** was only 48%. Unfortunately, almost half of products were converted to the isomeric form as seen by 22% yield. Therefore, the low yield of monomer **2** was found only 26%. Based on the proposed mechanism of isomerization of **1** (Scheme 1.51), high initial concentration of DMPA will increase the fragmentation rate of radical initiator which also favoring the isomerization of **1**. Thus, the thiol-ene coupling efficiency will be decreased if high initial concentration of DMPA is presented at the beginning of the reaction.

The last parameter was considered the concentration of benzyl thiol. As mentioned before, the thiyl radical is a key intermediate in this thiol-ene reaction. Therefore, increasing the amount of benzyl thiol in the reaction should improve the thiol-ene coupling efficiency. The reaction was performed with 0.25 M of **1** in CDCl$_3$ with 2 wt% of DMPA and changing the amount of benzyl thiol from 1.2 equiv. to 3.0 equiv. (entry 5 in Table 1.6). Interestingly, three in fourth of **1** was consumed after only 16 hours of UV irradiation. The formation of monomer **2** reached at 66% while the isomer of **1** was observed only at 1% determined by ^{1}H NMR. The conversion of **1** was then turned up to 85% after 36 hours of UV irradiation, whereas the monomer **2** was detected only in 68%. Moreover, the amount of isomer of **1** was increased and found by 5% yield. According to these results, changing the thiol concentration up to 3.0 equiv. also improves the thiol-ene coupling efficiency, although the reaction does not proceed properly after 16 hours. In the presence of high thiol concentration, the ratio of the addition/transfer rate to the decomposition rate of initiator will be increased, thus favoring the thiol-ene coupling rather than the formation of side products, i.e., the isomer of **1**.

According to the results above, the thiol-ene coupling efficiency will be increased if the reaction is considered by (1) lower the initial concentration of **1** to 0.25 M, (2) better to use the high polar solvent (CDCl$_3$) rather than the low one (C$_6$D$_6$), (3) better to use 2 wt% of DMPA as a low initial concentration than the other (6 wt% of DMPA), and (4) higher the initial benzyl thiol concentration to 3.0 equiv. *So, can we improve the coupling efficiency to reach more than 90 % of monomer **2** and less than 10 % of the side products?*

Back to the initiation step, the fragmentation of DMPA is occurred to generate the primary intermediate radicals ($I_{1,2}*$) during the initial period of UV irradiation. Subsequently, these primary radicals are consumed by further radical reactions. Therefore, the initial concentration of DMPA will not only optimize the ratio of thiol-ene coupling rate (addition/tranfer) to the DMPA decomposition rate, but also increase the rate of isomerization (Scheme 1.50 and 1.51). Based on the results described above, the thiol-ene reaction did not proceed properly after 16 hours leading to the low efficiency of thiol-ene coupling, meanwhile, the side reactions could be performed. In addition, high concentration of DMPA at the beginning of UV irradiation increased the formation of isomer of **1**. Therefore, the next attempt for the optimization was planned to do the second addition of DMPA after 16 hours of thiol-ene coupling process (Table 1.7). The second amount of DMPA (2 wt%) was added into the reaction at 16 hours of photoreaction and stirred under UV irradiation for 4 hours longer. The results showed that only 8% of the isomer of **1** was detected, and the thiol-ene coupling product was reached to 85% determined by ^{1}H NMR. By the end, the starting material (**1**) was completely consumed after 24 hours of the photoreaction yielding 91 % of monomer **2** and only 7% of the isomer of **1**, noted that total [DMPA] = 4 wt%.

Table 1.7 Optimization of thiol-ene reaction by the second addition of DMPA after 16 hours

	Total DMPA (wt%)	Reaction time (h)	Conv. of 1 (%)[a]	2 (%)[a]	Isomer (%)[a]
	2	16	84	77	6
Adding 2 wt% of DMPA ➡	4	20	94	85	8
	4	24	>99	91	7

As observed by the approximate rate of the isomerization (8% in 12 h with the presence of DMPA under UV irradiation) and the effect of second addition of DMPA after 16 hours: therefore, the optimization was further adapted by a sequential addition of DMPA (Scheme 52). According to the sequential addition of DMPA, the first addition was done after 8 hours and then the second addition at 16 hours was followed, (final [DMPA] = 6 wt%). The obtained results after 20 hours of UV irradiation reached up to 96% of monomer **2**, and only 3% of the isomer of **1** was found.
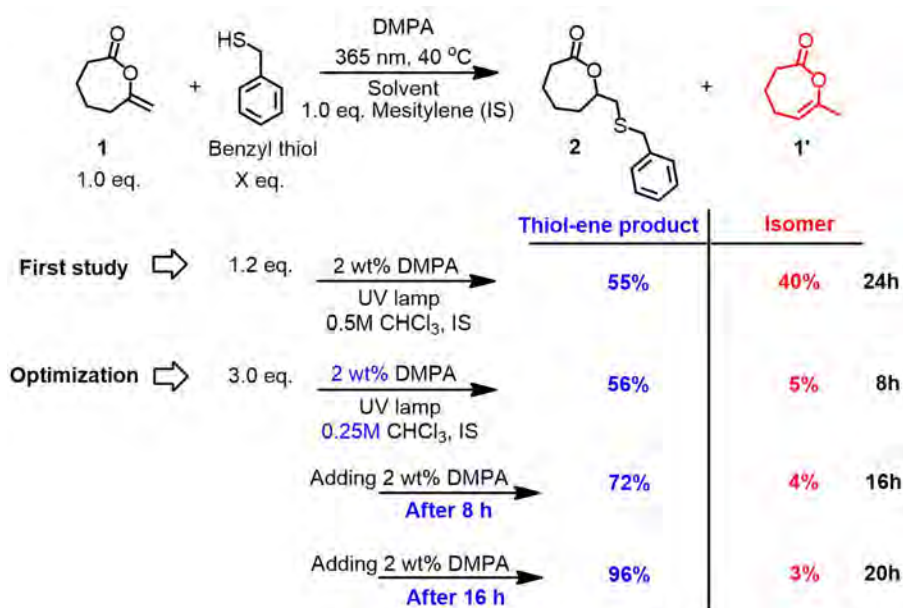
Scheme 1.52 Optimized thiol-ene reaction versus the initial study.

The optimization of thiol-ene reaction conditions was achieved by using the mixture of 0.25 M of **1** in CHCl$_3$, 3 equiv. of benzyl thiol, and 2 wt% of DMPA and under UV irradiation generated by UV lamp with a sequential addition of DMPA, at 8 hours and 16 hours after setting photoreaction. In addition, this protocol could be applied up to 1 gram scale displaying a similar result with an excellent yield (80%).

As proposed before, the functionalization of compound **1** by benzyl thiol *via* thiol-ene reaction will be used as a model study. The optimized thiol-ene reaction conditions for the synthesis of monomer **2** will lead to a new protocol for the preparation of new functionalized lactone at ε-position. Besides the conditions for the synthesis of monomer **2**, the second ε-functionalized ε-lactone monomer (**3**), which is the targeted monomer in protected form, was prepared by the coupling of compound **1** with benzyl 2-mercaptoacetate (Benzyl ester thiol). This benzyl ester thiol was prepared easily by the esterification of mercaptoacetic acid with benzyl alcohol following the reported procedure in literature (Scheme 1.53).[69]
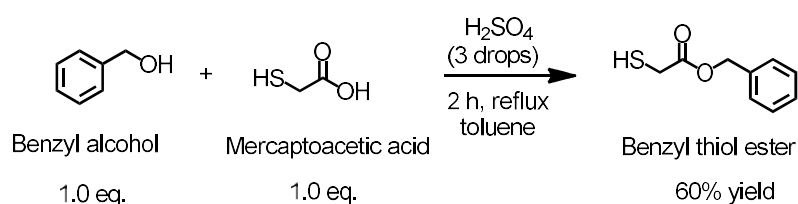
Scheme 1.53 The synthesis of benzyl ester thiol by the esterification of mercaptoacetic acid with benzyl alcohol.[69]

The thiol-ene reaction of compound **1** (0.25 M in CHCl₃) with benzyl ester thiol (3 equiv.) was initially performed similarly to the optimized reaction conditions under UV irradiation from UV lamp (Scheme 54). Surprisingly, this thiol-ene reaction was completely achieved after only 4 hours without a sequential addition of DMPA. In addition, none of the side products was observed (e.g., the isomer of **1**, thiol dimer, and ring-opened form of **1**). With its high thiol-ene coupling efficiency, the synthesis of the targeted monomer was then planned with a lower amount of benzyl ester thiol. As mentioned before, lower the amount of thiol may affect to the thiol-ene coupling rate as well as the coupling efficiency. Thereafter, several experiments were studied by decreasing the amount of benzyl ester thiol from 3.0 equiv. to 2.5, 2, 1.5, and 1 equiv. (see Scheme 1.54). Interestingly, all studies showed a relevant result to the one using 3 equiv. of benzyl ester thiol. None of the side products were observed, and the reactions were achieved within the operated time (4 hours). Moreover, this thiol-ene reaction can be scaled up to 3 grams in an excellent yield (83%).

	Thiol X eq.	Thiol-ene product	Isomer	
First study	3.0 eq.	97% (58%)	N.D.	4h
Optimization	2.0 eq.	95% (70%)	N.D.	2h
Reducing the amount of thiol	1.5 eq.	98% (83%)	N.D.	4h
	1.0 eq.	94% (55%)	N.D.	4h
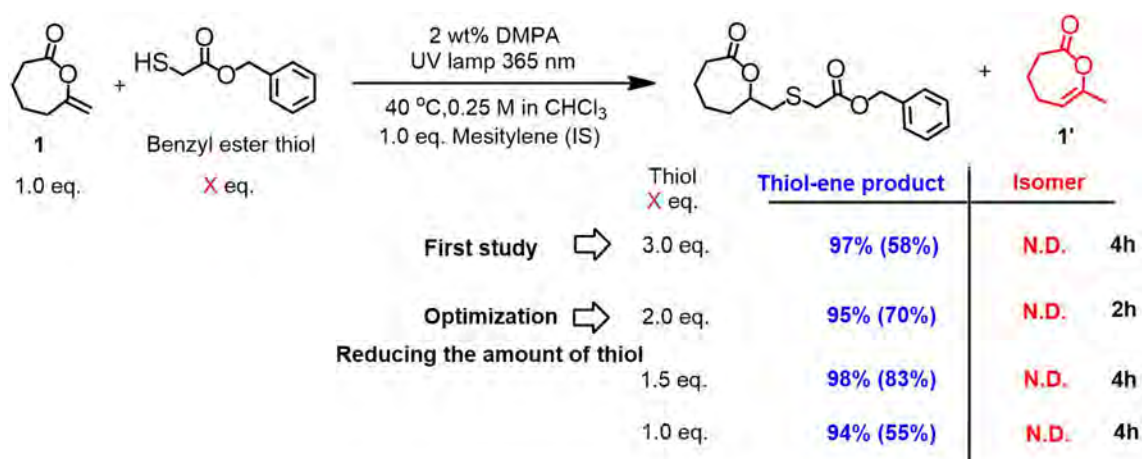
Scheme 1.54 The synthesis of monomer **3** by the thiol-ene reaction of **1** with benzyl ester thiol and also the optimization of reaction conditions by reducing the amount of benzyl ester thiol.

*Why this thiol-ene coupling reaction of compound **1** and benzyl ester thiol worked so efficiently?* Following the radical addition mechanism as mentioned before, the key intermediate of this thiol-ene reaction is the thiyl radical (RS•) behaving as an electrophilic radical. The ester functional group in this thiol compound may promote the weak inductive effect on this thiyl radical. Increasing the electrophilic character of thiyl radical, the thiyl is then very likely to react with an electron rich alkene of compound **1**. The thiol-ene radical addition is therefore faster than the proton abstraction of the active allylic from compound **1**, thus reducing the formation of the isomer **1'**.

The crude product containing the targeted monomer was then purified by column chromatography using 1:2 pentane: ethyl acetate mixture to obtain the pure form of benzyl 2-{[(7-oxooxepan-2-yl)methyl]thio} acetate or ε-benzyl ester thiol-ε-caprolactone (**3**) as a yellow oil. The structure of monomer **3** was confirmed by 1D NMR (Figure 1.16) and 2D NMR (COSY), which also showed more information about the correlation of proton and its neighbouring protons for their coupling to each other.

^{1}H NMR spectrum of pure monomer **3** represents the characteristic signals of one proton (a) of –CHO at 4.42–4.35 ppm that are changed from α-olefinic functional group of **1**. The signals of two diastereotopic protons of –CH$_2$–S– (b) which are not chemically equivalent are also observed at 2.95 and 2.74 ppm with the ABX system, due to being adjacent to a stereocenter (a). The signals of two protons (c) of methylene functional group (-CH_2-CHO-), which is next to the stereocenter (a) are also detected at 2.69–2.61 ppm and 2.56–2.46 ppm. The monomer **3** was also characterized by ^{13}C NMR, and the spectrum showed the characteristic signal of C=O (in ester from lactone) at 174.70 ppm and C=O (in ester from benzyl ester) at 170.24 ppm without the observation of any signals of C=O in ketone. The elemental analysis also reported that the amount of C and H from measurement is close to those calculations without any different in significant, thus confirming a high purity of the monomer **3**.

Figure 1.16 ^{1}H NMR spectrum (CDCl$_3$, 300 MHz) of **3** represents the coupling of characteristic proton signals.

1.3 Conclusions

In conclusion, a new strategy for the preparation of ε-functionalized-ε-caprolactone has been described. A sequential transition metal catalyzed cycloisomerization and then free radical thiol-ene coupling process figured out the regioselectivity problem, compared with Baeyer-Villiger oxidation of functionalized ketones. The pre-functionalized lactone (**1**) can be easily prepared in large scale (5 grams) by Pt pincer complexes catalyzed cycloisomerization of heptynoic acid in a good yield (72%). Then, the functionalization of compound **1** with benzyl thiol was carried out as a model study for the optimization of reaction conditions. Based on the results, lower initial concentration of **1** and higher amount of thiol increase the coupling efficiency. The sequential addition of DMPA was also applied to tune the ratio of the addition/transfer rate to the initiator decomposition rate. Finally, the coupling efficiency reached more than 95% of monomer **2**, and less than 5 % of the side products was observed. Thanks to the efficiency of these conditions, the synthesis of monomer **3** was achieved. Interestingly, the formation of monomer **3** was achieved only after 4 hours of UV irradiation, so that the sequential addition of DMPA was not applied to the reaction. As a result of the inductive effect from ester increases an electrophilic character of thiyl radicals, thus favoring the thiol-ene coupling efficiency and inhibiting the side reactions. In addition, both new functionalized monomers, **2** and **3**, can be synthesized in large scale with excellent yields (Scheme 1.55).

Scheme 1.55 The summary protocol for the synthesis of new functional monomers *via* thiol-ene functionalization

The targeted monomer, **3**, will be used as a comonomer for copolymerization with ε-DL leading an opportunity to modulate the PDL properties. But before doing that, the ring-opening polymerization (ROP) of ε-DL still has plenty issues to fulfil, due to the only few examples that have been reported in the literature. For example, it needs to be improved by

finding a good catalyst that works under mild condition and enables living and controlled polymerization. This work will be discussed in next chapter.

1.4 Experimental Part

7-Methylene-oxepan-2-one (1) synthesis: This pre-functional monomer was prepared according to the procedure described by our group.[47] In a Schlenk flask under stirring, the dried 6-heptynoic acid (2.5 g, 20 mmol) and dimeric complex {Pt[(iPr₂P=S)₂(C₉H₄)]}₂ (1 mol%) were dissolved in CHCl₃ (40 mL, 0.5 M) and heated at 90 °C for 21 hours under argon atmosphere. The reaction mixture was transferred to another round bottom Schlenk tube, and the solvent was evaporated. To the flask was adapted a cold finger and the residue was sublimated under vacuum at room temperature. The pure form of **1** then slowly volatizes and condenses on the cold finger containing liquid nitrogen inside. Once the cold finger is saturated, it was rinsed by DCM to obtain the pure **1**. This purification was repeated several times, and 2 grams of **1** (79%) were recovered.

1
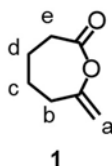
¹H NMR (300 MHz, CDCl₃) δ (ppm) = 4.80 – 4.78 (m, 1H, H$_a$), 4.67 – 4.65 (m, 1H, H$_a$'), 2.62 – 2.54 (m, 2H, H$_e$), 2.38 – 2.28 (m, 2H, H$_b$), 1.81 – 1.72 (m, 4H, H$_c$ and H$_d$).

7-[(benzylthio)methyl]oxepan-2-one (2) synthesis: To a solution of **1** (1 equiv., 1 g, 7.93 mmol) and benzyl thiol (3 equiv., 2.95 g, 23.79 mmol) in chloroform (32 mL, 0.25M) was added a solution of 2,2-dimethoxy-2-phenylacetophenone (DMPA, 20 mg, 2.0 wt%) in chloroform (1 mL) and stirred for 1 h to form a homogeneous solution in a quartz vessel. The quartz vessel containing the mixture was degassed three consecutive times by Freeze-pump-thaw process. Then, the reaction was initiated by UV lamp (365 nm). The reaction was stirred for 20 hours under UV irradiation, and a sequential addition of 2.0 wt% of DMPA was introduced to the mixture, first addition after 8 hours and the second addition at 16 hours (Total [DMPA] = 6 wt%). The crude product was purified by column chromatography. The isomer and undesired products were eluted first by 1:9 of pentane and ethyl acetate mixture, and the pure thiol-ene product was collected by 1:4 of pentane and ethyl acetate mixture. After solvent evaporation, the monomer **2** was dried under vacuum, and 1.6 grams (80%) of **2** were obtained as yellow oil.
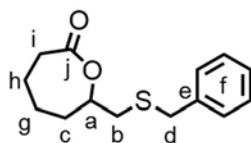
Monomer **2**

¹H NMR (300 MHz, CDCl₃) δ (ppm) = 7.35 – 7.20 (m, 5H, H_f), 4.08 – 3.98 (m, 1H, H_a), 3.79 (d, J = 2.6 Hz, 2H, H_d, AB system), 2.74 (dd, J = 14.0, 6.1 Hz, 1H, H_b, ABX system), 2.63 – 2.55 (m, 1H, H_b', ABX system), 2.54 (dd, J = 14.0, 6.9 Hz, 1H, H_c, ABX system), 2.42 – 2.32 (m, 1H, H_c', ABX system), 2.12 – 1.80 (m, 3H, -CH_2-, H_{i+h+g}), and 1.60 – 1.32 (m, 3H, -CH_2-, H_{i+h+g}). **¹³C NMR (300 MHz, CDCl₃)** δ (ppm) = 174.77 (C_j), 138.38 (C_e), 128.92, 128.48, and 127.07 (C_f), 80.07 (C_a), 37.27 (C_d), 36.76 (C_b), 34.60 (C_c), 33.28 (C_i), 27.98 (C_h), and 22.73 (C_g). **Elemental analysis calculated for C₁₄H₁₈O₂S;** C = 67.16% and H = 7.25%, Found C = 66.93% and H = 7.25%.

Benzyl 2-mercaptoacetate (benzyl ester thiol) preparation

2-Mercaptoacetate was synthesized following the reported procedure in the literature:[69] mercaptoacetic acid (8 mL, 65.6 mmol), benzyl alcohol (6.8 mL, 65.8 mmol), and concentrated sulfuric acid (3 drops) in toluene (200 mL) was added to a flask fitted with a Dean-Stark apparatus. The mixture was stirred and refluxed for 2 hours. The toluene was evaporated, and the crude was purified by distillation under vacuum at 130 °C to obtain the pure product as a colorless oil, 7.2 g (60%). The structure of benzyl ester thiol was confirmed by ¹H NMR corresponding to the reported reference.
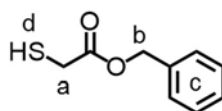
Benzyl thiol ester

¹H NMR (300 MHz, CDCl₃) δ (ppm) = 7.42 – 7.34 (m, 5H, H_c), 5.18 (s, 2H, H_b), 3.30 (d, J = 8.3 Hz, 2H, H_a), and 2.03 (t, J = 8.3 Hz, 1H, H_d).

Benzyl 2-{[(7-oxooxepan-2-yl)methyl]thio} acetate synthesis (3): To a solution of **1** (1 equiv., 1 g, 7.93 mmol) and benzyl ester thiol (1.5 equiv., 2.16 g, 11.9 mmol) in chloroform (32 mL, 0.25M) was added a solution of DMPA (20 mg, 2.0 wt%) in chloroform (1 mL) and stirred for 1 h to form a homogeneous solution in a quartz vessel. The quartz vessel containing the mixture was degassed three consecutive times by Freeze-pump-thaw process and the reaction was then initiated by UV lamp (365 nm). The reaction was stirred for 4 hours under UV irradiation. The crude product was purified by column chromatography using 1:2 pentane

and ethyl acetate mixture to obtain the pure form of monomer **3**. The solvent was evaporated, and the pure form of **3** was dried under vacuum yielding 2 grams (85%) as yellow oil.

Monomer **3**
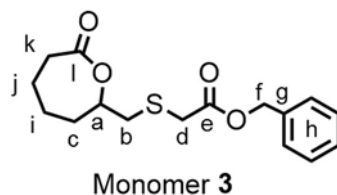
^{1}H NMR (300 MHz, CDCl$_3$) δ (ppm) = 7.38 – 7.31 (m, 5H, H$_h$), 5.16 (s, 2H, H$_f$), 4.42 – 4.35 (m, 1H, H$_a$), 3.37 (d, J = 8.2 Hz, 2H, H$_d$, AB system), 2.95 (dd, J = 14.1, 6.8 Hz, 1H, H$_b$, ABX system), 2.74 (dd, J = 14.1, 5.8 Hz, 1H, H$_b$', ABX system), 2.69 – 2.61 (m, 1H, H$_c$, ABX system), 2.56 – 2.46 (m, 1H, H$_c$', ABX system), 2.06 – 1.86 (m, 3H, -CH$_2$-, H$_{i+j+k}$), and 1.67 – 1.45 (m, 3H, -CH$_2$-, H$_{i+j+k}$).**^{13}C NMR (300 MHz, CDCl$_3$)** δ (ppm) = 174.70 (C$_l$), 170.24 (C$_e$), 135.45 (C$_g$), 128.57, 128.39, and 128.30 (C$_h$), 80.01 (C$_a$), 67.14 (C$_f$), 38.11 (C$_b$), 34.70 (C$_c$), 34.54 (C$_d$), 33.60 (C$_k$), 27.95 (C$_j$), and 22.77 (Ci). **Elemental analysis calculated for C$_{16}$H$_{20}$O$_4$S;** C = 62.31% and H = 6.54%, Found C = 62.33% and H = 6.53%.

1.5 Bibliography

1. Middleton, J. C.; Tipton, A. J. *Biomaterials*, **2000**, *21*, 2335.

2. Sudesh, K.; Abe, H.; Doi, Y. *Prog. Polym. Sci.* **2000**, *25*, 1503.

3. Zhu, Y.; Romain, C.; Williams, C. K. *Nature*, **2016**, *540*, 354.

4. Auras, R.; Harte, B.; Selke, S. *Macromol. Biosci.* **2004**, *4*, 835.

5. Woodruff, M. A.; Hutmacher, D. W. *Prog. Polym. Sci.* **2010**, *35* (10), 1217.

6. Ikada, Y.; Tsuji, H. *Macromol. Rapid Commun.* **2000**, *21* (3), 117.

7. Nair, L. S.; Laurencin, C. T. *Prog. Polym. Sci.* **2007**, *32* (8–9), 762.

8. Langer, R. *Acc. Chem. Res.* **2000**, *33* (2), 94.

9. Odian, G. *Ring-Opening Polymerization. Principles of Polymerization*; John Wiley & Sons, Inc.: Hoboken, NJ, **2004**, 544.

10. Williams, C. K. *Chem. Soc. Rev.* **2007**, *36*, 1573.

11. Duda, A.; Kowalski, A.; Libiszowski, J.; Penczek, S. *Macromol. Symp.* **2005**, *224* (1), 71.

12. (a) Duda, A.; Kowalski, A. Thermodynamics and Kinetics of Ring Opening Polymerisation. In *Handbook of Ring Opening Polymerization*; Dubois, P., Coulembier, O., Raquez, J-M. John Wiley & Sons: Weinheim, Germany, **2009**, pp. 1–51. (b) Olsén, P.; Odelius, K.; Albertsson, A. C. *Biomacromolecules*, **2016**, *17* (3), 699. (c) Schneiderman, D. K.; Hillmyer, M. A. *Macromolecules*, **2016**, *49* (7), 2419. (d) Delcroix, D.; Couffin, A.; Susperregui, N.; Navarro, C.; Maron, L.; Martin-Vaca, B.; Bourissou, D. *Polym. Chem.* **2011**, *2*, 2249. (e) Dove, A. P. *ACS Macro Lett.* **2012**, *1*, 1409. (f) Küllmer, K.; Kikuchi, H.; Uyama, H.; Kobayashi, S. *Macromol. Rapid Commun.* **1998**, *19*, 127. (g) Kikuchi, H.; Uyama, H.; Kobayashi, S. *Polym. J.* **2002**, *34*, 835.

13. Tong, R. *Ind. Eng. Chem. Res.* **2017**, *56* (15), 4207.

14. Jérôme, C.; Lecomte, P. *Adv. Drug Deliv. Rev.* **2008**, *60*, 1056.

15. Lou, X.; Detrembleur, C.; Jérôme R. *Macromol. Rapid Commun.* **2003**, *24* (2), 161.

16. Ponsart, S.; Coudane, J.; Vert, M. *Biomacromolecules*, **2002**, *1*, 275.

17. (a) Riva, R.; Schmeits, S.; Stoffelbach, F.; Jérôme, C.; Jérôme R.; Lecomte, P. *Chem. Commun.* **2005**, 5334. (b) Parrish, B.; Breitenhkamp R. B.; Emrick, T. *J. Am. Chem. Soc.* **2005**, *127*, 7404.

18. Gimenez, S.; Ponsart, S.; Coudane, J.; *M. J. Bioact. Compat. Polym.* **2001**, *16*, 32.

19. Ponsart, S.; Coudane, J.; McGrath, J. *M. J. Bioact. Compat. Polym.* **2002**, *17*, 417.

20. Riva, R.; Schmeits, S.; Jérôme, C.; Jérôme R.; Lecomte, P. *Macromolecules*, **2007**, *40*, 796.

21. (a) Al-Azemi T. F.; Mohamod, A. A. *Polymer*, **2011**, *52*, 5431. (b) Xu, N.; Wang, R.; Du, F. -S.; Li, Z. -C. *J. Polym. Sci. Part A: Polym. Chem*. **2009**, *47*, 3583.

22. (a) Lenoir, S.; Riva, R.; Lou, X.; Detrembleur, C.; Jérôme R.; Lecomte, P. *Macromolecules*, **2004**, *37*, 4055. (b) Massoumi, B. *Polym. Sci., Series B*. **2015**, *57*, 85.

23. (a) Jazkewitsch O.; Ritter, H. *Macromolecules*, **2011**, *44*, 375. (b) Jazkewitsch, O.; Mondrzyk, A.; Staffel R.; Ritter, H. *Macromolecules*, **2011**, *44*, 1365.

24. (a) Parrish, B.; Quansah J. K.; Emrick, T. *J. Polym. Sci., Part A: Polym. Chem*. **2002**, *40*, 1983. (b) Darcos, V.; Antoniacomi, S.; Paniagua C.; Coudane, J. *Polym. Chem*. **2012**, *3*, 362.

25. Garg, S. M.; Xiong, X. -B.; Lu, C.; Lavasanifar, A. *Macromolecules*, **2011**, *44*, 2058.

26. (a) Christoffers, J.; Oertling, H.; Fischer, P.; Frey, W. *Tetrahedron*. **2003**, *59*, p. 3769. (b) Li, H. Jéröme R.; Lecomte, P. *Polymer*, **2006**, *47*, 8406.

27. (a) Lowe, J. R.; Martello, M. T.; Tolman W. B.; Hillmyer, M. A. *Polym. Chem*. **2011**, *2*, 702. (b) Lowe, J. R.; Tolman W. B.; Hillmyer, M. A. *Biomacromolecules*, **2009**, *10*, 2003.

28. (a) Winkler, M.; Raupp,Y. S.; Köhl, L. A. M.; Wagner, H. E.; Meier, M. A. R. *Macromolecules*, **2014**, *47* (9), 2842. (b) Zhang, D.; Hillmyer, M. A.; Tolman, W. B. *Biomacromolecules*, **2005**, *6* (4) 2091. (c) Wang, Y.; Hillmyer, M. A. *Macromolecules* **2000**, *33* (20) 7395. (d) Baran, J.; Duda, A.; Kowalski, A.; Szymanski, R.; Penczek, S. *Macromol. Rapid Commun*. **1997**, *18* (4), 325.

29. (a) Gao, Y.; Mori, T.; Manning, S.; Zhao, Y.; Nielsen, A. D.; Neshat, A.; Sharma, A.; Mahnen, C. J.; Everson, H. R.; Crotty, S.; Clements, R. J.; Malcuit C.; Hegmann, E. *ACS Macro Lett*. **2016**, *5*, 4.

30. Detrembleur, C.; Mazza, M.; Halleux, O.; Lecomte, P.; Mecerreyes, D.; Hedrick J. L.; Jérôme, R. *Macromolecules*, **2000**, *33*, 14.

31. Riva, R.; Lazzari, W.; Billiet, L.; Du Prez, F.; Jérôme C.; Lecomte, P. *J. Polym. Sci., Part A: Polym. Chem.* **2011**, *49*, 1552.

32. (a) Tian, D.; Dubois, Ph.; Grandfils, Ch.; Jérôme, R. *Macromolecules*, **1997**, *30*, 406. (b) Latere, J.-P. ; Lecomte, P.; Dubois, P.; Jérôme, R. *Macromolecules*, **2002**, *35*, 7857.

33. Prime, E. L.; Hamid, Z. A. A.; Cooper-White, J. J.; Qiao, G. G. *Biomacromolecules*, **2007**, *8*, 2416.

34. Dai, W.; Zhu, J.; Shangguan, A.; Lang, M. *Eur. Polym. J*. **2009**, *45*, 1659.

35. Mecerreyes, D.; Humes, J.; Miller, R. D.; Hedrick, J. L.; Detrembleur, C.; Lecomte, P.; Jérôme, R.; Roman, J. S. *Macromol. Rapid Commun.* **2000**, *21*, 779.

36. Vaida, C.; Mela, P.; Keul, H.; Möller, M. *J. Polym. Sci.*, *Part A*: *Polym. Chem.* **2008**, *46*, 6789.

37. Lou, X.; Jérôme, C.; Detrembleur, C.; Jérôme, R. *Langmuir.* **2002**, *18*, 2785.

38. Rieger, J.; Butsele, K. V.; Lecomte, P.; Detrembleur, C.; Jérôme, R.; Jérôme, C. *Chem. Commun.* **2005**, 274.

39. Vaida, C.; Mela, P.; Kunna, K.; Sternberg, K.; Keul, H.; Möller, M. *Macromol. Biosci.* **2010**, *10*, 925.

40. Mecerreyes, D.; Atthoff, B.; Boduch, K. A.; Trollsås, M.; Hedrick, J. L. *Macromolecules*, **1999**, *32*, 5175.

41. Garle, A.; Kong, S.; Ojha, U.; Budhlall, B. M. *ACS Appl. Mater. Interfaces.* **2012**, *4*, 645.

42. Itoh, Y.; Yamanaka, M.; Mikami, K. *J. Org. Chem.* **2013**, *78*, 146.

43. (a) Mecerreyes, D.; Miller , R. D.; Hedrick, J. L.; Detrembleur, C.; Jerome, R. *J. Polym. Sci., Part A: Polym. Chem.* **2000**, *38*, 870. (b) *Polym. Chem.* **2016**, *7*, 4630. (c) Zhang, Y.; Li, J. H.; Du Z. Z.; Lang, M. D. *J. Polym. Sci., Part A*: *Polym. Chem.* **2014**, *52*, 188. (d) Dong, J.; Fernández-Fueyo, E.; Hollmann, F.; Paul, C. E.; Pesic, M.; Schmidt, S.; Wang, Y.; Younes, S.; Zhang, W. *Angew. Chem. Int. Ed.* **2018**, *57*, 9238. (e) Hollmann, F.; Kara, S.; Opperman, D. J.; Wang, Y. *Chem. Asian J.* **2018**, *13*, 3601. (f) Messiha, H. L.; Ahmed, S. T.; Karuppiah, V.; Suardiaz, R.; Avalos, G. A. A.; Fey, N.; Yeates, S.; Toogood, H. S.; Mulholland, A. J.; Scrutton, N. S. *Biochemistry*, **2018**, *57* (13), 1997.

44. Oulié, P.; Nebra, N.; Saffon, N.; Maron, L.; Martin-Vaca, B.; Bourissou, D. *J. Am. Chem. Soc.* **2009**, *131*, 3493.

45. Oulié, P.; Nebra, N.; Ladeira, S.; Martin-Vaca, B.; Bourissou, D. *Organometallics*, **2011**, *30*, 6416.

46. (a) Nebra, N.; Monot, J.; Shaw, R.; Martin-Vaca, B.; Bourissou, D. *ACS Catal.* **2013**, *3*, 2930. (b) Espinosa-Jalapa, N. Á.; Ke, D.; Nebra, N.; Le Goanvic, L.; Mallet-Ladeira, S.; Monot, J.; Martin-Vaca, B.; Bourissou, D. *ACS Catal.* **2014**, *4*, 3605. (c) Monot, J.; Brunel, P.; Kefalidis, C. E.; Espinosa-Jalapa, N. Á; Maron, L.; Martin-Vaca, B.; Bourissou, D. *Chem. Sci.* **2016**, *7*, 2179.

47. Ke, D.; Espinosa-Jalapa, N. Á; Mallet-Ladeira, S.; Monot, J.; Martin-Vaca, B.; Bourissou, D. *Adv. Synth. Catal.* **2016**, *358*, 2324.

48. Long, T. R.; Wongrakpanich, A.; Do, A.-V.; Salem, A. K.; Bowden, N. B. *Polym*. *Chem*. **2015**, *6*, 7188.

49. Thillaye du Boullay, O.; Saffon, N.; Diehl, J.-P.; Martín-Vaca, B.; Bourissou, D. *Biomacromolecules*, **2010**, *11*, 1921.

50. Lowe, A. B. *Polym*. *Chem*. **2010**, *1*, 17.

51. Hoyle, C. E.; Bowman, C. N. *Angew*. *Chem*. *Int*. *Ed*. **2010**, *49*, 1540.

52. Nair, D. P.; Podgorski, M.; Chatani, S.; Gong, T.; Xi, W.; Fenoli, C. R.; Bowman, C. N. *Chem*. *Mater*. **2014**, *26*, 724.

53. Liu, Meina; Tan, Beng Hoon; Burford, Robert P.; Lowe, Andrew B. *Polym*. *Chem*. **2013**, *4* (11), 3300.

54. Chan, Justin W.; Yu, Bing; Hoyle, Charles E.; Lowe, Andrew B. *Polymer*, **2009**, *50* (14), 3158.

55. (a) Klemarczyk, P. *Polymer*, **2001**, *42*, 2837. (b) Heilmann, S. M.; Rasmussen J. K.; Krepski, L. R. *J*. *Polym*. *Sci*., *Part A*: *Polym*. *Chem*. **2001**, *39*, 3655.

56. Nilsson, C.; Simpson, N.; Malkoch, M.; Johansson, M.; Malmström, E. *J*. *Polym*. *Sci*. *A Polym*. *Chem*. **2008**, *46*, 1339.

57. Fuoco,   T.;   Finne-Wistrand,   A   *Polymer   reviews*, https://doi.org/10.1080/15583724.2019.1625059

58. Nottelet, B.; Tambutet, G.; Bakkour, Y.; Coudane, J. *Polym*. *Chem*. **2012**, *3*, 2956.

59. Babinot, J.; Renard, E.; Le Droumaguet, B.; Guigner, J.-M.; Mura, S.; Nicolas, J.; Couvreur, P.; Langlois, V. *Macromol*. *Rapid Commun*. **2013**, *34*, 362.

60. Kalelkar, P. P.; Alas, G. R.; Collard, D. *M*. *Macromolecules*, **2016**, *49*, 2609.

61. Ates, Z.; Thornton, P. D.; Heise, A. *Polym*. *Chem*. **2011**, *2*, 309.

62. Kim, H.; Olsson, J. V.; Hedrick, J. L.; Waymouth, R. M. *ACS Macro Lett*. **2012**, *1*, 845.

63. Fuoco, T.; Finne-Wistrand, A.; Pappalardo, D. *Biomacromolecules*, **2016**, *17*, 1383.

64. Sandner, M. R.; Osborn, C. L. *Tetrahedron Letters*. **1974**, *15* (5), 415.

65. (a) Uygun, M.; Tasdelen, M. A.; Yagci, Y. *Macromol*. *Chem*. *Phys*. **2010**, *211*, 103. (b) Derboven, P.; D'hooge, D. R.; Stamenovic, M. M.; Espeel, P.; Marin, G. B.; Du Prez, F. E.; Reyniers, M.-F. *Macromolecules*, **2013**, *46* (5), 1732.

66. (a) Cramer, N. B.; Davies, T.; O'Brien, A. K.; Bowman, C. N. *Macromolecules*, **2003**, *36*, 4631. (b) Cramer, N. B.; Reddy, S. K.; O'Brien, A. K.; Bowman, C. N. *Macromolecules*, **2003**, *36*, 7964.

67. (a) Xu, J.; Jung, K.; Boyer, C. *Macromolecules*, **2014**, *47*, 4217. (b) Xu, J.; Jung, K.; Corrigan, N. A.; Boyer, C. *Chem*. *Sci*. **2014**, *5*, 3568.

68. Xu, J. ; Boyer, C. *Macromolecules*, **2015**, *48*, 520.

69. Tietze, L.F.; Gericke, K.M.; Güntner, C. *Eur. J. Org. Chem.* **2006**, *21*, 4910.

Chapter II: A simple In-based dual catalyst enables significant progress in ε-decalactone ring-opening (co)polymerization

This chapter corresponds to an article in Macromolecules, see reference: Macromolecules 2019, 52, 21, 8103-8113.

2.1 Catalytic System for Ring-opening polymerization of ε-DL

As mentioned in the general introduction, the replacement of ε-caprolactone (ε-CL) by δ- and ε-decalactones (δ- and ε-DL), derived from biomass, has attracted growing attention. These lactones, obtained from castor oil as a mixture of stereoisomers *via* fungal transformations, are widely used in flavor and fragrance industries, which proofs their low toxicity .[1,2,3]

Over the past few years, ε-DL has in particular been envisioned as a co-monomer in the preparation of random and block copolymers with modified properties compared to PCL. In contrast to the interest devoted to ε-DL as co-monomer to modulate polymer properties, only few studies have focused on the ROP of this monomer whose polymerization is challenging, and for which known catalysts present significant drawbacks and limitations. Most of the studies involving ε-DL as (co)-monomer make use of SnOct$_2$ and operate in bulk conditions at high temperatures (110-180 °C).[4-9]

The *n*-butyl substituent present on the propagating position significantly affects the polymerization kinetics, reducing the reaction rate.[10,11] Despite the required harsh polymerization conditions and long reaction times (few days at 110 °C), PDLs with M_n in range of the targeted ones (up to 40 000 g/mol) and rather narrow molecular distributions ($Đ < 1.30$) have been reported with SnOct$_2$. The organocatalyst TBD has also been evaluated in the ROP of ε-DL under similar reaction conditions (bulk at 110 °C).[4,12] Shorter reaction times are observed, but the polymerization is less controlled ($Đ < 1.45$). Considering the high application potential of PDL materials, it is necessary to develop new alternative catalytic systems able to promote the controlled ROP of ε-DL. Better knowledge is needed about the different classes of catalysts, to assess their behavior towards ε-DL and enable ultimately rational choice of the most suitable system to a given target / application. Last but not least, the reported ROP promoted by SnOct$_2$ or TBD were carried out in bulk conditions. This implies that the catalyst remains inside the polymer material. This may be an issue from a toxicity viewpoint,[13,14] and can also dramatically alter the polymer properties during thermal treatments at high

temperatures, thermo-modeling or extrusion for instance.[15,16,17] Therefore, while the results obtained with SnOct$_2$ and TBD are to be valued, new catalysts operating in solution under milder conditions are highly desirable to develop further the use of ε-DL.

Only few examples of catalysts promoting ROP of ε-DL in solution have been reported, and for most of them (La(OAr)$_3$,[18] Ca and Zn aryloxiamine complexes,[19] and the dual system MgI$_2$/cyclic isothiourea[20]), a unique example of ε-DL ROP has been reported. Only in the work of C. C. Lin with NNO tridentate ketimines Zn complexes, the control of the polymerization has been briefly explored, although the advantages and limitations of the catalyst have not been explored.[21] Nevertheless, PDL of $M_n > 15\,000$ and narrow molecular distributions ($\mathcal{D} < 1.15$) can be prepared in mild conditions (50 °C, 3-5h), which is also the case of the sole example reported using the dual catalytic system combining MgI$_2$ and a cyclic isothiourea.[20]

Dual catalysis, based on the cooperativity between a metallic Lewis acid and an organic Lewis base, is a concept widely used in organic synthesis[22] that has only been extended over the last decade to the field of polymer chemistry, and more particularly to the ROP of lactones and cyclic carbonates.[23,24] The strength of dual catalysis is the association of a Lewis acid with a Lewis base (to activate the monomer and the protic initiator, respectively), that are inactive separately while their combination and cooperation enables polymerization under mild conditions. This constitutes an interesting approach to increase activity, while maintaining good selectivity towards chain-transfer reactions (transesterifications).

Most of the recent reports involve simple, readily available Lewis acids (MgX$_2$, ZnX$_2$ LiX …) with a more sophisticated Lewis base such as N-heterocyclic carbenes (NHCs)[25,26] N-heterocyclic olefins (NHOs)[27,28,29] or cyclic isothioureas.[19,30] However, dual catalysts based on readily available Lewis acids and Lewis bases are rare. We recently used the association of [Zn] derivatives with tertiary amines (DMAP, TMP) to polymerize lactide (and ε-caprolactone) and access macrocyclic polymers.[31,32]

In addition, M Hillmyer reported in 2010[33] a detailed study on the ability of the InCl$_3$/NEt$_3$ association to act as catalyst for the controlled ROP of lactide.[34,35,36,37,38] In the same article, preliminary results were disclosed on the ROP of several lactones including one example with ε-Me-ε-CL, suggesting that this dual catalytic system is able to propagate ROP *via* secondary In-alkoxide moieties. Using benzylic alcohol as initiator, 115 equivalents of ε-Me-ε-CL were polymerized in 24 hours at 60 °C, in toluene solution to yield a polymer of M_n 20 000 and $\mathcal{D}$ of 1.30.

This result prompted us to investigate the behavior of this very simple dual catalyst towards ε-DL, which is a heavier analog of ε-Me-ε-CL. As reported hereafter, the InCl$_3$/NEt$_3$ association InCl$_3$/NEt$_3$ indeed promotes the ROP in a controlled and living manner, leading to PDL free of residual catalyst. Different types of initiators can be used (alcohols, amines) leading to ester and amide end-capped PDLs. Block and random copolymers with PLC can also be easily prepared.

2.2 Results and Discussions

2.2.1 ROP of ε-DL promoted by InCl$_3$/NEt$_3$

ROP of ε-DL promoted by the InCl$_3$/NEt$_3$ association (1/2 ratio) and initiated by benzyl alcohol with a ε-DL/BnOH ratio of 50 was first achieved in 3 mol/L toluene solution at 60 °C. The dual system was then compared with SnOct$_2$ and TBD under similar reaction conditions. As depicted by Figure 2.1, the reaction is significantly faster for the InCl$_3$/NEt$_3$ association. Only 4 h is needed to achieve full conversion, while after 24 h of reaction, 90% and 5 % of conversion are reached with TBD and SnOct$_2$, respectively. Due to the very low conversions observed for SnOct$_2$ at 60 °C, the reaction was also carried out at 110 °C, but even at this temperature, conversion is slower than with the InCl$_3$/NEt$_3$ association (~24 h to reach full conversion). The association of InCl$_3$ and NEt$_3$ is thus a rare catalyst to promote the ROP of ε-DL in solution under mild conditions. The PDL sample obtained with InCl$_3$/NEt$_3$ (after quenching the polymerization with an excess of PhCO$_2$H and precipitation) features a molecular weight of 9800 g/mol ($M_{n\,th}$ 8600 g/mol) and low molar distribution ($Đ$ = 1.13), suggesting rather good control of the polymerization, as in the case of the ROP of ε-DL with SnOct$_2$ at 110 °C (M_n = 6 116 g/mol, vs $M_{n\,th}$ = 6978 g/mol, and $Đ$ = 1.19).
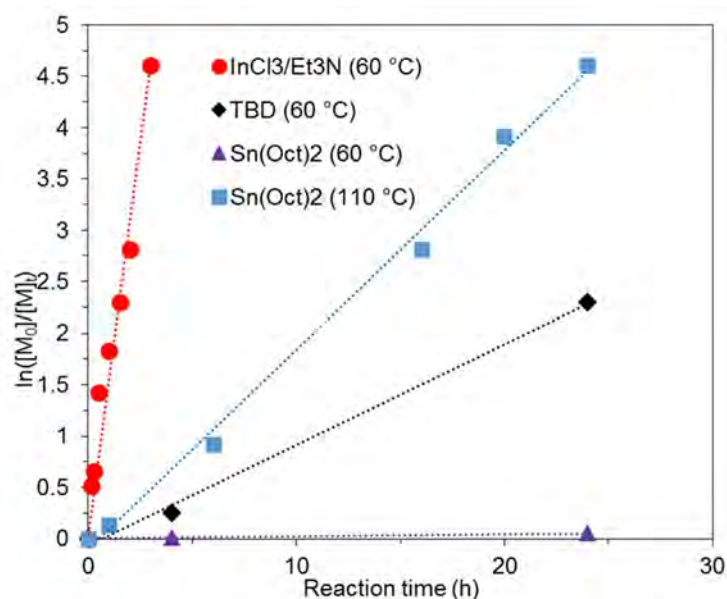
Figure 2.1 Comparative kinetic plot of ROP of ε-DL (toluene, $[\varepsilon\text{-DL}]_0$ = 3 mol/L) catalyzed by $InCl_3/NEt_3/BnOH$ 1:2:1 at **60 ºC DP50** (red line and dots), TBD/BnOH 1:1 at **60 ºC DP50** (black line and rhombus), $Sn(Oct)_2/BnOH$ 1:1 at **60 ºC DP50** (violet line and triangles), $Sn(Oct)_2/BnOH$ 1:1 at **110 ºC DP50** (blue line and squares).

Using the same reaction conditions, and benzyl alcohol or 3,5-dimethoxybenzyl alcohol (DMBA) as initiator (depending on the M/I ratio, so that accurate integration of the ^1H NMR spectra could be done for calibration), the control of the polymerization was probed for monomer to initiator ratios of 20 to 175 (Table 2.1, runs 1 to 8). For these M/I ratios, all the typical characteristics of a controlled and living polymerization were observed (Figure 2.2). As showed in Figure 2a,b, the molecular weight of the resulting PDL increases linearly with the M_0/I_0 ratio, while maintaining low molecular distributions ($Đ$ = 1.08-1.13). Moreover, the number of active-growing chains remains constant all over the polymerization process, as demonstrated by the kinetic semi-logarithmic plot, consistent with a first partial kinetic order in monomer, and by the linear evolution of the molecular weight of the polymer with monomer conversion (Figures 2.2c and 2.2d, respectively).

Table 2.1 Polymerization of ε-DL promoted by InCl$_3$/NEt$_3$ and initiated by BnOH or DMBA[a]
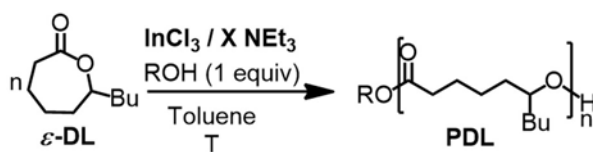
Run	M_0/I_0[a]	InCl$_3$/NEt$_3$	I/ InCl$_3$	ROH (I)	T (°C)	t (h)	Conv[b](%)	$M_{n\,(Th)}$	M_n[c]$_{NMR}$	M_n[d]$_{SEC}$	$Đ$[d]
1	50	1:2	1	BnOH	60	4	>99	8600	9000	9100	1.09
2	20	1:2	1	BnOH	60	1	>99	3500	3800	5400	1.10
3	25	1:2	1	BnOH	60	2	>99	4400	4500	6000	1.08
4	30	1:2	1	BnOH	60	2	>99	5200	4900	5600	1.10
5	70	1:2	1	BnOH	60	8	98	11 700	11 500	11 400	1.10
6	90	1:2	1	BnOH	60	12	99	15 300	15 800	13 100	1.12
7	150	1:2	1	DMBA	60	18	>99	25 700	26 700	25 100	1.13
8	175	1:2	1	DMBA	60	20	>99	29 900	29 900	19 300	1.09
9	50	1:2	1	BnOH	30	12	12	1100	1100	n.d.	n.d.
10	150	1:2	1	DMBA	80	20	>99	25 700	26 300	25 500	1.39
11[f]	325	1:2	1	DMBA	60	40	98	55 500	n.d.	57 500	1.35
12	50	1:2	0	DMBA	60	24	NR	-	-	-	-
13	20	1:0	1	BnOH	60	24	26	1000	1000	n.d.	n.d.
14	50	0:1	1	BnOH	60	18	NR	-	-	-	-

[a]I_0 = initiator, (benzyl alcohol BnOH or 3,5-dimethoxybenzyl alcohol, DMBA). [b]Calculated by ^{1}H NMR spectroscopy. [c]$M_{n\,NMR}$ = [(DP$_{NMR}$)*170.25 (M_w of ε-DL)] + M_w of initiator. [d]$M_{n\,SEC}$ from polymer after purification, using PS calibration. [e]DP$_{NMR}$ = Integration of CH-O polymer signal in ^{1}H NMR at 4.80 ppm divided by integration of the reference signal of the initiator. [f]Reaction performed with two monomer feeds 175 + 150. n.d. = not determined, NR = no reaction.
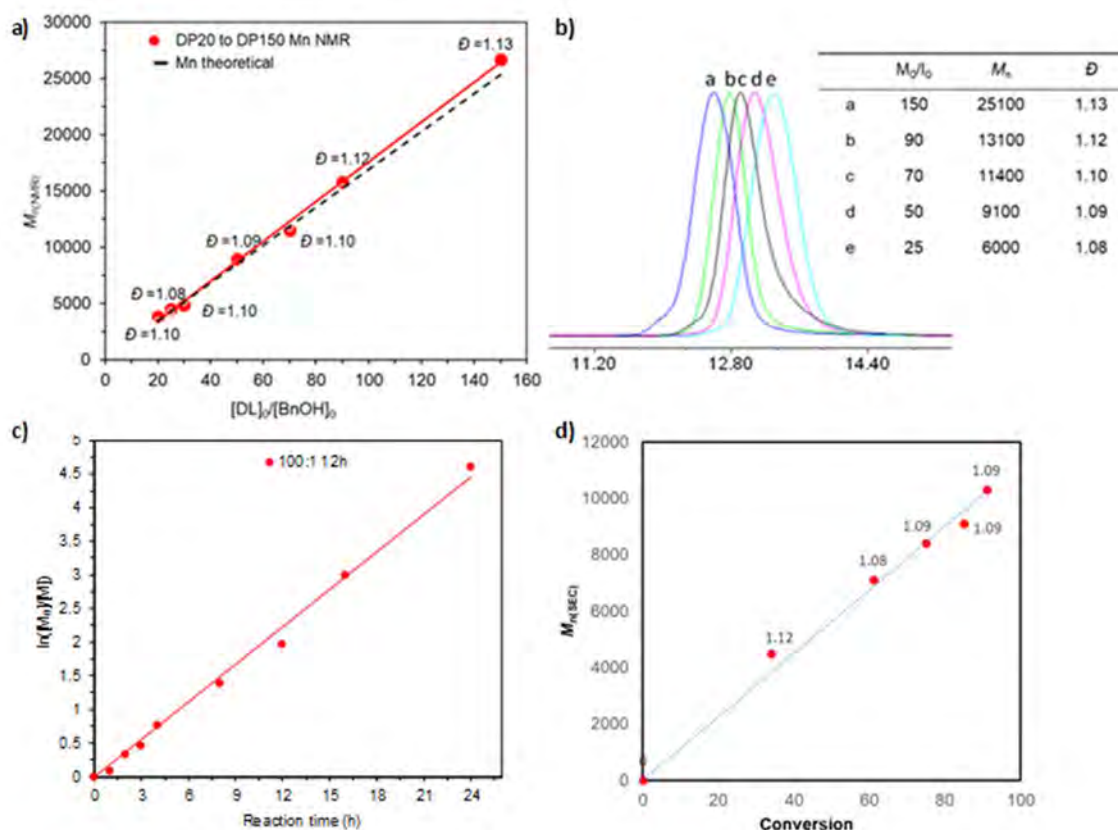
Figure 2.2 Controlled character of ROP of ε-DL catalyzed by InCl$_3$/ NEt$_3$/BnOH 1:2:1 in toluene ([ε-DL]$_0$ = 3 mol/L) at 60 °C for DP20 to DP175: a) Plot of M_n *vs* [ε-DL]$_0$/[BnOH]$_0$. b) Stack of SEC traces of the obtained PDL. c) Semi-logarithmic plot for [ε-DL]$_0$/[BnOH]$_0$ = 100. d) Evolution of M_n with the conversion for [ε-DL]$_0$/[BnOH]$_0$ = 50, Đ values on the graph.

Chain-end group fidelity was investigated by ^{1}H NMR spectroscopy and MALDI-Tof MS. The ^{1}H NMR spectrum in Figure 2.3a depicts the typical signals expected for a PDL polymer chain at 4.85 (a), 2.52 (i), 1.71-1.45 (b,c,d,f,g,h) and 0.87 (e) ppm. In addition, the spectrum also displays two singlet signals at 7.30 (k) and 5.10 (j) ppm corresponding to the benzyl ester group resulting from ROP initiation by BnOH, and a broad signal at 3.55 (a') ppm corresponding to the terminal C*H*OH group. The relative 2 to 1 value of the integration of signals j and a' is consistent with all the chains featuring the same ester/alcohol chain-ends and demonstrates high end-group fidelity. Moreover, the relative integration value between signals a and a' (or a+a' and j) is close to 20, indicating that the DP$_{NMR}$ value matches well the initial monomer / initiator feed.
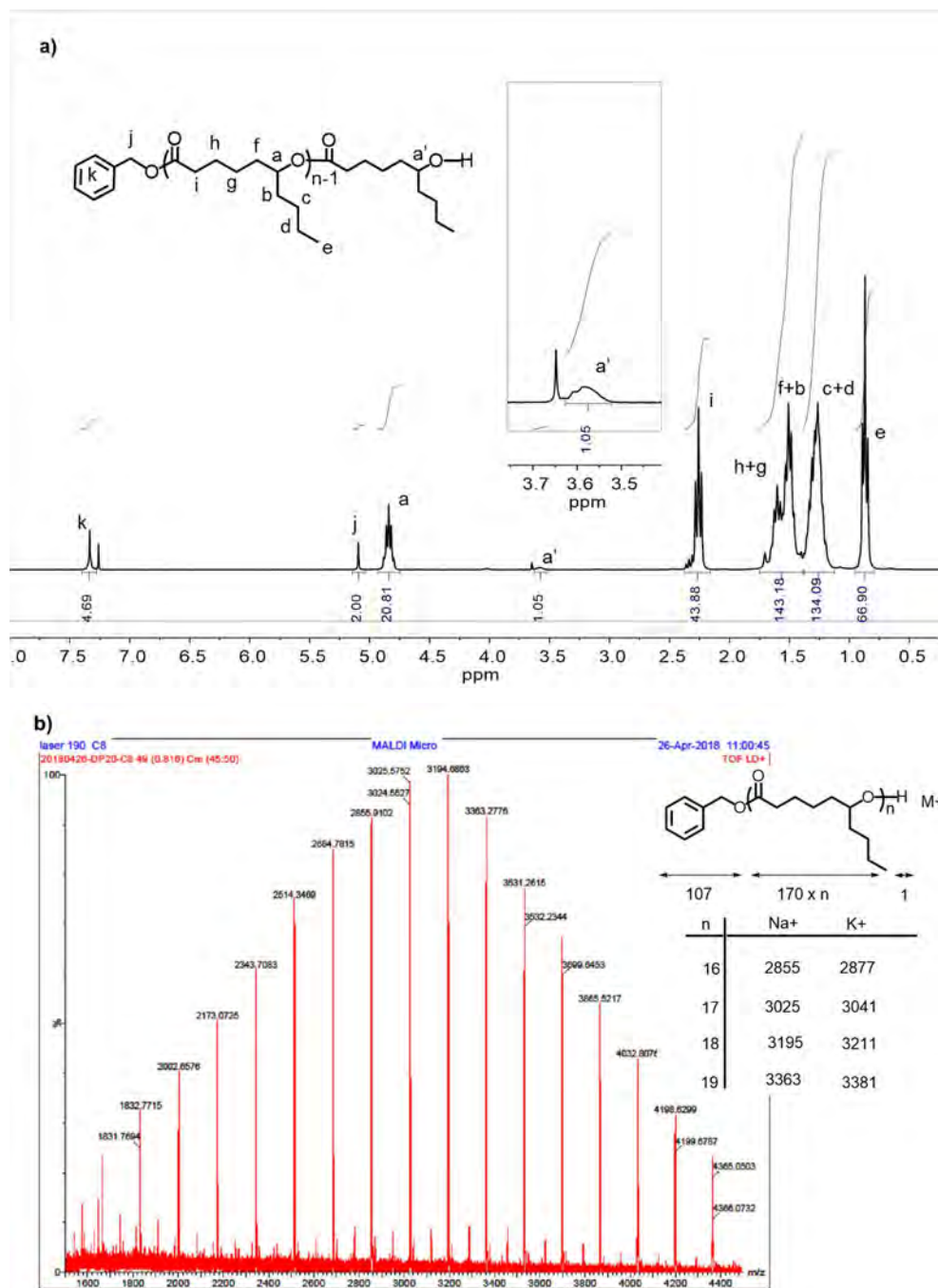
Figure 2.3 a) ^{1}H NMR spectrum (CDCl$_3$, 300 MHz) of a PDL of DP 21. b) Mass spectrum (MALDI-TOF) (region m/z 1700 to 4500 g/mol) of a PDL sample prepared with a [ε-DL]$_0$/[BnOH]$_0$/[InCl$_3$]$_0$/[NEt$_3$]$_0$ = 20/1/1/2 in toluene at 60 °C, [ε-DL]$_0$ = 3 mol/L (SEC analysis; M_n = 5400, Đ = 1.10)

Further information is supplied by the MALDI-Tof MS analysis (Figure 2.3b). No sign of macrocycles is detected. A very major population is observed with molar mass M = n × 170(M_{DL}) + 107(M_{BnOH}) + 23(M_{Na+}), corresponding to the linear polymer chains initiated by BnOH and terminated by a hydroxyl group. All these data indicate that PDL of well-defined structures with M_n up to ~30 000 g/mol and narrow molar distributions (Đ < 1.13) can be prepared in a controlled manner by fixing the M/I ratio. Another noticeable point is that ICP-

OES analysis of the polymers, obtained after precipitation by addition of a concentrated DCM solution on cold methanol, showed an In content of ~ 10 ppm which means that more than 99 % of the introduced In catalyst has been removed. This low content in catalyst residue should limit the risk of polymer alteration upon thermal treatments at high temperature.[15,16,17]

Table 2.2 Polymerization of ε-DL promoted by InCl$_3$/NEt$_3$ and initiated by BnOH or DMBA[a]
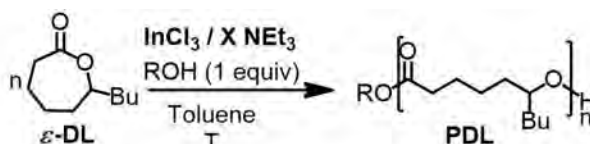
Run	M_0/I_0[a]	InCl$_3$/NEt$_3$	I/ InCl$_3$	ROH (I)	Solvent	T (°C)	t (h)	Conv[b] (%)	$M_{n\,(Th)}$	M_n[c] (NMR)	M_n[d] (SEC)	$Đ$[d]	DP[e] (NMR)
1	50	1:2	1	BnOH	Toluene	60	4	>99	8600	9000	9100	1.09	52
2	20	1:2	1	BnOH	Toluene	60	1	>99	3500	3800	5400	1.10	22
3	25	1:2	1	BnOH	Toluene	60	2	>99	4400	4500	6000	1.08	26
4	30	1:2	1	BnOH	Toluene	60	2	>99	5200	4900	5600	1.10	28
5	70	1:2	1	BnOH	Toluene	60	8	98	11 700	11 500	11 400	1.10	67
6	90	1:2	1	BnOH	Toluene	60	12	99	15 300	15 800	13 100	1.12	92
7	150	1:2	1	DMBA	Toluene	60	18	>99	25 700	26 700	25 100	1.13	156
8	175	1:2	1	DMBA	Toluene	60	20	>99	29 900	29 900	19 300	1.09	175
9	50	1:2	1	BnOH	Toluene	30	12	12	1100	1100	n.d.	n.d.	6
10	150	1:2	1	DMBA	Toluene	80	20	>99	25 700	26 300	25 500	1.39	154
11	20	1:0	1	BnOH	Toluene	60	24	26	1000	1000	n.d.	n.d.	5
12	50	0:2	0	DMBA	Toluene	60	24	NR	-	-	-	-	-
13	20	1:2	1	BnOH	CDCl$_3$	60	3	94	3300	3300	5000	1.14	19
14	50	1:2	1	BnOH	CDCl$_3$	60	4	97	8400	8500	8700	1.12	49
15	70	1:2	1	BnOH	CDCl$_3$	60	8	>99	12 000	12 000	10 700	1.14	70
16	90	1:2	1	BnOH	CDCl$_3$	60	12	97	14 900	13 900	12 500	1.26	81
17	20	1:1	1	BnOH	Toluene	60	2	>99	3500	3500	4600	1.08	20
18	25	1:1	1	BnOH	Toluene	60	3	>99	4400	4400	6100	1.08	25
19	50	1:1	1	BnOH	Toluene	60	4	98	8400	8600	8800	1.08	50
20	70	1:1	1	BnOH	Toluene	60	8	92	11 000	10 800	10 800	1.09	63
21	90	1:1	1	BnOH	Toluene	60	24	94	14 500	15 400	15 500	1.09	90
22	25	1:2	2	BnOH	Toluene	60	1	>99	4200	4500	6000	1.12	26
23	50	1:2	2	DMBA	Toluene	60	4	>99	8700	8500	9400	1.15	49
24	100	1:2	2	DMBA	Toluene	60	12	>99	17 200	17 200	16 000	1.08	100
25	150	1:2	2	DMBA	Toluene	60	18	>99	25 700	25 700	21 000	1.10	150
26[f]	50	1:2	1	DMBA	-	100	1	>99	8700	9 190	10 000	1.50	53

[a]I_0 =initiator, DMBA = 3,5-dimethoxybenzyl alcohol. [b]Calculated by ^{1}H NMR spectroscopy. [c]$M_{n\,NMR}$ = [(DP$_{NMR}$)*170.25 (M_w of ε-DL)] + M_w of alcohol used as initiator. [d]M_n SEC for polymer after purification, using PS calibration. [e] DP$_{NMR}$ = Integration of CH-O polymer signal in ^{1}H NMR at 4.80 ppm divided by integration of the reference signal of the initiator initiator. [f]Carried out in bulk conditions. n.d. = not determined, NR = no reaction.

We then explored the impact of the reaction conditions on the polymerization process and the polymer properties. Carrying out the reaction at 30°C resulted in very slow conversion (less than 12% after 12 h., run 9, Table 2.1), while increasing the temperature reaction to 80 °C (run 10) enabled rapid conversion and yielded high molecular weight PDL (M_n = 26 300 g/mol). However, lower control of the polymerization is indicated by the higher molar distributions observed ($Đ$ of 1.39 vs 1.13 at 60 °C). In line with this result, bulk polymerization at 100 °C led to higher $Đ$ values (entry 26 in Table 2.2, 1.50 vs 1.15 at 60 °C, using DMBA as

initiator and M/I = 50). Chloroform can be used as solvent instead of toluene without impact on kinetic or controlled character of the polymerization (entries 1-4 in Table 2.2, Figure 2.4a).
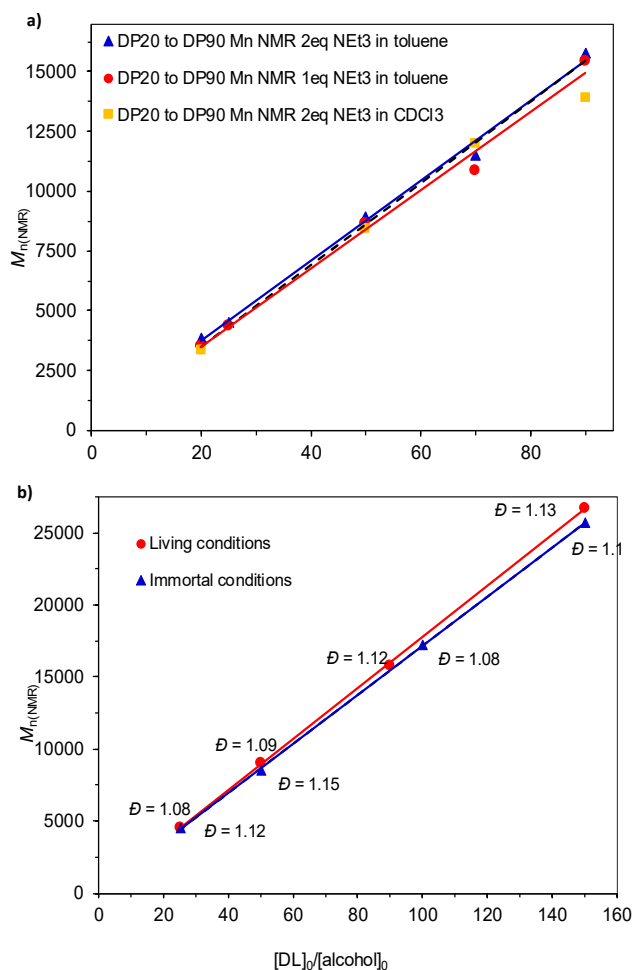
Figure 2.4 a) Plot of $M_{n,NMR}$ *vs* ($[\varepsilon\text{-DL}]_0/[\text{BnOH}]_0$) for DP20 to DP90) for the polymerization at 60 °C of ε-DL by BnOH/InCl$_3$/NEt$_3$ 1:1:2 in Toluene (blue line, triangles), in CDCl$_3$ (yellow line, squares) and BnOH/InCl$_3$/NEt$_3$ 1:1:**1** in Toluene (red line, circles) ($[\varepsilon\text{-DL}]_0$ = 3M). b) Plot of $M_{n,NMR}$ *vs* ($[\varepsilon$-DL]$_0$/[BnOH]$_0$) for DP20 to DP90) for the polymerization at 60 °C in Toluene of ε-DL by by BnOH/InCl$_3$/NEt$_3$ **1:1:2** (red line, circles) and BnOH/InCl$_3$/NEt$_3$ **2:1:2** as immortal conditions (blue line, triangles).

Toluene was preferred for the rest of study. To push further the system in terms of DP, a polymerization was performed with two consecutive feeds of 175 and 150 equiv. of ε-DL. A PDL with M_n = 57 490 g/mol and $\DJ$ = 1.35 was thereby obtained (run 11, Table 2.1). Although the $\DJ$ value increases slightly, the M_n value is in the range of the targeted one ($M_{n\ th}$ 55 500 g/mol).

The presence of the two partners InCl$_3$ and NEt$_3$ is necessary for the polymerization to take place efficiently. Removing any of them resulted in low or no conversion (runs 13&14 in Table 2.1 for ROP in the absence of NEt$_3$ or InCl$_3$, respectively). This observation is consistent

with a dual character of the catalytic system. In the case of lactide, Hillmyer proposed that $InCl_3$ and NEt_3 form alkoxy-bridged dinuclear In compounds as key species for a coordination-insertion polymerization. An alternative scenario consists in the concomitant activation of the monomer and alcohol by $InCl_3$ and NEt_3, respectively. Both mechanisms are conceivable with ε-DL. The ability of $InCl_3$ to bind and activate ε-DL has been evidenced by NMR spectroscopy. ^{1}H and ^{13}C NMR analyses of 1:1 and 1:2 of *ε*-DL:$InCl_3$ mixtures in $CDCl_3$ revealed shifts to lower fields of the signals corresponding to the C(=O)O–C*H* and *C*(=O)O–CH moieties.

The initiator/$InCl_3$/NEt_3 ratio was varied. As showed in Figure 2.4a, using one equivalent of NEt_3 ([BnOH]$_0$/[InCl$_3$]$_0$/[NEt$_3$]$_0$ = 1/1/1, runs 18-22) instead of two gives similar results, but from a practical point of view, it makes the purification of the polymer easier. Moreover, the ratio between the initiator (benzyl alcohol, runs 23-26 in Table 2.2) and the two partners $InCl_3$/NEt_3 can be raised to 2, without marked impact on the polymerization control (Figure 2.4b), which means that the $InCl_3$/NEt_3 association can be used in sub-stoichiometric conditions related to the initiator, in so-called immortal conditions.[39]

The possibility of varying the initiator, so that one of the polymer chain-ends can be modified, was also evaluated. In addition to primary alcohols, such as BnOH, DMBA and 1-pentanol (runs 1&2, Table 2.3), secondary alcohols can be used (run 3). In all cases, the incorporation of the initiator is complete and the M_n value of the obtained PDL matches well that expected. Notably, initiation with 1,4-benzenedimethanol (run 4) yielded a telechelic dihydroxylated PDL (^{1}H NMR spectroscopy indicates initiation from both alcohol moieties, see Figure 2.5).
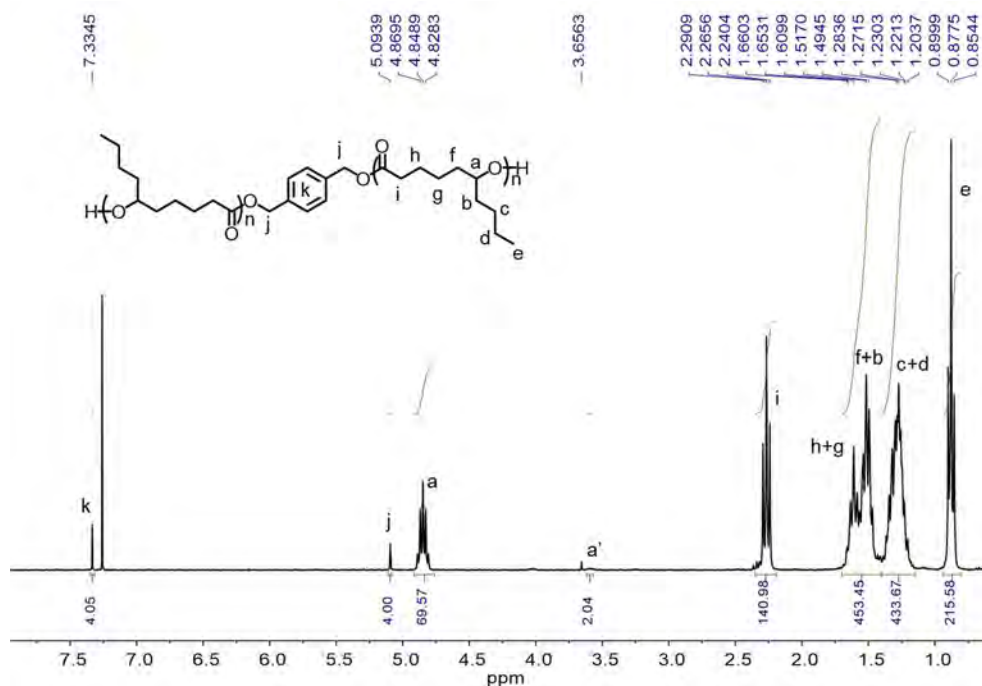
Figure 2.5 ^{1}H NMR spectrum (CDCl$_3$, 300 MHz) of the PDL DP70 initiated by 1,4-benzenedimethanol.

Table 2.3 Polymerization of ε-DL, promoted by InCl$_3$/NEt$_3$ and initiated by various initiators[a]

Run	M_0/I_0	I	t (h)	$M_{n\,Th}$	$M_n^d{}_{NMR}$	$M_n^c{}_{SEC}$	$Đ^c$
1	50	DMBA[b]	3	8700	8800	11200	1.11
2	25	1-Pentanol	2	4400	4200	5600	1.11
3	50	2-propanol	3	8700	8700	8700	1.09
4	70	HOBnOH[b]	4	12000	12000	13600	1.12
5	30	BnNH$_2$	2	5200	5600	7300	1.12
6	60	BnNH$_2$	4	10000	10500	11300	1.18
7[f]	1	BnNH$_2$	18	NR	-	-	-
8[g]	20	PEGNH$_2$	4	5400	5600	6700	1.13
9[g]	50	PEGNH$_2$	14	10500	11200	14300	1.18
10[h]	50	BnSH	24	8600	n.d.	n.d.	n.d.
11[h]	50	BzCH$_2$SH	24	8700	n.d.	n.d.	n.d.

[a]Reaction conditions: InCl$_3$/NEt$_3$ 1:2, 3 M solution in toluene at 60 °C, conv > 96%. [b]DMBA = 3,5-dimethoxybenzyl alcohol, HOBnOH = 1,4-benzenedimethanol. [c]M_n (SEC) from polymer (after purification) calibrated by polystyrene standards. [d]M_n (NMR) = [(DP$_{NMR}$)*170.25, Mw of DL] + Mw of initiator. [e]DP$_{NMR}$ = Integration of ^{1}H at CH-O, 4.8 ppm divided by integration of ^{1}H of the initiator signal used as reference. [f]InCl$_3$:NEt$_3$ 0:2. [g]MeOPEG-NH$_2$, $M_{n\,SEC}$ = 2100, $Đ$ = 1.03. [h]Monomer conversion < 20 % NR = No reaction. n.d. = not determined.

Interestingly, primary amines can also be used as initiators, enabling the preparation of PDLs capped with amide end groups which are noticeably stronger than the ester moieties.[40,41,42] More precisely, ROP of 30 equiv. of ε-DL using benzyl amine as initiator (BnNH$_2$/InCl$_3$/NEt$_3$ 1/1/2 resulted in a PDL of targeted M_n (7300 g/mol, run 5 Table 2.3) and low $Đ$ (1.12). Note that in the absence of InCl$_3$/NEt$_3$, polymerization does not occur. Benzyl

amine alone is not able to promote the polymerization, neither to ring open ε-DL. This last point markedly contrasts with the ROP of lactide promoted by DBU and initiated by primary amines in a two-step one-pot process (first ring opening of one unit of lactide by the amine alone, and then addition of the catalyst DBU to promote polymerization).[43] The incorporation of the benzyl amine as an amide chain-end was carefully analyzed by ^{1}H NMR to determine whether one or the two N-H bonds were implicated in the initiation (Figure 2.6).[43,44]

Besides the expected signals for the PDL chain, the spectrum displays a multiplet and a doublet signals at 7.25 and 4.45 ppm (integrating for 5 and 2 H, respectively) that can be attributed to the Ph and the CH_2-N groups of the benzyl moiety. An additional broad signal that disappears when the NMR analysis is performed in the presence of D_2O is observed at 6.00 ppm, which is consistent with the presence of an NH group and suggests initiation of only one polymer chain. Final confirmation of the incorporation of the amine as an amide chain-end was obtained by a 2D COSY analysis, where cross-marks between the signals attributed to the NH and CH_2N groups were clearly observed (Figure 2.6b). This result also confirms the initiation of a unique polymer chain per amine unit. We then took advantage of the ability of amines to act as initiators to prepare amphiphilic block copolymers featuring a robust link between the two blocks using a PEG-NH$_2$ ($M_{n\ SEC}$ = 2100, $Đ$ = 1.03) as macro-initiator.[40,41,42]
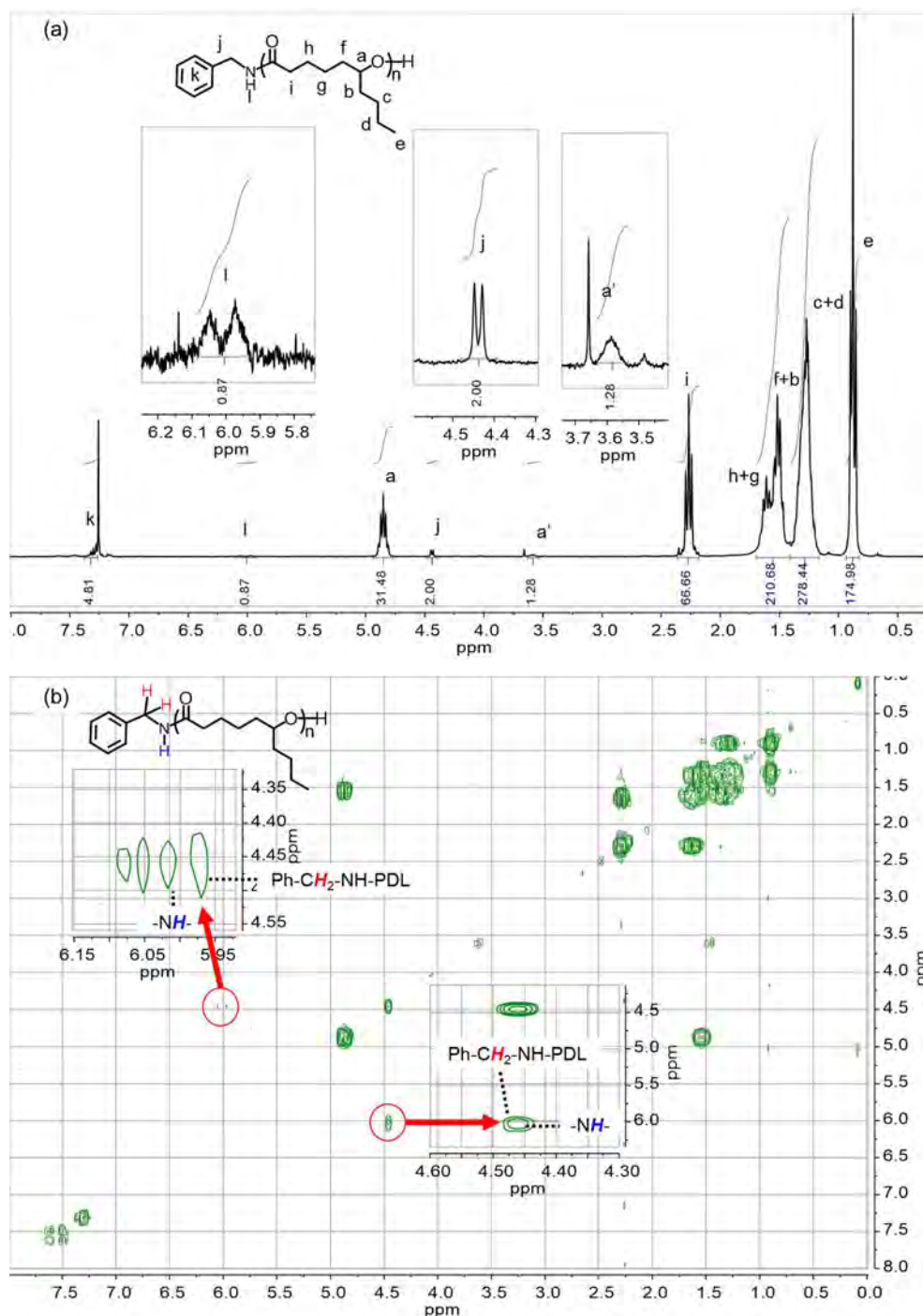
Figure 2.6. a) ^{1}H NMR spectrum (CDCl$_3$, 300 MHz) and b) Extract of the 2D COSY, of a PDL of DP 30 initiated by BnNH$_2$, [ε-DL]$_0$/[BnNH$_2$]$_0$/[InCl$_3$]$_0$/[NEt$_3$]$_0$ = 30/1/1/2 in toluene at 60 °C, [ε-DL]$_0$ = 3 mol/L.

The poly(ethylene glycol) polymer chain did not prevent the polymerization reaction, but ROP took place at a slower rate (runs 8&9). Nevertheless, block copolymers exempt of any homo-polymer (non-incorporated macro-initiator or PDL initiated by other protic residues), featuring M_n values close to those expected and narrow molecular distributions could be obtained ($Đ$ < 1.18) (see Figures 2.7 and 2.8 for the ^{1}H NMR spectra of the PEG-NH$_2$ macro-initiator and of the PEG-NH-PDL block copolymer). As observed with the initiating alcohols,

modifying the monomer over amine ratio allows to finely tune the molecular weight of the polymers (runs 5&6 and 8&9 for activation with $BnNH_2$ and $PEG-NH_2$, respectively).

In line with the growth of only one PDL polymer chain with primary amines as initiator, no polymerization reaction occurred with the secondary amine benzyl-methyl amine. Thiols were also tried as initiators (entries 10&11), but low conversions (< 20%) were observed even after 24 h of reaction. The low polarity of the In-S bond probably makes the transfer of the thiolate to the ester group of the lactone unfavorable.
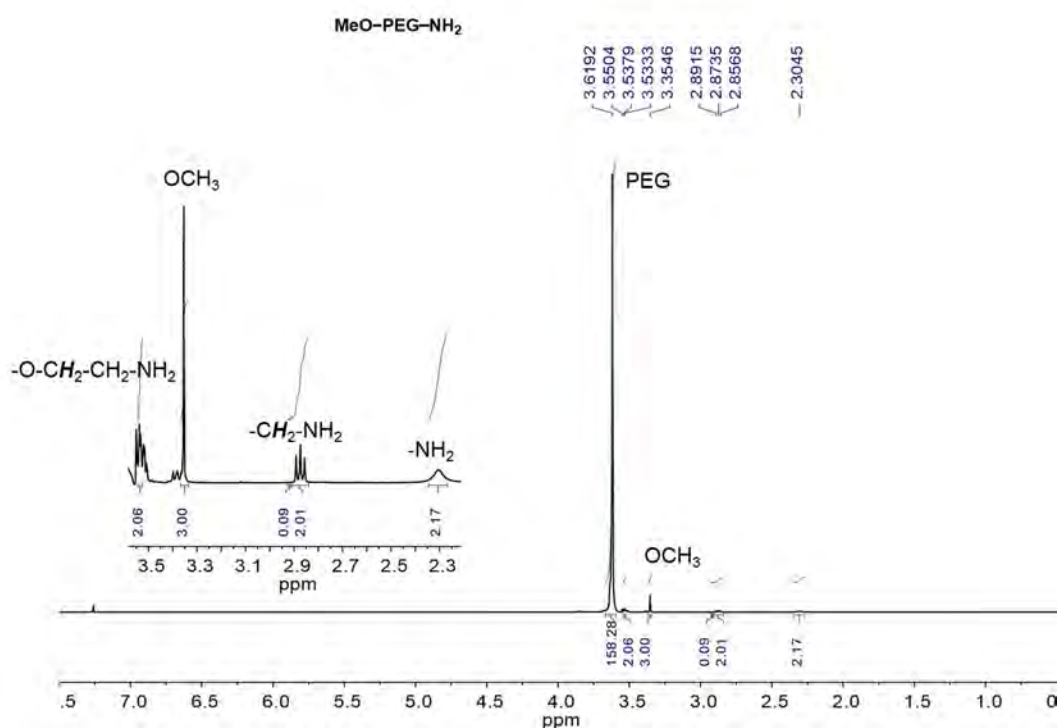
Figure 2.7 ^{1}H NMR spectrum (CDCl$_3$, 300 MHz) of the MeO-PEG-NH$_2$ used as macroinitiator.
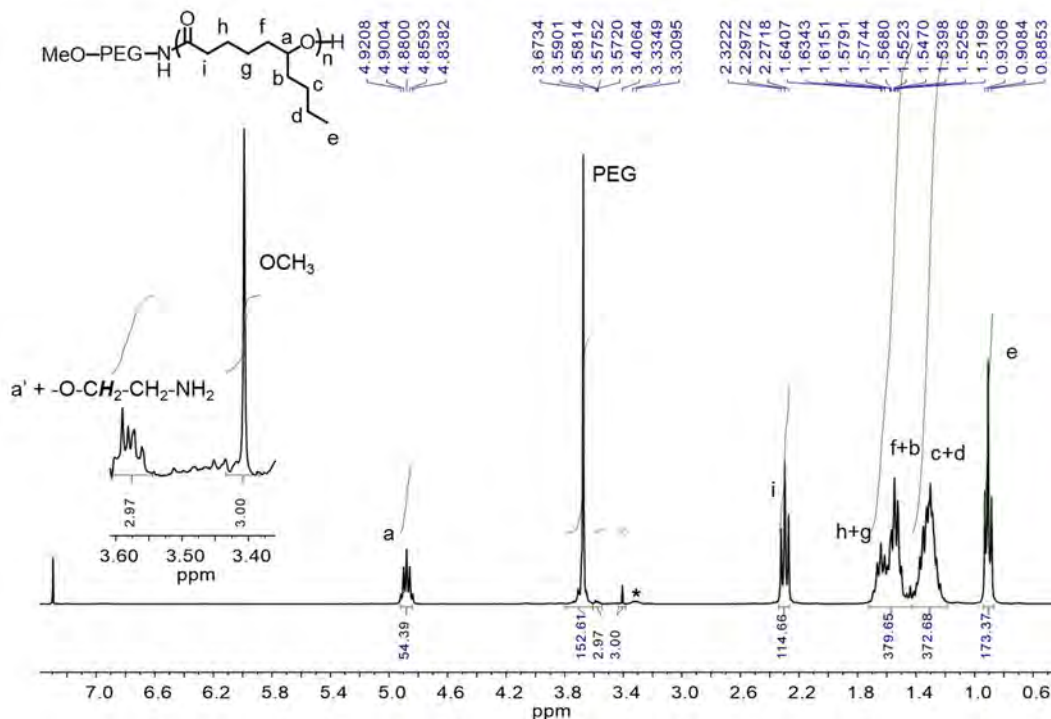
Figure 2.8 ^{1}H NMR spectrum (CDCl$_3$, 300 MHz) of the PEG-NH-PDL block copolymer DP50. *ammonium salt.

2.2.2 Preparation of ε-DL and ε-CL random and block copolymers

At this stage, we decided to probe the capacity of this catalytic system to copolymerize ε-DL and ε-CL in a controlled manner to give access to well-defined block and random copolymers. A PDL-*b*-PCL block copolymer was first prepared by addition of 50 equiv. of ε-CL to the reaction media after polymerization of 50 equiv. of ε-DL in the presence of [BnOH]$_0$/[InCl$_3$]$_0$/[NEt$_3$]$_0$ = 1/1/2 in toluene at 60 °C (Table 2.4, run 3). Formation of the block copolymer was confirmed by NMR spectroscopy and by SEC analysis (Figure 2.9a, right&left, respectively).

Table 2.4 Preparation of PCL/PDL block and copolymers by ROP with $InCl_3/NEt_3$[a]

Run	polymer	CL_0/DL_0	t (h)	$M_{n\,Th}$	$M_n^b{}_{NMR}$	$M_n^c{}_{SEC}$	$Đ^c$	$DP^d{}_{NMR}$ CL/DL	T_g^e (°C)	T_m^e (°C)	T_d^e (°C)	$χ^f$
1	PDL	0:50	3	8700	8800	11200	1.11	-/52	-53	-	356	-
2	PCL	60:0	0.5	7000	6900	7200	1.18	59/-	-61[g]	55[g]	300	55[g]
3	PCL-b-PDL	50:50	5.5	14400	14400	22000	1.24	50/50	-57.8	55.2	337	27
4	PDL-b-PCL	50:50	10	14400	15000	16300	1.25	56/50	-54.8	55.2	362	30
5	P(CL-r-DL)	50:50	2.5	14400	15500	19400	1.17	55/53	-60	-	351	-
6	P(CL-r-DL)	40:40	3.2	11500	11000	11700	1.13	40/37	-60.2	-	339	-

[a]Polymerizations carried out in toluene, $[monomer]_0$ = 3M, at 60 °C, using DMBA = 3,5-dimethoxybenzyl alcohol as initiator, and $InCl_3/Et_3N/DMBA$ = 1:2:1. [b]Calculated by ^{1}H NMR, $\{[(DP_{NMR\,of\,DL})*170.25, Mw\ of\ \varepsilon\text{-DL}] + [(DP_{NMR\,of\,CL})*114.14, Mw\ of\ \varepsilon\text{-CL}\,]\} + M_w$ of DMBA. [c]M_{nSEC} determined on polymer after purification using calibration by polystyrene standards. [d]DP_{NMR} = Integration of the CH-O (PDL) or CH_2-O (PCL) signal in ^{1}H NMR divided by the integration of the reference signal of the initiator (DMBA = 6H, reference position at $-(OCH_3)_2)$. [e]Determined by DSC. [f]Determined by DSC, using a heat of fusion value for a 100% crystalline PCL[45] of 136.0 J g^{-1}. [g]Data from ref 24.

The ^{1}H NMR spectrum shows the disappearance of the broad signal at 3.58 ppm, corresponding to the $CHOH_{PDL}$ chain-end of the PDL block, giving rise to the typical triplet signal (b') at 3.65 ppm for the CH_2OH_{PCL} chain-end of the added PCL block. Moreover, SEC analysis clearly shows the increase of M_n upon monomer feeding (from 11 800 g/mol at the end of consumption of ε-DL, to 16 300 g/mol for the diblock copolymer), while rather narrow molar mass distributions are retained ($Đ \sim 1.25$).
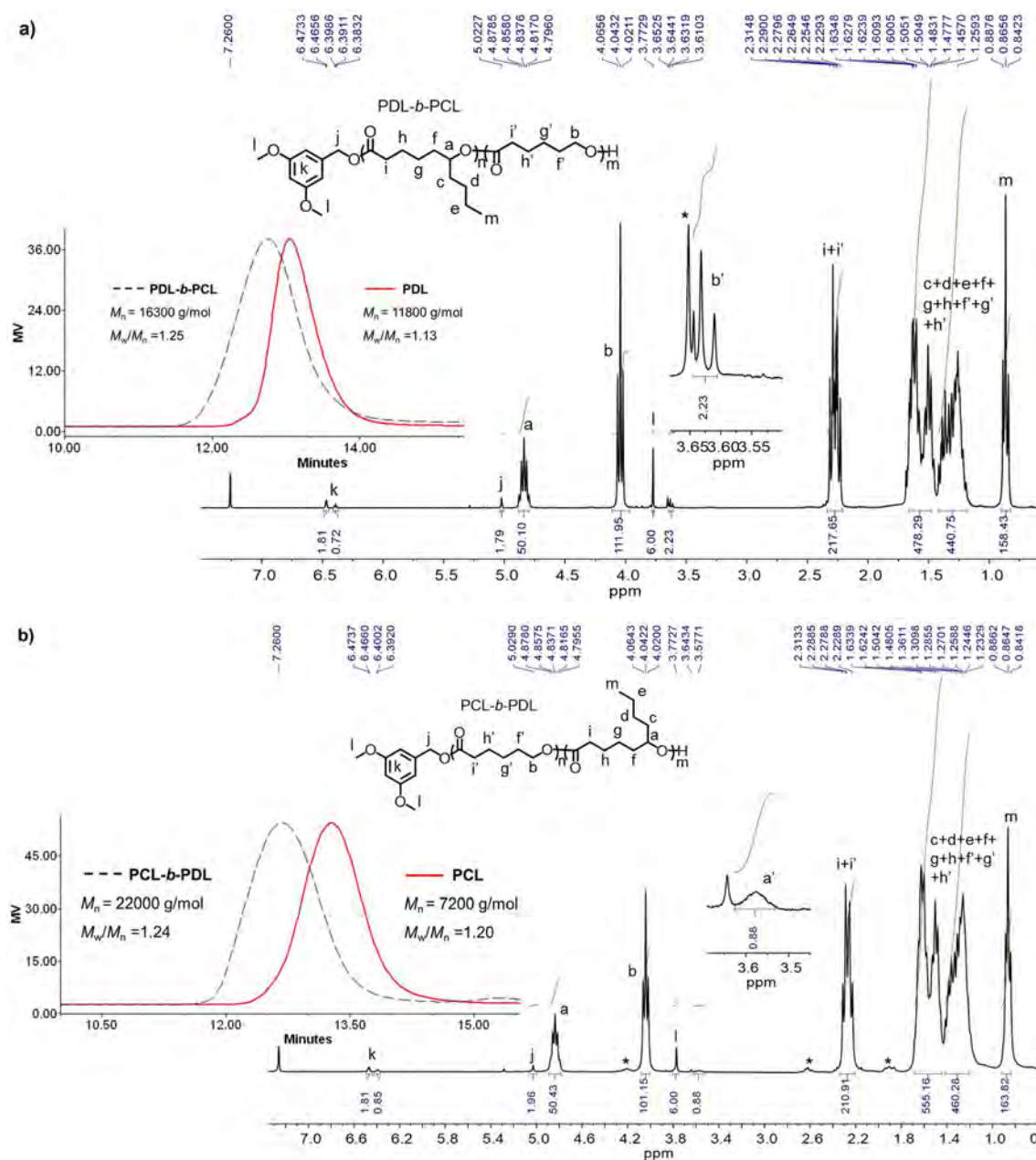
Figure 2.9 ^{1}H NMR spectrum (CDCl$_3$, 300 MHz) of a) a PDL-*b*-PCL block coplolymer, and b) a PCL-*b*-PDL block copolymer. initiated by BnOH, [ε-DL]$_0$/ [ε-CL]$_0$/[BnNH$_2$]$_0$/[InCl$_3$]$_0$/[NEt$_3$]$_0$ = 50/50/1/1/2 in toluene at 60 °C, [ε-DL]$_0$ or [ε-CL]$_0$ = 3 mol/L.

Sequential copolymerization with reverse order of addition of the monomers (first ε-CL then ε-DL, with similar conditions to the previous one, run 4) provides a PCL-*b*-PDL block copolymer. Again, ^{1}H NMR spectroscopy and SEC analysis are diagnostic for the formation of the block copolymer (Figure 2.9b right&left, respectively). We can note the disappearance on the ^{1}H spectrum of the triplet signal at 3.65 ppm associated to the C*H$_2$*OH$_{PCL}$ chain-end of the first PCL block and the appearance of the broad signal (a') at 3.58 ppm attributed to the C*H*OH$_{PDL}$ chain-end of the PDL block. SEC analysis shows an increase of M_n upon monomer feeding (from 7 200 to 22 000 g/mol, with Đ ~ 1.24). In addition, the ^{13}C NMR spectra of

these two block copolymers display only one signal for each type of C=O groups at δ 173.54 ppm (PDL) and 173.26 ppm (PCL) (Figures 2.10 and 2.11),[46] confirming the block architecture of the copolymers.
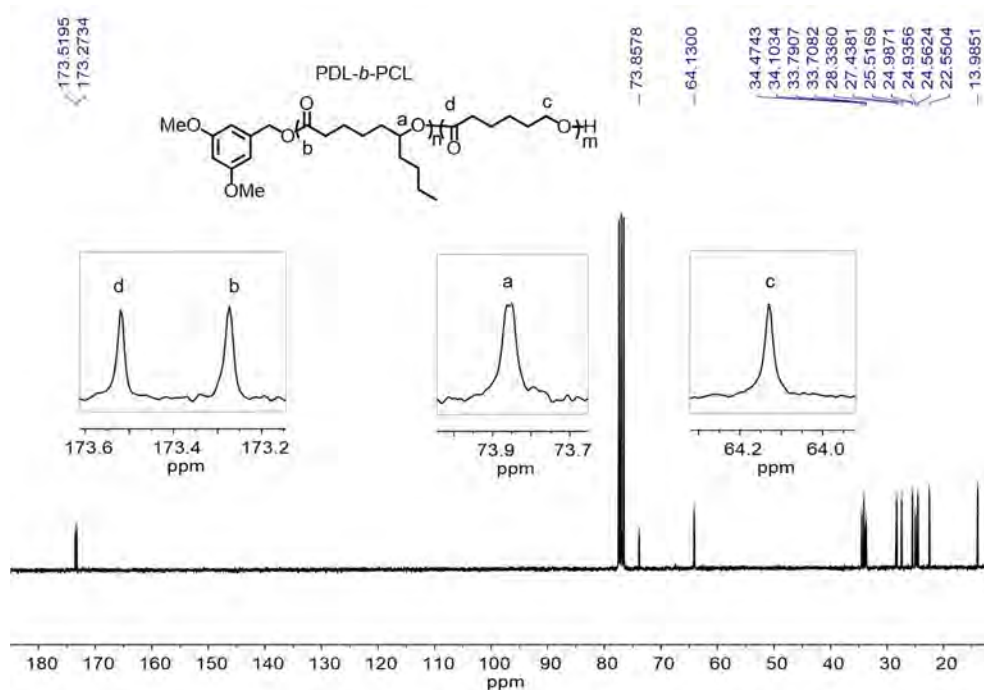
Figure 2.10 ^{13}C NMR spectrum (CDCl$_3$, 300 MHz) of a PDL-b-PCL block copolymer.
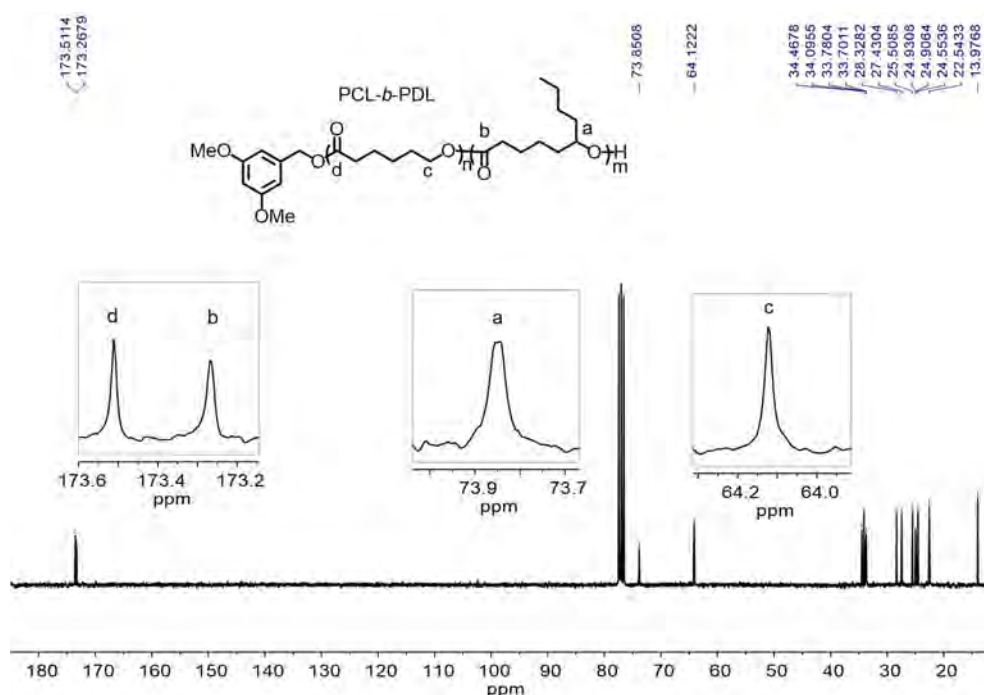
Figure 2.11 ^{13}C NMR spectrum (CDCl$_3$, 300 MHz) of a PCL-b-PDL block copolymer.

Two important conclusions can be drawn from these results. First, cross–propagation occurs efficiently, as demonstrated by the initiation of the ROP of ε-CL and ε-DL by the hydroxyl chain-end of PDL and PCL homopolymers, respectively. Secondly, the fact that the block architecture is retained at the end of the polymerization indicates very low, if any,

occurrence of side–reactions leading to redistribution of polymer segments (chain reshuffling). All these features suggest that simultaneous copolymerization of ε-DL and ε-CL is possible, although the different reactivity of these monomers in homo-polymerization may favor the formation of copolymers with blocky rather than random structure (60 equiv. of ε-CL are fully converted in less than 30 min while 3 h are necessary for ε-DL under the same conditions, see entries 1&2 of Table 2.4). The simultaneous polymerization of ε-DL and of ε-CL was carried out at 60 °C in toluene solution with InCl$_3$/NEt$_3$ in the presence of 1 equiv. of DMBA (ε-DL/ε-CL of 50/50 and 40/40 for entries 5&6, respectively). ^{1}H NMR monitoring of the monomer conversion showed full conversion of the two monomers in a little bit more than three hours, and, more surprisingly, a slow-down on the consumption rate of CL (less than 80 % of conversion in 30 min, Figure 12a). Consequently, a random P(CL-r-DL) copolymer with regular monomer distribution along the polymer chain was obtained, as supported by NMR spectroscopy. The ^{1}H NMR spectrum displays the triplet and broad signals at δ 3.63 and 3.58 ppm characteristic of the presence of CH_2OH$_{PCL}$ and CHOH$_{PDL}$ hydroxyl chain-ends, respectively (Figure 12b). Furthermore, the ^{13}C NMR spectrum shows, in marked contrast with those of the PDL-PCL block copolymers, broad or multiplet signals in the C=O region n, indicating the presence of different environments for the CO groups of each monomer as a result of a statistical distribution (Figure 2.13). With the dual catalyst InCl$_3$/NEt$_3$, it is thus possible to prepare block as well as random PCL/PDL copolymers of controlled structures under mild conditions. Thanks to the high initiation efficiency and low impact of chain-redistribution side-reactions, the nature of the chain-ends can also be finely tuned. DSC analysis illustrates the impact of the block or random structure of the copolymers on their thermal properties. Both block copolymers feature a glass transition at T_g values (-54.8 and -57.8 °C for PDL-b-PCL and PCL-b-PDL, respectively) in the range of those of the two homopolymers (-53 and -60 °C, for PDL and PCL, respectively), and a melting transition at T_m = 55.5 °C associated to the semi-crystalline PCL block. The value of the T_m is slightly lower to that of PCL, as is the crystallinity parameter (27 and 30 % compared to the typical 45-50 %). In marked contrast, the random copolymer is totally amorphous and presents only a glass transition at -60 °C. Although CL is converted at a slightly higher rate, the CL sequences are not long enough to bring crystallinity, which is consistent with the random character of the copolymer.
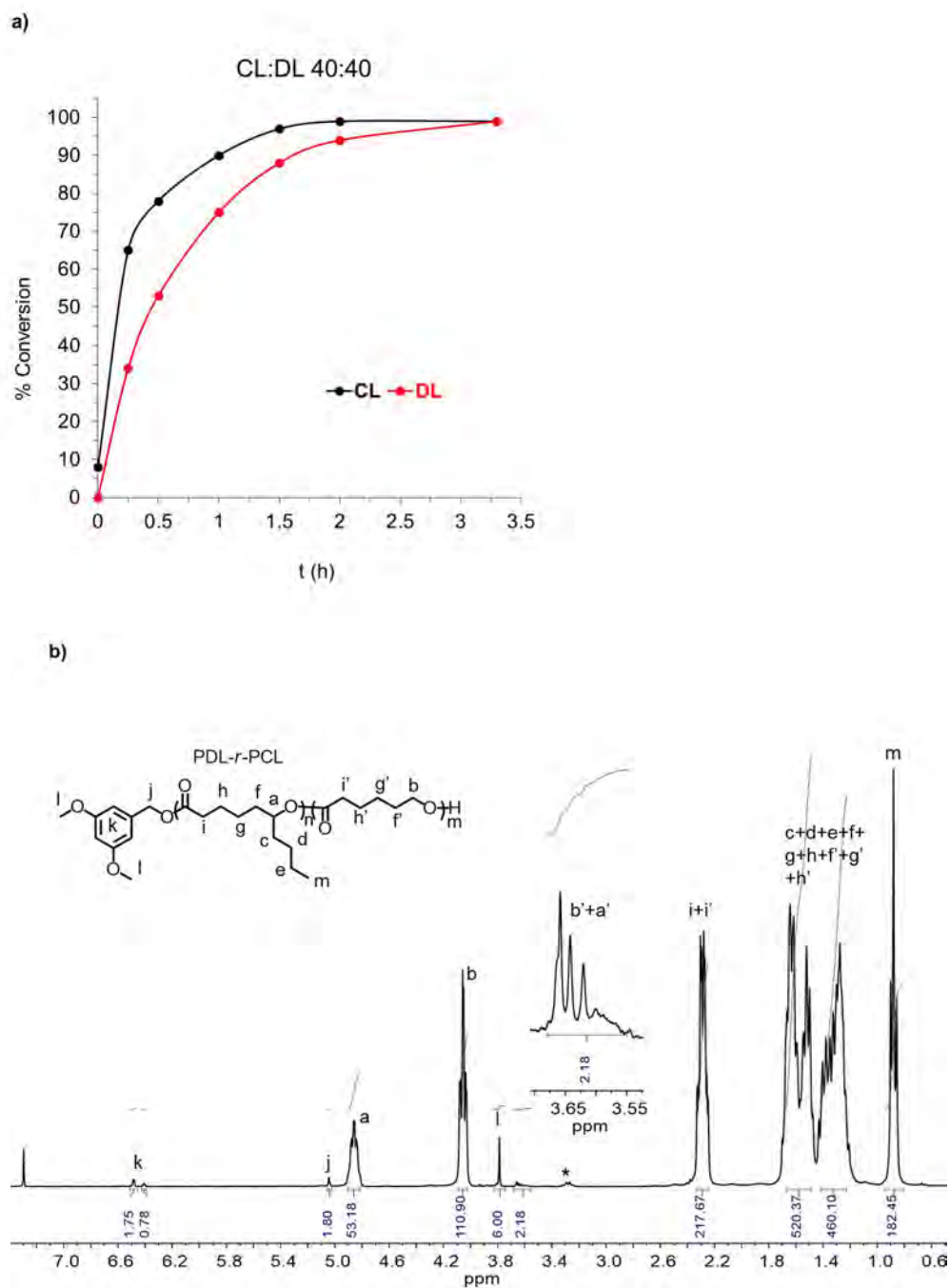
Figure 2.12 Simultaneous ROP of ε-DL and ε-CL, [ε-DL]/[ε-CL]/DMBA/InCl$_3$/NEt$_3$ = 40/40/1/1/2 a) Kinetic plot of ROcoP of ε-DL and ε-CL showing that both monomers are consumed at similar rate, b) ^{1}H NMR spectrum (CDCl$_3$, 300 MHz) of the obtained copolymer.
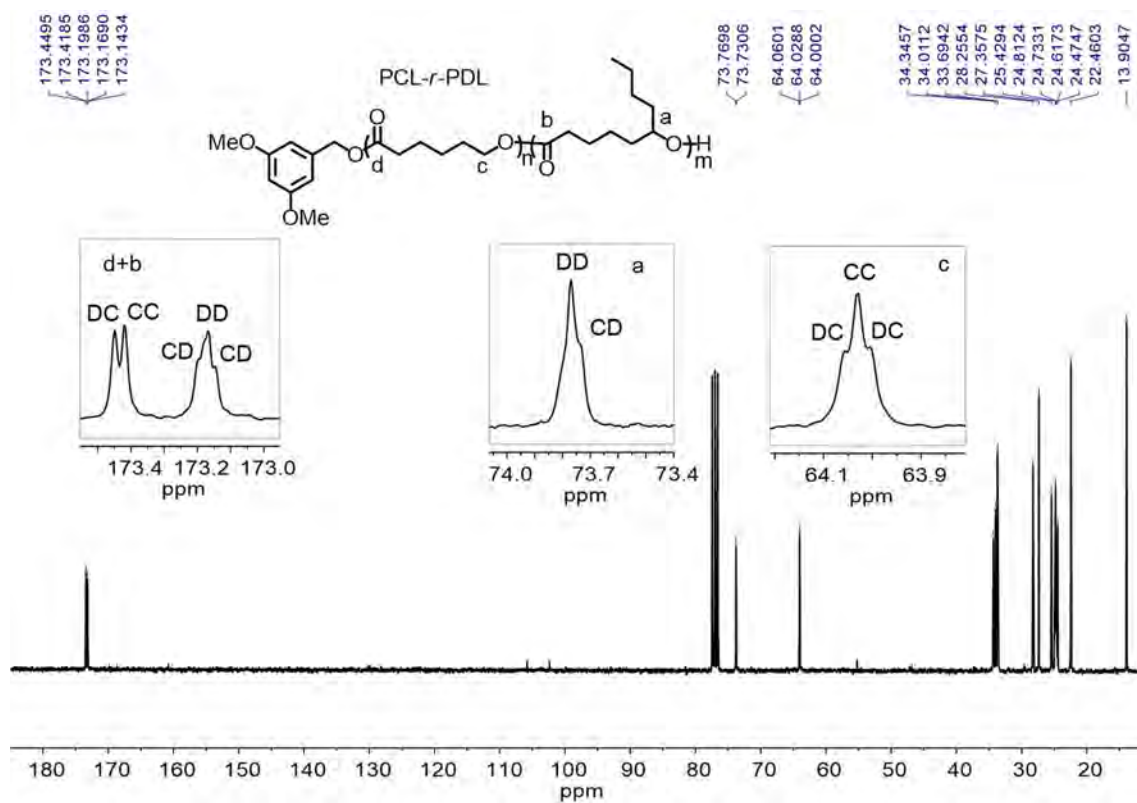
Figure 2.13 ^{13}C NMR spectrum (CDCl$_3$, 300 MHz) of a P(CL-*r*-DL) random copolymer.

2.3 Conclusions

In summary, we have demonstrated that the association of InCl$_3$ and NEt$_3$ is a readily available, easy to remove and efficient catalyst for the ROP of ε-DL under mild conditions (toluene, 3M, 60 °C). Besides the typical ester end-capped PDLs obtained by initiation of the polymerization with alcohols (primary or secondary), amide end-capped PDLs were prepared thanks to the ability of this dual catalyst to perform with primary amines as initiators. As a result, amphiphilic PEG-NH-PDL block copolymers, with a strong amide bond between the two blocks could be prepared. PDL-*b*-PCL / PCL-*b*-PDL and P(DL-*r*-CL) copolymers were also prepared by sequential or simultaneous ROP with ε-caprolactone. NMR spectroscopy, SEC and DSC analyses confirmed their well-defined structures, substantiating the controlled character of the polymerization and the low impact of transfer reactions.

The use of the InCl$_3$ / NEt$_3$ association thus enables significant progress ε-DL polymerization under mild conditions, and is complementary to SnOct$_2$, the latter being more adapted for ROP at high temperatures in bulk conditions. It provides access to a variety of polymers and copolymers derived from this renewable monomer. This work also highlights further the interest of dual catalysis and expands its application scope to ε-DL, a lactone propagating *via* a sterically hindered secondary alcohol and thus rather challenging to polymerize.

2.4 Experimental Part

Typical procedure for homopolymerization of ε-DL. Polymerization experiments were performed under Ar atmosphere at ambient temperature by adding ε-DL in a stirring suspension of initiator (1 equiv.), NEt$_3$ (2 equiv.), and InCl$_3$ (1 equiv.), [M]$_0$ = 3M in Toluene. The reaction mixture was stirred at 60 °C for the desired time until the complete consumption of ε-DL as determined by ^{1}H NMR spectroscopy. An excess of benzoic acid was added to quench the catalyst, and the solvent was evaporated under vacuum. The polymer was then dissolved in a minimum of DCM and precipitated two consecutive times in cold methanol, then filtered, and dried under vacuum, only 10 ppm of Indium remained in pure polymer. Conversion: 92% to >99%; isolated yield: 85% to 95%;

> *Benzyl alcohol as initiator, example for M/I = 20*: ^{1}H NMR (CDCl$_3$, 300 MHz, ppm): 7.30 (s Br, 5H, Ph), 5.10 (s, 2H, PhCH_2O), 4.88 – 4.79 (m, 21H, -CHO-), 3.58 (br s, 1H, -CH-OH, chain end), 2.28 – 2.23 ppm (m, 44H, CH$_2$), 1.60-1.46 (m, 142H, CH$_2$), 0.89-0.84 (m, 66H, CH$_3$). DP$_{NMR}$ = 22; SEC (THF): M_n = 3800, $Đ$ = 1.10.

> *Benzyl amine as initiator, example for M/I = 30:* ^{1}H NMR ($δ$, CDCl$_3$, 300 MHz, ppm): 7.30 –7.24 (m, 5H, CH), 6.09 – 6.01 (br t, 1H, NH), 4.85 – 4.81 (m, 31H, -CHO-), 4.42 (d, 2H, J = 5.6 Hz, PhCH_2N-), 3.58 (br s, 1H, -CH-OH, chain end), 2.28 – 2.23 (m, 60H, CH$_2$), 1.60-1.46 (m, 360H, CH$_2$), 0.89-0.84 (m, 90H, CH$_3$). DP$_{NMR}$ = 31; SEC (THF): M_n = 7300, $Đ$ = 1.12.

Typical procedure for the preparation of block copolymer PCL-*b*-PDL. Copolymerization experiments were performed under Ar atmosphere at ambient temperature by adding ε-CL in a stirring suspension of dimethoxybenzyl alocohol (DMBA) (1 equiv.), NEt$_3$ (2 equiv.), and InCl$_3$ (1 equiv.), [CL]$_0$ = 3M in Toluene. The reaction mixture was stirred at 60 °C for the desired time until the complete consumption of ε-CL, as determined by ^{1}H NMR spectroscopy. ε-DL in Toluene was then added to the stirring solution of PCL and catalysts. The reaction mixture was stirred at 60 °C until the complete consumption of ε-DL. An excess of benzoic acid was added to quench the catalyst, and the solvent was evaporated under vacuum. The block copolymer was then dissolved in a minimum of DCM and precipitated in cold methanol, then filtered, and dried under vacuum. Conversion: > 99% (for both monomers); yield: 90%. SEC: M_n = 22000 g/mol, $Đ$ = 1.24. DSC: T_g = −57.8 °C and T_m = 55.2 °C. TGA: T_d = 337

°C. ^{1}H NMR (CDCl$_3$, 300 MHz, ppm): 6.47 (d, J = 2.3 Hz, 2H, *ortho*-C$_6$H$_3$- CH$_2$-O-), 6.37 (t, J = 2.3 Hz, 1H, *para*-C$_6$H$_3$-CH$_2$-O-), 5.03 (s, 2H, ArCH$_2$O-), 4.88 − 4.79 (m, 50H, -CHO-), 4.04 (m, 100H, -CH$_2$O-), 3.75 (s, 6H, 2(-OCH$_3$)), 3.58 (br s, 1H, -CH-OH, chain end by DL unit), 2.29 − 2.22 (m, 200 H, CH$_2$), 1.60-1.46 (m, 450 H, CH$_2$), 1.40 − 1.22 (m, 450 H, CH$_2$), 0.89-0.84 (m, 150 H, CH$_3$).

Typical Procedure for the Preparation of sequential block copolymer PDL-*b*-PCL

The block copolymer PDL-*b*-PCL was synthesized by adding ε-DL in a stirring suspension of DMBA (1 equiv.), NEt$_3$ (2 equiv.), and InCl$_3$ (1 equiv.), [ε-DL]$_0$ = 3M in Toluene. The reaction mixture was stirred at 60 °C until the complete consumption of ε-DL. ε-CL, in Toluene, was then added to the stirring suspension of PDL and catalysts. The reaction mixture was stirred at 60 °C until the complete consumption of ε-CL. An excess of benzoic acid was added to quench the catalyst, and the solvent was evaporated under vacuum. The block copolymer was then dissolved in a minimum of DCM and precipitated in cold methanol, then filtered, and dried under vacuum. Conversion: > 99% (for both monomers); yield: 92%. SEC: M_n = 16300 g/mol, Đ = 1.25. DSC: T_g = −54.8 °C and T_m = 55.2 °C. TGA: T_d = 362 °C. ^{1}H NMR (CDCl$_3$, 300 MHz, ppm): 6.47 (d, J = 2.3 Hz, 2H, *ortho*-C$_6$H$_3$- CH$_2$-O-), 6.39 (t, J = 2.3 Hz, 1H, *para*-C$_6$H$_3$-CH$_2$-O-), 5.02 (s, 2H, ArCH$_2$O-), 4.88 − 4.79 (m, 50H, -CHO-), 4.06 − 4.02 (m, 100H, -CH$_2$O-), 3.77 (s, 6H, 2(-OCH$_3$)), 3.67 − 3.60 (m, 2H, -CH$_2$-OH, chain end by CL unit), 2.31 − 2.22 (m, 200 H, CH$_2$), 1.69 − 1.46 (m, 450 H, CH$_2$), 1.40 − 1.22 (m, 450 H, CH$_2$), 0.89 − 0.84 (m, 150 H, CH$_3$).

Typical Procedure for the Preparation of random copolymer P(CL-*r*-DL). Copolymerization experiments were performed under Ar atmosphere at ambient temperature by adding ε-CL and ε-DL in a stirring suspension of DMBA (1 equiv), NEt$_3$ (2 equiv.), and InCl$_3$ (1 equiv.), [CL+DL]$_0$ = 3M in Toluene. The reaction mixture was stirred at 60 °C for the desired time until the complete consumption of both monomers, as determined by ^{1}H NMR spectroscopy. An excess of benzoic acid was added to quench the catalyst, and the solvent was evaporated under vacuum. The copolymer was then dissolved in a minimum of DCM and precipitated in cold methanol, then filtered, and dried under vacuum. Conversion: >99% (for both monomers); yield: 95%. SEC: M_n = 19400 g/mol, Đ = 1.17. DSC: T_g = −60 °C. TGA: T_d = 351 °C. ^{1}H NMR (CDCl$_3$, 300 MHz, ppm): 6.45 (d, J = 2.3 Hz, 2H, *ortho*-C$_6$H$_3$- CH$_2$-O-), 6.37 (t, J = 2.3 Hz, 1H, *para*-C$_6$H$_3$-CH$_2$-O-), 5.01 (s, 2H, ArCH$_2$O-), 4.88 − 4.79 (m, 50H, -CHO-), 4.04 − 3.99 (m, 100H, -CH$_2$O-), 3.75 (s, 6H, 2(-OCH$_3$)), 3.64 − 3.58 (m, 2H, -CH$_2$-OH, chain

end by CL unit), 3.56 (br, 1H, -C*H*-OH, chain end by DL unit), 2.30 – 2.22 (m, 200 H, CH_2), 1.67 – 1.43 (m, 450 H, CH_2), 1.41 – 1.16 (m, 450 H, CH_2), 0.86 – 0.82 (m, 150 H, CH_3).

2.5 Bibliography

1   Romero-Guido, C.; Belo, I.; Ta, T. M. N.; Cao-Hoang, L.; Alchihab, M.; Gomes, N.; Thonart, P.; Teixeira, J. A.; Destain, J.; Waché, Y. *Appl. Microbiol. Biotechnol.* **2011**, *89* (3), 535.

2   Endrizzi, A.; Pagot, Y.; Clainche, A. L.; Nicaud, J. M.; Belin, J. M. *Crit. Rev. in Biotechnol.* **1996**, *16* (4), 301.

3   For other bio resourced lactones see: Hillmyer, M. A.; Tolman, W. B. *Acc. Chem. Res.* **2014**, *47* (8), 2390.

4   Olsén, P.; Borke, T.; Odelius, K.; Albertsson, A. C. *Biomacromolecules*, **2013**, *14* (8), 2883.

5   Glavas, L.; Olsén, P.; Odelius, K.; Albertsson, A. C. *Biomacromolecules*, **2013**, *14* (11), 4150.

6   Glavas, L.; Odelius, K.; Albertsson, A. C. *Polym. Adv. Technol.* **2015**, *26* (7), 880.

7   Martello, M. T.; Schneiderman, D. K.; Hillmyer, M. A. *ACS Sustainable Chem. Eng.* **2014**, *2* (11), 2519.

8   Schneiderman, D. K.; Hill, E. M.; Martello, M. T.; Hillmyer, M. A. *Polym. Chem.* **2015**, *6* (19), 3641.

9   Lee, S.; Lee, K.; Kim, Y. W.; Shin, J. *ACS Sustainable Chem. Eng.* **2015**, *3* (9), 2309.

10   Olsén, P.; Odelius, K.; Albertsson, A. C. *Biomacromolecules*, **2016**, *17* (3), 699.

11   Schneiderman, D. K.; Hillmyer, M. A. *Macromolecules*, **2016**, *49* (7), 2419.

12   Kakde, D.; Taresco, V.; Bansal, K. K.; Magennis, E. P.; Howdle, S. M.; Mantovani, G.; Irvine, D. J.; Alexander, C. *J. Mater. Chem. B.* **2016**, *4* (44), 7119.

13   Although Sn(Oct)2 is approved by the FDA as a food additive, the tin content in polymers should be lower than 20 ppm as it has been found to have some cytotoxicity. See: Tanzi, M. C.; Verderio, P.; Lampugnani, M. G.; Resnati, M.; Dejana, E.; Sturani, E. *J. Mater. Sci.: Mater. Med.* **1994**, *5* (6), 393.

14   Moderate cytotoxicity has been reported for TBD related to other organocatalysts such as thioureas. See: Nachtergael, A.; Coulembier, O.; Dubois, P.; Helvenstein, M.; Duez, P.; Blankert, B.; Mespouille, L. *Biomacromolecules*, **2014**, *16* (2), 507.

15   Cam, D.; Marucci, M. *Polymer.* **1997**, *38* (8), 1879.

16   Mori, T.; Nishida, H.; Shirai, Y.; Endo, T. *Polym. Degrad. Stab.* **2004**, *84* (2), 243.

17   Coulembier, O.; Moins, S.; Raquez, J. M.; Meyer, F.; Mespouille, L.; Duquesne, E.; Dubois, P. *Polym. Degrad. Stab.* **2011**, *96* (5), 739.

18 Lin, J. O.; Chen, W.; Shen, Z.; Ling, J. *Macromolecules*, **2013**, *46* (19), 7769.

19 Jasinska-Walc, L.; Bouyahyi, M.; Rozanski, A.; Graf, R.; Hansen, M. R.; Duchateau, R. *Macromolecules*, **2015**, *48* (3), 502.

20 Bai, J.; Wang, J.; Wang, Y.; Zhang, L. *Polym. Chem.* **2018**, *9* (39), 4875.

21 Chuang, H. J.; Chen, H. L.; Huang, B. H.; Tsai, T. E.; Huang, P. L.; Liao, T. T.; Lin, C. C. *J. Polym. Sci. A Polym. Chem.* **2013**, *51* (5), 1185.

22 Peters, R. Cooperative Catalysis. Wiley, New York. **2015**.

23 Piedra-Arroni, E.; Amgoune, A.; Bourissou, D. *Dalton Trans*. **2013**, *42* (25), 9024.

24 Hong, M.; Chen, J.; Chen, E. Y. X. *Chem. Rev.* **2018**, *118* (20), 10551.

25 Naumann, S.; Schmidt, F. G.; Frey, W.; Buchmeiser, M. R. *Polym. Chem.* **2013**, *4* (15), 4172.

26 Naumann, S.; Scholten, P. B. V.; Wilson, J. A.; Dove, A. P. *J. Am. Chem. Soc.* **2015**, *137* (45), 14439.

27 Naumann, S.; Wang, D. *Macromolecules*, **2016**, *49* (23), 8869.

28 Walther, P.; Naumann, S. *Macromolecules*, **2017**, *50* (21), 8406.

29 Walther, P.; Frey, W.; Naumann, S. *Polym. Chem.* **2018**, *9* (26), 3674.

30 Bai, J.–H.; Wang, X. –Q.; Wang, J.–H.; Zhang, L. –F. *J. Polym. Sci. A Polym. Chem.* **2019**, *57* (11), 1189.

31 Piedra-Arroni, E.; Ladavière, C.; Amgoune, A.; Bourissou, D. *J. Am. Chem. Soc.* **2013**, *135* (36), 13306.

32 Wang, B.; Wei, Y.; Li, Z. J.; Pan, L.; Li, Y. S. *ChemCatChem*, **2018**, *10* (22), 5287.

33 Pietrangelo, A.; Knight, S. C.; Gupta, A. K.; Yao, L. J.; Hillmyer, M. A.; Tolman, W. B. *J. Am. Chem. Soc.* **2010**, *132* (33), 11649.

34 For other articles reporting in well-defined ROP complexes as promotors, see: Osten, K. M.; Mehrkhodavandi, P. *Acc. Chem. Res.* **2017**, *50* (11), 2861.

35 Kremer, A. B.; Andrews, R. J.; Milner, M. J.; Zhang, X. R.; Ebrahimi, T.; Patrick, B. O.; Diaconescu, P. L.; Mehrkhodavandi, P. *Inorg. Chem.* **2017**, *56* (3), 1375. and references therein.

36 Dagorne, S.; Normand, M.; Kirillov, E.; Carpentier, J. F. *Coord. Chem. Rev.* 2013, *257* (11–12), 1869.

37 Myers, D.; White, A. J. P.; Forsyth, C. M.; Bown, M.; Williams, C. K. *Angew. Chem. Int. Ed.* **2017**, *56* (19), 5277.

38 Maudoux, N.; Roisnel, T.; Dorcet, V.; Carpentier, J. F.; Sarazin, Y. *Chem. Eur. J.* **2014**, *20* (20), 6131.

39   Ajellal, N.; Carpentier, J. F.; Guillaume, C.; Guillaume, S. M.; Helou, M.; Poirier, V.; Sarazin, Y.; Trifonov, A. *Dalton Trans*. **2010**, *39* (36), 8363.

40   Buwalda, S. J.; Dijkstra, P. J.; Calucci, L.; Forte, C.; Feijen, J. *Biomacromolecules*, **2010**, *11* (1), 224.

41   Buwalda, S. J.; Dijkstra, P. J.; Feijen, J. *J. Control. Rel*. **2010**, *148* (1), 23.

42   Buwalda, S. J.; Calucci, L.; Forte, C.; Dijkstra, P. J.; Feijen, J. *Polymer*, **2012**, *53* (14), 2809.

43   Alba, A.; Thillaye du Boullay, O.; Martin-Vaca, B.; Bourissou, D. *Polym. Chem*. **2015**, *6* (6), 989.

44   Coulembier, O.; Kiesewetter, M. K.; Mason, A. F.; Dubois, P.; Hedrick, J. L.; Waymouth, R. M. *Angew. Chem. Int. Ed*. **2007**, *46* (25), 4719.

45   Determined by DSC, using a heat of fusion value for 100 % crystalline PCL of 136.0 J g-1: Avella, M.; Errico, M. E.; Rimedio, R.; Sadocco, P. *J. Appl. Polym. Sci*. **2002**, *83* (7), 1432.

46   Similar observation can be made in the CH_2O and CH_2CO region.

Chapter III: Preparation of biodegradable functionalized polyesters by InCl₃/NEt₃ catalyzed ROcoP of new ε-functionalized-ε-CL and ε-DL

3.1 *"We are now in the plastic age" How can we move further to the sustainable, renewable, and <u>biodegradable polymers?</u>*

As discussed in the general introduction, the side effects of using such high amounts of plastics is largely associated with the increase of environmental problems. The interest on biodegradable and biocompatible materials as alternatives to non-degradable plastics has therefore been increasing over the last years.[1,2,3] It would be desirable that these biodegradable materials are synthesized from bio-based renewable monomers, rather than from petroleum-based feed-stock (i.e., ε-CL).

Is there any alternative lactone derived from renewable sources? These concerns have motivated investigations into the replacement of ε-CL by other lactone-type monomers. Due to its origin from renewable sources, ε-decalactone (ε-DL) is a good alternative to ε-CL. ε-DL is a 7-membered ring lactone with a similar structure to ε-CL, except the pendant butyl group at ε-position (Figure 3.1).
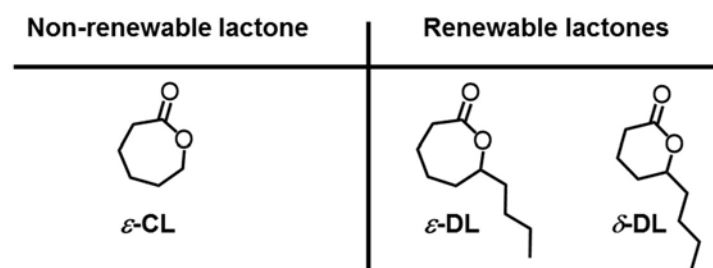
Figure 3.1 Structure of non-renewable lactone (ε-CL) and renewable lactones (ε-DL, δ-DL).

The key advantages of ε-DL are: (1) it is derived from a sustainable source, i.e. castor oil[4], (2) it is already used in industry as a food additive, (3) it has a good polymerizability due to the properties originating from its ring size, promoting low monomer concentration at equilibrium and high ceiling temperature, as compared to other decalactones such as δ-DL, and (4) the pendant butyl groups impact polymer properties (PDL is an amorphous polymer) differently from PCL (semi-crystalline).[4] As a consequence, increased attention has been focused on PDL, not only as an alternative to PCL but also to introduce new properties, particularly in the context of (block)copolymers.

mPEG-*b*-PDL block copolymers were synthesized using TBD and PEG−OH as an organocatalyst and an initiator, respectively, to compare their ability in drug loading/releasing with the corresponding mPEG-*b*-PCL (Scheme 3.1). The core volume of micelles based on amorphous mPEG-*b*-PDL was significantly larger than that of semi-crystalline mPEG-*b*-PCL-based micelles, as a result of the self-assembly behavior, thus increasing its ability in drug loading. The effect of core crystallinity also plays an important role in drug release properties, as PDL core micelles with amorphous phase were able to release 80% of the drug over a period of 72 h compared to 110 h needed for the semi-crystalline PCL core micelles.
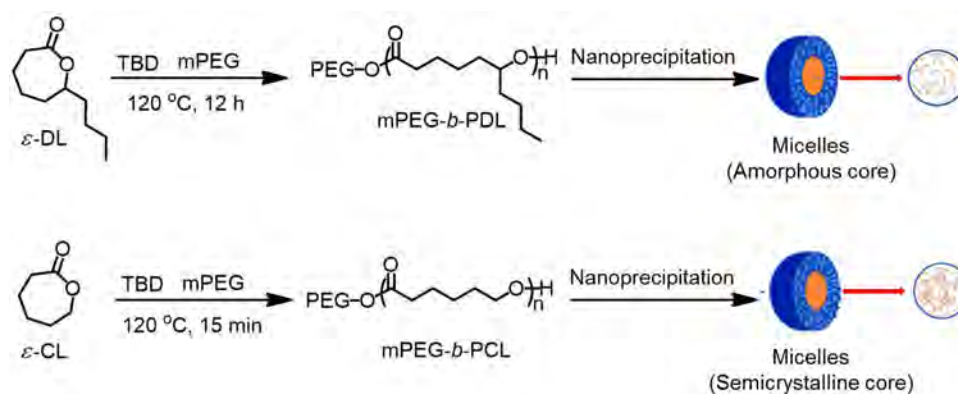
Scheme 3.1 Synthetic route for the preparation of amphiphilic block copolymers (mPEG-*b*-PDL and mPEG-*b*-PCL) to generate micelles with different core properties.[4]

The use of *ε*-DL as a comonomer in ROP with either *L*-LA or *ε*-CL has been investigated in the last few years in order to study the effect of the *ε*-DL units on thermal and mechanical properties of the copolymers. Albertsson reported the first copolymerization of *ε*-DL with *L*-LA, using Sn(Oct)$_2$ or TBD as a catalyst.[10] Thanks to the high ceiling temperature for both monomers, the copolymerization rate of *ε*-DL and *L*-LA can be easily tuned *via* temperature, while retaining the architectural control. A study of highly tough material with a very high strain-at-break values (e.g., 250 times greater for the triblock copolymer than pure PLA) was also reported, confirming the benefits of using *ε*-DL as a thermoresilient and toughening partner to *L*-LA (Figure 3.2).[5] So, *ε*-DL is a good renewable comonomer to *L*-LA, since their copolymers show a significant change in thermal stability (higher) and brittleness (softer) compared with PLLA. Moreover, the thermal stability of the obtained copolymers increased corresponding to the amount of *ε*-DL in the copolymer chains. These properties also highlight the result in phase separation for soft (*ε*-DL) and hard (*L*-LA) domains, which provides the basis for the elastomeric behavior of the block copolymers.[5]
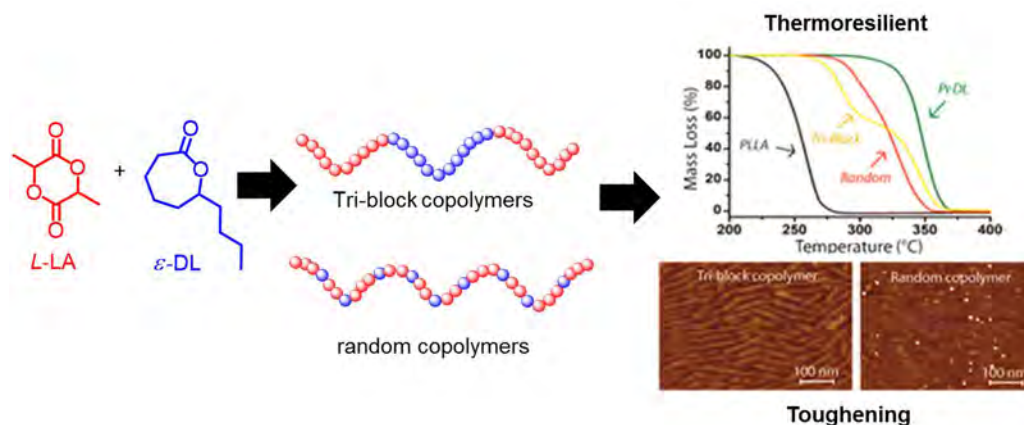
Figure 3.2 A thermoresilient and Toughening copolymers of *L*-LA and ε-DL presented by thermal decomposition patterns and AFM phase images. The text insets describe the polymer architectures and compositions.[5]

The same type of copolymers were efficiently synthesized by Hillmyer and col. by a two-step process of ROP of ε-DL and *L*-LA using Sn(Oct)$_2$ as a catalyst and diethylene glycol (DEG) as a difunctional initiator in bulk conditions (Figure 3.3).[6] The length of soft and hard blocks can be easily tuned by varying the monomer ratio, so that mechanical properties of copolymers are modulated as well.
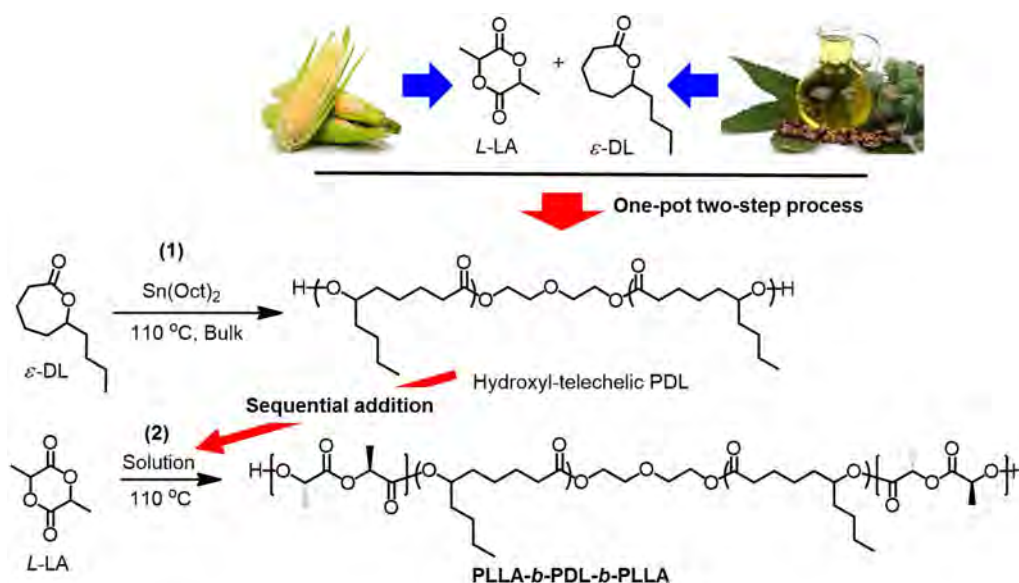
Figure 3.3 Synthesis of semi-crystalline thermoplastic polyester and renewable PSA formulation.[6]

The mechanical properties of these ABA block copolymers were investigated by dynamic mechanical analysis (DMA) and tensile test, demonstrating an elastomeric behavior depending on the composition ratio between the amorphous and semi-crystalline blocks. In addition, self-adhesive properties were also evidenced, demonstrating the interest of these plant-based copolymers in the field of pressure-sensitive adhesives (PSAs).[6]

Multiblock copolymers have also been prepared from triblock copolymers PLLA-PDL-PLLA. The alternating multiblock polymers of PLA and PDL were prepared by a sequential ROP and subsequent coupling reaction with 4,4′-Methylenebis(phenyl isocyanate), MDI, (Scheme 3.2).[7] The multiblock polymers were analyzed by differential scanning calorimetry (DSC) and small-angle X-ray scattering (SAXS) to demonstrate their bulk properties and microphase separation. The combination of PDL (soft–flexible block) and PLA (hard–rigid block) results in phase separation in the material. This combination of hard-soft domains, in particular, reveals the basis for a highly flexible material originating from renewable resources.[7]
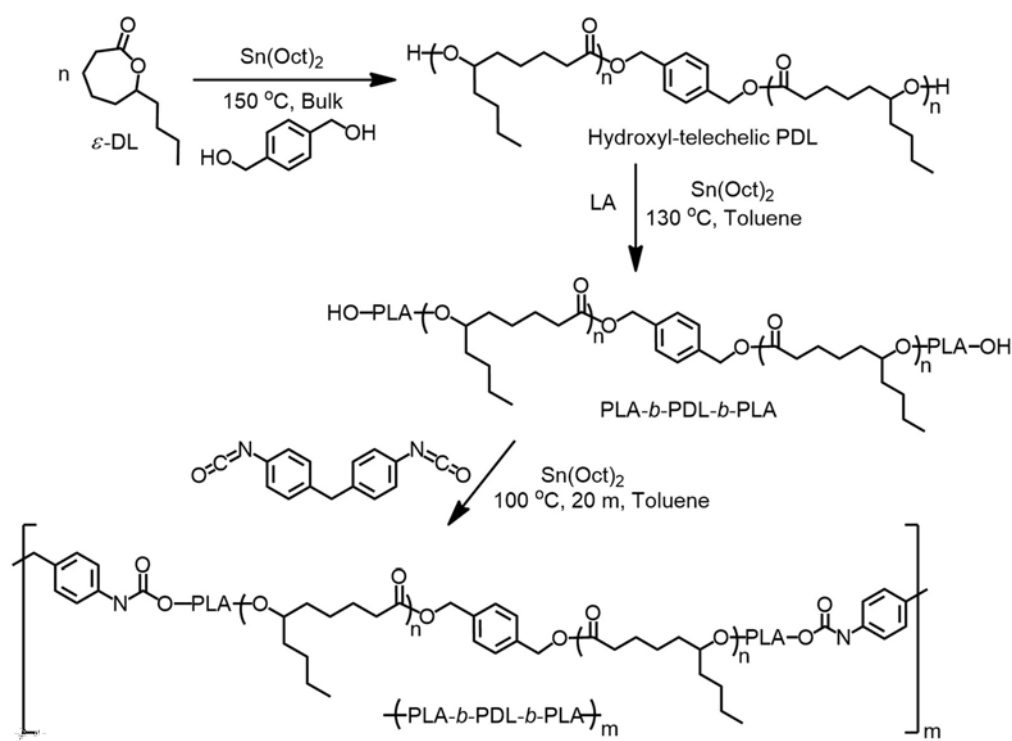
Scheme 3.2 Synthesis of multiblock PDL-based polymers.[7]

Not only the study of di, tri, or multiblock copolymers of ε-DL and L-LA has been reported, but a series of well-defined multiarm star block copolymers has also been investigated, revealing the improvement of the thermal and mechanical properties of these plant-based thermoplastic elastomers (Figure 3.4).[8]

Figure 3.4 Semi-crystalline PLLA/PDL-based block copolymers with different multiarm shapes.[8]

Multiarm star block copolymers were prepared in one-pot with two-step process by controlled ROP of ε-DL with multiarm initiators in bulk conditions (Sn(Oct)$_2$, 110 °C), to form the hydroxyl-terminated PDL, and subsequent block copolymerization with L-LA.[8] The more compact microphase-separated structures of hard and soft domains from PLA and PDL, respectively, in these block copolymers was observed by structural analysis, and the results were related to the increase of the number of arms. In addition, these star-shaped copolymers showed a higher thermal stability compared to the linear block. Tensile tests also suggested that these star-shaped materials behave like typical thermoplastic elastomers, while the ultimate tensile strength was also found to be strongly dependent on the number of PDL−PLLA chains.

What about the combination of amorphous and semi-crystalline polymers derived from ε-DL and ε-CL? Statistical copolymers of ε-DL and ε-CL were prepared in bulk conditions using Sn(Oct)$_2$ as a catalyst at 120 °C to yield the α,ω-hydroxy telechelic polymers (PCD).[9] The resultant copolymers were used as macroinitiatiors for the further preparation of PLA-PCD-PLA triblock copolymers (Scheme 3.3). Using different midblock compositions and different amounts of L-LA, it was possible to modify the mechanical behavior of these block copolymers. In addition, a combination of ε-DL and ε-CL in PCD (midblock) also promoted a higher tensile stress at failure stage, compared to the one with homoPDL midblock.

Scheme 3.3 The preparation of a PCD statistical copolymer midblock and subsequent chain extension to yield LCDL block copolymers.[9]

All examples described above mainly reveal the impacts of ε-DL on both the thermal and mechanical properties of copolymers with LA and/or ε-CL, which leads to elastomer materials with high thermal stability.

What about the impact of this bio-based monomer on the degradation rates? Very few examples have been reported, revealing the strong impact of the lateral *n*-butyl chain on degradability. It is better to start with simpler examples, in particular to compare with PCL.

The study of a selective degradation based on the heterogeneity of the amorphous phase in aliphatic block copolyesters has been reported.[10] A set of degradable materials based on PLLA, PDL, and PCL with various compositions was synthesized to demonstrate the predominant impact of heterogeneity of the amorphous phase on the degradation processes (Scheme 3.4).
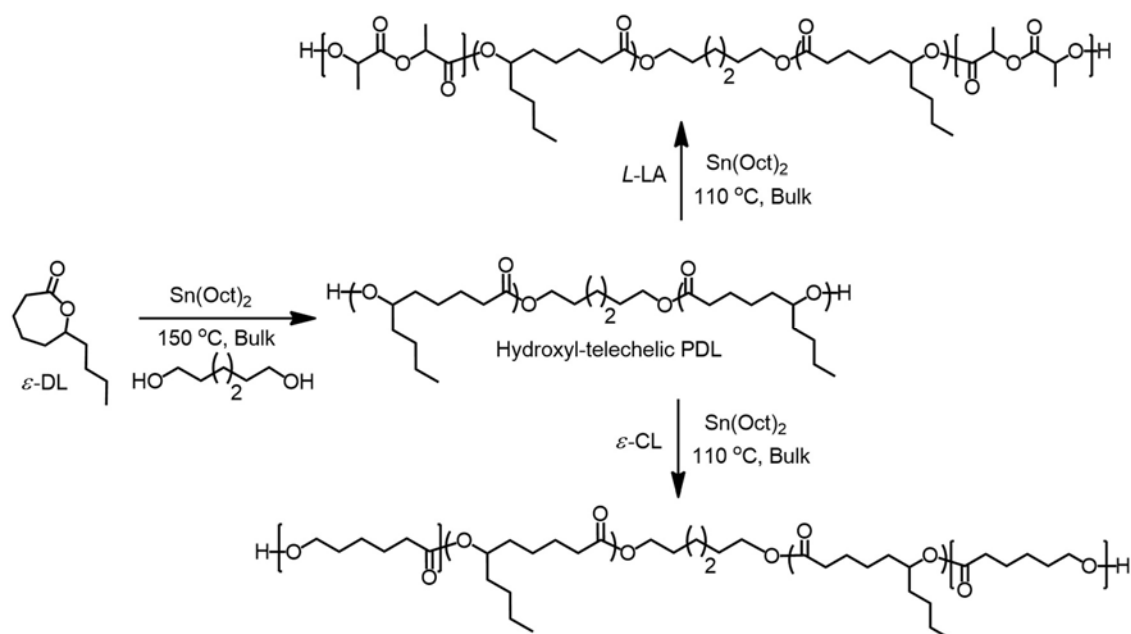
Scheme 3.4 Copolymerization of ε-DL with either *L*-LA or ε-CL for the preparation of homogeneous and heterogeneous amorphous materials, respectively. ROP condition: Sn(Oct)$_2$ as catalyst and 1,6-hexanediol as initiator at 110 °C.[10]

For each composition, PDL$_{50}$PLA$_{50}$ and PLA$_{33}$PDL$_{33}$PLA$_{33}$, two different T_gs were observed. The presence of two different T_gs indicated two separated amorphous phases corresponding to the PDL and PLA blocks, thus exhibiting a heterogeneous amorphous phase. In contrast, copolymer combining of PCL and PDL displayed a more homogeneous phase, since both compositions, PDL$_{50}$PCL$_{50}$ and PCL$_{33}$PDL$_{33}$PCL$_{33}$, presented only one T_g each. Based on the heterogeneity of the amorphous phase in the samples, the degradation process could proceed in two different pathways by the selective chain scission for the homogenous amorphous material and the random chain scission for the heterogeneous phase material (Figure 3.5). Hydrolytic degradations were performed in water at 37 °C for 6 months. The slowest degradation rate was detected for the most homogeneous and the least hydrophilic compositions of PCL and PDL, as driven by a more selective chain scission. (Figure 3.6b). A random chain scission process results in a faster degradation rate as was observed in the heterogeneous amorphous phase PLA/PDL-based materials (Figure 3.6a). However, more than 80% of remaining mass was observed for all materials after 6 months of degradation, revealing the difficulty of the degradation of these aliphatic polyesters.
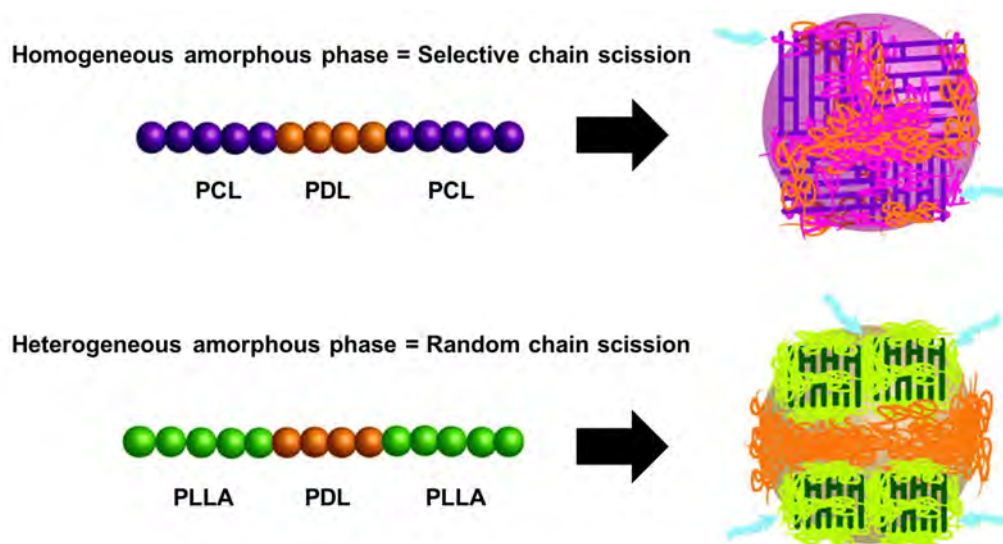
Figure 3.5 Proposed degradation routes for copolymers presenting more homogeneous amorphous phase regions and for copolymers with heterogeneous amorphous regions under hydrolysis in water at 37 °C.[10]

The polymer degradation depends not only on the degree of crystallinity but also on the hydrophilicity of polymer. These results (Figure 3.6) revealed that the degradation of PDL is significantly faster than that of PCL but still slower than the one of PLLA. This means that the amorphous character of the polymer backbone predominantly affects the degradation rate over the hydrophobicity imparted by the *n*-butyl lateral groups, as compared the similar polymer backbone between PDL (amorphous) and PCL (semi-crystalline).
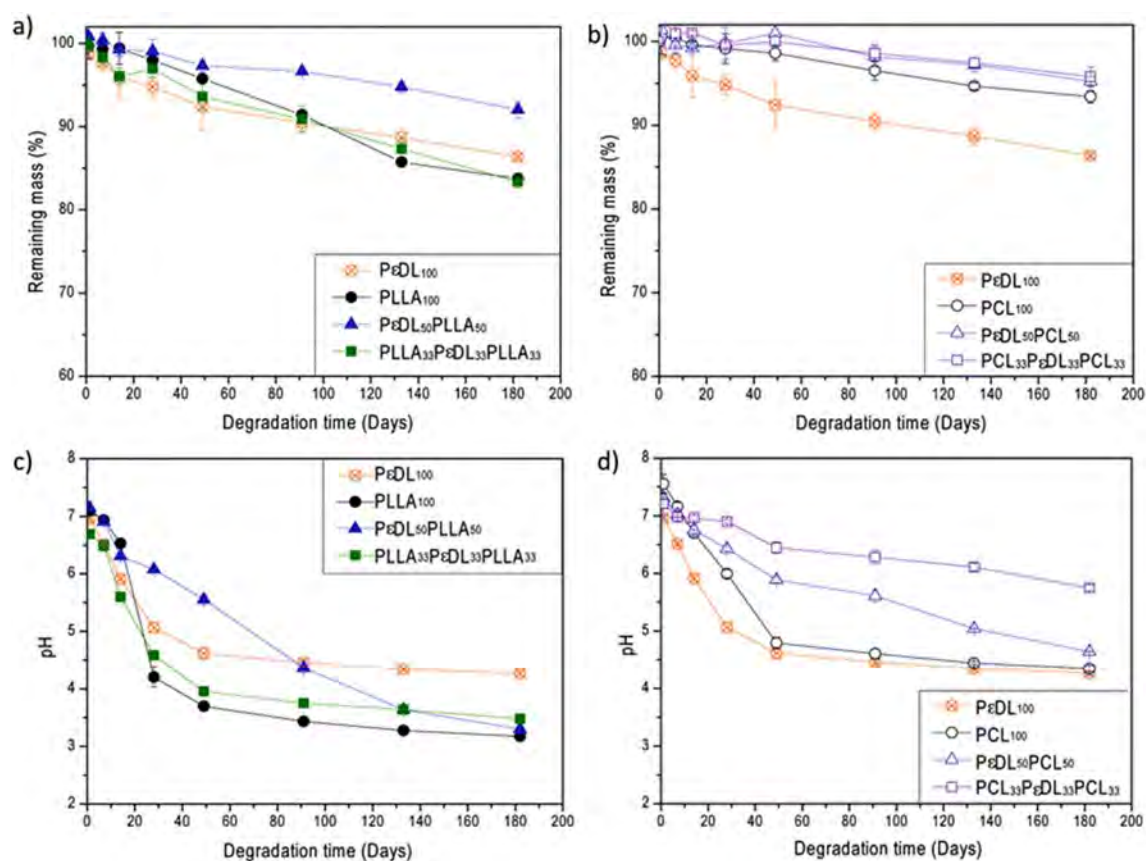
Figure 3.6 Remaining mass of (a) PDL/PCL-based copolymers, and (b) PDL/PLA-based copolymers; (c) pH of PDL/PCL-based copolymers; (d) pH of PDL/PLA-based copolymers after different hydrolysis times in water at 37 °C.[10]

To further increase the degradation rate of PDL-based materials, the modulation of the PDL properties by synthesizing a new ε-CL-based monomer with close structure to the ε-DL monomer but bearing functional group is required. Ideally, the new polyester-based functional materials will feature tailored structures with increasing hydrophilicity and thereby with controlled degradation process.

3.1.1 Hydrophilic aliphatic polyesters

The introduction of hydrophilic functional groups would be a highly efficient means of tailoring the polyesters properties including some features such as (bio)degradation rate and water affinity.[11,12] Basically, the presence of hydrophilic functional groups (i.e., alcohols and carboxylic acids) in polyesters will increase the degradation rates.[11-19] For example, a hydrolytic degradation study of hydroxyl-functionalized PLA was reported by Hennink, demonstrating the effect of hydroxyl lateral groups in LA-based functionalized monomer.[13] These functionalized lactide monomers were synthesized in benzylether-protected form.

Thereafter, they were homo- and copolymerized in bulk conditions with various amounts of LA using $Sn(Oct)_2$ and benzyl alcohol as the catalyst and initiator, respectively (Scheme 3.5).[13]

R = Me, 1a
R = H, 1b

R = Me, 2a
R = H, 2b
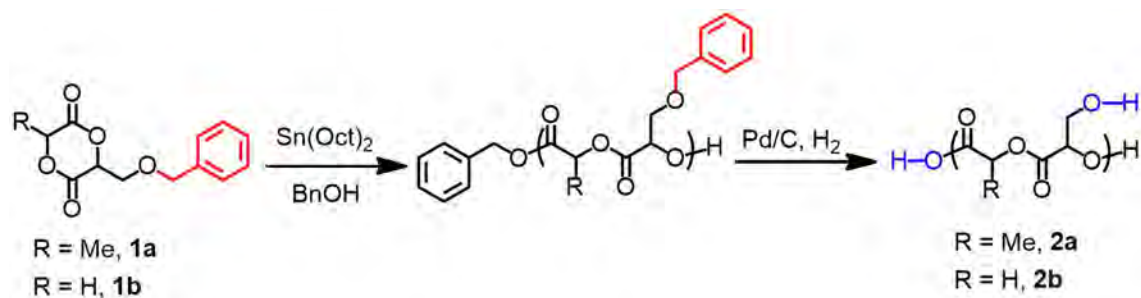
Scheme 3.5 Synthesis of the α-hydroxylated PLA from benzylether-protected LA monomers.[13]

Then, the benzyl protecting groups were removed by hydrogenolysis using a Pd/C catalyst under H_2 atmosphere to yield either poly(lactic acid-co-hydroxymethyl glycolic acid) (**2a**) or poly(lactic acid-co-glycolic acid-co-hydroxymethyl glycolic acid) (**2b**), both substituted with hydroxyl functional groups. Note that the degradation time of the LA/GA-based polymers for completely amorphous PLGA 50/50 was frequently observed in several months, whereas semi-crystalline PLA have degradation times about 1−2 years.[14] The samples for degradation tests were prepared with a thickness of ∼0.4 mm and a diameter of 13 mm corresponding to a weight of about 60 mg of polymer. The degradation study of these hydroxyl-functionalized copolymers was performed with the incubation of pellets in phosphate buffer (pH 7.4) at 37 °C and was monitored by mass-loss measurements, SEC analysis, and ^{1}H NMR.

The PLGA samples retained their mass for more than 20 days and were fully dissolved after 45 days of degradation, whereas the copolymers containing 25% of hydroxyl pendant groups (**2a/2b**) exhibited significant mass loss after 20 days with ≈ 20% weight loss and 40% weight loss, respectively (Figure 3.7). While both copolymers (**2a/2b**) with 50% of hydroxyl pendant groups showed faster degradation with 80% weight loss in 20 days (Figure 3.7).
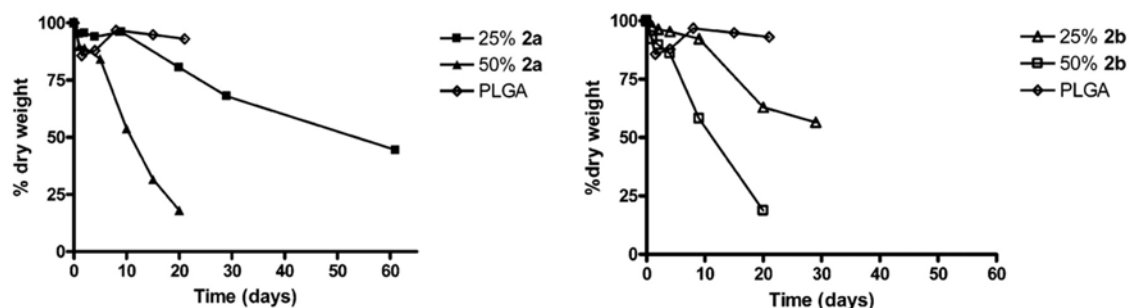

Figure 3.7 Relative mass loss profiles of PLGA and copolymers **2a** and **2b** containing either 25% or 50% of hydroxyl pendant groups (averages of two measurements at each time point).[13]

By increasing the amount of hydroxyl pendant groups in **2a** or **2b** up to 75%, the degradation profiles showed a rapid hydrolysis rate, and the copolymers were then completely dissolved in 4 and 1 days, respectively (Figure 3.8). Notably, an extreme weight loss was observed for homopolymer of **2a** after only 4 h of hydrolysis, and then the samples were completely dissolved after 16 h.
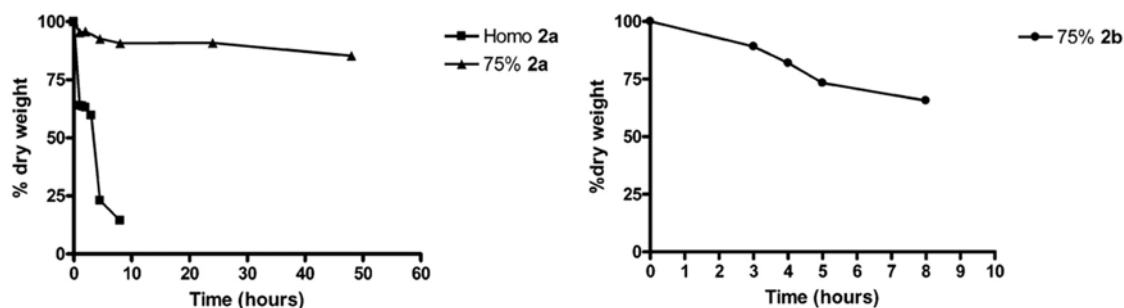

Figure 3.8 Relative mass loss profiles of PLGA and copolymers **2a** and **2b** containing 75% of hydroxyl pendant groups (averages of two measurements at each time point).[13]

The degradation profiles of PLGA and hydroxylated polymers are associated with the water affinity of these polymers, therefore the higher amount of hydroxyl pendant groups in polymer backbone increases significantly the rate of hydrolysis. This study revealed the fact that the degradation rate of PLGA can be tailored by changing the content of hydroxyl pendant groups in the polymers, leading to suitable PLA(GA)-based materials for biomedical and pharmaceutical applications.[13]

What effect would changing from alcohol to carboxylic acid have on the degradation rates of polyesters? To investigate this fact, the carboxyl-functionalized PLA-based copolymers were prepared by copolymerization with Sn(Oct)$_2$, in bulk conditions at 160 °C, from 3-(*S*)-[(benzyloxycarbonyl)methyl]-l,4-dioxane-2,5-dione (BMD) with various amount of *L*-LA (85 – 95 mol%) and subsequent hydrogenolysis of the pendant benzyl esters (Scheme 3.6).[15]
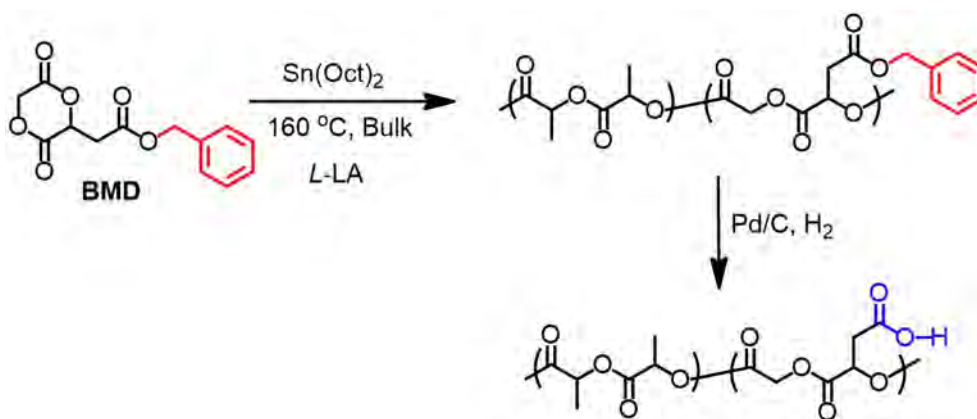
Scheme 3.6 Copolymerization of *L*-LA and BMD and subsequent hydrogenolysis.[20]

The degradation study was set up at 37 °C with several samples of these copolymer films (50 x 5 x 0.1 mm), placed in glass ampoules containing 10 ml of phosphate buffer (pH 7.2). The M_n of these copolymers, observed by SEC analysis, decreased significantly for all samples after a week of hydrolysis. The copolymer containing 5% of carboxylic acids retained a half of M_n after a week of hydrolysis, whereas for the other copolymers with 10 and 15 %, less than 4000 g/mol remained (Figure 3.9). These results show that the hydrolysis is much faster, resulting from the presence of higher amounts of carboxyl groups in the copolymer. Additionally, the exponential decrease in M_n of the materials is attributed to the pendant carboxyl groups that will bind water in both surface and also inside of the polymer film, so that the main chain esters are hydrolyzed rapidly.
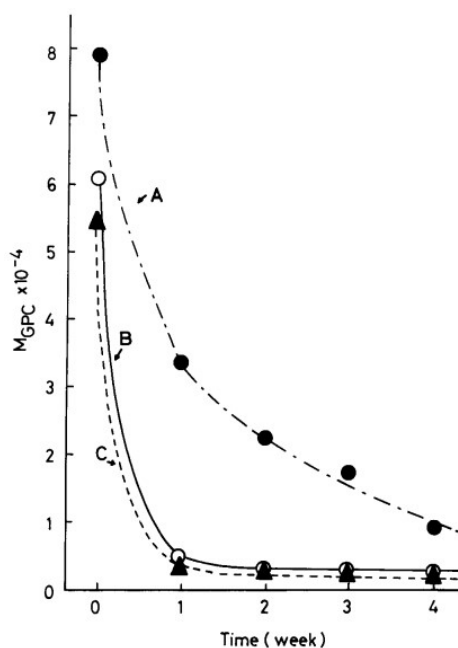

Figure 3.9 Decrease in molecular weight as a function of immersion time for films of 4 with LAC/BMD ratio of 95/5 (**A**), 90/10 (**B**) and 85/15 (**C**).[15]

Comparing both cases of hydroxyl- and carboxyl-functionalized PLA-based materials described above, the M_n from the remaining materials of hydroxyl-functionalized PLA (**2a**) barely changed during the hydrolysis. This suggests that the hydrolysis is performed *via* a surface erosion, thereby conserving the M_n of interior material (Figure 3.10).
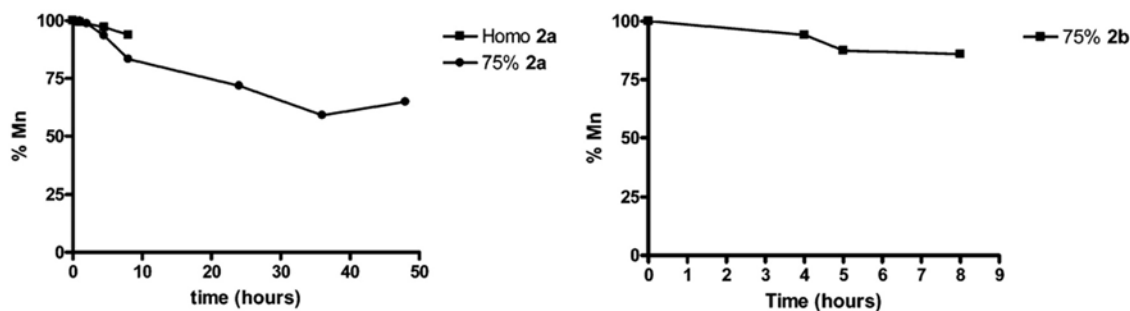
Figure 3.10 Relative decrease in M_n as a function of time for hydroxyl-functionalized PLA (**2a**) and copolymers with 75% of hydroxyl groups.[13]

In contrast, the copolymer with 75% **2a** showed a constant M_n during 40 h of hydrolysis with approximately 40% mass loss (Figure 3.10, left) referring to the degradation pathway as a bulk erosion process. Besides, the copolymers with 25% and 50% of **2a** showed decreasing M_ns with roughly 50% loss after 20 days of hydrolysis (Figure 3.11, left).
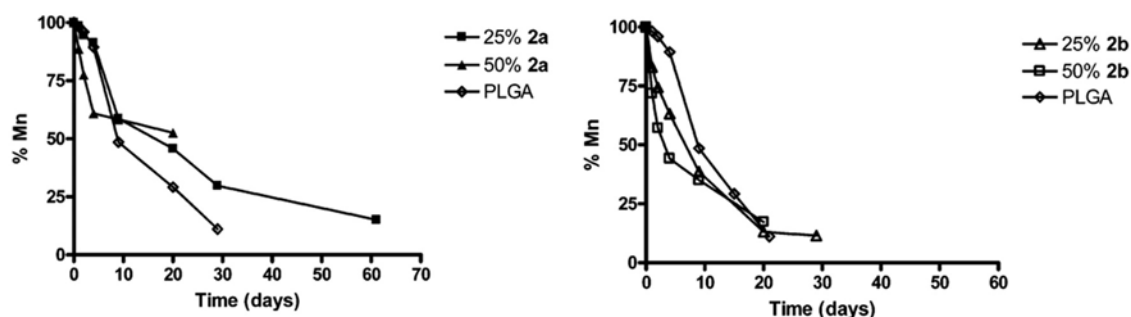
Figure 3.11 Relative decrease in M_n as a function of time for PLGA and copolymers with either 25% or 50% of hydroxyl groups.[13]

However, the copolymers with carboxyl pendant groups showed much more decrease in M_n. Having only 5% of carboxyl groups in copolymer, a half of M_n loss after a week of hydrolysis, while the other copolymers with 10 and 15% loss more than 90% of polymer (Figure 3.9). Note that the M_n of hydroxylated polymer is around 10 – 25 kg/mol, whereas the carboxylated polymer is over 35 kg/mol.[13,15]

The degradation rates of the hydroxyl-functionalized PLA-based polymers are slower than that of carboxyl substituted, because of their higher crystallinity and less water affinity.[16] In contrast to the hydroxyl groups, the carboxyl groups in the polymer backbone inhibit the

polymer crystallization, which results in a more flexible amorphous phase, thereby promoting the degradation. The pendant carboxyl groups impart higher water affinity and may also catalyze the degradation, leading to more rapid rate of hydrolysis as driven by both surface (at initial state) and bulk erosions.[17] Obviously, the presence of hydrophilic carboxyl pendant groups in polymer promotes the degradation much faster than that of hydroxyl pendant groups.

Are there any examples for the carboxyl-functionalized PCL-based polymer? The introduction of carboxyl groups onto a PCL backbone has rarely been reported.[18a,19] Only one example described the degradation of carboxyl-functionalized PCL,[18a] whereas the others are focused on the functional modification, i.e., amidation with 4-amino-TEMPO,[19a] or the modulation of the physico-chemical and biological properties of PCL, such as hydrophilicity or bioadhesion ability.[19b,c]

The benzyloxycarbonylmethyl-ε-functionalized-ε-CL (**BCL**) was obtained in a multistep synthesis in a moderate global yield of 48% (Scheme 3.7a).[18a] Thereafter, copolymerization of **BCL** with CL was achieved using Sn(Oct)$_2$ as a catalyst (Scheme 3.7b) yielding the functionalized copolymers with pendant benzyloxycarbonylmethyl group (PCL-*co*-PBCL). Finally, the benzyl protecting groups were removed by hydrogenolysis using Pd/C as a catalyst under H$_2$ atmosphere (Scheme 3.7c) to obtain PCL-based copolymer containing pendant carboxylic acid groups (PCL-*co*-PCCL).
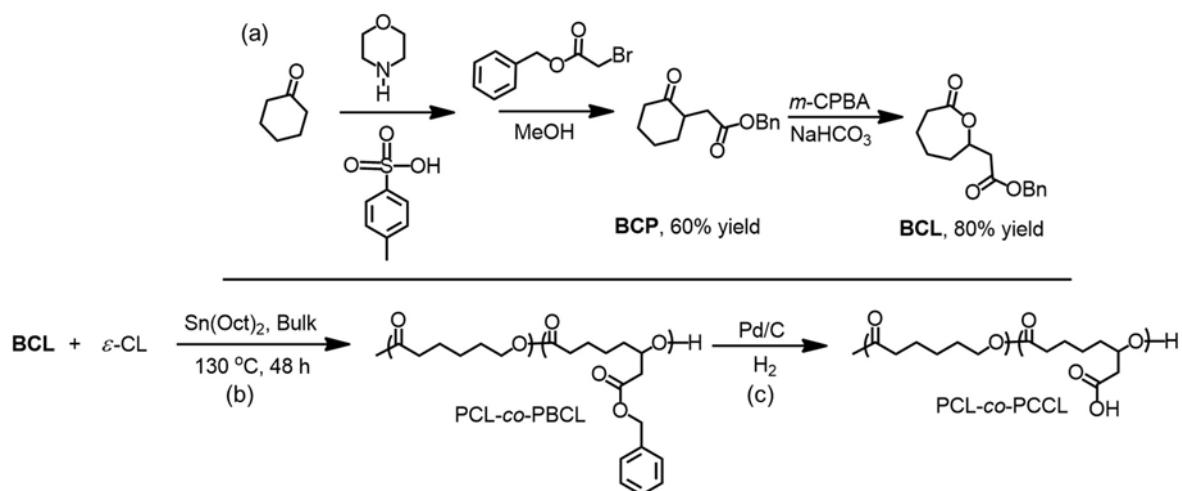
Scheme 3.7 Synthesis of carboxyl-ε-functionalized CL (a), its copolymerization with ε-CL (b), and post-polymerization deprotection (c).[18a]

The degradation of both copolymers, PCL-*co*-PBCL and PCL-*co*-PCCL, was studied in phosphate buffered solution (pH 7.4).[18a] After 10 days of hydrolysis, significant decrease in mass was observed for PCL-*co*-PCCL (9% - 28%), whereas less than 5% weight loss was

observed for PCL-*co*-PBCL (Figure 3.12). At day 55, PCL-*co*-PCCL showed more than 40% weight loss, which is 2-2.5 times faster than that of PCL-*co*-PBCL. In addition, in this study, PCL showed only 2% of weight loss after almost 3 months. Note that the degradation of PCL in buffer pH 7.4 solution requires 4-6 months for mass loss to begin, and then the degradation is complete in 2-3 years.[18b]
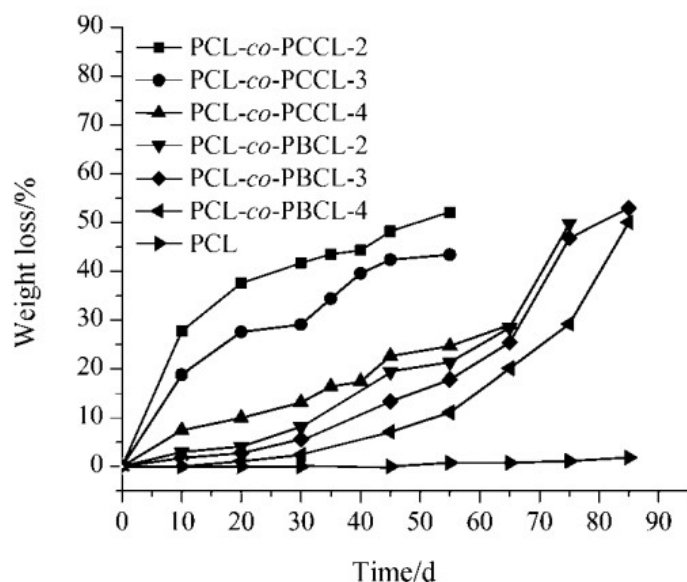
Figure 3.12 Comparative mass loss profiles of PCL and copolymers containing carboxylic acid pendant groups from the degradation in a buffer pH 7.4 at 37 °C.[18a]

According to the mass loss profiles, the degradability of PCL is greatly improved by the pendant carboxylic acid groups, and the degradation rates can be controlled by varying the amount of the pendant carboxylic acid groups onto the PCL backbone. The hydrophilic carboxyl end groups can support significantly the degradation of polyesters by (1) increasing the water affinity of polymer and (2) catalyzing the hydrolysis of polymer backbone from the acid ended chain fragments.[20,21] It is also reported that the carboxyl end groups formed by chain cleavage can catalyze the degradation, so that the hydrolyzed shorter polymer chains/oligomers are readily degraded.[20]

Our objective: we envision the synthesis of a carboxyl-functionalized PCL-based polymer, with the lateral group posted at ε-position so that its behavior in ROP is close of that of ε-DL. As mentioned in Chapter I, a well-controlled approach for the preparation of ε-functionalized-ε-CL monomer remains a challenge due to the regioselectivity problem of the BV reaction depending on the stereo-electronic properties of the substituent. In contrast to the typical multistep synthesis of carboxyl-ε-functionalized CL monomer (Scheme 3.8).[19a] we

propose the two-step synthesis of monomer **2** and **3**. This strategy is thus shorter, atom economical, and more versatile.
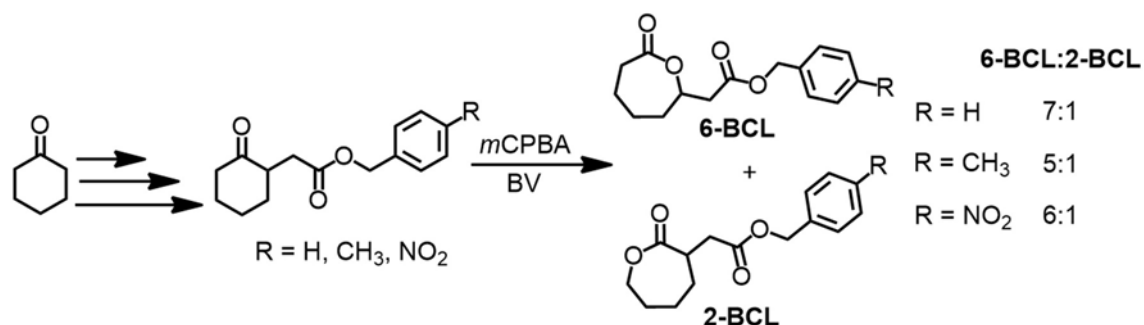
Scheme 3.8 Synthesis route of carboxyl functionalized caprolactone with different protecting groups.[19a]

The new functional monomers (**2** and **3**) have a substituent at ε-position, so that the study of homo- and copolymerization with a close structure monomer like ε-DL were planned to ensure similar behavior in ROP and to investigate their controlled polymerization conditions. ROP of ε-DL was already studied using In-based catalyst under mild conditions, as seen in Chapter II. So now the homo- and copolymerization of the new monomers, **2** and **3**, with ε-DL using similar catalytic system will be presented. Their post-polymerization modification to obtain the targeted carboxyl-functionalized PCL-based polymer will be discussed as well (Scheme 3.9). Finally, the degradation profiles of these copolymers will be discussed in both hydrolytic and enzymatic conditions in the next chapter (IV).
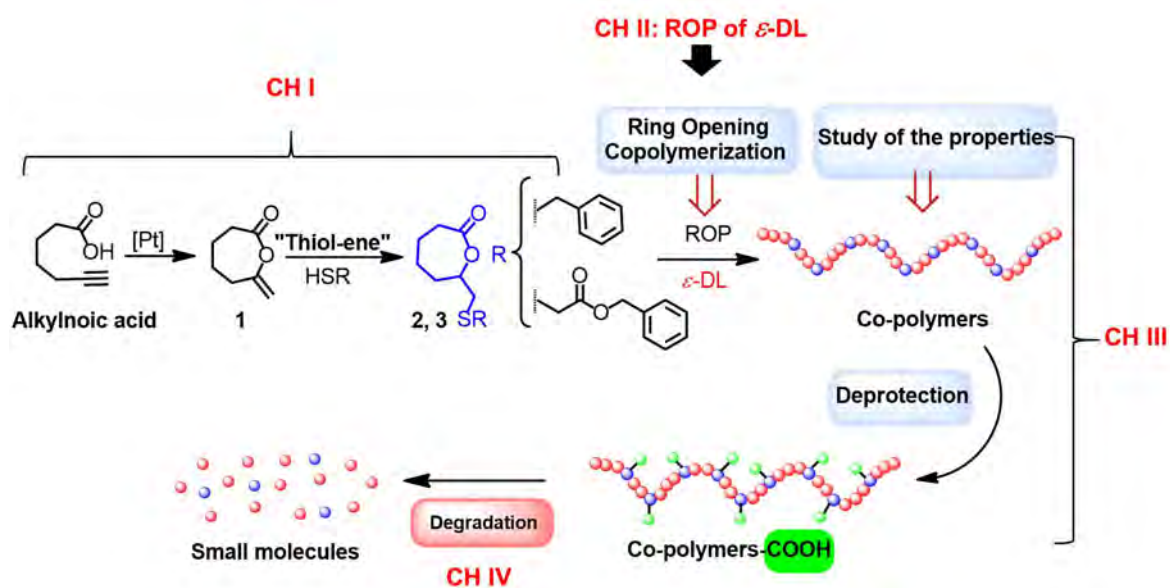
Scheme 3.9 The overview of this project to reach the carboxylated PCL-based polymer and their features in biodegradability.

3.2 Results and discussions

In Chapter II, we described the association of InCl$_3$ and NEt$_3$ for the controlled ROP of ε-DL under mild conditions (Toluene, 3M, 60 °C). Besides the typical ester end-capped PDLs obtained by the initiation of the polymerization with alcohols, amide end-capped ones were obtained using amines. Thanks to the ability of this dual catalyst, block PDL-*b*-PCL and PCL-*b*-PDL, and random PDL-*r*-PCL copolymers were efficiently synthesized by sequential or simultaneous RcoOP with ε-CL. As a result, this catalytic system is a good choice for the ROP of ε-functionalized-ε-CL (e.g., Monomer **2** and **3**). According to the results from Chapter I, Monomer **2** and **3** were efficiently synthesized in gram scale with good yields. Here, we decided to study the homo and copolymerization of new monomers under mild conditions (Toluene, 3M, 60 °C) following the described protocol for ROP of ε-DL.

3.2.1 Homopolymerization of the ε-functionalized-ε-lactones catalyzed by InCl$_3$/NEt$_3$

Homopolymerization of monomers **2** or **3** promoted by the association InCl$_3$/NEt$_3$ (1/2 ratio) was first evaluated initiated by 2,2-dimethyl-1-propanol, with a monomer/alcohol ratio of 25, in 3 mol/L toluene solution at 60 °C (Scheme 3.10).
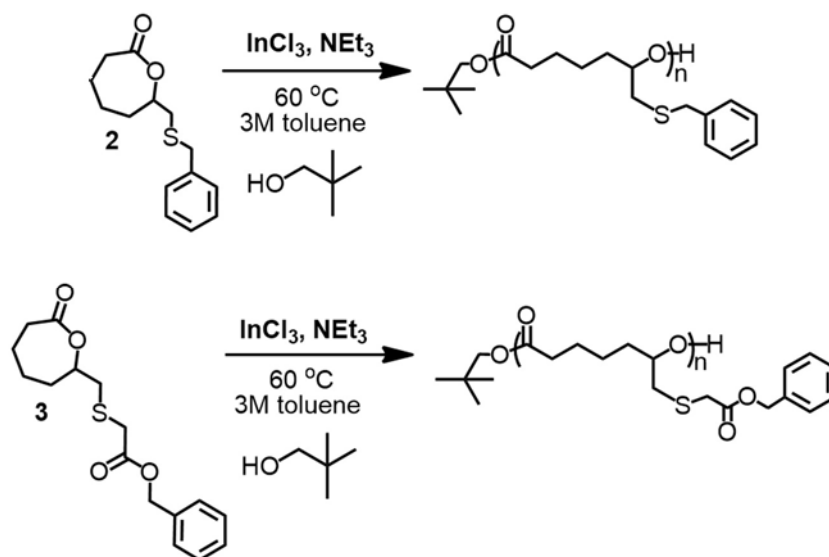
Scheme 3.10 ROP of new functionalized CL, either monomer **2** or **3**, promoted by InCl$_3$/NEt$_3$.

HomoROP of **2** is quite slow (94% of conversion was observed after 60 hours), while the ROP of **3** is even slower with only 30% conversion after 48 hours, as determined by ^{1}H NMR. These results contrast markedly with those described in chapter 2 for the ROP of ε-DL

under similar conditions. PDL of controlled properties was obtained in 2 hours (M_n = 5600 g/mol, $Đ$ = 1.11). Both ROPs were quenched with an excess of PhCO$_2$H, and then the crudes were analyzed by ^{1}H NMR spectroscopy and SEC analysis. Interestingly, the thiol moiety is stable under the polymerization conditions without performing any side reaction such as elimination, as evidenced by ^{1}H NMR spectroscopy. However, low M_ns values (1100 g/mol for P**2** and 900 g/mol for P**3**) were observed by SEC analyses, differing from the theoretically expected values . Additionally, in contrast to the ROP of ε-DL, these functional polymers showed multimodal signals in chromatogram (Figure 3.13).
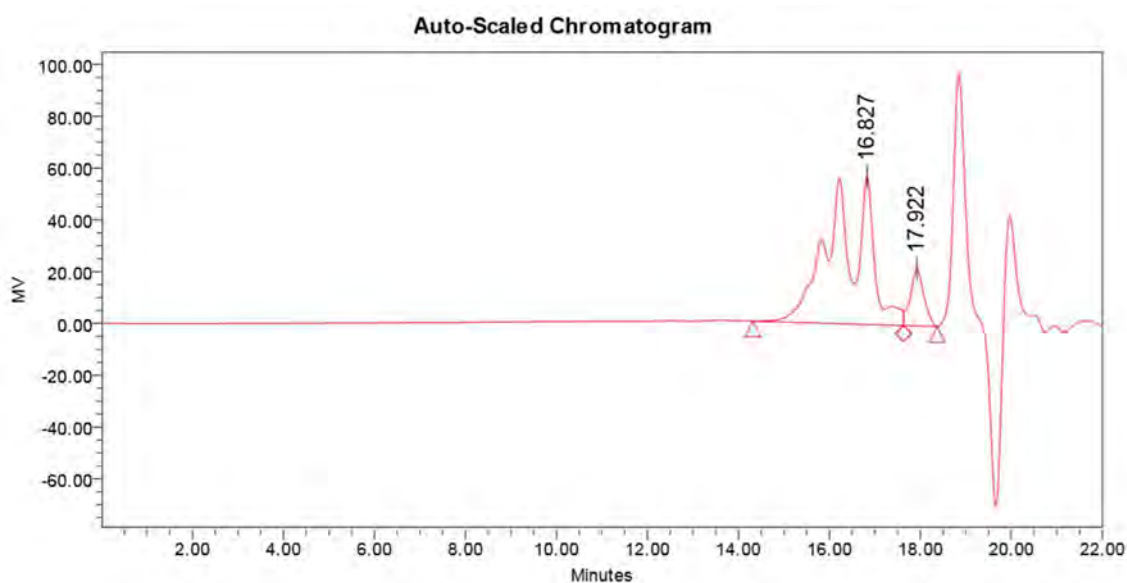
Figure 3.13 SEC trace of P**2** represents multimodal in chromatogram.

Thus, it appears that homopolymerization of **2** and **3** is not only very slow but also occurs with low control. As described in Chapter 2 for simultaneous copolymerization of ε-DL with ε-CL, a random PCL-*r*-PDL copolymer with regular monomer distribution along the polymer chain was obtained, despite the different reactivity of these monomers in homopolymerization that could favor the formation of copolymers with blocky structure rather than true random copolymers. Interestingly, monomer conversion monitoring revealed that both monomer were consumed at similar rate. A slow-down on the consumption rate of ε-CL was observed, while ε-DL was converted at a slightly higher rate compared with the homoROP of ε-DL and of ε-CL. These results revealed that the more reactive monomer can actually promote higher rates of the ROP of the less reactive monomer. This prompted us to directly investigate the copolymerization of new monomers (**2** and **3**) with ε-DL.

3.2.2 Copolymerization of ε-DL with the new monomers (2 and 3)

Taking advantage of the living and controlled character of the ROP of ε-DL promoted by InCl$_3$/NEt$_3$, copolymerization of ε-DL with **2** was initially carried out at 60 °C with various ε-DL/**2** ratios of 45:5, 40:10, 35:15, and 25:25 for 18 h, 24 h, and 48h, respectively (Scheme 3.11).
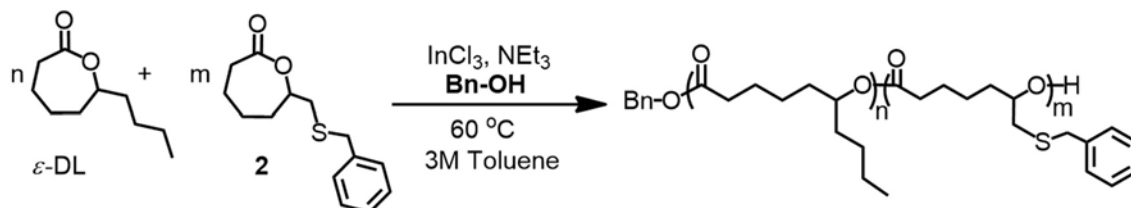
Scheme 3.11 Copolymerization of ε-DL with **2** catalyzed by InCl$_3$/NEt$_3$ using BnOH as an initiator.

The reactions were performed by adding a mixture of ε-DL and the new monomer (**2**) into a stirring suspension of BnOH (1 equiv.), NEt$_3$ (2 equiv.), and InCl$_3$ (1 equiv.) in Toluene ($[\mathbf{2}]_0 = [\mathrm{DL}]_0 = 3$ mol/L). The consumption of both monomers was monitored by ^{1}H NMR spectroscopy (see Figure 3.14 for an example). Looking at the results in Table 3.1 (entry 1) for the ROcoP with the ε-DL/**2** ratio of 45:5, ε-DL and **2** were completely consumed after 18 hours. The crude from copolymers containing 10 mol% of **2** was quenched with an excess of benzoic acid, and the solvent was evaporated under vacuum. The crude was then dissolved in a minimum volume of DCM following by the precipitation in cold methanol (two consecutive times), and then filtered and dried under vacuum to yield yellowish sticky materials in an excellent yield (90%). First of all, we can note that although full conversion of the two monomers is achieved, it takes place in significantly longer times than that of homoROP of ε-DL (3 h for homoROP ε-DL *vs* 18 h for copolymerization of ε-DL with **2**).
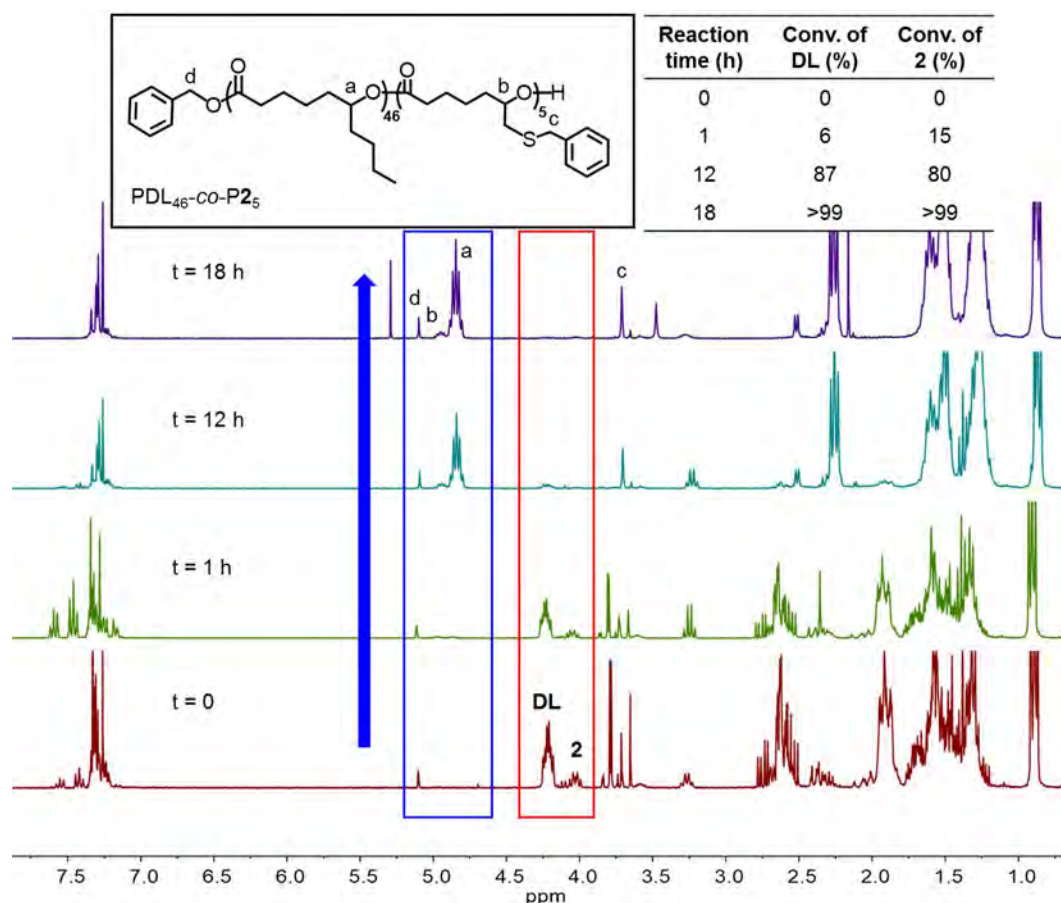
Figure 3.14 Stacked ^{1}H NMR Spectra (CDCl$_3$, 300 MHz) represents the growth of copolymer of ε-DL with **2 for** the ratio of 45:5.

A copolymer with a molecular weight of 9200 g/mol and low molecular distributions ($\DJ$ = 1.17) was obtained according to SEC analysis. The ^{1}H NMR spectrum shows the disappearance of proton signals from both monomers (at 4.22 ppm and at 4.04 ppm, corresponding to the –CHO– proton from ε-DL and **2**, respectively), giving rise to the multiplet signals (a) at 4.88 – 4.80 ppm for the –CHO–$_{PDL}$ and (b) at 4.97 – 4.90 ppm for the –CHO–$_{P2}$. In addition, the spectrum also displays two singlet signals at 5.09 (d) and at 3.71 (c) ppm corresponding to the two protons of benzyl ester group resulting from ROP initiation by BnOH and the two protons of the methylene group from –S–CH_2Ar (Figure 3.15). The chain-end group was also investigated by ^{1}H NMR spectroscopy, as seen by a broad signal at 3.59 (a'+ b') ppm corresponding to the terminal CHOH group. The relative 2 to 1 value of the integration of signals d and (a'+ b') is consistent with most of the chains bearing the same chain-ends ester/alcohol, confirming efficiency of the initiation. Additionally, the relative integration value between signals of proton from PDL and P**2** (a and b) and from BnOH (d) close to 46:5 (ε-DL: **2**) which indicates a composition and DP$_{NMR}$ in accordance with the M$_0$/I$_0$ (see ^{1}H NMR spectrum in Figure 3.15).
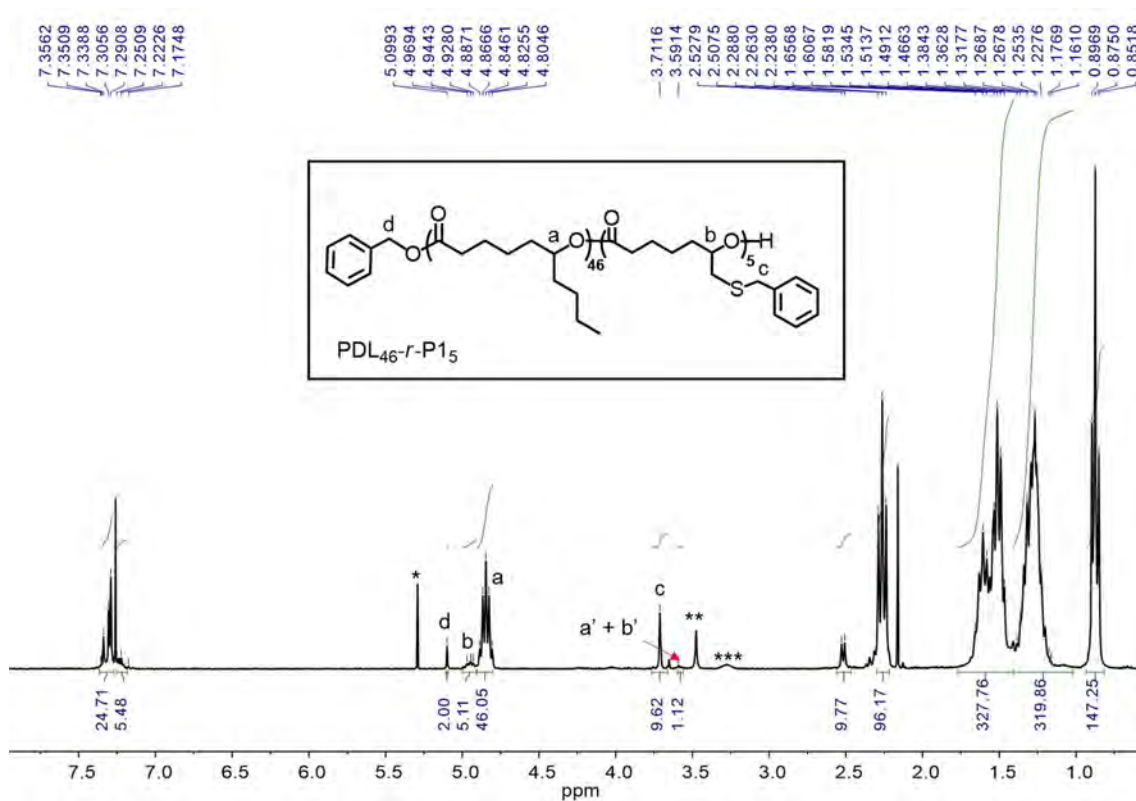
Figure 3.15 ^{1}H NMR spectrum (CDCl$_3$, 300 MHz) of copolymers of ε-DL and **2** as PDL$_{46}$-co-P**2**$_5$ (residual of *DCM, **MeOH, and ***ammonium salt).

We decided then to increase the amount of **2** in the ROcoP with the ε-DL/**2** ratio of 40:10 (Table 3.1, entry 2). This copolymerization took longer time than the first one, and it was not complete. Conversion of 98% and 87% for ε-DL and **2**, respectively, were achieved after 24 hours, and the conversion of both monomers did not change even after an additional 24 hours. Low M_n (SEC) that significantly differ from the theoretically expected value and also the M_n value calculated from DP$_{NMR}$ was obtained (5300 g/mol), although Đ are narrow (1.10). With the increase of the amount of monomer **2** up to 30 mol% and 50 mol% (Table 3.1, entry 3 and 4), no copolymerization was observed after 48 hours (none of the monomers were consumed).

Table 3.1 Copolymerization of ε-DL with **2** promoted by InCl$_3$:NEt$_3$ using BnOH as an initiator.

Entry	ε-DL:**2**:Initiator	Amount of **2** (mol%)	Reaction time (h)	Conv. of ε-DL (%)	Conv. of **2** (%)	Mn^a (Theo.)	M_n (g/mol)^b	$Đ^b$	DP^a DL/**2**
1	45:5:1	10	18	>99	>99	8900	9200	1.17	46/5
2	40:10:1	20	24	98	87	9100	5300	1.10	32/8
3	35:15:1	30	48	No reaction					
4	25:25:1	50	48	No Reaction					

^{a}Determined from ^{1}H NMR spectra, ^{b}Calculated from SEC traces.

Using the same polymerization conditions and 3,5-dimethoxybenzyl alcohol (DMBA) as initiator (to acquire accurately the integration of protons from the ^{1}H NMR spectra for the DP calculation), copolymerization of ε-DL with **3** was then investigated with various ε-DL/**3** ratio of 49:1, 47.5:2.5, 45:5, 42.5:7.5, 40:10, and 35:15 (Scheme 3.12).
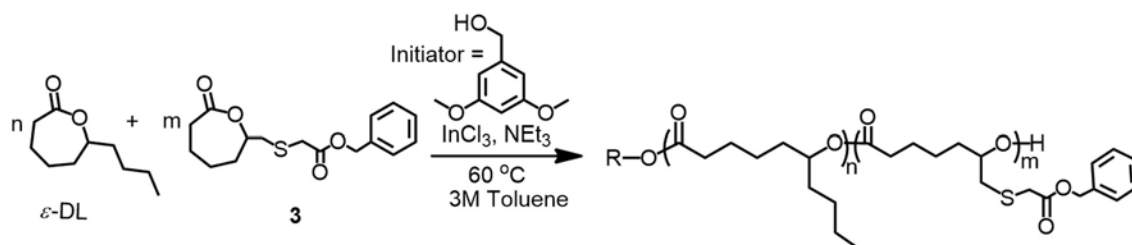
Scheme 3.12 Copolymerization of ε-DL with **3** catalyzed by InCl$_3$/NEt$_3$ using DMBA as an initiator.

Looking at the result in Table 3.2 (entry 1-5), full conversion was observed after 4, 8, 12, 18 hours. Copolymers containing 2% to 20% of **3** with M_ns ranging from 5700 to 11700 g/mol were obtained after quenching the polymerization with an excess of benzoic acid and precipitation in cold methanol. The obtained M_ns (SEC) slightly differ from the theoretically expected value, especially for the copolymers containing high amounts of **3** (Table 3.2, entry 4 and 5) and relatively broad molecular distributions ($Đ$) were observed (1.33-1.38). Note that these M_n values are relative, since we are working with RI detection and calibration with polystyrene standards. Currently, we do not have information about the behavior of these copolymers or about the impact of the lateral groups on the hydrodynamic radius of the polymer chains.

Table 3.2 Copolymerization of ε-DL with **3** promoted by InCl$_3$:NEt$_3$ using DMBA as an initiator

Entry	ε-DL:3:Initiator	Amount of 3 (mol%)	Reaction time (h)	Conv. of ε-DL (%)	Conv. of 3 (%)	Mn^a (Theo.)	M_n (g/mol)^b	$Đ^b$	DP^a DL/3
1	49:1:1	2	4	>99	>99	8800	11700	1.33	49/1
2	47.5:2.5:1	5	8	>99	>99	9000	11100	1.34	47/3
3	45:5:1	10	12	>99	>99	9300	9100	1.36	45/5
4	42.5:7.5:1	15	18	>99	>99	9700	7900	1.46	43/7
5	40:10:1	20	18	>99	>99	10000	5700	1.38	40/10
6	35:15:1	30	48			No Reaction			

^{a}Determined from ^{1}H NMR spectra, ^{b}Calculated from SEC traces.

Similar to the case of **2**, the reactions took longer time than that of homoROP of ε-DL (3 hours), and the M_ns/$Đ$s were found slightly different from the PDL (for example, PDL DP50 with $M_n/Đ$ = 11200/1.11 *vs* copolymer containing 10 mol% of **3** with $M_n/Đ$ = 9100/1.36). For the higher amounts of **3**, the benzyl ester thiol pendant groups impact not only the ROP rates but also the hydrodynamic volume of PDL. To confirm the limitation of ε-DL/**3** ratio that can used for this copolymerization, higher amounts of monomer **3** were used (30 mol%, see Table 2, entry 6). No copolymerization occurred after 48 hours, since none of the monomers was consumed.

Figure 3.16 shows the ^{1}H NMR spectrum of copolymer containing 10 mol% of **3** (ε-DL/**3** ratio of 45:5). It depicts the typical signals expected for a PDL polymer chain at (a) 4.85 ppm corresponding to the –CHO– proton, at 1.64 – 1.20 ppm for the –CH_2– groups, and at 0.87 ppm for the methyl group. In addition, the multiplet signals (b) at 5.03 – 4.98 ppm for the –CHO–P3, a signal (d) at 3.29 – 3.15 ppm for the S–CH_2–COOBn, and (c) at 2.86 – 2.67 for the –OCH–CH_2–S– are detected. The spectrum also shows a singlet signal at 5.09 (e) corresponding to the two protons of the benzyl ester group from monomer **3** (Figure 3.16).
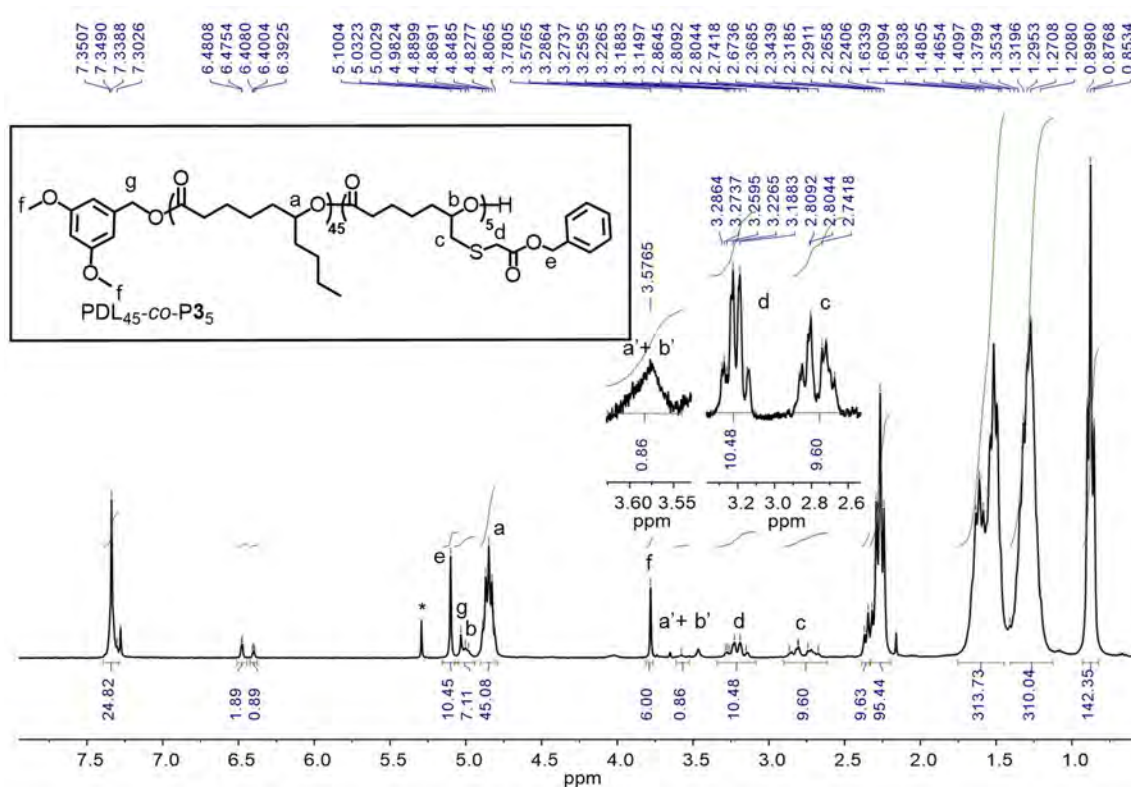
Figure 3.16 ^{1}H NMR spectrum (CDCl$_3$, 300 MHz) of copolymers of ε-DL and **2** as PDL$_{46}$-co-P**2**$_5$ (*DCM).

DP$_{NMR}$ was determined accurately using six protons (f) of (–OCH$_3$)$_2$ groups from DMBA. The chain-end group fidelity was also investigated by ^{1}H NMR spectroscopy. A broad signal at 3.58 ppm (a'+ b') corresponding to the terminal CHOH group is observed in close agreement with the relative 6 to 1 value of the integration of signals f and (a'+b').

As both monomers (ε-DL and **3**) display a markedly different reactivity in homo-polymerization, a block copolymer could be formed rather than a random one. To explore the copolymer architecture, monitoring of the monomer conversions by ^{1}H NMR spectroscopy was investigated using the ε-DL/**3** ratio of 80:20, promoted by InCl$_3$:NEt$_3$ with DMBA as an initiator at 60 °C in Toluene solution ([M]$_0$ = [DL]$_0$ =3M). The results showed more than 80% conversion of the two monomers in 72 hours (Figure 3.17). A slow-down on the consumption rate of ε-DL was observed (less than 40 % of conversion in 12 hours), while a faster consumption rate of monomer **3** was also found (more than 45 % of conversion in 12 hours). These results revealed that simultaneous conversion of the two monomers and are consistent with a random structure.
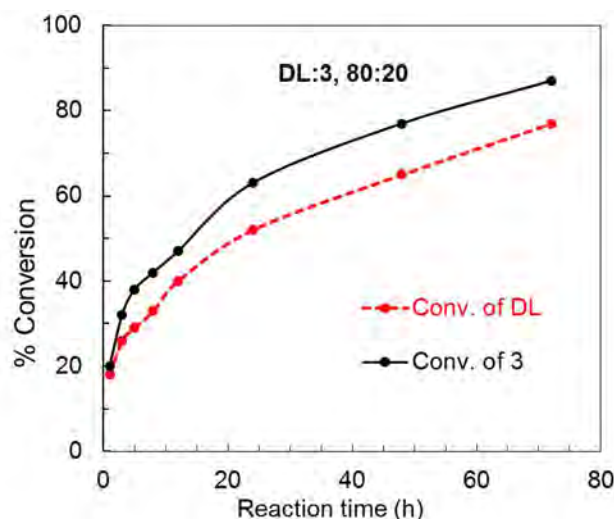
Figure 3.17 Monomers conversion of ROcoP of ε-DL and **3** monitored by ^{1}H NMR, showing that both monomers are consumed at similar rate.

Furthermore, ^{13}C NMR spectroscopy is diagnostic for the formation of the random copolymer (Figure 3.18). The ^{13}C NMR spectra of these copolymers reveal broad or multiple signals at ~173.54 and 170.05 ppm for C=O groups from PDL and P**3**, indicating the presence of different environments for the CO groups of each monomer as a result of a statistical distribution. Notably, similar spectral characteristics are observed in the –C*H*O– region, as seen by the multiple signals at 73.85 ppm (PDL) and 66.12 ppm (P**3**) in the ^{13}C NMR spectrum.
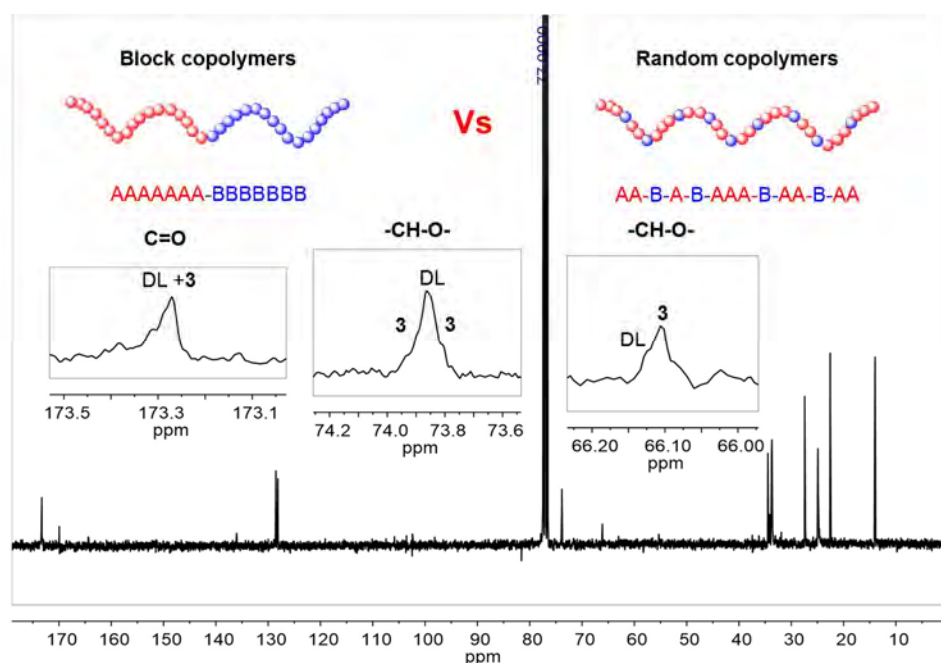
Figure 3.18 ^{13}C NMR spectrum (CDCl$_3$, 300 MHz) of random PDL-*r*-P3 copolymer (40:10).

As a result, a random PDL-*r*-P**3** copolymer with regular monomer distribution along the polymer chain was obtained, as suggested by the monitoring of the monomers conversion and ^{13}C NMR spectroscopy.

What about the thermal properties of these copolymers? DSC analysis illustrates the impact of the benzyl ester thiol pendant groups on the thermal properties of these copolymers (Table 3.3). Copolymers containing 2% to 20% of monomer **3** feature decreasing glass transition (T_g) values with the increasing amount of **3** (-73, -68, -69, -56, and -54 °C for 20%, 15%, 10%, 5%, and 2% of monomer **3** in copolymers, respectively) that differ from the homoPDL DP50 (-53°C). No melting transition (T_m) was detected in all cases, as expected for amorphous polymers. Finally, there is slight difference on the degradation temperature of these copolymers and PDL DP50.

Table 3.3 Thermal analysis data for copolymers of ε-DL and **3**, and PDL DP50.

ε-DL:**3**:Initiator	Amount of **3** (mol%)	T_g (°C)	T_d (°C)
PDL DP50	0	-53	356
49:1:1	2	-54	339
47.5:2.5:1	5	-56	344
45:5:1	10	-69	345
42.5:7.5:1	15	-68	346
40:10:1	20	-73	345

3.2.3 End-capping by acetylation and debenzylation by hydrogenolysis

3.2.3.1 End-capping by acetylation

As the targeted functional groups in the prepared copolymers were introduced in a protected form, the deprotection of the pendant functional groups is required. Before doing this, the terminal hydroxyl groups of the polymer chains were acetylated with acetic anhydride to avoid competitive reactions (especially lactonization with an adjacent COOH group or depolymerization) (Scheme 3.13).
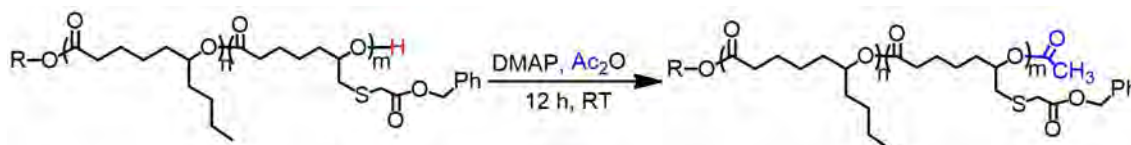
Scheme 3.13 Acetylation of copolymers using DMAP as a catalyst.

The acetylation of the copolymers containing 2% or 5% of benzyl ester thiol pendant groups was successfully achieved using DMAP as a catalyst with the copolymer/DMAP/acetic anhydride ratio of 1:1:2 in DCM. The mixture was stirred for 12 hours at room temperature, and the complete acetylation of the terminal alcohol units was confirmed by ^{1}H NMR spectroscopy (Figure 3.19). DMAP, acetic acid, and residue of acetic anhydride were removed by acidic aqueous work-up, and the solvent was removed under vacuum. The crude was then dissolved in a minimum volume of DCM and precipitated twice in cold methanol, filtered, and dried under vacuum to yield the acetylated copolymer as a sticky material in good yields (80% and 82% isolated yield for 2 gram scale of 2% and 5% acetylated copolymer, respectively). Looking at the ^{1}H NMR spectrum in Figure 3.19, the disappearance of the broad signal corresponding to the –CHOH proton at 3.59 ppm is noted, while the typical signals expected for a PDL polymer chain are observed in the ^{1}H NMR spectrum. In addition, a singlet signal appears at 2.02 ppm (h) corresponding to the methyl ester group (–CH_3) resulting from the end-capping by acetate. Notably, all characteristic signals of DMBA are retained, and the relative integration of signals f and (a + b) confirms that no transesterification reactions have occurred.
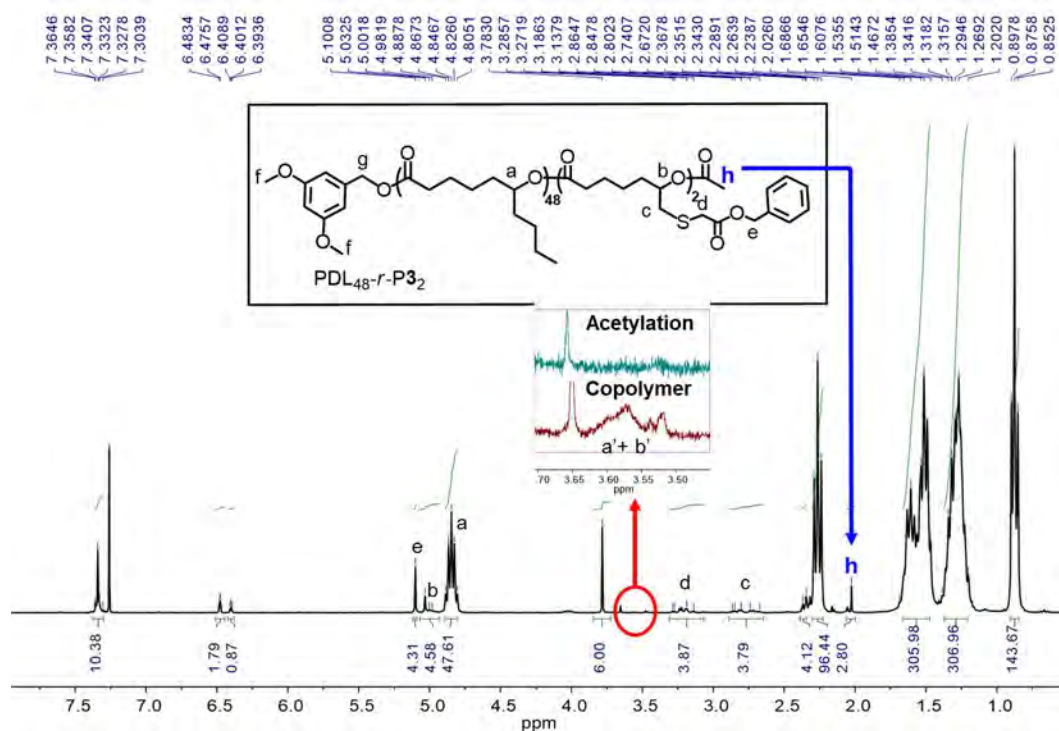

Figure 3.19 ^{1}H NMR spectrum (CDCl$_3$, 300 MHz) of acetylated copolymers of ε-DL and **3**, PDL$_{48}$-r-P3$_2$

3.2.3.2 Debenzylation by hydrogenolysis

Palladium on carbon (Pd/C) is known as an efficient catalyst for hydrogenolysis or debenzylation.[22,23] Following the conventional hydrogenolysis protocols (Scheme 3.14), the benzyl ester thiol pendant groups (2%) in acetylated copolymers were initially deprotected using the commercially available Pd/C catalyst (20 % w/w) in EtOH/EtOAc (1:9) under H_2 atmosphere (Table 3.4, entry 1). The benzyl ester was completely removed after 48 hours of hydrogenolysis, as demonstrated by ^1H NMR. However, the polymer backbone was also affected, as the spectrum showed the disappearance of the signals attributed to DMBA as well as the apparition of several unexpected broad or multiple signals at 5.00-5.75 ppm.
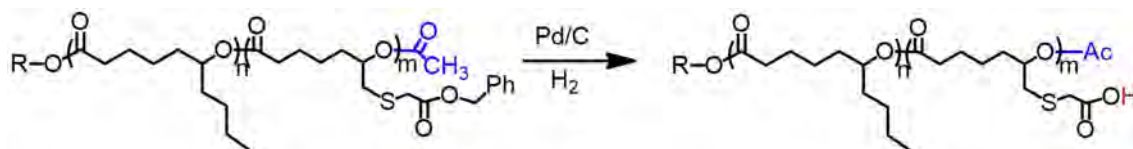
Scheme 3.14 The debenzylation of acetylated copolymers containing benzyl ester thiol groups using commercially available Pd/C as a catalyst.

Increasing the amount of Pd/C to 50% w/w, led to similar result after 24 hours (Table 3.4, entry 2). Changing the solvent mixture from EtOH/EtOAc (1:9) to EtOH/DCM (1:5) and using 20 % w/w of Pd/C for 18 h did not affect the polymer but only 22 % of conversion was observed (Table 3.4, entry 3). The debenzylation was undertaken using more Pd/C catalyst (50% w/w); however, the polymer decomposition was also detected (Table 3.4, entry 4). Adjusting the ratio of solvent mixture of EtOH/DCM to 2:1 and using 50 % w/w of Pd/C, led to 68 % of conversion without polymer decomposition after 12 hours. Unfortunately, the degradation of PDL backbone was still observed after 18 hours (Table 3.4, entry 5&6).

Table 3.4 The screening of reaction conditions applied for the debenzylation of acetylated copolymer containing 2% of benzyl ester thiol.

Entry	Solvent & ratio		Pd/C (% w/w)	t (h)	Conv. (%)	Polymer decomposition
1	EtOH:EtOAc	1:9	20%	48	>99	Found
2	EtOH:EtOAc	1:9	50%	24	>99	Found
3	EtOH:DCM	1:5	20%	18	22	Not found
4	EtOH:DCM	1:5	50%	12	99	Found
5	EtOH:DCM	2:1	50%	12	68	Not found
6	EtOH:DCM	2:1	50%	18	99	Found

Despite the number of applications described in the literature, the hydrogenolysis following a standard protocol with Pd/C as a catalyst shows some drawbacks.[22,23] For example, the quality of commercially available batches of Pd/C and the random distribution and size of Pd^0 nanoparticles over the charcoal are unpredictable.[22a,22b,23]

In the last few years, an alternative protocol based on the preparation of Pd/C nanoparticles was reported as a catalytic system for hydrogenation and for the hydrogenolysis of O-benzyl groups.[23] The i*n situ* preparation of an active Pd^0/C catalyst was achieved by mixing charcoal (90wt% to Pd) and $Pd(OAc)_2$ (0.05 mol%) in a THF solution, and then stirring the mixture for 30 minutes prior to use. Following this procedure, the hydrogenolysis of the benzyl ester thiol pendant groups in the copolymers was initially carried out using similar reaction conditions (10 % w/w of Pd nanoparticles at room temperature under H_2 atmosphere) except the solvent that was changed to EtOH (Table 3.5, entry 1). After 12 hours, the debenzylation was completed, but some polymer decomposition was also detected by SEC analysis (a small signal of 600 g/mol was found with Đ of 1.08). No polymer decomposition was found when the reaction time was decreased to 6 hours. However, only 56 % of conversion was detected (Table 3.5, entry 2). Using a higher amount of Pd^0/C nanoparticles (15 % w/w, see Table 3.5, entry 3 and 4), 72 % of conversion was observed without the decomposition of polymer backbone after 6 hours. Performing the debenzylation with similar conditions for 9 hours, a small removal of initiator (DMBA) was also found.

Table 3.5 The optimization of hydrogenolysis conditions using *in situ* preparation of Pd/C.

Entry	Pd/C (% w/w)	t (h)	Conv. (%)	Polymer decomposition	M_n /Đ (SEC)
1	10	12	>99	Found	7100/1.29 with a small chromatogram of 600/1.08
2	10	6	56	Not Found	10500/1.24
3	15	6	72	Not Found	10500/1.29
4	15	9	92	a small removal of initiator	10800/1.21
5	20	9	98	Not found	10800/1.20
6[a]	20	12	>99	Not found	11500/1.23
7[b]	20	14	>99	Not found	11600/1.22
8[c]	20	16	>99	Not found	10200/1.18

[a]400 mg scale with 70% isolated yield. [b]500 mg scale with 88% isolated yield. [c]1 g scale with 92% isolated yield.

All these results reveal that decomposition of the polymer backbone is a major issue of the hydrogenolysis. This issue may arise from the competitive reaction (i.e., transesterification,

as the solvent is EtOH). To address this observation, higher amounts of Pd/C nanoparticles were used to drive the debenzylation rather than the polymer decomposition. 20% w/w of Pd/C catalyst was then introduced for this hydrogenolysis, and the reaction with 400 mg scale was set up for 12 hours (Table 3.5, entry 6 – 8). Gratifyingly, the reaction was completely achieved without observing any decomposition of polymer or the removal of the initiator. Moreover, this protocol can even be applied to 1-2 gram scale reactions, obtaining similar results (without decomposition) in excellent isolated yields (92 % yield for 1 gram scale). After the complete removal of benzyl protecting groups, an excess amount of charcoal was added to the mixture, and then the Pd/C was removed by filtration over Celite following by solvent evaporation. The crude was dissolved in DCM, precipitated in cold pentane, and dried under vacuum overnight to yield a sticky material. The complete removal of the benzyl protecting groups (–OBn) is easily verified from the disappearance of all aromatic signals belonging to the –OBn in the ^{1}H NMR spectrum, compared to the ^{1}H NMR spectra of protected copolymers (Figure 3.20).
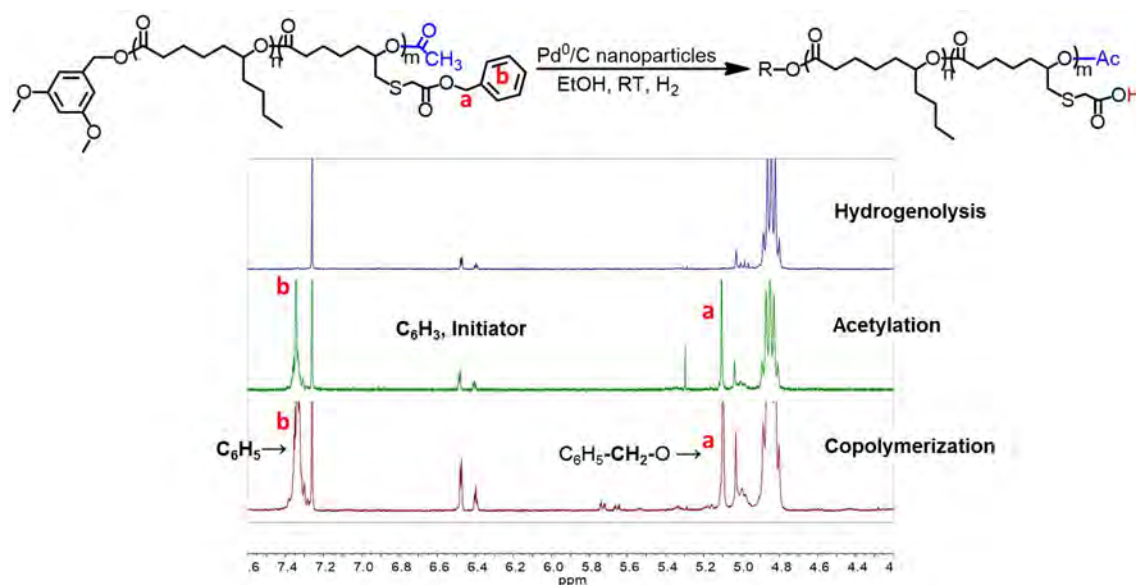
Figure 3.20 Stacked ^{1}H NMR spectra (CDCl$_3$, 300 MHz) of copolymers containing 2% of benzyl ester thiol (Copolymerization), acetylated copolymers (Acetylation), and deprotected copolymer (Hydrogenolysis).

The hydrogenolysis of copolymer containing 5% of benzyl ester thiol pendant groups was attempted using the same reaction conditions. However, the debenzylation of these copolymers was not complete, as 60 % of conversion was found after 14 hours. We thus decided to use higher amounts of Pd/C nanoparticles, from 20% w/w to 40% w/w. With these reaction conditions, the hydrogenolysis was also successfully achieved in 18 hours without degradation of the polymer backbone. Moreover, this protocol can be used in 2 gram scale

yielding the copolymers containing 5% of carboxylic acid pendant groups in an excellent isolated yield (85%) without polymer decomposition.

The structure of copolymers containing 5% of carboxylic acid pendant group was confirmed by ^{1}H NMR spectroscopy. Again, the complete removal of the benzyl protecting groups was confirmed by the disappearance of all aromatic signals belonging to the –OBn in the ^{1}H NMR spectrum (Figure 3.21). In addition, the ^{1}H spectrum shows all the typical characteristics signal of a PDL polymer chain (e.g., at 4.85 ppm (a) corresponding to the –CHO$_{PDL}$) as well as the multiplet signals of two protons (b) from –CHO$_{P3}$ at 5.01 ppm.
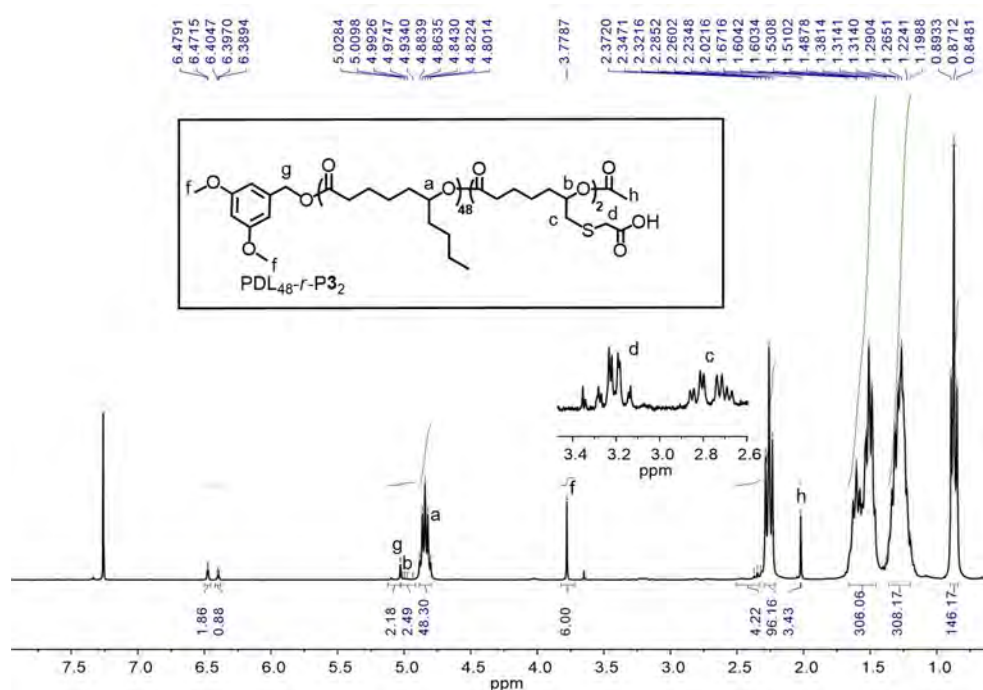
Figure 3.21 ^{1}H NMR spectrum (CDCl$_3$, 300 MHz) of copolymers containing 5% of carboxylic acid, PDL$_{48}$-r-P3$_2$-COOH.

Notably, SEC analyses showed that none of these three steps affect the polymer backbone, as evidenced by the fairly constant M_n with narrow Đ (Table 3.6). Thermal analysis reveals a slight change in a glass transition temperature, as more negative Tg values were detected from copolymers to acetylated and deprotected copolymers.

Table 3.6 SEC and thermal analysis from copolymers of ε-DL and **3**, acetylated copolymers, and carboxyl-functionalized copolymers.

PDL$_{47.5}$-r-P3$_{2.5}$	M_n (g/mol)	Đ	T_g (ºC)	PDL$_{49}$-r-P3$_1$	M_n (g/mol)	Đ	T_g (ºC)
Polymerization	11000	1.32	-51.8	Polymerization	10400	1,23	-54
Acetylation	9000	1,27	-53.8	Acetylation	11000	1,19	-54.3
Hydrogenolysis	8200	1.19	-58.5	Hydrogenolysis	10300	1,17	-55,9

3.3 Conclusions

In summary, we described the preparation of copolymers of ε-DL and monomers **2** or **3** using the dual catalyst (InCl$_3$/NEt$_3$) with either BnOH or DMBA as an initiator, under mild conditions (toluene, 3M, 60 °C). Copolymers with DP and compositions close to the targeted ones were prepared. Based on the monitoring of monomer conversions by NMR spectroscopy, the architecture of these copolymers were confirmed as random copolymers, e.g. P(DL-*r*-**3**). To obtain the carboxyl-functionalized PDL-based copolymers, the post-polymerization modification of copolymers containing 2% and 5% of benzyl ester thiol was achieved in two steps: (1) acetylation and (2) hydrogenolysis. First, the terminal hydroxyl groups were acetylated with acetic anhydride to avoid the competitive reactions. Then, the carboxylic acid pendant groups in copolymers are obtained using a simply and reliable protocol for hydrogenolysis of O-benzyl group, the *in situ* preparation of an active Pd^0/C catalyst under H$_2$ atmosphere. The complete removal of the benzyl protecting groups is demonstrated by the disappearance of all aromatic signals from ^{1}H NMR spectrum. In addition, this protocol also respects the integrity of the polymer backbone, as none of post-polymerization steps affect the polymer backbone, a fairly constant M_n is maintained with narrow Đ evidenced by SEC analysis.

In the next chapter (Chapter IV), we will explore and discuss the impact of these acidic lateral groups on the degradation rates of PDLs based on a degradation study of the copolymers containing 2% and 5% of COOH pendant groups.

3.4 Experimental Part

Typical procedure for homopolymerization of monomers 2 and 3.

Polymerization experiments are performed under Ar atmosphere at ambient temperature by adding either monomer **2** or monomer **3** into a stirring suspension of 2,2-Dimethyl-1-propanol (1 equiv.), NEt$_3$ (2 equiv.), and InCl$_3$ (1 equiv.) in Toluene ([M]$_0$ = 3M) with a monomer/alcohol ratio of 25. The reaction mixture was stirred at 60 °C for 60 hours and 48 hours (for ROP of **2** and **3**, respectively), and the crude was analyzed by ^{1}H NMR spectroscopy to determine the consumption of monomer.

Typical Procedure for the preparation of random copolymer of ε-DL with monomers 2 or 3: an example for 10 mol% content.

Copolymerization is performed by adding ε-DL (45 equiv.) and the new monomer (5 equiv.) (**2** or **3**) into a stirring suspension of BnOH or DMBA (1 equiv.), NEt$_3$ (2 equiv.), and InCl$_3$ (1 equiv.), [M]$_0$ = [DL]$_0$ = 3 M in Toluene. The reaction mixture is stirred at 60 °C for the desired time until complete consumption of both monomers, as determined by ^{1}H NMR spectroscopy. An excess of benzoic acid is then added to quench the catalyst, and the solvent is evaporated under vacuum. The crude is then dissolved in a minimum volume of DCM and precipitated two consecutive times into cold methanol, filtered, and dried under vacuum.

PDL-r-P2: 18h, Conversion: >99% (for both monomers), isolated yield: 90%. SEC: M_n = 9200 g/mol, $Đ$ = 1.17. Monomer ratio: ε-DL:**2** = 45:5 for DP50 initiated with BnOH

^{1}H NMR (CDCl$_3$, 300 MHz) δ (ppm) = 7.35 – 7.29 (m, 25H, -S-CH$_2$-C$_6$H$_5$), 7.25 – 7.17 (m, 5H, C$_6$H$_5$-CH$_2$-O), 5.10 (s, 2H, ArCH$_2$-O), 4.97 – 4.92 (m, 5H, -OCH-), 4.88 – 4.80 (m, 45H, O-CH-), 3.71 (s, 10H, -S-CH$_2$Ar), 3.59 (br, 1H, -CH-OH), 2.52 (d, J = 6.1 Hz, 10H, -O-CH-CH$_2$-S-), 2.28 – 2.23 (m, 90H, -CH$_2$-), 1.65 – 1.46 (m, 270H, -CH$_2$-), 1.39 – 1.16 (m, 270H, -CH$_2$-), and 0.89 – 0.85 (m, 135H, -CH$_3$).

PDL-r-P3: 12h, Conversion: >99% (for both monomers), isolated yield: 92%. SEC: M_n = 9200 g/mol, $Đ$ = 1.36. DSC: T_g = −49.7 °C. TGA: T_d = 345°C. Monomer ratio: ε-DL:**3** = 45:5 for DP50 initiated with DMBA

^{1}H NMR (CDCl$_3$, 300 MHz) δ (ppm) = 7.35 – 7.30 (m, 25H, C$_6$H$_5$-CH$_2$-O), 6.48 (d, J = 2.3 Hz, 2H, *ortho*-C$_6$H$_3$- CH$_2$-O-), 6.40 (t, J = 2.3 Hz, 1H, *para*-C$_6$H$_3$- CH$_2$-O-), 5.10 (s, 10H, ArCH$_2$-O), 5.03 (s, 2H, ArCH$_2$-O-), 5.03 – 4.98 (m, 5H, -OCH-), 4.89 – 4.80 (m, 45H, O-CH-

), 3.78 (s, 6H, -(OCH_3)$_2$), 3.57 (br, 1H, -CH-OH), 3.29 – 3.15 (m, 10H, S-CH_2-COO), 2.86 – 2.67 (m, 10H, -OCH-CH_2-S-), 2.34 (t, J = 7.5 Hz, 10H, -CH_2-CO- (From P**3**)), 2.28 – 2.24 (m, 90H, -CH_2-CO- (from PDL)), 1.63 – 1.46 (m, 270H, -CH$_2$-), 1.40 – 1.20 (m, 270H, -CH$_2$-), and 0.89 – 0.85 (m, 135H, -CH$_3$).

Typical procedure for kinetic study.

Kinetic experiment of copolymerization is performed by adding ε-DL (80 equiv.) and **3** (20 equiv.) into a stirring suspension of DMBA (1 equiv.), NEt$_3$ (2 equiv.), and InCl$_3$ (1 equiv.), in Toluene ([**3**]$_0$ = [DL]$_0$ = 3 M) at room temperature. After adding the monomer, an aliquot, t = 0, is withdrawn from the reaction and quenched by benzoic acid before solvent evaporation. The crude material is analyzed by ^{1}H NMR spectroscopy in CDCl$_3$ to determine the monomer conversion and degree of polymerization. The mixture is then stirred at 60 °C. The other aliquots are withdrawn from the reaction in each designed time (1h, 3h, 5h, 8h, 12h, 24h, and 48h) and then treated similarly.

Deprotection of copolymers, acetylation and hydrogenolysis.

Typical procedure to prepare the acetylated copolymers (according to the reported procedure in the literature.[22c]

Acetic anhydride (0.5 mL) and DMAP (50 mg) are added to the solution of copolymers (2 g) in 10 mL of DCM, and the mixture is stirred for 12 hours at room temperature. The complete protection of the terminal alcohols is confirmed by ^{1}H NMR spectroscopy. DMAP, acetic acid, and residue of acetic anhydride are removed by acidic aqueous work-up (20 mL of cold 2 M HCl). The solvent is removed under vacuum. The crude is then dissolved in a minimum volume of DCM and precipitated two consecutive times in cold methanol, then filtered, and dried under vacuum to yield the acetylated copolymer as a sticky material.

Acetylated copolymer: CP-X%-OAc

CP-2%-OAc: monomer ratio: ε-DL:**3** = 49:1 for DP50, Conversion: 99%, isolated yield: 80%. SEC: M_n = 11000 g/mol, $Đ$ = 1.19. DSC: T_g = −54.3 °C.

^{1}**H NMR (CDCl$_3$, 300 MHz)** δ (ppm) = 7.36 – 7.30 (m, 5H, C$_6$H$_5$-CH$_2$-O), 6.48 (d, J = 2.3 Hz, 2H, *ortho*-C$_6$H$_3$- CH$_2$-O-), 6.40 (t, J = 2.3 Hz, 1H, *para*-C$_6$H$_3$- CH$_2$-O-), 5.10 (s, 2H, ArCH_2-O), 5.03 (s, 2H, ArCH_2-O-), 5.01 – 4.93 (m, 1H, -OCH-), 4.89 – 4.80 (m, 49H, O-CH-), 3.78 (s, 6H, -(OCH_3)$_2$), 2.34 (m, J = 7.5 Hz, 2H, -CH_2-CO- (From P**3**)), 2.28 – 2.24 (m, 98H, -CH_2-

CO- (from PDL)), 2.02 (s, 3H, -OOC-CH$_3$), 1.68 – 1.46 (m, 294H, -CH$_2$-), 1.38 – 1.20 (m, 294H, -CH$_2$-), and 0.89 – 0.85 (m, 147H, -CH$_3$).

CP-5%-OAc: monomer ratio: ε-DL:**3** = 48:2 for DP50, Conversion: 99%, isolated yield: 82%. SEC: M_n = 9000 g/mol, $Đ$ = 1.27. DSC: T_g = −53.8 °C.

^{1}H NMR (CDCl$_3$, 300 MHz) δ (ppm) = 7.36 – 7.30 (m, 10H, C$_6$H$_5$-CH$_2$-O), 6.48 (d, J = 2.3 Hz, 2H, *ortho*-C$_6$H$_3$- CH$_2$-O-), 6.40 (t, J = 2.3 Hz, 1H, *para*-C$_6$H$_3$- CH$_2$-O-), 5.10 (s, 2H, ArCH$_2$-O), 5.03 (s, 2H, ArCH$_2$-O-), 5.01 – 4.93 (m, 2H, -OCH-), 4.89 – 4.80 (m, 48H, O-CH-), 3.78 (s, 6H, -(OCH$_3$)$_2$), 3.28 – 3.13 (m, 4H, S-CH$_2$-COO), 2.86 – 2.67 (m, 4H, -OCH-CH$_2$-S-), 2.34 (t, J = 7.5 Hz, 4H, -CH$_2$-CO- (From P**3**)), 2.28 – 2.24 (m, 96H, -CH$_2$-CO- (from PDL)), 2.02 (s, 3H, -OOC-CH$_3$), 1.68 – 1.46 (m, 288H, -CH$_2$-), 1.38 – 1.20 (m, 288H, -CH$_2$-), and 0.89 – 0.85 (m, 144H, -CH$_3$).

Typical procedure to prepare the deprotected copolymers (adapted from reported procedure in literature).[23]

CP-2%-COOH:

A solution of the acetylated copolymers (2 g) in dried and degassed EtOH (40 mL) is added to the stirred solution of 20% w/w of Charcoal (90wt%/Pd) and Pd(OAc)$_2$ in 2.5 mL of THF at 30 °C. The resulting mixture is stirred under H$_2$ atmosphere (1 atm, balloon) for 16 hours. After the reaction is completed, an excess amount of Charcoal is added to the mixture, and the Pd/C is then removed by filtration over Celite following by solvent evaporation. The deprotected copolymers are dissolved in a minimum volume of DCM, precipitated in cold pentane, and dried under vacuum overnight to yield CP-2%-COOH as a sticky material. The complete removal of the benzyl protecting groups are confirmed by ^{1}H NMR spectroscopy.

CP-2%-COOH: monomer ratio: ε-DL:**3** = 49:1, Conversion: 99%, isolated yield: 92%. SEC: M_n = 10300 g/mol, $Đ$ = 1.17. DSC: T_g = −55.9 °C.

^{1}H NMR (CDCl$_3$, 300 MHz) δ (ppm) = 6.48 (d, J = 2.3 Hz, 2H, *ortho*-C$_6$H$_3$- CH$_2$-O-), 6.41 (t, J = 2.3 Hz, 1H, *para*-C$_6$H$_3$- CH$_2$-O-), 5.03 (s, 2H, ArCH$_2$-O-), 5.01 – 4.93 (m, 1H, -OCH-), 4.89 – 4.80 (m, 49H, O-CH-), 3.79 (s, 6H, -(OCH$_3$)$_2$), 2.34 (t, J = 7.5 Hz, 2H, -CH$_2$-CO- (From P**3**)), 2.28 – 2.24 (m, 98H, -CH$_2$-CO- (from PDL)), 2.03 (s, 3H, -OOC-CH$_3$), 1.69 – 1.47 (m, 294H, -CH$_2$-), 1.39 – 1.20 (m, 294H, -CH$_2$-), and 0.89 – 0.85 (m, 147H, -CH$_3$).

CP-5%-COOH:

A solution of the acetylated copolymers (2 g) in dried and degassed EtOH (40 mL) is added to the stirred solution of 50% w/w of Charcoal (90wt%/Pd) and Pd(OAc)$_2$ in 2.5 mL of THF at 30 °C. The resulting mixture is stirred under H$_2$ atmosphere (1 atm, balloon) for 22 hours. After the reaction is complete, an excess amount of Charcoal is added to the mixture, and the Pd/C is then removed by filtration over Celite following by solvent evaporation. The deprotected copolymers are dissolved in a minimum volume of DCM, precipitated in cold pentane, and dried under vacuum overnight to yield a CP-5%-COOH as a sticky material. The complete removal of the benzyl protecting groups are confirmed by ^{1}H NMR spectroscopy.

CP-5%-COOH: monomer ratio: ε-DL:**3** = 48:2, Conversion: 99%, isolated yield: 85%. SEC: M_n = 8200 g/mol, $Đ$ = 1.19. DSC: T_g = −58.5 °C.

^{1}H NMR (CDCl$_3$, 300 MHz) δ (ppm) = 6.48 (d, J = 2.3 Hz, 2H, *ortho*-C$_6$H$_3$- CH$_2$-O-), 6.40 (t, J = 2.3 Hz, 1H, *para*-C$_6$H$_3$- CH$_2$-O-), 5.03 (s, 2H, ArCH$_2$-O-), 5.01 – 4.93 (m, 2H, -OCH-), 4.89 – 4.80 (m, 48H, O-CH-), 3.78 (s, 6H, -(OCH$_3$)$_2$), 2.34 (t, J = 7.5 Hz, 4H, -CH$_2$-CO- (From P**3**)), 2.28 – 2.24 (m, 96H, -CH$_2$-CO- (from PDL)), 2.02 (s, 3H, -OOC-CH$_3$), 1.67 – 1.46 (m, 288H, -CH$_2$-), 1.38 – 1.20 (m, 288H, -CH$_2$-), and 0.89 – 0.85 (m, 144H, -CH$_3$).

3.5 Bibliography

1   Williams, C. K. *Chem. Soc. Rev.* **2007**, *36*, 1573.

2   Bednarek, M. *Prog. Polym. Sci.* **2016**, *58*, 27.

3   Vert, M. Biomacromolecules, **2005**, *6*, 538.

4   Kakde, D.; Taresco, V.; Bansal, K.K.; Magennis, E. P.; Howdle, S. M.; Mantovani, G.; Irvine, D. J.; Alexander, C. *J. Mater. Chem. B*. **2016**, *4*, 7119.

5   Olsén, P.; Borke, T.; Odelius, K.; Albertsson, A.-C. *Biomacromolecules*, **2013**, *14* (8), 2883.

6   Lee, S.; Lee, K.; Kim, Y.-W.; Shin, J. *ACS Sustainable Chem. Eng.* **2015**, *3* (9), 2309.

7   Martello, M. T.; Schneiderman, D. K.; Hillmyer, M. A. *ACS Sustainable Chem. Eng.* **2014**, *2* (11), 2519.

8   Lee, S.; Lee, K.; Jang, J.; Choung, J. S.; Choi, W. J.; Kim, G.-J.; Shin, J. *Polymer*, **2017**, *112*, 306.

9   Schneiderman, D. K.; Hill, E. M.; Martello, M. T.; Hillmyer, M. A. *Polym. Chem.* **2015**, *6*, 3641.

10   Arias, V.; Olsén, P.; Odelius, K.; Höglund, A.; Albertsson, A.-C. *Polym. Chem.* **2015**, *6*, 3271.

11   Valverde, C.; Lligadas, G.; Ronda, J. C.; Galià, M.; Cádiz, V. *Polym. Degrad. Stabil.* **2018**, *155*, 84.

12   Zhang, J.; Xiao, Y.; Xu, H.; Zhou, C.; Lang, M. *Polym. Chem.* **2016**, *7* (28), 4630.

13   Leemhuis, M.; Kruijtzer, J. A. W.; F. van Nostrum, C.; Hennink, W. E. *Biomacromolecules*, **2007**, *8*, 2943.

14   Lewis, D. H. Controlled release of bioactive agents from lactide/glycolide polymers. In *Biodegradable Polymers as Drug Delivery Systems*; Chasin, M.; Langer, R., Eds.; Marcel Dekker: New York, **1990**.

15   Kimura, Y.; Shirotani, K.; Yamane, H.; Kitao, T. *Polymer*, **1993**, *34*, 1741.

16   (a) Miller, R. A.; Brady, J. M.; Outright, D. E. *J. Biomed. Mater. Res.* **1977**, *11*, 711. (b) Gilding, D. K.; Reed, A. M. *Polymer*, **1979**, *20*, 1459.

17   Kimura, Y.; Shirotani, K.; Yamane, H.; Kitao, T. *Macromolecules*, **1988**, 21, 3338.

18   (a) Sun, Y.; Dai, W.; Zhang, Q.; Zhang, Y.L.; Lang, M., *Acta Chim. Sinica* **2009**, 67, 1259. (b) Gabelnick, H. L. Advances in Human Fertility and Reproductive Endocrinology, Raven Press, New York, **1983**, 149.

19 (a) Zhang, J.; Xiao, Y.; Xu, H.; Zhou, C.; Lang, M. *Polym*. Chem. **2016**, *7*, 4630. (b) Valverde, C.; Lligadas, G.; Ronda, J.C.; Galià, M.; Cádiz, V. *Polym. Degrad. Stabil.* **2018**, *155*, 84. (c) Rowe, M.D.; Eyiler, E.; Walters, K.B. *Polym. Test.* **2016**, *52*, 192.

20 Gleadall, A.; Pan, J.; Kruft, M.-A.; Kellomäki, M. *Acta Biomater.* **2014**, *10*, 2223.

21 Pitt, C. G.; Gratzel, M. M.; Kimmel, G. L.; Surles, J.; Schindler, A. *Biomaterials*, **1981**, *2*, 215.

22 (a) Nikouei, N. S.; Lavasanifar, A. *Acta Biomater.* **2011**, *7*, 3708. (b) Mahmud, A.; Xiong, X.-B.; Lavasanifar, A. *Macromolecules*, **2006**, *39* (26), 9419. (c) Thillaye du Boullay, O.; Saffon, N.; Diehl, J.-P.; Martin-Vaca, B.; Bourissou, D. *Biomacromolecules*, **2010**, *11*, 1921.

23 Felpin, F. -X. and Fouquet, E. *Chem. Eur. J.* **2010**, *16*, 12440.

Chapter IV: Study of the hydrolytic and enzymatic degradation of ε-carboxyl-functionalized PDL-based copolymers

4.1 Hydrolytic and enzymatic degradation of polyester-based materials

4.1.1 General considerations

As previously mentioned, over the last decades plastics waste have become an environmental issue due to their high persistence in nature.[1] This problem is exacerbated by the increase of convenience plastics with short-term use. Seeking to tackle this problem, the investigation and development of biodegradable polymers has attracted more and more attention.[2] Biodegradable polymers are promising alternatives to non-degradable petroleum-based polymers, as they can be used widely, not only in commodity applications such as packaging, but also in biomedical, and tissue engineering applications.[3] Biodegradable polymers are designed to degrade into small molecules, and to be released in the environment as biomass, carbon dioxide (CO_2), and water.[3] Based on the literature, most of the biodegradable plastics are derived from polyesters, especially the compostable PLA and PCL.[4]

However, the degradation times for PLA and PCL may be still long for some of the targeted applications, from 6 months to 2 years depending on the hydrolysis conditions, as mentioned in Chapter III. To increase the degradation rates of these polyesters, especially for PCL-based polymers, the introduction of lateral polar groups such as hydroxyl or carboxyl functional groups on the polymer backbone can be an option. The lateral functional groups will affect the polymer chains by breaking their crystallinity and increasing their hydrophilicity, thus modulating the water-affinity and degradability of the polymer.[5] In particular, the increase of hydrophilicity also leads to a higher water absorbing capacity of the polymers, thus enhancing the degradation and facilitating the release of polymer fragments in water-soluble form prior to small molecules.[6]

What about the polymer degradation processes? We first need to distinguish between spontaneous degradation in natural medium, and forced degradation while investigating the polymer properties in the laboratory (*in vitro*). The polymers that are susceptible to degradation by a decrease of their mass *via* biological activity in natural medium are defined as biodegradable polymers, according to the International Union of Pure and Applied Chemistry (IUPAC).[7] Additionally, other definitions (from technical report established by the European committee for standardization, PD CEN/TR 15351:2006) require the biodegradable polymer

to be converted into biomass, CO_2, and water during biodegradation processes, which is particularly suitable for biomedical applications.[8]

In nature, the <u>biodegradation processes of polymers</u> can be separated into 4 different phases: 1) biodeterioration, 2) depolymerization, 3) bioassimilation, and 4) mineralization (Figure 4.1).[3,9,10] The first phase is associated with superficial degradation, in which a microbial biofilm is formed on the polymer surface. Then, the depolymerization of the polymer chains catalyzed by microorganisms of the biofilm starts, releasing oligomers, dimers, or monomers. The third phase, bioassimilation, is the consumption of small molecules, degraded from the oligomers during the second phase, by microbial cells or bacteria, leading to the production of primary and secondary metabolites. In the final phase, the metabolites are converted to the final products, e.g., biomass, CO_2, water, CH_4, and N_2, which are released into the environment. Note that the final products released at the end of the biodegradation depend on the initial composition of the polymer (Figure 4.1).[9]
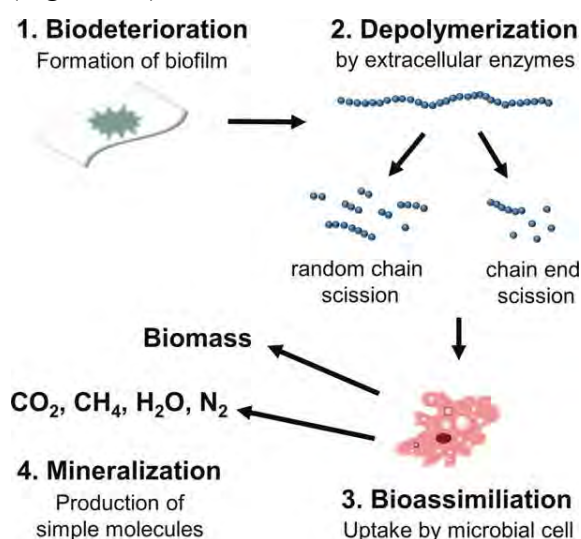

Figure 4.1 The different steps involved in biodegradation.[3]

In contrast to spontaneous degradation, *in vitro* degradation of polymers in the laboratory can be carried out in different well-controlled conditions such as photo-, thermal-, mechanical, chemical, and enzymatic degradation.[3,11] The sensitivity of the ester linkage to hydrolysis makes aliphatic polyesters easy to degrade. Chemical (hydrolytic) degradation at different pH, and enzymatic degradation are then the most common conditions used to investigate the degradability of polyesters. Applying these *in vitro* conditions, aliphatic polyesters are degraded by a two-step process.[11,12] First, the chain scission of the polymer backbone takes place by hydrolysis or by enzyme-catalyzed hydrolysis of the ester linkages to

yield oligomers. Subsequently, these oligomers are broken down to small molecules such as biomass, CO_2 and water.[13]

Are there any factors that influence the hydrolysis/degradation? The degradation rates are, in general, influenced by the structure of polymer backbone, including the electrophilicity of the carbonyl atoms and the presence or absence of bulky substituents. Besides, polymer morphology also affect the rates of degradation. For example, the degradation rate of crystalline and semi-crystalline polyesters is slower than that of amorphous ones. Furthermore, M_n and the water affinity of polyesters are shown to have a marked impact on degradation.[18]

Hydrolysis is the major pathway in chemical and enzymatic degradation for aliphatic polyesters, and it proceeds *via* either a bulk or surface erosion mechanism (Figure 4.2).[9,14,15] The bulk erosion is a uniform degradation through the whole material, characterized by a decrease of mass and M_n throughout the entirety material. The surface erosion, conversely, shows a decrease of mass from its surface area, whereas the M_n of remaining material barely changes.[3,14,15]
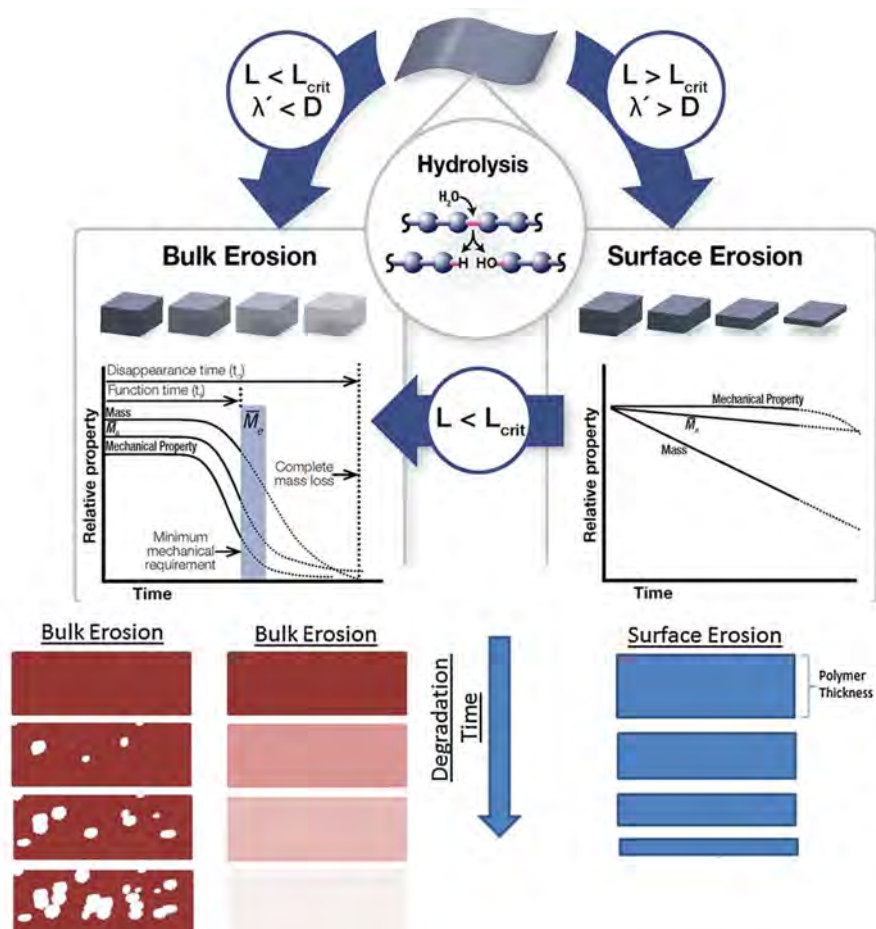

**Figure 4.2** Surface *vs* bulk erosion during polymer degradation.[15]

There are 4 critical factors that affect the mechanism of both bulk and surface polymer erosions: (1) The rate of water diffusion into the bulk polymer (D), (2) the rate of hydrolysis (λ'), (3) the thickness of the specimen (L), and (4) the critical thickness (L_{crit}).[15] Note that L_{crit} indicates the transition point where the erosion changes from surface to bulk degradation. Briefly, surface erosion occurs when the hydrolysis rate (λ') is faster than the water diffusion rate into the bulk polymer (D). It should be noted that the surface erosion in enzymatic degradation takes place when the enzymes cannot penetrate the bulk polymer, and are therefore only able to catalyze hydrolysis on the surface. In general, the surface erosion represents the predominating mechanism for most of the semi-crystalline and hydrophobic polymers, revealing a rapid initial hydrolysis rate. In contrast, bulk erosion is favored for amorphous, hydrophilic polymers, as a result of an easy uptake of water into the whole polymer. So, bulk erosion occurs when the rate of water diffusion (D) is faster than the hydrolysis rate (λ'), showing a very slow rate of mass loss at the beginning of degradation. Note that the hydrolysis mechanism can change from surface to bulk erosion during the degradation process, when the sample thickness (L) is lower than a critical sample thickness (L_{crit}).[16,17]

.

4.1.2 Experimental conditions for *in vitro* degradation tests

As previously mentioned, the *in vitro* degradation studies of polyesters are frequently carried out in hydrolytic conditions with controlled pH (buffer solution) and temperature or in enzymatic conditions, using appropriate enzymes.

Hydrolytic degradation of polyesters in buffered solutions: In general, water-initiated degradation processes are governed by several external factors which affect the hydrolysis rate in the degradation tests.[3,19-21] For example, high temperatures favor a rapid rate of hydrolysis as well as a change of pH in the degradation media.[3,19] As observed in the reported degradation studies of PLGA, the hydrolysis rate of the corresponding polymer increased in both acidic and basic conditions.[21] Interestingly, the erosion mechanism was found to be different in acidic and basic conditions, i.e., bulk erosion occurred at a low pH (acidic conditions), whereas surface erosion was observed at high pH values (basic conditions).[19] Moreover, a change in pH significantly impacts the acid–base hydrolysis, as a difference of one pH unit increases the rate of hydrolysis by 10 fold.[20] Accordingly, the degradation of PLA and PCL is slow in neutral conditions, but it takes place at higher rates in basic and in acid conditions (basic conditions being the highest).[21a] This is consistent with the degradation of

polyesters being more pronounced by the basic-catalyzed hydrolysis. In general, the hydrolysis of PLA (as an example) can be initiated by two different pathways: (1) intra chain and (2) end chain cleavage (Scheme 4.1).[3,9,10] The intra chain pathway (1) occurs by a random nucleophile, such as hydroxide attack on an ester group in the polymer backbone, and subsequent cleavage of the ester link, therefore leading to shorter polymer chains. In contrast, the end chain degradation, also called dezipping mechanism, (2) is mainly associated with an intramolecular transesterification. Thus, the polymer is shortened by only one unit of LA, which is subsequently hydrolyzed into two molecules of lactic acid.[3,10]
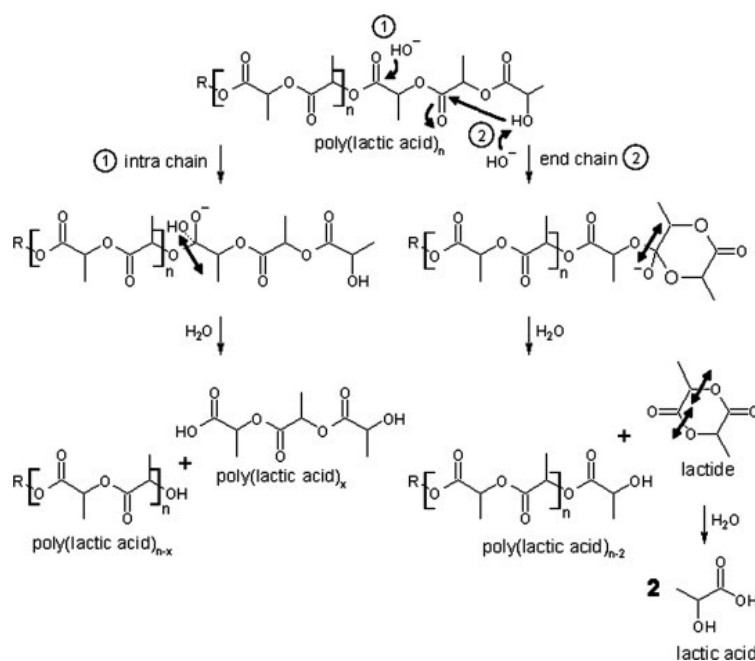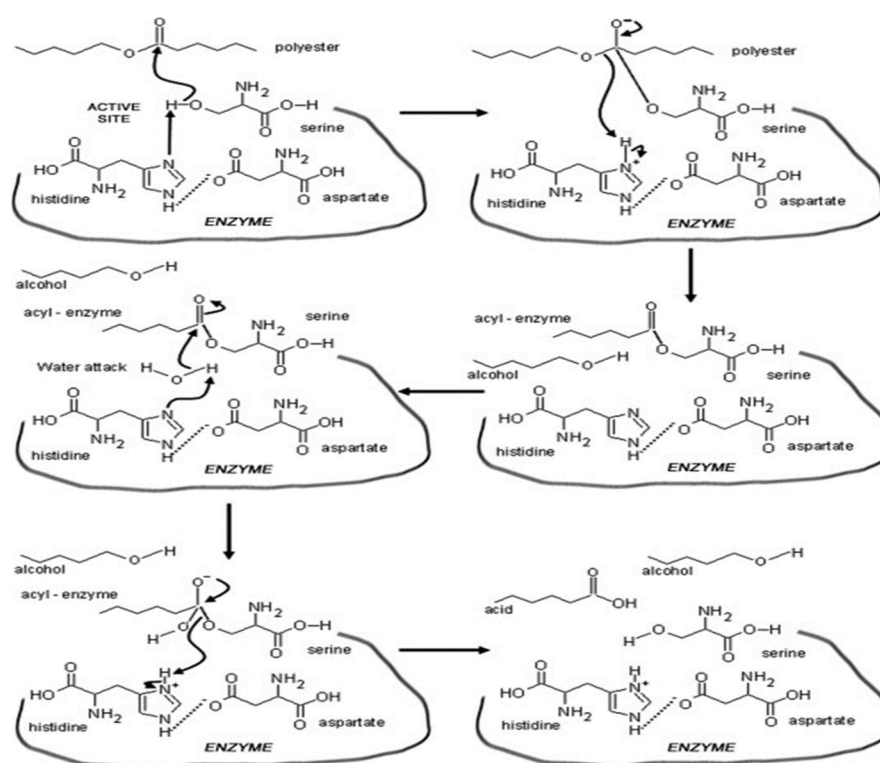

Scheme 4.1 Basic-catalyzed hydrolysis of PLA *via* end chain and intra chain pathways.[3, 10]

Enzymatic-catalyzed hydrolysis of polyesters: PLA and PCL have a very slow hydrolysis rate (several years) in neutral conditions, so that the use of enzymes is often required to catalyze the polymer degradation.[3,20,21] For instance, PCL degradation is completely achieved within 4 days in the presence of *Pseudomonas* lipase, while several months or even more than one year are required in neutral aqueous conditions.[21b] Generally, enzymes have high activities in neutral pH solutions and at moderate temperatures, due to stability issues. They can increase the hydrolysis rates from 100 to 1000 times.[22] Note that enzyme-catalyzed degradation studies are typically performed in phosphate-buffered saline solution (pH 7.4), which is a simple model system.[15] However, the high molecular weights of some enzymes makes them unable to penetrate the sample. Thereby, the enzyme-catalyzed hydrolysis mainly occurs at the material surface which is referred to as surface erosion.[15] The enzymes have been classified based on their activity towards polyesters degradation, for example: the enzymes that specifically attack carboxylic linkages are called lipases and esterases, while the enzymes that

cleave the amide group are endopeptidases.[23-27a] Note that the enzymatic degradation of PCL has been largely studied using lipase obtained from fungi or bacteria.[27]

Here is an example of the proposed mechanism for depolymerase promoted degradation of PLA, which uses a triad of amino acids to catalyze the hydrolysis of polyester, i.e., aspartate, histidine and serine. (Scheme 4.2).[28] The basicity of the histidine moiety is activated by the aspartate so that it deprotonates the serine unit, which attacks the ester group. This leads to the formation of an alcohol end group including an acyl-enzyme complex. The acyl-enzyme bond is then attacked by a water molecule yielding a carboxyl end group and the free enzyme. This arrangement of three amino acids is typically known as a catalytic triad.

Scheme 4.2 Enzymatic-catalyzed hydrolysis of PLA.

4.1.3 Polymer film preparation for the degradation tests

Different devices such as microparticles, pellets, and films can be used for the preparation of the samples used in the degradation experiments, and one of the most used devices are films. It is necessary to have approximately the same surface area, weight, and thickness in each sample prior to investigating degradation in various conditions. The definition of a film is a thin layer or membrane of any material.[29] The film can be considered thin if its thickness is much smaller than all the other critical dimensions. The degradation of thin polymer films is of significant importance given the changes in the chemical structure and

mechanical properties of the polymer at this thickness. Thus, not all degradation processes will occur with equal significance in films of different thicknesses.[29]

Several examples of polymer films preparation have been reported, in which the prepared films were subjected to the degradation experiments.[30-35] Film preparation is mainly achieved in 2 steps, as follows: (1) the slow solvent evaporation of the polymer solution of known concentration (e.g., in Chloroform, DCM, or THF) at room temperature and (2) drying under vacuum for at least 2 days to ensure complete removal of the solvent.[30,31] It should be noted that the solvent must be evaporated slowly to create a uniform structure of polymer for the entire film, both surface and bulk.[32] For example, PCL thin films were prepared from a solution of commercial PCL (43 – 50 kg/mol) in THF and subsequent solvent evaporation at room temperature for a week. Thereafter, the PCL films were cut into discs with diameter of 6 mm and a thickness of 2.5 mm corresponding to a weight of ≈70 mg.[31] In this study, the films were placed into test-tubes, followed by the addition of the degradation solution (sample/degradation solution ratio of 1:50) at either pH 1 or pH 13.[31] In another example, the PLA-PDL-PLA triblock copolymer was dissolved in chloroform (~6% w/w) and subsequently placed in glass Petri dishes before evaporating the solvent slowly. After that, the films were dried under vacuum for a week prior to the hydrolysis experiments (hydrolytic degradation in 10 mL of water at 37 °C in a thermostatically controlled oven for 6 months). Each hydrolyzed sample had an approximate weight of 30 mg ± 1 mg with a square shape that had the dimensions of 1 cm × 1 cm and 0.200–0.300 mm thickness.[33]

Next, the preparation of PCL-*b*-PEG films was achieved using the solvent casting technique from a 10 wt % chloroform solution, and the prepared films were dried at 50 °C for 2 days under vacuum. The films had a diameter of 8 mm and a thickness of 80 μm (≈ 20 mg) before using in the degradation experiments (either pH 7.4 or 9.5 at 37 °C for 20 weeks).[34] For the last selected example, films of about 0.1 mm thickness were prepared from a mixed solution of PCL and PEOs in DCM by slow solvent evaporation at room temperature for a week.[35] The discs of polyester elastomer with 4.3 mm (inner) diameter were prepared by a technique called circular die cut, in which all obtained films have an equal surface area.[36]

Several experimental parameters have to be considered in order to provide accurate results concerning the rates of degradation and erosion of the polymer.[10] These parameters are associated with the monitoring of mass loss in an aqueous solution.[37] For the relative

degradation studies in physiological conditions, samples are typically exposed to phosphate-buffered saline solutions (PBS), pH = 7.4 ± 0.2 with constant temperature at 37 ± 1 °C.[10, 37] However, these "natural conditions" have a drawback, since a very slow degradation time can be observed, over 2-3 years for some polyesters.[38,39] Thus, polyester degradation tests are often conducted under "accelerated" conditions, i.e., at extreme pH values.[40] In addition, the testing parameters have been outlined in American Society for Testing and Materials (ASTM F1635) as a standard test method for *in vitro* degradation. Key features of the standard include: (1) a solution-to-specimen mass ratio of greater than 30:1 to provide adequate buffer capacity, (2) a sealable container to prevent solution loss by evaporation, (3) a minimum number of specimens (N) of N = 3 per time period, (4) packaged specimens consistent with that of the final device, and (5) removal of the dried and weighed specimens from a mass loss study.[10]

How can we monitor the degradation process? Several characterization techniques can serve to determine polymer properties during degradation, while the key observations should reveal the early signs of polymer cracking corresponding to the surface and/or bulk erosion behavior.[14a]

After hydrolytic degradation for predetermined periods of time, the weight loss percentage of the degraded polymers and blends was determined by the following equation:

$$\text{Weight loss (\%)} = [(W_0 - W_t)/W_0] \times 100 \qquad (1)$$

Where W_0 and W_t are the initial weight and the weight of the remaining material after a predetermined period of time. Additionally, water uptake into the material, indicating the degree of swelling of the remaining material, can also be determined roughly for each time point.[41]

For the selected characterization techniques, size exclusion chromatography (SEC) allows the observation of a clear change in M_n and $Đ$ of the polymer during the degradation process, thereby giving indications towards the polymer's erosion behavior.[42,43,44] For multicomponent polymer systems, NMR can be a useful characterization technique to monitor the composition change during and after the degradation process (Figure 4).[45] Additionally, several studies also report analysis by DSC and TGA to reveal the changes in thermal and mechanical properties as well as thermal stability during the degradation of the samples.[38, 46] To analyze the fragments from polymer cracking, HPLC–MS can help identify released fragments and compounds.[47]

To summarize, the transformation of polymers to small molecules can proceed through mechanical, light, thermal, enzymatic and chemical degradation.[3,7] Among these transformations, chemical degradation *via* hydrolysis is a well-known pathway for polymers containing hydrolysable functional groups like esters.[7] The hydrolysis of polyesters takes place *via* either a bulk or a surface erosion, depending on the working conditions, including the polymer properties. Bulk erosion is characterized by uniform degradation throughout the whole material, and a large decrease in M_n and mass of polymer. In contrast, surface erosion typically occurs under either highly basic or acidic conditions, while minimal changes in M_n occur, a marked loss of mass profile is usually observed.

In general, the temperature and pH of the degradation medium affect the hydrolysis rate of the polyester.[48] Additionally, base-catalyzed degradation occurs at higher rates than acid-catalyzed ones. In basic conditions, PLA is degraded faster than PCL due to the higher electrophilicity of PLA's carbonyl carbon atoms than that of PCL, thus increasing the possibility of hydroxide ion attack.[21] The pH-buffered *in vitro* degradation tests of polyesters is useful, but some studies report its limitations. For instance, a long degradation time is observed for crystalline polymers that have an ability to limit water diffusion, thus preventing access of water to hydrolysable ester bonds.[10] In marked contrast, enzymes catalyze degradation with high specificity for polymers containing hydrolytically labile bonds, including crystalline polymers. Moreover, the presence of hydrophilic pendant groups like carboxyl groups promotes polyester degradation.[49]
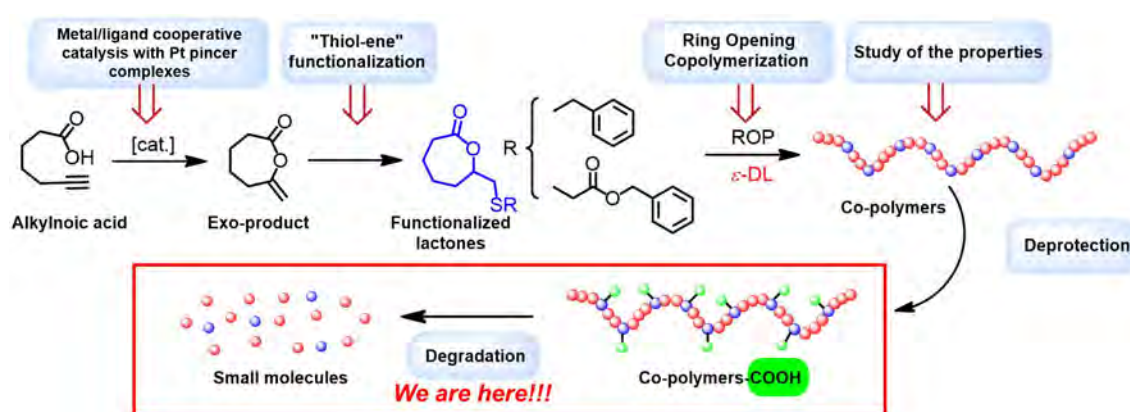
Scheme 4.3 Project's overview: from monomer synthesis, copolymerization, and post-polymerization modification as well as the degradation study, for this Chapter.

The project's overview in Scheme 4.3 represents the pathway for the preparation of carboxyl-functionalized PDL-based copolymers as described before in Chapter I, II, and III. In the present chapter, the degradation study will be discussed thoroughly to demonstrate the

influence of the carboxyl pendant groups on the degradation rates of PDL. As presented in Chapter I and III, the targeted functionalized lactone monomer (**3**) was successfully prepared in multi-gram scale in excellent yields. Accordingly, monomer **3** was introduced in protected form, which was facile to deprotect after the copolymerization with ε-DL based on the results in Chapter III. For the prospective of the carboxyl pendant groups along the PDL chains, these carboxylic acid groups will affect the polymer properties, especially increasing the degradation rates of PDL (Scheme 4.4).
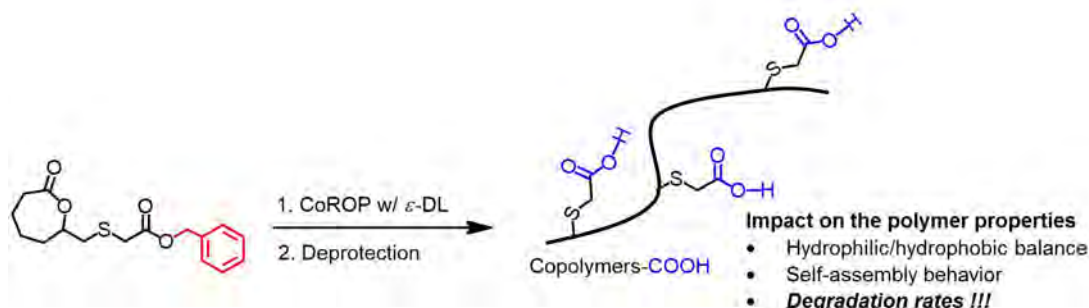
Scheme 4.4 The targeted monomer (**3**) and its prospective for the modulation of PDL degradation.

As described in Chapter III, the deprotection of the pendant carboxyl groups was achieved using mild conditions, respecting the integrity of the polymer backbone, according to ^{1}H NMR and SEC analysis. Carboxyl-functionalized copolymers (PDL-*r*-P**3**-COOH) with controlled ratios of functional group were thus obtained, and their degradability will be compared to that of pure PDL. Three different polymers will then be subjected to the degradation study: PDL DP50, CP-2%-COOH, and CP-5%-COOH; M_n/ $Đ$ = 11800/1.16, 10300/1.17, and 8200/1.19, respectively).

The chosen strategy for the degradation studies is as follows: we have chosen to work with films in hydrolytic and enzymatic conditions. We have chosen a lipase as enzyme at pH 7.4. For the hydrolytic condition, we will work at pH 7.4 (to compare with enzymatic degradation) and at pH 9 (basic conditions). The degradation tests consist in 4 steps as follows (Figure 4.3): (1) preparation of the polymer films, (2) addition of the hydrolysis media such as the buffered solution pH 9, pH 7.4, and the enzyme solution, (3) *in vitro* degradation tests at constant controlled temperature (40 °C), without shaking, and (4) the post-degradation analysis of samples such as %weight loss, the compositions of remaining polymer, and degradation products (3 samples each).

Figure 4.3 Illustration of degradation tests.

4.2 Results and discussions

4.2.1 Polymer Films preparation

Is it possible to prepare polymer films from the amorphous functionalized PDL? Firstly, we investigated the preparation of polymer films using non-functionalized PDL, DP50 and DP100, as model materials. Two solutions of PDL, DP 50 and DP 100, in DCM (300 mg in 6 mL) were placed in a borosilicate glass petri dish, and the solvent was allowed to evaporate slowly at room temperature for 2 days. Thereafter, the dishes containing a sticky polymer film on the bottom were dried under vacuum at 40 °C for 1, 3, or 5 days, and at 55 °C for 3 and 5 days. This treatment allowed for the total elimination of the solvent without affecting the properties of the polymer, but unfortunately, all of the samples were too soft and sticky to be taken out as films.

We decided then to prepare the film of the sticky polymer directly in a flat-bottom glass vial, although this meant that only the upper surface would initially be in contact with the degradation media. Initial attempts were done using PDL DP50. The polymer was dissolved in DCM (30 mg/mL) and placed (1 mL) in flat-bottom glass vials. The solvent was allowed to evaporate slowly at room temperature overnight, thus obtaining a homogenous phase for the whole sample (both surface and bulk). Subsequently, the vials were dried using a high vacuum oven at 60 °C for 2 days. Thin films were obtained with a diameter of 13 mm and a thickness of ≈ 0.5 mm, corresponding to a weight of approximately 30 mg (Figure 4.4). To ensure that the high temperature did not affect the polymer backbone, the obtained films (after drying over 2 days at 100 °C) were analyzed by SEC and ^{1}H NMR revealing similar properties to the starting material. Thereafter, this procedure was applied to the film preparation of copolymers containing 5% and 2% of carboxylic acid pendant groups with similar results.
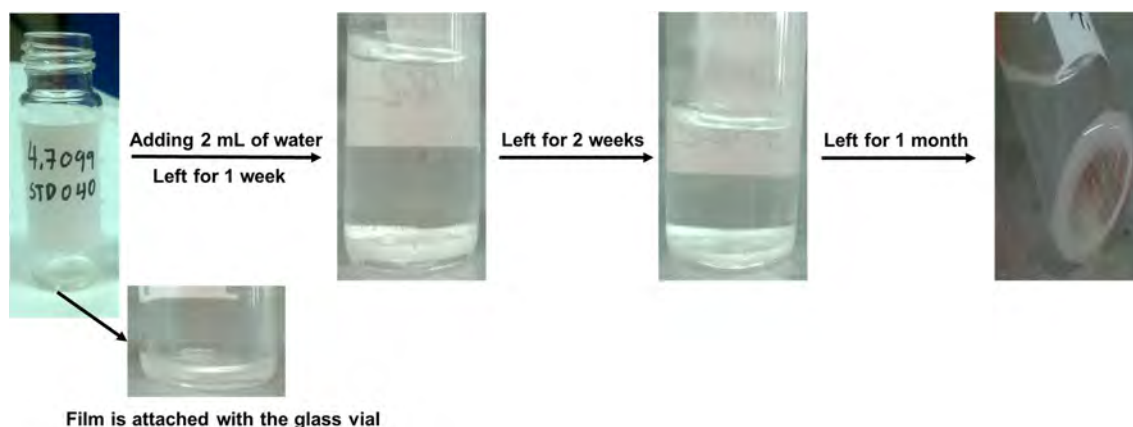
Figure 4.4 The selected example of polymer films using PDL DP50, and the study of its behavior in water.

4.2.2 Hydrolytic and Enzymatic degradation of copolymers containing 0%, 2% and 5% of carboxyl pendant groups (PDL, CP-2%-COOH and CP-5%-COOH)

The samples of the functionalized PDLs, CP-2%-COOH and CP-5%-COOH, were then submitted to the degradation study together with the samples of non-functionalized PDL, so that the impact of the pendant carboxyl group could be determined. As a reminder, the degradation studies were carried out at 40 °C, without shaking, and using three different degradation conditions: pH 7.4 and 9 buffer solutions, and enzymes in pH 7.4 buffer solution. Degradation tests were performed, in triplicate, over 15-30 days, during which data were collected at predetermined time points. Firstly, the degradation profiles in terms of weight loss, and the aspect of the samples along the study will be quickly summarized. The analysis of the constituents of the two phases (remaining polymer and released species) will be then discussed.

4.2.2.1. Degradation profiles

Over the 30 days of incubation of the non-functionalized PDL, very little change, if any, was observed on the aspect of the samples. Concerning the CP-2%-COOH samples, they were initially homogenously attached to the bottom of the glass vial. However, as the degradation proceeds, they appeared like a drop at the bottom of the degradation media at day 2 for pH 7.4 and 9 buffered solutions, whereas they are still stuck at the bottom of the glass vial in the case of the enzyme solution (Figure 4.5a). The degradation medium of the pH 9 buffered solution became turbid starting from day 4 as the CP-2%-COOH seemed to disperse into the basic buffered solution (Figure 4.5b). In contrast, the CP-2%-COOH samples in both

pH 7.4 buffer and enzymatic media retained its shape until the end of degradation experiments. As for the CP-5%-COOH samples, they acquire the same turbid aspect as the CP-2%-COOH samples, shown in figure 4.6b, after one week.
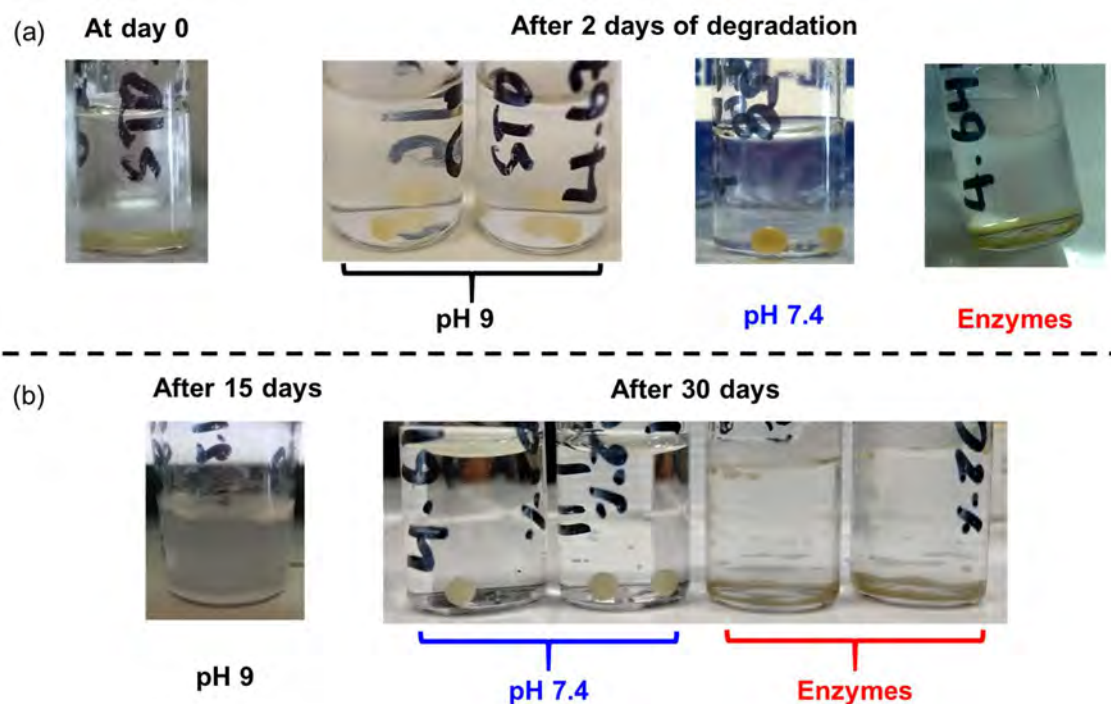

Figure 4.5 The external form of CP-2%-COOH in three different degradation conditions.

As evidenced by mass loss profiles of PDL DP50 in Figure 4.7, after 30 days of hydrolysis, very little degradation (less than 10% of weight loss) of the PDL chain was found in both hydrolytic and enzymatic conditions. This is consistent with the quite slow degradation of the hydrophobic non-functionalized PDL.[50]

For CP-2%-COOH noticeable weight loss was observed from the first day in all degradation conditions (Figure 4.6 and see data in Table 4.1). For example, mass loss of about 17% was observed in pH 9 buffer media. During the first 6 days, an exponential mass loss was found, from 17% to 41% of weight loss. However, only minor further mass loss was observed between days 6 to 15, reaching a plateau of ≈ 44% weight. In pH 7.4 buffer solutions, only 5% of weight loss was found after 1 day. Between days 3 to 12, weight loss percentages displayed a similar trend to that of day 1, observing only 6 – 10% of weight loss. Finally, 25% of weight loss was detected after 30 days. After 1 day, enzymatic degradation and pH 7.4 buffer media presented similar results (around 7 % mass loss). Interestingly, a significant increase in mass loss was observed the following days for enzymatic degradation, with mass loss reaching 25% and 43%, after 6 and 15 days, respectively. A marked decrease in mass of 47% of weight loss

was observed after 30 days. This result is different from the one performed in pH 7.4 buffer media in the absence of enzymes, but close to what was observed in pH 9.
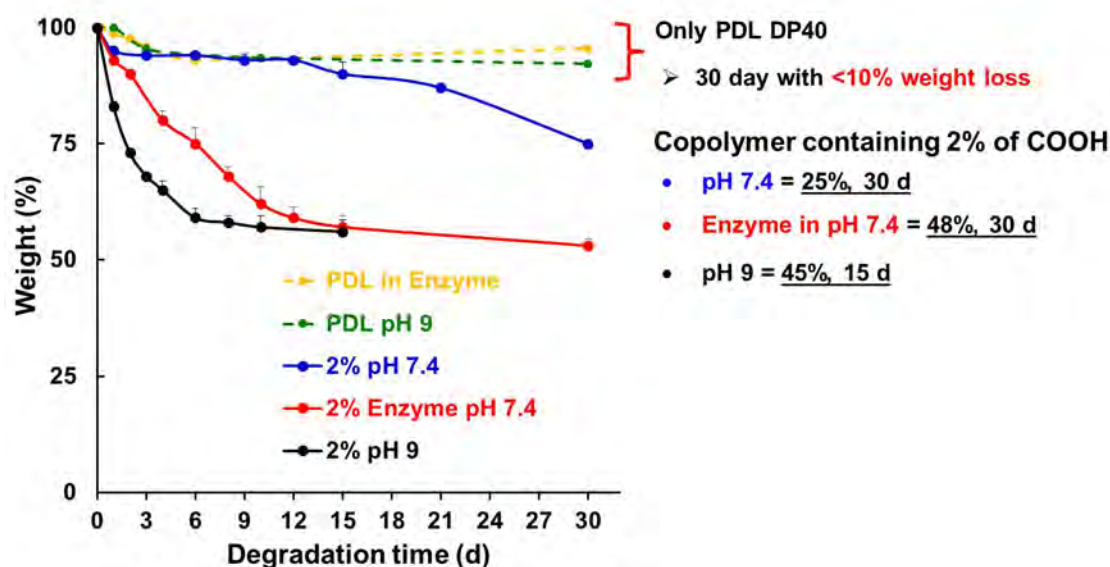

Figure 4.6 Mass loss profiles for the degradation of CP-2%-COOH in three different conditions and PDL DP50 in buffer pH 9 and enzymes solution.

Table 4.1 Mass loss data for CP-2%-COOH in three different conditions.

CP-2%-COOH, buffer pH 9			CP-2%-COOH, buffer pH 7.4			CP-2%-COOH, Enzymes		
Time (d)	% weight loss	STD	Time (d)	% weight loss	STD	Time (d)	% weight loss	STD
1	17	±2	1	5	±2	1	7	±1
2	27	±1	3	6	±1	2	10	±2
3	32	±1	6	6	±1	4	20	±4
4	35	±4	9	7	±3	6	25	±7
6	41	±4	12	7	±1	8	32	±4
8	42	±3	15	10	±5	10	38	±7
10	43	±5	21	13	±2	12	40	±5
15	44	±5	30	25	±1	15	43	±5
						30	47	±3

For Standard deviation ±1 ≈ 0.5 mg corresponding to ≈ 1.7 % weight loss

In general, weight loss percentage of the degraded polymers is determined using the weight of the remaining sample by the equation: [(Initial mass (mg) – Remaining mass (mg)) / Initial mass] × 100. *What about the weight loss percentage from released mass?* In order to confirm that the method is accurate, we decided to determine the weight loss percentage using the released mass after degradation, according to the equation below.

$$\text{Weight loss (\%)} = [(W(R)_t)/W_0] \times 100 \qquad (2)$$

Where W_0 and $W(R)_t$ are the initial weight and weight of released products after the predetermined time period (determined after evaporation of the sample to dryness).

We can then compare the degradation results of CP-2%-COOH using the two methods of determining weight loss percentage (Figure 4.7). Comparative plots of weight (%) and degradation time show that there is no difference in both methods for all degradations. These results suggest that during manipulation of the samples there is very little loss of material, despite the very low amounts and volumes being manipulated.
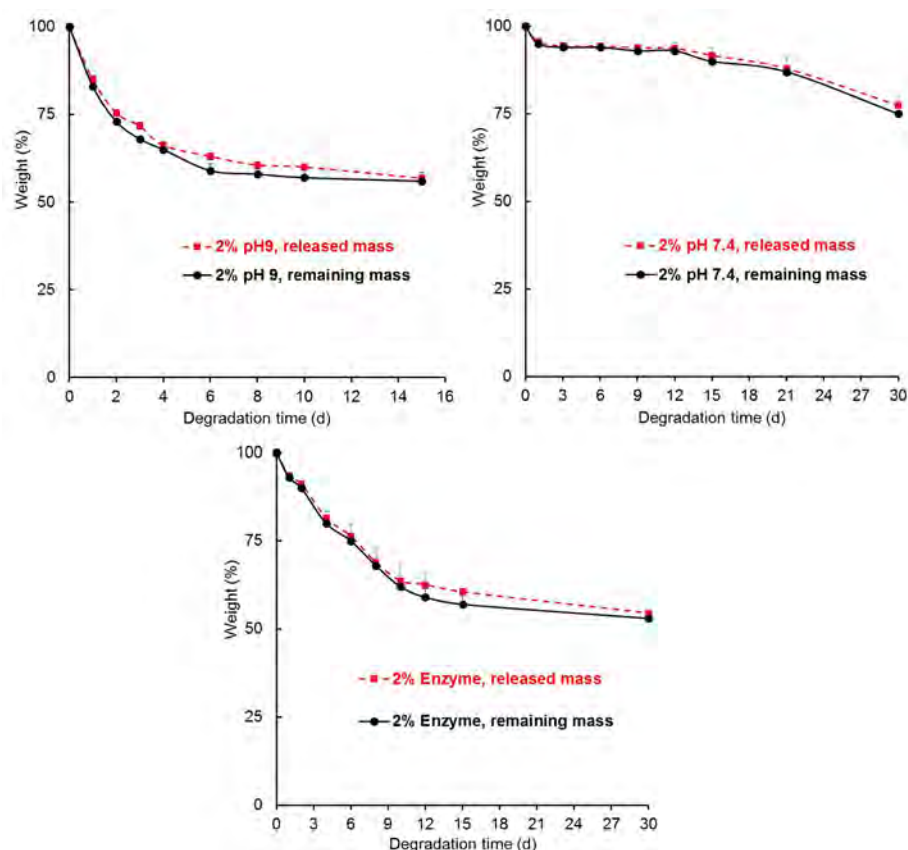

Figure 4.7 Comparative mass loss profiles for the degradation of CP-2%-COOH in three different conditions: weight loss percentage determined by the remaining mass (black line) and weight loss percentage determined by the released mass (dashed red line)

The results obtained with PDL and CP-2%-COOH polymers support the fact that the presence of carboxylic acid pendant groups significantly affect the degradation process of the polymer. In addition, the enzymes at pH 7.4 promote the degradation at double the rates of those at neutral conditions (pH 7.4 buffer), proving the efficiency of the enzymatic media in the polymer degradation. It should be noted that the mass loss profile of CP-2%-COOH in enzyme solution reached a plateau of degradation after 10 days, similar to that in pH 9 buffer after 6 days. The degradation in both conditions reached almost 50% of weight loss, probably

because non-functionalized PDL chains might be the main constituents of the remaining polymer.

The degradation of copolymers containing 5% of carboxyl pendant groups (CP-5%-COOH) was also investigated in the three different conditions at 40 °C: (1) pH 9 buffer solution (for 15 days), (2) pH 7.4 buffer solution (for 21 days), and enzymes in pH 7.4 buffer solution (for 12 days). After only 12 hours, a weight loss of 9 % was already observed in pH 9 buffer (Figure 4.8). Then, a significant increase in mass loss up to 20% was measured after 1 day, and up to 42 % after 8 days. Finally, the mass loss reached ≈ 52 % after 15 days. Unfortunately, at this stage, there were no more samples to continue the study.
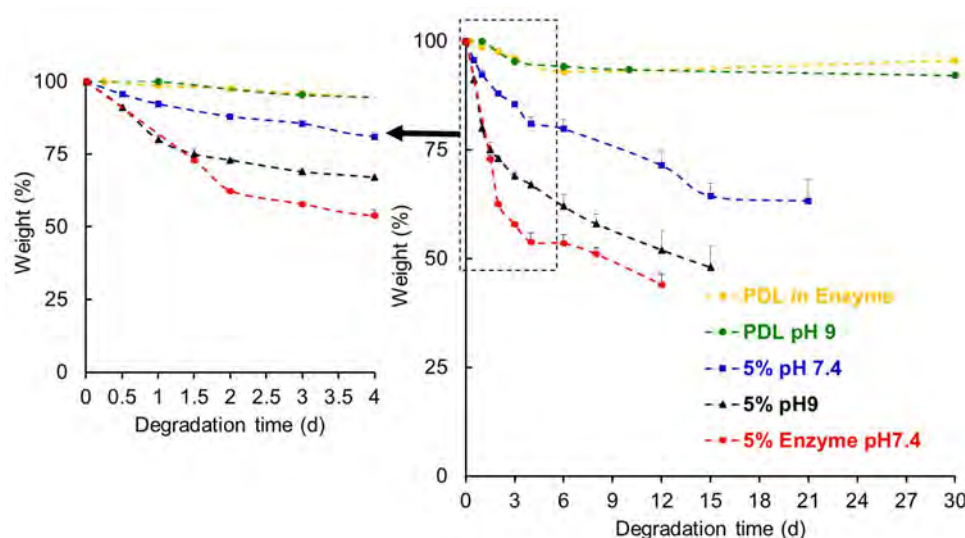

Figure 4.8 Mass loss profiles from the degradation of PDL DP50, and CP-5%-COOH in different hydrolysis conditions.

In pH 7.4 buffer, 4 % and 8 % of weight loss were observed after 12 hours and 1 day, respectively. From days 2 to 6, a slight change in mass loss was found, reaching 20% of weight loss. After 12 days, mass loss profiles showed a significant decrease in mass, as 29 % of copolymers was released into the degradation medium. Finally, the results after 15 to 21 days revealed a plateau of ≈ 36 % weight loss. For the enzymatic degradation, the results are different from those of hydrolytic degradations. At the beginning, a mass loss of 27% and 38% was found after a day and a half, and 2 days, respectively. At 8 days, a slight increase in weight loss was observed, reaching 49%. Finally, the last sampling showed 56% weight loss after 15 days.

Comparing the mass loss profiles between the degradation of CP-2%-COOH and CP-5%-COOH (Table 4.2 and Figure 4.9), the degradation of CP-5%-COOH showed greater weight loss percentages than that of CP-2%-COOH in all conditions, although they were quite

close for pH 9. Comparing the mass loss profiles of both PDL and CP-2%-or-5%-COOH, the very small weight loss from the degradation of PDL is consistent with the higher hydrophobicity, caused by the butyl pendant groups along the PDL backbone. Therefore, the rate of water diffusion into the bulk polymer is very slow, resulting in low possibility of chain cleavage caused by hydroxide ions. In marked contrast, the carboxyl pendant groups in the copolymer chains promote the diffusion of water into the polymer, as it should increase the hydrophilicity of PDL chains. This leads to a significant decrease in mass of copolymer, which may result from the increase of the water-affinity and the subsequent increase of the rate of polymer chain cleavage.

Table 4.2 Comparative mass loss data for the degradation of CP-2%-COOH and CP-5%-COOH after 15 days in three different conditions.

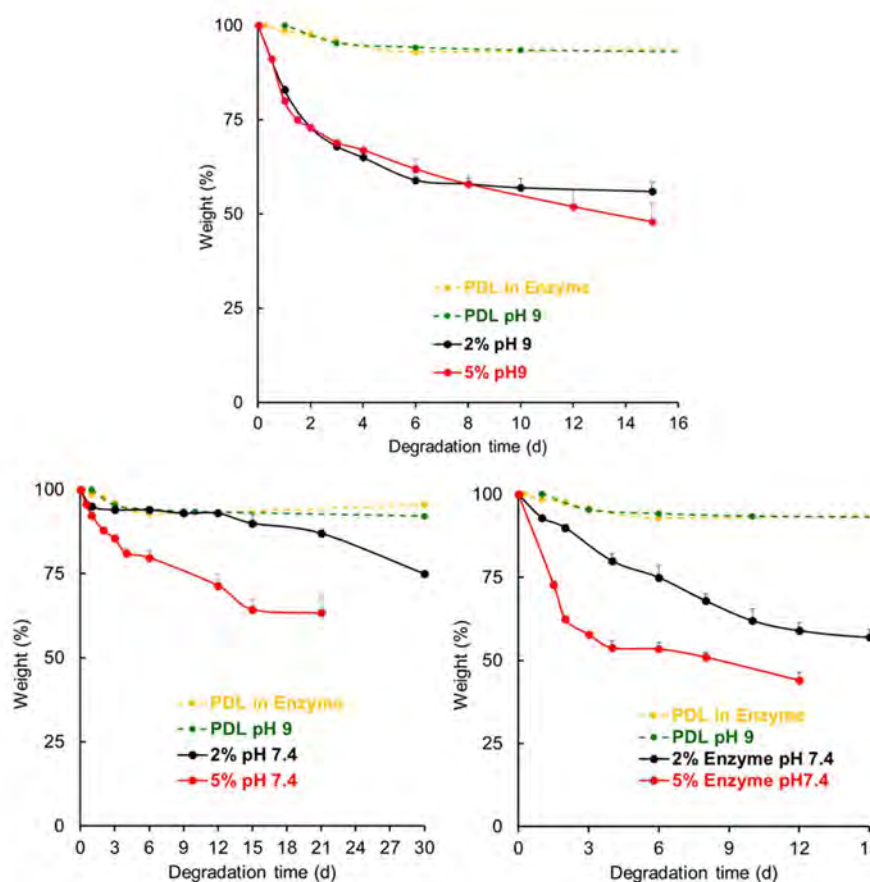| Polymer, condition	Time (d)	% weight loss	STD
CP-2%-COOH, pH 7.4	15	10	±5
CP-2%-COOH, pH 9	15	45	±5
CP-2%-COOH, Enzyme in pH 7.4	15	43	±5
CP-5%-COOH, pH 7.4	15	36	±6
CP-5%-COOH, pH 9	15	52	±5
CP-5%-COOH, Enzyme in pH 7.4	12	56	±5

Figure 4.9 Comparative mass loss profiles from the degradation of CP-2%-COOH (black), and CP-5%-COOH (red) in pH 9 buffer (top); in pH 7.4 buffer (bottom left) and in enzymatic solution (bottom right).

In contrast to base-promoted degradation, degradation of CP-5%-COOH in pH 7.4 buffer and in enzymatic medium showed markedly different hydrolysis rates compared to those of CP-2%-COOH (Figure 4.9 bottom). The higher amount of carboxylic acid pendant groups may also promote enzyme or water penetration into the material, increasing thereby the rate of hydrolysis.

We can also remark that a plateau of mass loss is clearly observed in pH 9 buffer for both materials, CP-2%-COOH and CP-5%-COOH; the plateau is reached much earlier in enzymatic conditions (Figure 4.9). These results may suggest a limit extent of degradation resulting from reduced water diffusion and hydrolysis. This is probably related to the fact that only a small amount of carboxylic acid pendant groups were introduced per polymer chain (for example, only one unit of carboxylic acid pendant group in CP-2%-COOH of DP 50, see in Figure 4.10). However, it is enough to strongly affect the degradation when compared with PDL.
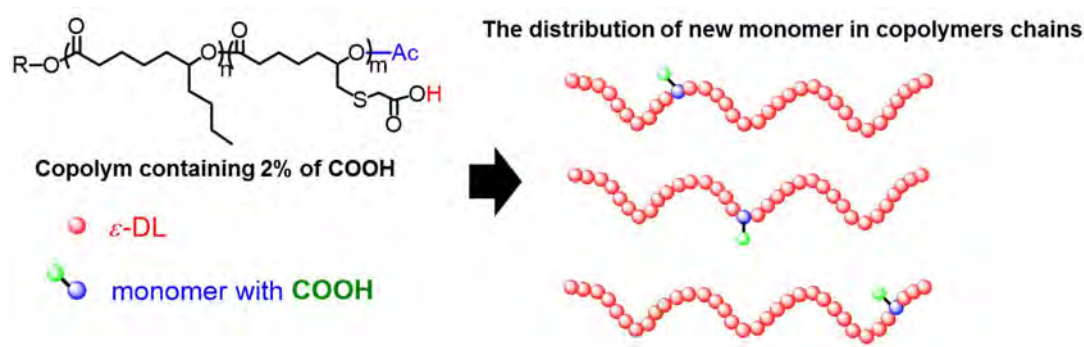

Figure 4.10 Proposed the structure of CP-2%-COOH with the distribution of COOH group.

4.2.2.2. Analysis of the degraded polymers and Discussion

All samples (remaining polymer and released products in the degradation media) were analyzed by SEC, and some of them by ^{1}H NMR and MALDI-TOF mass spectrometry.

For the CP-2%-COOH samples in pH 9, SEC analysis of the remaining copolymers reveal the gradual but weak decrease of M_n by 100 – 300 g/mol (M_n of 10300 g/mol for the initial polymer and M_n of 9900 g/mol after 15 days) with a broadening of Đ (from 1.17 to ≈ 1.34) (Figure 4.11). In addition, a minor population is observed at lower M_n (≈ 1000 g/mol) (Figure 4.11, bottom). These results may indicate that the random chain scission occurs most probably in intra-chain mode at a unit close to a carboxyl pendant group, thus cutting the CP-2%-COOH chains into two parts of hydroxyl and carboxyl end-chains. Therefore, the small

signal observed in the SEC traces represent the oligomers that somehow are not fully soluble in pH 9 buffer medium.
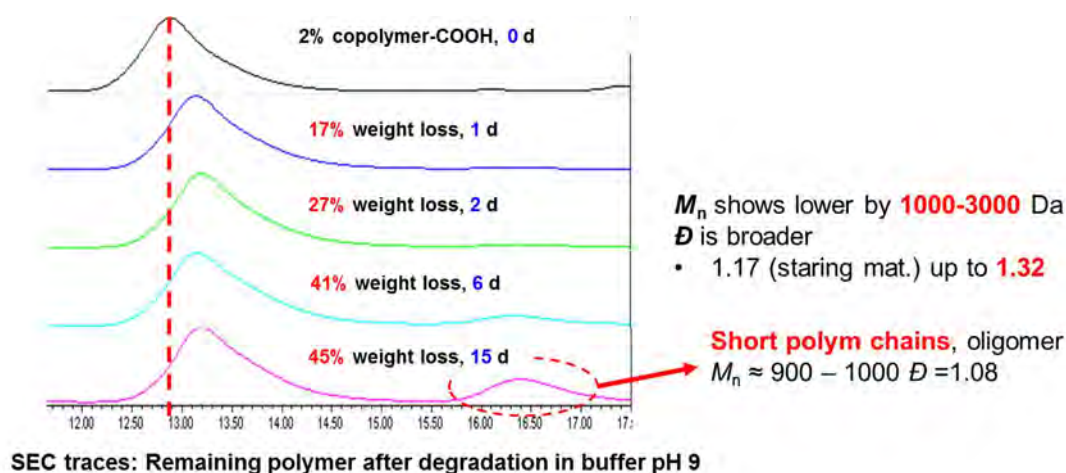

Figure 4.11 SEC traces of remaining copolymer after degradation in pH 9 buffer.

In the case of enzymatic degradation, the decrease of M_n was also very weak, although slightly higher, around 700 g/mol of decrease ($Đ = 1.31$ after 15 days) (Figure 4.12 (left)). In contrast to what was observed for the pH 9 samples, there is only one population in the SEC traces. Surprisingly, using physiological conditions (pH 7.4) led to the highest decrease in M_n (over 900 g/mol with a broadened $Đ$ of about 1.41) (Figure 4.12 (right)). However, as all these values are quite close, it is difficult to draw conclusions other than the fact that despite the marked weight loss, there was little impact on the M_n.
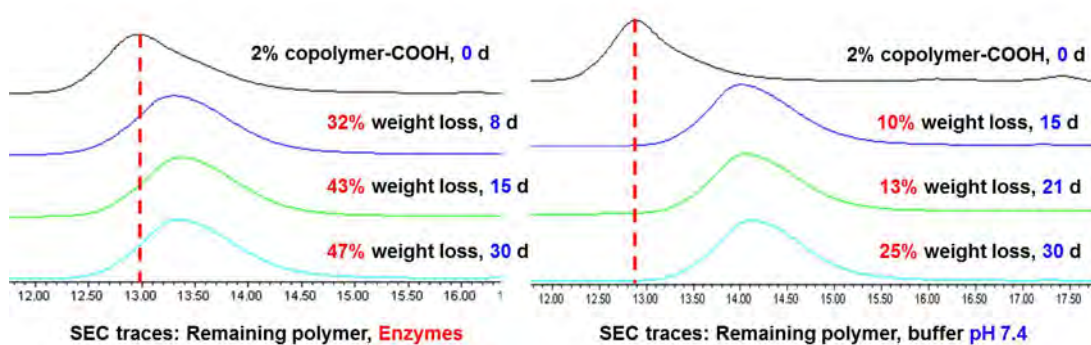
Figure 4.12 SEC traces of remaining copolymer after degradation in enzymatic solution (left) and in pH 7.4 buffer (right).

Bulk vs surface erosions: From all these data we can propose that the degradation of CP-2%-COOH in the three different conditions occurs probably *via* surface erosion, as significant mass of CP-2%-COOH is lost, but there is only a minor change in the molecular weight of the remaining copolymers. These results also suggest that the diffusion of small fragments or oligomers from the bulk is slower than the cleavage of polymer bonds, since the

degradation/chain scission mainly occurs at the surface of polymer film. As the hydrolysis rate is higher than the rate of water diffusion into the polymer, the degraded products should diffuse into the degradation media.

What about the released product in the degradation media? Based on the principle of surface degradation, the released products should be detected as lower molecular weight polymer chains and small molecules related to the monomer unit. First, the degradation media were extracted with $CHCl_3$. The two phases were then evaporated to dryness and analyzed by SEC analysis, MALDI-TOF, and ^1H NMR.

SEC traces of released product in organic phase from the degradation in pH 9 buffer showed very weak signals of polymer populations of similar M_n to those observed in the remaining polymer samples, including the second minor population at low M_n (but again, the intensity of the signals is really weak) (Figure 4.13). In addition, the growth in relative intensity of this minor population matches with the increase of short chains/oligomers in buffer solution during the degradation. Similar observations are done for the degradation in pH 7.4 buffer and in enzymatic conditions, including the minor population (Figure 4.14).
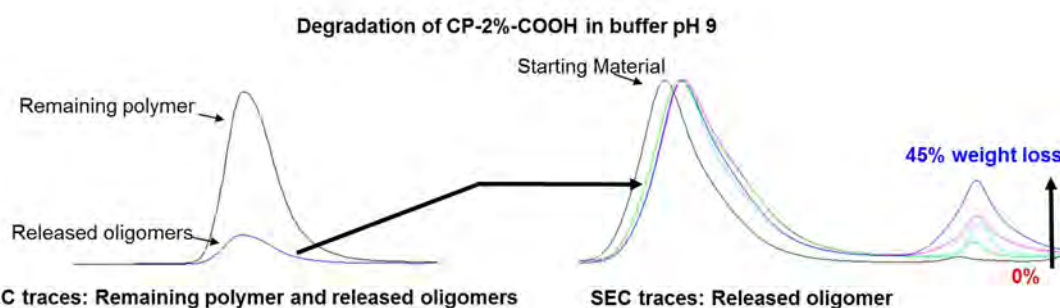
Figure 4.13 SEC traces of remaining copolymer and released products after degradation in buffer pH 9.

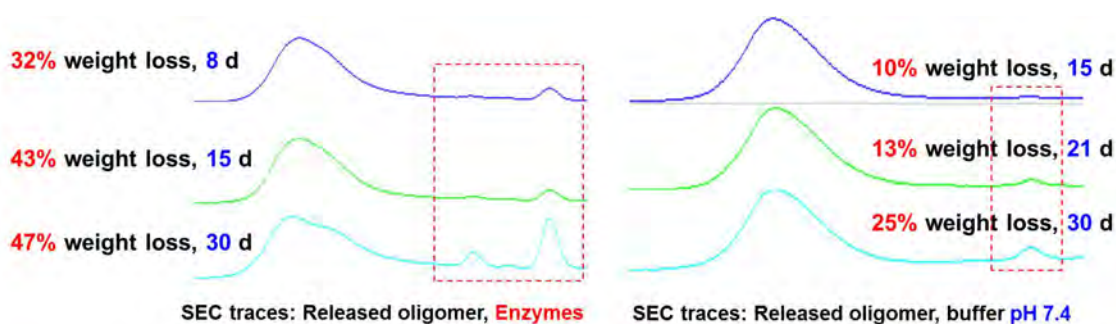**Figure 4.14** SEC traces of released products after degradation in buffer pH 7.4 and Enzyme.

Interestingly, the released products extracted in the organic phase were also analyzed by MALDI-TOF revealing the presence of low to moderate molecular-weight oligomer (Figure 4.15 as an example). For instance, the observed oligomers consist of 12 units of ε-DL monomer

and a unit of monomer **3** in deprotected form. Note that these oligomers are probably finely dispersed in the degradation media (e.g., pH 9 buffer and enzymatic solutions in pH 7.4 buffer containing enzymes), and dissolve in CHCl₃ during the extraction process. What is surprising is that the spectrum shows only one mass pic and no the distribution of mass pics typically observed for polymers.
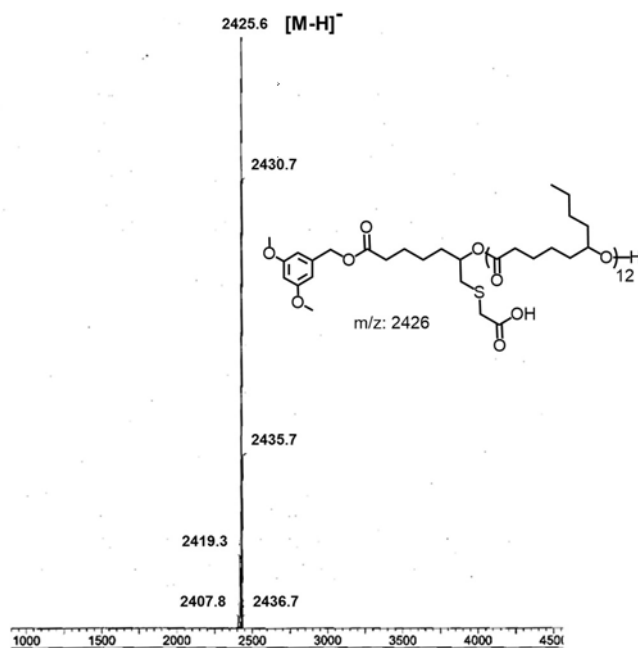
Figure 4.15 MALDI-TOF spectrum released products in organic phase after degradation in pH 9 buffer and in enzymes solution.

It is necessary to also identify the nature of the released products in water phase. First, the released products in water phase from the degradation in pH 9 buffer were analyzed by ^{1}H NMR (D₂O, 300MHz). However, only broad signals difficult to assign were observed. We moved next to the released products in the enzymatic medium, which were analyzed by ^{1}H NMR in D₂O (Figure 4.16). The spectrum depicts characteristic signals corresponding to the enzyme, in addition to signals that can be attributed to 6-hydroxydecanoate or to 6-hydroxydecanoic acid. A signal (a) at 3.70 – 3.62 ppm can be attributed to the –CH–OH, as well as the signal (b) at 2.20 ppm, integrating for two protons, to the –CH_2–COOH group. In addition, the signal (c) at 0.89 ppm (three protons) is consistent with the methyl group (–CH₃) from the butyl pendant chain.
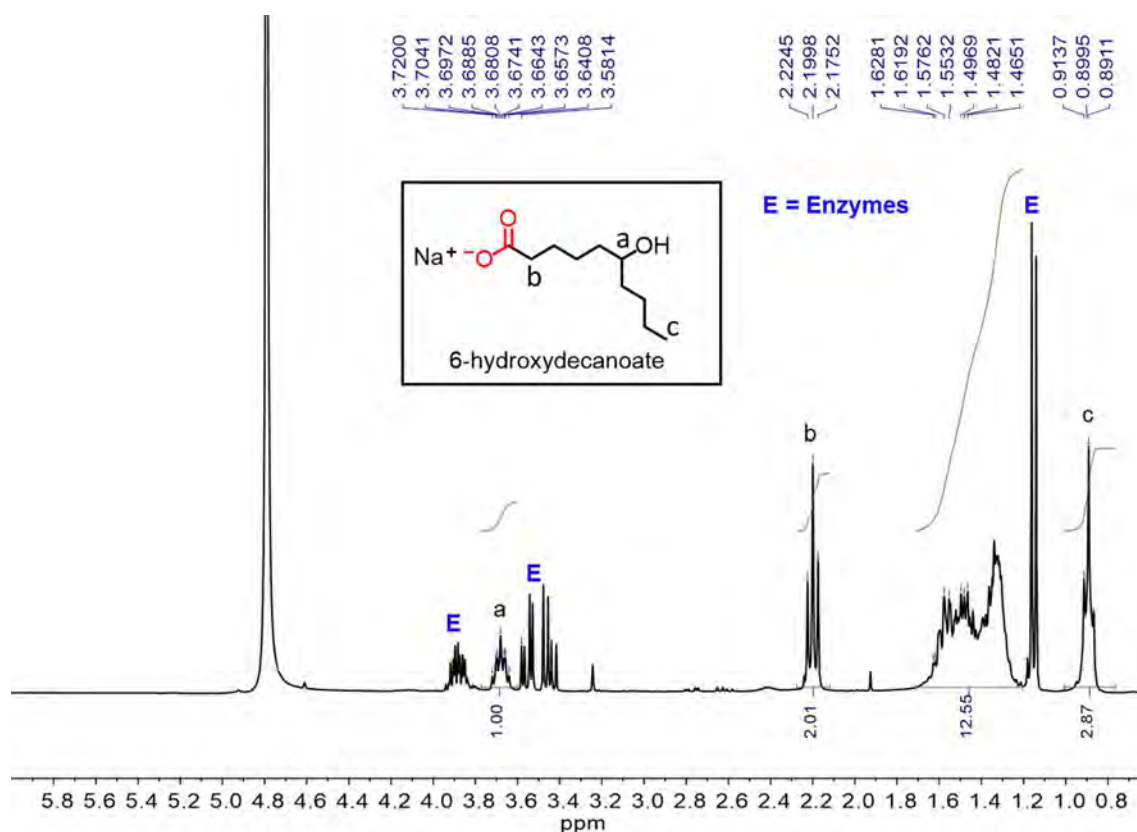
Figure 4.16 ^{1}H NMR Spectrum (D_2O, 300 MHz) of released products from the enzymes medium.

To conclude about the structure of the released products, authentic samples of 6-hydroxydecanoate and 6-hydroxydecanoic acid were prepared by hydrolysis of ε-DL using the reaction conditions reported for the hydrolysis of ε-CL (for more detail see the experimental section).[51] The hydrolysis products were characterized by ^{1}H NMR before and after acidic treatment (to analyze both the acid and the carboxylate). Figure 4.17 shows both spectra, which are almost identical except for the chemical shift of signal b, at 2.28 ppm for the carboxylic acid (top spectrum) and 2.18 ppm for the carboxylate (bottom spectrum). From all these data we can conclude that the released product is the 6-hydroxydecanoate, which is consistent with the pH of the degradation media. More importantly, it confirms the degradation of the polymers chains in monomer-like units.
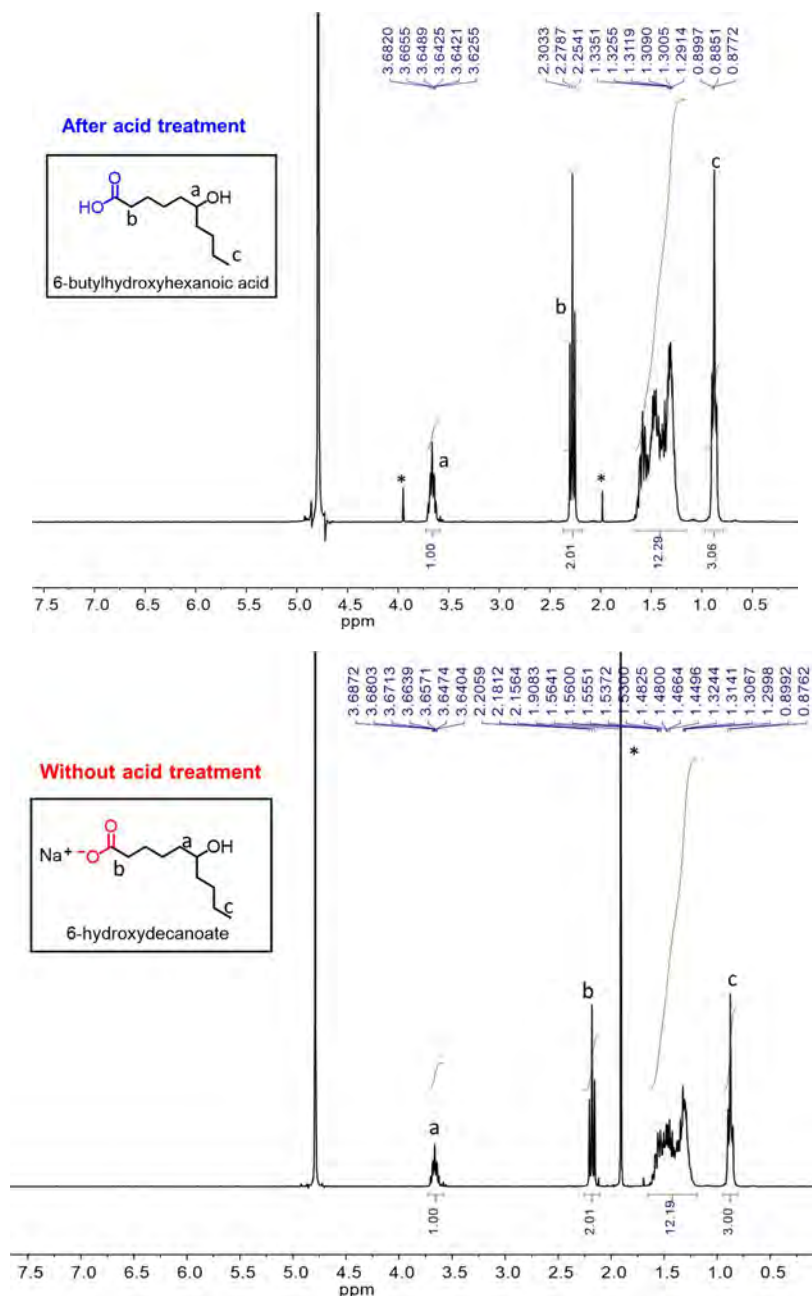
Figure 4.17 ¹H NMR spectrum (D$_2$O, 300 MHz) of 6-hydroxydecanoic acid (top) and 6-hydroxydecanoate (bottom).

What about PDL-based copolymer containing 5% of carboxyl pendant groups? Before discussing the post-degradation analysis of CP-5%-COOH, it would be beneficial to investigate their water-affinity/solubility. To do so, 20 mg of copolymers containing 5% of carboxyl pendant groups was dispersed in 0.5 mL of D$_2$O and the sample was analyzed by ¹H NMR (D$_2$O, 300 MHz as shown in Figure 4.18). The obtained ¹H NMR spectrum showed exclusively signals corresponding to water, thus confirming the insolubility of these copolymers in water.
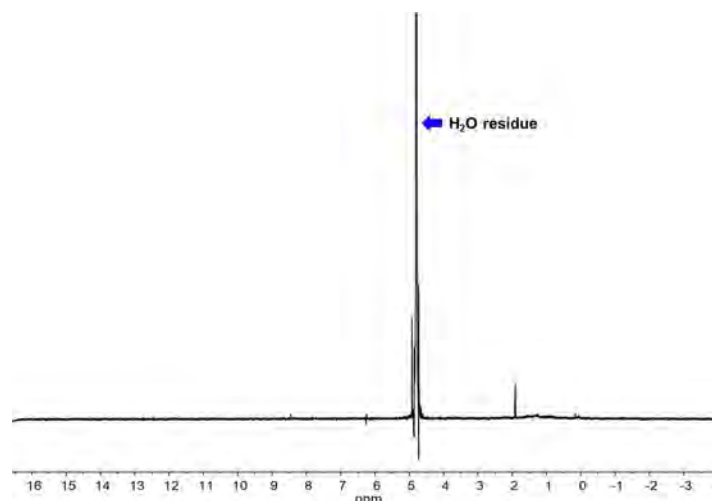
Figure 4.18 ^{1}H NMR spectrum (D$_2$O, 300 MHz) of CP-5%-COOH.

After the degradation, the remaining copolymers were analyzed by SEC, and the results were found different to those obtained for CP-2%-COOH. The SEC traces revealed significant changes in M_n and Đ during the degradation (Figure 4.19a). For example, the remaining CP-5%-COOH after 8, 12, and 15 days of degradation in pH 9 buffer had M_n, around 3000 – 4000 g/mol lower than the initial one (8 200 and 4 900 for the initial polymer and the remaining one after 15 days, respectively), with broadening Đ of 1.49 (1.19 for the initial sample) (Figure 4.19a (left)). At day 21, the remaining CP-5%-COOH from the degradation in pH 7.4 buffer also showed significant changes in M_n over 4 300 g/mol and Đ of 1.50 (Figure 4.19a (center)). Finally, the remaining polymer from degradation in enzymatic conditions displayed a decrease in M_n and broadening of Đ even more marked than the two hydrolytic degradations (Figure 4.19 (right). After 6 days of enzymatic degradation, a significant change in M_n was observed, lower by 5000 g/mol with a broad Đ of 1.52. After 12 days, M_n is 2700 g/mol and Đ is 1.53. In contrast to the remaining copolymers from the degradation of CP-2%-COOH, no minor populations were detected by SEC in all degradation conditions.

The composition of the remaining polymer after enzymatic degradation was analyzed by ^{1}H NMR spectroscopy, and the result was compared with the starting material (CP-5%-COOH), see in Figure 4.19b. In the stacked ^{1}H NMR spectra, the spectrum of remaining polymer mainly displays the signals of protons from PDL, –CHO$_{PDL}$ (a) for example, whereas none of the signals from –CHO$_{P3}$ (b), neither (c) nor (d), remained. This is consistent with the remaining polymer being exclusively non-functionalized PDL.

Figure 4.19 (a) SEC traces of remaining copolymers from the degradation of CP-5%-COOH in three different conditions. (b) Stacked ^{1}H NMR spectra of remaining polymer after enzymatic degradation and CP-5%-COOH.

Based on these results between the mass loss profiles and the M_n analyzed by SEC, the degradation of CP-5%-COOH, in the three different conditions, is most likely initiated *via* surface erosion mode but during the process changes to bulk erosion.

What about the released product in the degradation media? The degradation media were also extracted using a similar procedure to that of CP-2%-COOH. In contrast to the results from the degradation of CP-2%-COOH, SEC traces of the released products, extracted in the organic phase, from the degradation of CP-5%-COOH in all conditions showed extremely low intensity of signals in the chromatogram. It was thus impossible to determine both M_n and $Đ$.

Therefore, the released products in organic phase were directly analyzed by MALDI-TOF MS, and the results showed very low molecular-weight oligomers (Figure 4.20a). These oligomers mostly consist of 2 units of monomer **3** in deprotected form and the initiator (DMBA). Notably, these oligomers are largely dispersed in the degradation media (e.g., pH 9 buffer and enzymes in pH 7.4 buffer) and are soluble in $CHCl_3$ during the extraction process. Next, the released products in water phase from the enzymatic degradation were also examined by HPLC-MS. Interestingly, small molecules corresponding to 1 and 2 units of hydrolyzed form of ε-DL units were detected (Figure 4.20b).
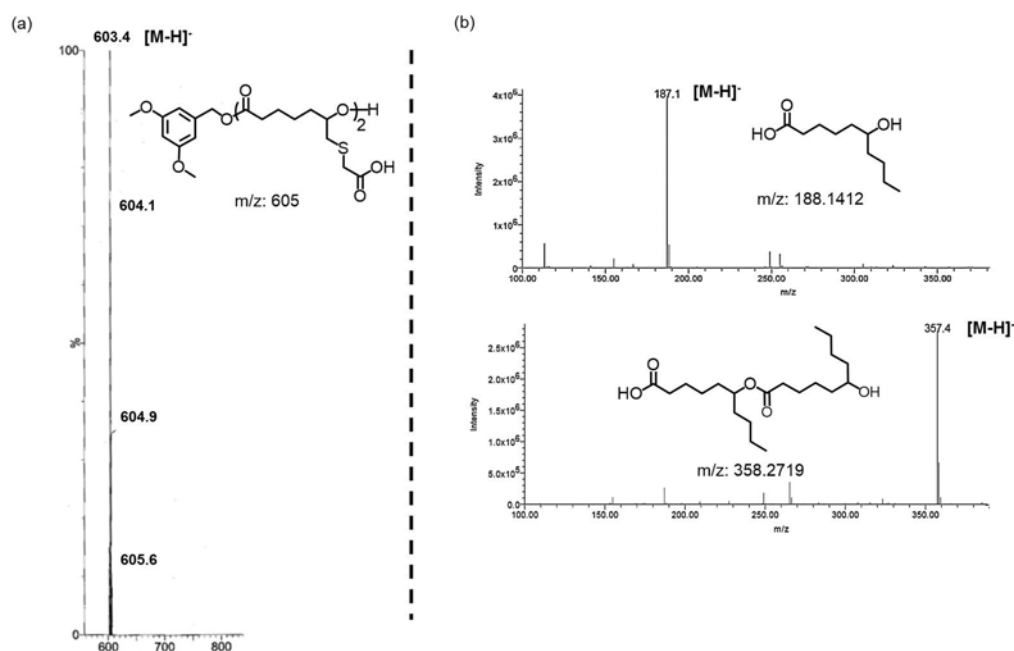

Figure 4.20 Mass spectra of released products from the degradation of CP-5%-COOH: (a) from organic phase analyzed by MALDI-TOF and (b) from water phase obtained from HPLC-MS.

Finally, the released products in aqueous phase for all degradations were analyzed by ^{1}H NMR spectroscopy. ^{1}H NMR spectrum of the released products from pH 7.4 buffer showed several broad signals that are similar to the hydrolyzed form of ε-DL monomer. However, the ^{1}H NMR spectrum was obtained with a very poor resolution, as a very small amount of degraded products was isolated. A similar ^{1}H NMR spectrum was obtained for the degradation in pH 9 buffer, but with slightly better resolution than the one of pH 7.4 buffer (Figure 4.21). Although the signals are not well resolved, they suggest the structure of this degraded product to be hydrolyzed ε-DL monomer.
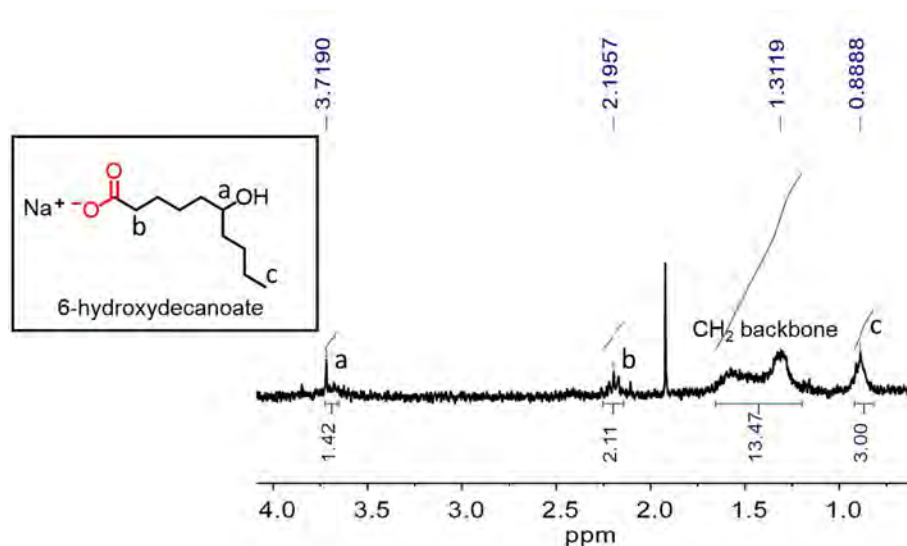
Figure 4.21 ^{1}H NMR spectrum (D$_2$O, 300 MHz) of released products from the degradation in pH 9 buffer.

Conversely, the ^{1}H NMR spectrum of released products from the enzymatic degradation were well resolved and revealed the characteristic signals of protons corresponding to the 6-hydroxydecanoate fragment (Figure 4.22). In addition, several signals were also observed with a very low intensity in the 2.40-2.90 ppm region (as marked by * in Figure 4.22) as well as at 3.25 and 4.15 ppm. Further inspection of the ^{1}H NMR spectrum in Figure 4.23 reveals signals that are consistent with : one proton of –CHO for the signal at 4.17 – 4.06 ppm (a), an AB system for –S–C**H**$_2$–CH–OH at 2.77 and 2.62 ppm (b), and two protons of methylene functional group next to the carboxylic acid group (–S–C**H**$_2$–COOH) at 3.24 ppm (c). These characteristic signals can be tentatively attributed to the hydrolyzed form of monomer **3** with carboxylic acid pendant chain, namely 7-((carboxymethyl)thio)-6-hydroxyheptanoic acid, probably in the basic form.
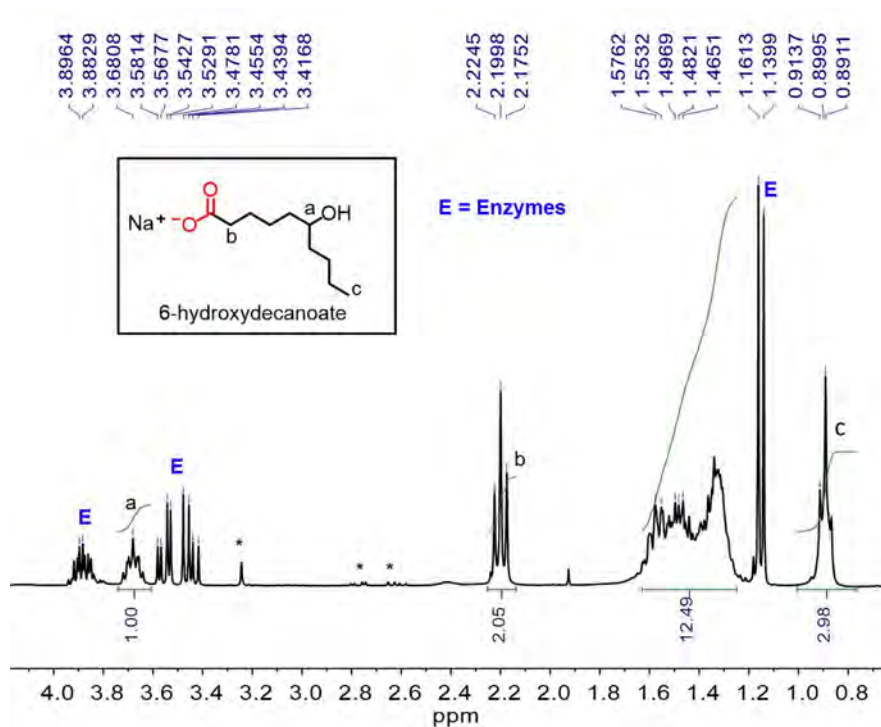
Figure 4.22 ^{1}H NMR spectrum (D$_2$O, 300 MHz) of released products from the degradation of CP-5%-COOH in enzymes solution.

Figure 4.23 ^{1}H NMR spectrum (D$_2$O, 300 MHz) of released product represents the hydrolyzed form of new monomer **3** as 7-((carboxymethyl)thio)-6-hydroxyheptanoic acid.
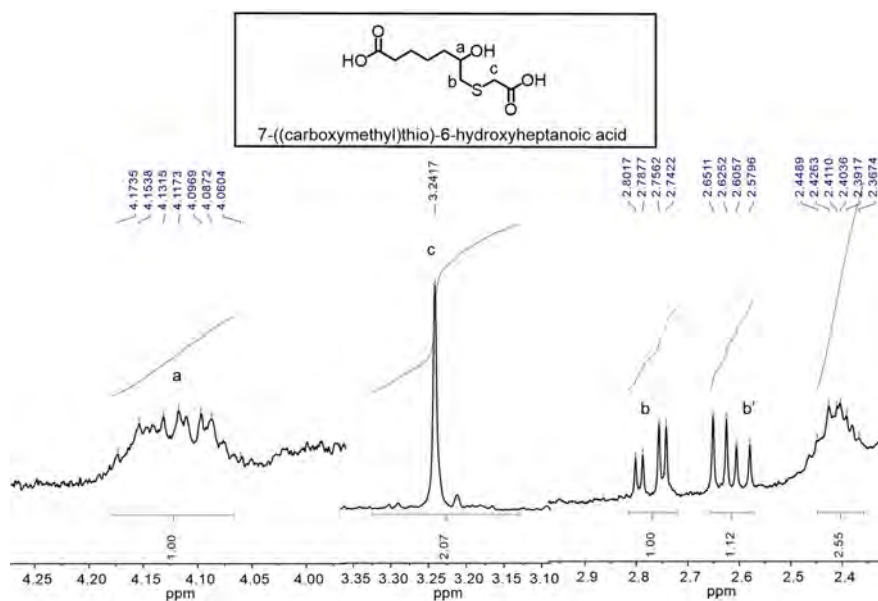
This observation strongly suggests the presence of the functionalized units in the degradation medium and is thus fully consistent with the non-functionalized PDL structure of the remaining polymer.

4.3 Conclusions

The degradation of CP-2%-COOH and CP-5%-COOH has been investigated in both hydrolytic and enzymatic conditions, and the results have also been compared with homo-PDL with DP50 revealing a significant impact of the carboxyl pendant groups on the PDL chains. First, polymer film preparation was examined using several techniques based on reported methods. As both PDL and the copolymers are sticky materials probably due to their amorphous character and low T_g, a method to cast the copolymer directly on the flat-bottom glass vial was applied. The thin films were carefully prepared by slow solvent evaporation, followed by drying process under vacuum to homogenize the surface and bulk of polymer film.
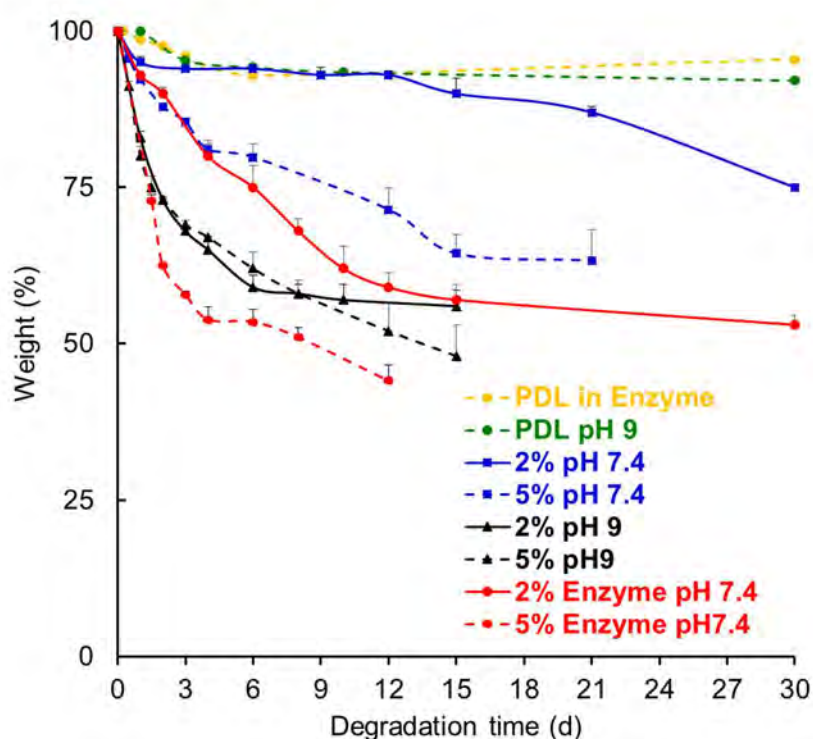
Figure 4.24 Mass loss profiles the degradation of PDL DP50, CP-2%-COOH, and CP-5%-COOH.

Mass loss profiles showed a large difference in hydrolysis rates between PDL DP50, CP-2%-COOH, and CP-5%-COOH (Figure 4.32). Having 2% or 5% loading inside the PDL backbone, degradation rates are 2.5-5 times and 4-6 times (for 2% loading and for 5% loading, respectively) faster than the homo-PDL. The degradation of CP-2%-COOH in hydrolytic conditions showed very little change in M_n and Đ observed by SEC. The remaining polymer revealed that M_n is only lower by 100-300 g/mol and the Đ is broader (up to 1.4) compared to the starting material. However, ^{1}H NMR spectra of released products from the degradation showed no signals corresponding to degraded products such as hydrolyzed forms of ε-DL and monomer **3**.

In contrast, the analysis by ^{1}H NMR spectroscopy of the released product in water phase demonstrated the presence of hydrolyzed ε-DL monomer for the enzymatic degradation. Hydrophilic oligomers which are finely dispersed in buffered solution were observed for all degradation studies by SEC analysis of the released product in organic phase. Then, the released products from degradation in organic phase were examined by MALDI-TOF, and oligomer with 12 DL units and a unit of monomer **3** in carboxylic acid form were detected in the mass spectra. It should be noted that the oligomers are actually soluble in degradation media (pH 7.4 and 9 buffer solutions).

Both hydrolytic and enzymatic degradation processes of CP-5%-COOH showed not only significant mass loss and a marked difference of M_n and $Đ$ observed by SEC, but also the hydrolyzed form of ε-DL and monomer **3** in deprotected form were detected by ^{1}H NMR spectroscopy. The remaining copolymers presented a large decrease in M_n (3000-5000 g/mol) from the starting material, and a broader of $Đ$, from 1.19 to 1.52. In addition, no signs of oligomers were observed by SEC, in which these results are totally different from the one of CP-2%-COOH. This confirms that not only the presence of the carboxylic units along the polymer chains promotes the degradation, but in addition, the number of functional groups impacts the degradation rates.

All these results reveal that the introduction of low amounts (2-5 %) of carboxyl group along the polymers chains of PDL, thanks to the new monomer **3**, has a marked impact on its hydrophilicity and its degradation rates, both in hydrolytic and enzymatic conditions. Furthermore, the different behavior between CP-2%-COOH and CP-5%-COOH also evidences that is possible to tune the degradation rate by adjusting the amount of functional group. The materials investigated here are therefore promising candidates as renewable and biodegradable alternatives to commercially available petroleum-based materials.

4.4 Experimental Part

Hydrolysis of ε-DL monomer as a reference degraded molecule.

ε-DL (34 g, 0.20 mol) was added into a solution of sodium hydroxide (0.2 mol in 50 mL of water), and then the reaction mixture was stirred at room temperature overnight. The solution was cooled in an ice bath and acidified with 10% HCl. The clear reaction mixture was then extracted with ethyl acetate (EtOAc) (4 × 15 mL), and the organic phase was washed with saturated NaCl (2 × 50 ml), dried over anhydrous sodium sulfate (Na_2SO_4), and filtered to give the product as a clear white solid.

Degradation study

Phosphate-Buffered Saline (pH 7.4) and pH 9 buffered solution were purchased from Aldrich and used as received. The enzymatic degradation solution was prepared from Novozym® 51032, which is a lipase originating from *Aspergillus* micro-organism (Strem Chemicals, Inc.), and **Phosphate Buffered Saline (pH 7.4)** to obtain a final lipase (enzymes) concentration of 4 mg/mL following the reported procedure[5]. All testing parameters of the degradation experiments were outlined according to ASTM F1635, standard test method for *in vitro* degradation.[10,12] Key features of the standard include: (i) a solution-to-specimen mass ratio of greater than 30:1 to provide adequate buffer capacity, (ii) a sealable container to prevent solution loss by evaporation, (iii) a minimum number of specimens (N) of $N = 3$ per time period, and (iv) removal of the dried and weighed specimens from a mass loss study.

A typical procedure to prepare the dried polymer films before exposure to hydrolytic/enzymatic degradation

The materials are dissolved in dichloromethane (30 mg/mL) and placed (1 mL) in a flat bottom glass vial. The solvent is slowly evaporated at room temperature overnight, and the materials are dried under high vacuum oven at 60 °C for 2 days. Finally, the thin films have a diameter of 13 mm and a thickness of ≈ 0.5 mm corresponding to a weight of 30 mg approximately.

Hydrolytic degradation study

The dried thin films of copolymers and homopolymer, PDL DP50, were subjected to hydrolytic degradation in **phosphate-buffered saline (pH 7.4) or pH 9 buffered solution at 40 °C for**

15-30 days. Each degradation study was composed of 24-30 samples for 8-10 sampling times. Each sample contained 2 mL of pH 7.4 or 9 buffered solutions (pH remains constant during all the degradation processes). The samples were placed in the thermostatically controlled oven without shaking. Triplicate samples were withdrawn from the degradation processes at the specific time: between 12 hours and 1 month. The buffered solutions were then carefully removed from the samples. The samples were rinsed with deionized water and dried under high vacuum oven at 60 °C for 2 days to yield constant weight before the various analyses: weight loss, ^{1}H NMR spectroscopy and SEC analysis.

Enzymatic degradation study

The enzymatic degradation tests were achieved in a similar way using **phosphate-buffered saline (pH 7.4, 2 mL) containing lipase from Novozym® 51032 (8 mg, freshly prepared). Samples were placed in** the thermostatically controlled oven and withdrawn at the specific time: between 12 hours and 15 days. The buffered enzyme solutions were carefully removed from the samples. The samples were rinsed with deionized water and dried under high vacuum oven at 60 °C for 2 days prior to analysis in a similar protocol in the hydrolytic degradation study.

Measurements

After hydrolytic degradation for predetermined periods of time, the percentage weight loss of the degraded polymers and blends was determined by the following equation:

$$\text{Weight loss (\%)} = [(W_0-W_t)/W_0] \times 100 \qquad (1)$$

Where W_0 and W_t are the initial weight and weight of material dried after the predetermined time period.

4.5 Bibliography

1. Barlow, C. Y.; Morgan, D. C.; *Resour. Conserv. Recycl.* **2013**, *78*, 74.

2. Tehrani, I. M.; Fathi, A.; Badr, H.; Daly, S.; Shirazi,A. N.; Dehghani, F. *Polymers*, **2016**, *8*, 1.

3. Haider, T.; Völker, C.; Kramm, J.; Landfester, K.; Wurm, F. R. *Angew. Chem. Int. Ed.* **2019**, *58*, 50-62.

4. Sevim, K.; Pan, J. *Acta Biomater*. **2018**, *66*, 192.

5. Ken, W.; Vladimir, H.; Patrick A. T. *J. Biomed. Mater. Res*. **1998**, *41*, 422.

6. Ghassemi, A. H.; van Steenbergen, M. J.; Talsma, H.; van Nostrum, C. F.; Jiskoot, W.; Crommelin, D. J. A.; Hennink, W. E. *J. Contr. Release*, **2009**, *138*, 57.

7. McNaught, A.D.; Wilkinson, A. *IUPAC. Compendium of Chemical Terminology,* 2nd ed. (the "Gold Book"), Wiley-Blackwell, Chichester. **1997**.

8. Guide for vocabulary in the field of degradable and biodegradable polymers and plastic items: PD CEN/TR 15351:2006, BSI, **2006**, 23.

9. Lucas, N.; Bienaime, C.; Belloy, C.; Queneudec, M.; Silvestre, F.; Nava-Saucedo, J. E. *Chemosphere*, **2008**, *73*, 429.

10. Woodard, L. N.; Grunlan, M. A. *ACS Macro Lett*. **2018**, *7* (8), 976.

11. Ottenbrite, R.; Albertsson, A.; Scott, G. Discussion on Degradation Terminology. In *Biodegradable Polymers and Plastics*; Vert, M.; Feijen, J.; Albertsson, A.; Scott, G.; Chiellini, E, The Royal Society of Chemistry: Cambridge, London, **1992**, 73.

12. ASTM Standard D6400 Standard Specification for Labelling of Plastics Designed to Be Aerobically Compostable in Municipal or Industrial Facilities; **2012** ASTM Annual Book of Standards ASTM International, West Conshohocken, PA (**2012**), 10.1520/D6400–D6412

13. Göpferich, A. *Biomaterials*, **1996**, *17* (2), 103.

14. I. (a) Kyrikou, D.; Briassoulis, J. *Polym. Environ*. **2007**, *15*, 125. (b) Emadian, S. M.; Onay, T. T.; Demirel, B. *Waste Manage*. **2017**, *59*, 526.

15. Laycock, B.; Nikolić, M.; Colwell, J. M.; Gauthier, E.; Halley, P.; Bottle, S.; George, G. *Prog. Polym. Sci*. **2017**, *71*, 144.

16. Lyu, S.; Untereker, D. *Int. J. Mol. Sci*. **2009**, *10*, 4033.

17. Andrady, A. L. *J. Macromol. Sci. Polym. Rev*. **1994**, *34*, 25.

18. Valverde, C.; Lligadas, G.; Ronda, J. C.; Galià, M.; Cádiz, V. *Polym. Degrad. Stabil*. **2018**, *155*, 84.

19. Shen, J.; Burgess, D. J. *J. Pharm. Pharmacol*. **2012**, *64*, 986.

20. Pierre, T.S.; Chiellini, E. *J. Bioact. Compat. Polym*. **1986**, *1*, 467.

21. (a) Jung, J. H.; Ree, M.; Kim, H. *Catal*. **2006**, *115*, 283. (b) Gan, Z.; Yu, D.; Zhong, Z.; Liang, Q.; Jing, X. *Polymer*, **1999**, *40*, 2859.

22. Rittié, L.; Perbal, B. *J. Cell Commun. Signaling*. **2008**, *2*, 25.

23. Eubeler, J. P.; Bernhard, M.; Knepper, T. P. *Trac-Trends Anal. Chem*. **2010**, *29*, 84.

24. Walter, T.; Augusta, J.; Müller, R. -J.; Widdecke, H.; Klein, J. *Microb. Technol*. **1995**, *17*, 216.

25. Hoshino, A.; Isono, Y. *Biodegradation*, **2002**, *13*, 141.

26. Sakai, K.; Kawano, H.; Iwami, A.; Nakamura, M.; Moriguchi, M. *J. Biosci. Bioeng*. **2001**, *92*, 298.

27. (a) Muller, R. -J. *Biochem*. **2006**, *41*, 2124. (b) He, F. *Polymer*, **2003**, *44*, 5145. (c) Lee, C.; Kimura, J.; Chung, J. D. *Macromol. Res*. **2008**, *16*, 651. (d) Fukuzaki, H.; Yoshida, M.; Asano, M.; Kumakura, M.; Mashimo, T.; Yuasa, H.; Imai, K.; Hidetoshi, Y. *Polymer*. **1990**, *31*, 2006. (e) Mochizuki, M.; Hirano, M.; Kanmuri, Y.; Kudo, K.; Tokiwa, Y.; *J. Appl. Polym. Sci*. **1995**, *55*, 289. (f) Gan, Z.; Liang Q.; Zhang, J.; Jing, X. *Polym. Degrad. Stab*. **1997**, *56*, 209. (g) Li, S. M.; Pignol, M. ; Gasc, F.; Vert, M. *Macromolecules*, **2004**, *37*, 9798.

28. (a) Abou Zeid, D.-M., **2001**. Anaerobic biodegradation of natural and synthetic polyesters. Ph.D thesis, Technischen Universität Carolo-Wilhelmina zu Braunschweig. (b) Belal, E.S., **2003**. Investigations on biodegradation of polyesters by isolated mesophilic microbes. Ph.D Thesis, Technischen Universität Carolo- Wilhelmina zu Braunschweig.

29. Cheneler, D.; Bowen, J. *Soft Matter*. **2013**, *9*, 344.

30. Rahaman, H.; Tsuji, H. *Polym. Degrad. Stab*. **2013**, *98* (3), 709.

31. Sailema-Palate, G. P.; Vidaurre, A.; Campillo-Fernández, A. J.; Castilla-Cortázar, I. *Polym. Degrad. Stab*. **2016**, *130*, 118.

32. Liao, C.J.; Chen C.F.; Chen, J.H.; Chiang S.F.; Lin, Y.J.; Chang, K.Y. *J. Biomed. Mater. Res*. **2002**, *59* (4), 676.

33. Arias, V.; Olsén, P.; Odelius, K.; Höglund, A.; Albertsson, A.C. *Polym. Chem*. **2015**, *6*, 3271.

34. Loh, X. J. *J. Appl. Polym. Sci*. **2013**, *127*, 2046.

35. Tsuji, H.; Ishizaka, T. *J. Appl. Polym. Sci.*, **2001**, *80*, 2281.

36. De Hoe, G.X.; Zumstein, M.T.; Tiegs, B.J.; Brutman, J.P.; McNeill, K.; Sander, M.; Coates, G. W.; Hillmyer, M. A. *J. Am. Chem. Soc.* **2018**, *140* (3) 963.

37. van de Wetering, P.; Metters, A. T.; Schoenmakers, R. G.; Hubbell, J. A. *J. Control. Release.* **2005**, *102* (3), 619.

38. Tsuji, H.; Ikada, Y. *Polym. Degrad. Stab.* **2000**, *67* (1), 179.

39. Lam, C. X.; Savalani, M. M.; Teoh, S.-H.; Hutmacher, D. W. *Biomed. Mater.* **2008**, *3* (3), 034108.

40. Xu, X.-J.; Sy, J. C.; Shastri, V. P. *Biomaterials*, **2006**, *27* (15), 3021.

41. Gu, B.; Sun, X.; Papadimitrakopoulos, F.; Burgess, D. J. *J. Control. Release.* **2016**, *228*, 170.

42. Choi, N.-S.; Kim, C.-H.; Cho, K. Y.; Park, J.-K. *J. Appl. Polym. Sci.* **2002**, *86* (8), 1892.

43. Lu, L.; Garcia, C. A.; Mikos, A. G. *J. Biomed. Mater. Res.* **1999**, *46* (2), 236.

44. Rahaman, H.; Tsuji, H. *Polym. Degrad. Stab.* **2013**, *98* (3), 709.

45. Jang, J.; Park, H.; Jeong, H.; Mo, E.; Kim, Y.; Yuk, J. S.; Choi, S.Q.; Kimac, Y. –W.; Shin, J. *Polym. Chem.* **2019**, *10*, 1245.

46. Saha, S. K.; Tsuji, H. *Polym. Degrad. Stab.* **2006**, *91* (8), 1665.

47. Gaona, L. A.; Gómez Ribelles, J. L.; Perilla, J. E.; Lebourg, M. *Polym. Degrad. Stab.* **2012**, *97* (9), 1621.

48. von Burkersroda, F.; Schedl, L.; Göpferich, A. *Biomaterials*, **2002**, *23* (21), 4221.

49. Valverde, C. ; Lligadas, G.; Ronda, J. C.; Galià, M.; Cádiz, V. *Polym. Degrad. Stab.* **2008**, *155*, 84.

50. Arias, V.; Olsén, P.; Odelius, K.; Höglund, A.; Albertsson, A.-C. *Polym. Chem.* **2015**, *6*, 3271.

51. Zhu, H.; Yang, Z.; Li, N.; Wang, X.-J.; Wang, F.; Su, H.; Xie, Q.; Zhang, Y.; Ma, Y.-X.; Lin, B.-H. *J. Organomet. Chem.* **2012**, *716*, 95.

General conclusion

The object of this work was to develop biodegradable polyesters based on a renewable monomer (ε-DL) with tunable properties, in particular enhanced degradability. To do so, the introduction of pendant functional groups along the polymer chains has been envisioned by the copolymerization of ε-DL with functionalized monomers of related structure. We have developed a new strategy for the preparation of ε-functionalized-ε-caprolactones, whose structure is close to that of ε-DL. A reaction sequence consisting of a transition metal-catalyzed cycloisomerization followed by a free radical thiol-ene coupling process leads selectively to the targeted lactones. Notably, this strategy allows overcoming the regioselectivity problem associated with the Baeyer-Villiger oxidation of functionalized dissymmetric ketones, which is the main drawback. The alkylidene-lactone (**1**) has been easily prepared in large scale (5 grams) in a good yield (72%) thanks to the catalytic cycloisomerization of 6-heptynoic acid with a Pt pincer complex. Then, the functionalization of compound **1** with benzyl thiol and benzyl ester thiol has been achieved yielding the monomers **2** and **3**, respectively. Notably, the two functionalized monomers **2** and **3** can be synthesized in large scale with good yields (>80%).

In chapter II, we described an alternative dual catalyst associating $InCl_3$ and NEt_3 to promote controlled ROP of ε-DL under mild conditions (toluene, 3M, 60 °C, 1-20 h). PDL of well-defined structures with M_n up to 30 000 g/mol ($Đ \sim 1.2$) and free of catalytic residues have been obtained. Besides the typical ester end-capped PDLs, amide end groups have been installed thanks to the ability of the dual catalyst to perform with primary amines as initiators. As a result, amphiphilic PEG-NH-PDL block copolymers, with a strong peptidic bond between the two blocks could be prepared. Block P(DL-*b*-CL)/P(CL-*b*-DL) and random P(DL-*r*-CL) copolymers have been also prepared by sequential and simultaneous ROP with ε-CL, respectively. NMR spectroscopy, SEC and DSC confirmed their well-defined block or random structures, evidencing the controlled character of the polymerization and the low impact of transfer reactions. The use of the $InCl_3/NEt_3$ association thus enables significant progress in ε-DL polymerization. This catalyst is complementary of those reported previously in terms of reaction conditions, chain-end functionality and purity quality of the polymer. In addition, it also highlights further the interest of dual catalysis and expands its application scope to ε-functionalized-ε-caprolactones (monomers **2** and **3**), lactone propagating via a sterically hindered secondary alcohol and thus rather challenging to polymerize.

In chapter III, we described the preparation of copolymers of ε-DL and monomer **2** or **3** using the dual catalyst (InCl₃/NEt₃) with either BnOH or DMBA as an initiator under mild conditions (toluene, 3M, 60°C). Based on the monitoring of monomer conversions by NMR spectroscopy, the obtained copolymers were confirmed to be random copolymers, e.g. P(DL-*r*-**3**). To obtain the carboxyl-functionalized PDL-based copolymer, the post-polymerization modification of copolymers containing 2% and 5% of benzyl ester thiol has been achieved in two steps: (1) acetylation of the terminal hydroxide and (2) Pd-catalyzed hydrogenolysis. The complete removal of the benzyl protecting groups was confirmed by ¹H NMR spectroscopy. In addition, this protocol respects the integrity of the polymer backbone. None of post-polymerization steps affects the polymer backbone, M_n remaining fairly constant and Đ remaining low, as evidenced by SEC analysis.

In the final chapter, the degradation of CP-2%-COOH and 5% CP-5%-COOH was investigated in both hydrolytic and enzymatic conditions, and the results were compared with homo-PDL. Mass loss profiles of PDL, CP-2%-COOH, and CP-5%-COOH showed that the degradation rates are 2.5-5 times and 4-6 times (for 2% loading and for 5% loading, respectively) faster than the homo-PDL. Analysis of the released products revealed the formation of hydrophilic oligomers, which are finely dispersed in the degradation media and detected by MS. Small amounts of 6-hydroxydecanoate, the hydrolysis product of ε-DL, and the hydrolysis product of monomer **3** were also detected by ¹H NMR. All these data reveal the impact of the lateral carboxyl groups on the hydrophilicity and degradation rates of PDL chains. The materials investigated here are promising candidates as renewable and biodegradable alternatives to commercially available petroleum-based materials.

This work is also a proof-of-concept of the impact of polar functionalized groups on PDL properties. It opens the way to other tailored structural modifications that may open new application opportunities for these polymers. As a medium term perspective, we propose an application of lactone **2** as a monomer for the preparation of reactive oxygen species (ROS)-responsive biodegradable polymers, by taking advantage of the presence of the thioether group. To do so, the ROS-responsive amphiphilic block copolymers could be prepared by ROP of monomer **2** using PEG-NH₂ as macroinitiator, so the diblock structure can resist during the application thanks to the strong amide bond between the two blocks. The ability of these block copolymers to form micellar nanoparticles in water should then be investigated. Then, their capacity to trap the oxidative species should be probed by the reaction with H₂O₂. In addition,

it may be worth investigating the hydrophilicity and degradability of these copolymers containing thiolate moieties of different polarity (e.g., thioether, sulfoxide, and sulfone).
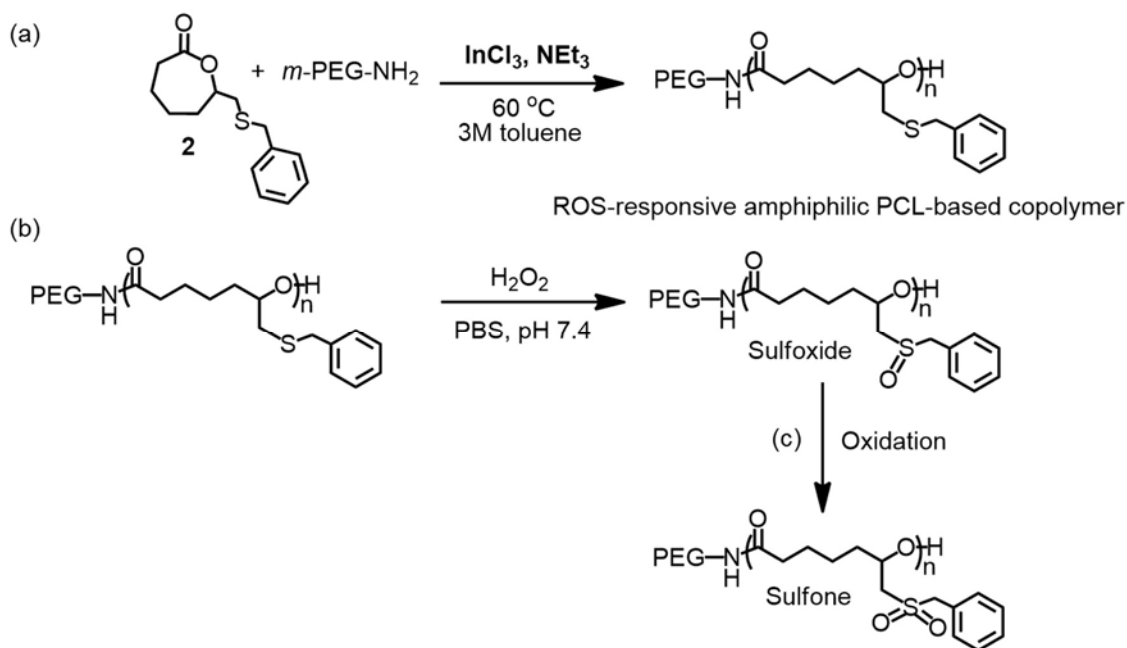
Scheme 1. Proposed strategy for the preparation of ROS-responsive amphiphilic PCL-based copolymers and the study of their oxidative response to H_2O_2: (a) Ring-opening polymerization of monomer **2** with *m*PEG-NH$_2$ to yield ROS-responsive PCL, (b, c) oxidation pathways of the related polymers in the presence of H_2O_2.

INTRODUCTION

De nos jours, les plastiques sont des matériaux omniprésents, à tel point qu'il est difficile d'envisager une vie sans eux.[1] La production mondiale de plastiques dépasse les 150 millions de tonnes par an, ce qui correspond à une croissance exponentielle de la production industrielle.[1a] Malheureusement, les plastiques sont associés à de graves problèmes environnementaux. L'intérêt porté aux matériaux renouvelables, biodégradables et biocompatibles en tant que solutions de remplacement des plastiques non dégradables s'est donc accru de manière notable ces dernières années. Les polymères biodégradables sont de plus en plus utilisés dans les applications quotidiennes (emballage et agriculture…) et spécifiques (matériaux biomédicaux, ingénierie des tissus…).[1b] Une quantité croissante de polymères pouvant être décomposés dans la nature est à l'étude.[1c] Parmi les polymères biodégradables, on peut différencier ceux d'origine naturelle (par exemple l'amidon) et ceux d'origine synthétique. Les polymères synthétiques sont principalement basés sur des liaisons sensibles en conditions hydrolytiques ou enzymatiques telles que les esters et les amides (par exemple, des polyesters, des polyamides, des polycarbonates et des polyanhydrides).[2] Parmi ces polymères dégradables, les polyesters ont suscité beaucoup d'intérêt en raison de leur bon équilibre entre stabilité et sensibilité à la dégradation hydrolytique.[1a,1b] De plus, certains polyesters aliphatiques, synthétisés à partir de lactones ou de diesters, présentent un intérêt particulier, car leur dégradation conduit à des petites molécules pouvant être directement éliminées ou métabolisées par l'organisme. Ils sont donc biocompatibles.

À ce jour, le polylactide (PLA), dérivé de l'acide lactique, est le polyester biodégradable le plus utilisé. C'est un polymère renouvelable produit industriellement. Le PLA peut être synthétisé par la polymérisation par ouverture de cycle (ROP) du lactide (LA), dérivé de la biomasse (maïs, blé …). Parmi les polymères industriels, la production de PLA a atteint l'échelle de la tonne, soit 24% de la production mondiale de plastiques biodégradables.[3] En conséquence, son prix est passé de 1 000 à ≈ 6 US $ par kg, un niveau de prix similaire à celui du polystyrène (1,6 US $ par kg).[4] Outre le PLA, d'autres polyesters biodégradables tels que les polyhydroxyalcanoates (PHA) et le poly (butylène succinate) (PBS) sont également produits à l'échelle industrielle (Figure 1).
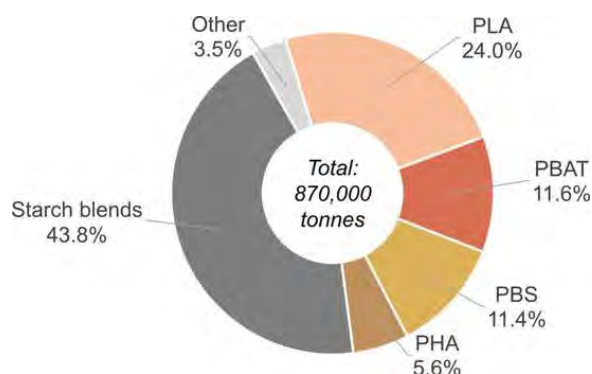
Figure 1 Production Globale de polymers biodégradables en 2017.[3]

Le PLA a un potentiel élevé de par ses propriétés mécaniques et thermiques, ce qui le rend approprié pour de nombreuses applications.[1a,1c] L'hydrolyse du PLA est principalement associée à un métabolite du cycle de l'acide carboxylique conduisant à la formation d'acide lactique, qui est ensuite transformé en CO_2 et H_2O *via* le cycle de Krebs (Figure 2).[5]
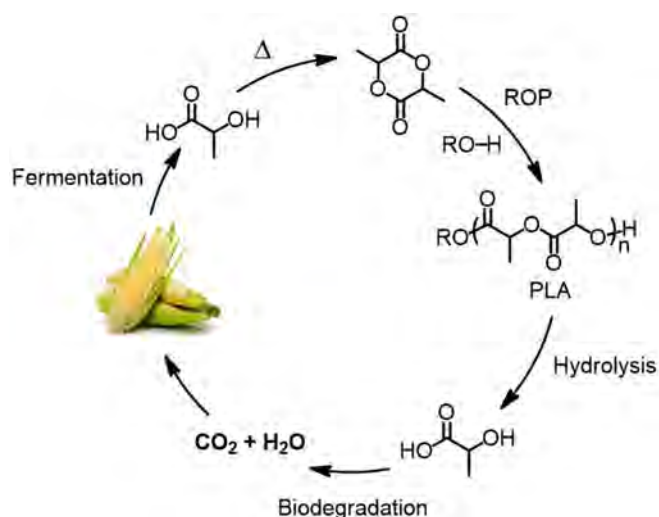

Figure 2 Cycle de vie du PLA.[5]

Les applications du PLA augmentent de manière exponentielle, grâce à sa capacité de dégradation et à sa compatibilité avec les domaines biomédicaux (par exemple, pour l'utilisation dans les implants dentaires, les greffes vasculaires, les vis à os et en tant que vecteur pour l'administration de médicaments).[6] Cependant, Le PLA présente des inconvénients qui entravent son utilisation pour certaines applications: par exemple, sa fragilité due à une cristallinité élevée et à sa faible stabilité thermique ($T_m \approx 160$ °C, $T_g \leq 60$ °C et $T_d \leq 280$ °C), son caractère hydrophobe et son faible degré de fonctionnalisation.

Les propriétés du PLA peuvent être modulées par la combinaison ou le remplacement par d'autres polyesters, tels que la polycaprolactone (PCL). La PCL est un polymère semi-cristallin

dont la T_m est d'environ 60 °C et la T_g d'environ -60 °C (les deux inférieures à celles du PLA).[7] Le PCL est également considéré comme un polymère biodégradable, bien que sa dégradation hydrolytique est plus lente (2 à 3 ans) que celle du PLA semi-cristallin (1 à 2 ans).[8] Ce polyester semi-cristallin a été largement utilisé dans les applications biomédicales, telles que les nanoparticules pour des systèmes de délivrance de médicaments, et dans l'ingénierie. Cependant, la PCL présente l'inconvénient important de ne pas être renouvelable, car c'est un polymère préparé par ROP de l'ε-CL, une lactone dérivée du pétrole (il faut cependant noter qu'une synthèse récente à partir de sucre a été rapportée[7b]). L'ε-décalactone (ε-DL), qui est dérivée de la biomasse, est un autre monomère lactone à 7 chaînons de choix, car elle est proche de l' ε-CL. L'ε-DL attire de plus en plus l'attention en tant que monomère renouvelable alternatif. Cependant, le groupe butyle pendant en position ε a un impact important non seulement sur la vitesse de polymérisation mais également sur les propriétés du polymère et en particulier sur les vitesses de dégradation. Il est à noter que la vitesse de polymérisation de l'ε-DL sont plus lents que ceux du l'ε-CL, tandis que les vitesses de dégradation de la PDL sont plus rapides que ceux de la PCL, mais restent plus lents que ceux du PLLA (voir le chapitre III pour plus de détails). Une possibilité pour moduler et / ou améliorer encore les propriétés de la PDL, et développer ainsi son utilisation, consiste à introduire des groupes latéraux fonctionnels en utilisant des ε-caprolactones modifiées. Par conséquent, il est très souhaitable de développer l'accès à des monomères fonctionnalisés de structure proche de l'ε-DL, afin d'assurer un comportement similaire en ROP, et de concevoir un procédé fiable pour leur (co) polymérisation contrôlée.

Les stratégies les plus utilisées pour la préparation de lactones cycliques de 6 à 9 chaînons peuvent être séparées selon trois méthodes différentes, comme suit:

(1) La cyclisation ou la lactonisation est similaire à la préparation de lactide.[9] La formation du cycle est essentiellement réalisée par activation de l'acide ou de l'alcool. Cependant, les lactones fonctionnalisées préparées par ce procédé sont souvent obtenues avec des rendements modérés à faibles en raison de la compétition avec des réactions intermoléculaires qui conduisent à la formation de produits non désirés (à savoir des oligomères).[10]

(2) L'alkylation en position α de lactones déjà existantes à l'aide d'une base forte est une méthode bien connue en chimie organique pour préparer des lactones spécifiquement fonctionnalisées en position α.[11] L'α-propargyl-ε-caprolactone est l'un des monomères préparés par cette méthode. Le groupe pendant propargyle peut être modifié par la suite par chimie «click» en tant que modification post-polymérisation.[12] Cependant, cette approche

présente des inconvénients: il s'agit d'un procédé en plusieurs étapes et est accompagné de produits secondaires dus à des réactions de transestérification et à la polymérisation anionique de la caprolactone.

(3) L'oxydation Baeyer-Villiger des cétones cycliques (fonctionnalisées) est probablement l'approche la plus largement appliquée pour produire des lactones (fonctionnalisées), par exemple, l'ε-caprolactone à partir de la cyclohexanone.[13] Le problème le plus important dans l'oxydation de Baeyer-Villiger est lié au manque de régiosélectivité dans le cas de lactones dissymétriques. En conséquence, très peu d'exemples d'ε-caprolactone fonctionnalisé en position ε ont été rapportés.

Ainsi, une nouvelle stratégie pour la préparation d'ε-CL ε-fonctionnalisées directe et plus efficace serait souhaitable. Nous proposons ici une approche alternative et sélective pour la préparation de ces lactones et leur application en tant que monomères pour la préparation de polymères biodégradables fonctionnalisés.

Au cours des dernières années, l'équipe LBPB a décrit des complexes pince originaux de Pd ou de Pt de type A, dans lesquels deux bras latéraux thiophosphinoyle soutiennent la coordination σ dans le plan du fragment indénediide avec le centre métallique, Pd et Pt (Figure 3).[14] Selon des études expérimentales et théoriques, ces complexes **A** présentent un centre métallique électrophile, tandis que le squelette indénediide est riche en électrons et présente un comportement non-innocent comme base.[15] En particulier, des complexes de type A ont été appliqués aux réactions d'hydrofonctionnalisation catalytique. Contrairement aux catalyseurs Pd habituels, ces catalyseurs Pd et Pt permettent de préparer efficacement des lactones à 5, 6 et même 7 chaînons incluant des ε-alkylidène-lactones avec d'excellents rendements >80% (Schéma 28).[16]
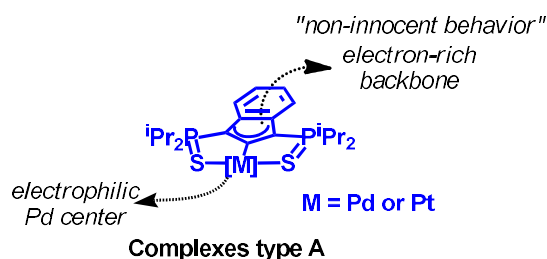

Figure 3. Complexes pince de Pd et de Pt comportant le ligand indediide à comportement chimiquement non-innocent.
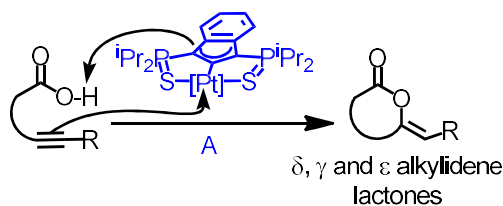
Schéma 1. Préparation de δ-, γ-, et ε-alkylidene lactones avec les complexes once de Pt.

De plus, la réaction a une économie d'atomes complète et se déroule dans des conditions douces sans aucune base ni additif. La cycloisomérisation des acides alcynoïques donne des produits exo-méthylène intéressants qui peuvent être utilisés en tant que précurseur de ε-caprolactones ε-modifiées. En particulier, Ces précurseurs révèlent une occasion unique de surmonter les problèmes de régiosélectivité précédemment mentionnés pour la préparation de ε-lactones-fonctionnalisées avec la réaction de BV. Sur la base des résultats obtenus précédemment,[17] des ε-alkylidène-ε-lactones dérivées de l'acide 6-heptynoïque seront préparées à l'échelle multi-gramme et seront ensuite modifiées en lactones ε-fonctionnalisées correspondantes par réaction click de thio-lène (Schéma 2).
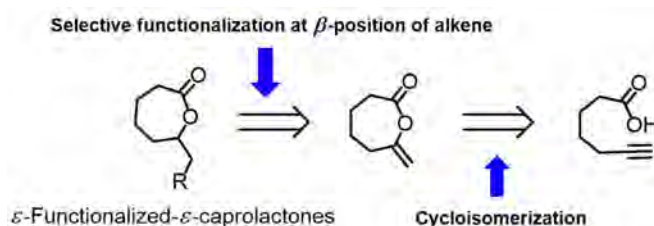

Schéma 2. Stratégie alternative proposée pour la préparation d'ε-caprolactonesε-fonctionnalisées

En ce qui concerne la réaction de thiol-ène, on utilisera les thiols portant le groupe fonctionnel souhaité, éventuellement sous forme protégée. En raison de sa bonne compatibilité avec le fragment ester, la réaction de thiol-ène est une réaction efficace et sélective qui a déjà été appliquée dans de nombreux exemples pour la fonctionnalisation post-polymérisation de polyesters fonctionnels ou pour la modification pré-polymérisation d'ε-CL fonctionnelles.[18] Dans le cas d'une modification de pré-polymérisation, les groupes fonctionnels cibles d'acide carboxylique, d'amide ou d'hydroxyle seront introduits sous une forme protégée, qui peut être éliminée facilement sans affecter le squelette du polymère.[19] Nous avons choisi de travailler en particulier avec des groupements fonctionnels de type acide carboxylique. Après copolymérisation des nouveaux monomères protégés avec la DL, les post-modifications (déprotection) des copolymères résultants seront réalisées en deux étapes, acétylation et hydrogénolyse. Ceci conduira aux copolymères comportant des groupes latéraux carboxyles.

Ces groupes fonctionnels carboxyles peuvent avoir un impact sur les propriétés du polymère, en particulier les vitesses de dégradation. Pour sonder la dégradabilité de ces copolymères fonctionnalisés, leur dégradation sera étudiée dans des conditions hydrolytiques et enzymatiques. L'influence de notre nouveau monomère (sous forme déprotégée) sur le squelette du PDL sera présentée sur la base des résultats des tests de dégradation.

Ce manuscrit traite donc de la synthèse de lactones fonctionnelles, et également de l'étude de catalyseurs doubles pour la ROP de l'ε-DL. Les travaux visent à utiliser un nouveau monomère fonctionnel pour la préparation de polyesters biodégradables comportant des groupes fonctionnels latéraux (Schéma 3). Le manuscrit est composé de quatre chapitres, comme illustré ci-après:
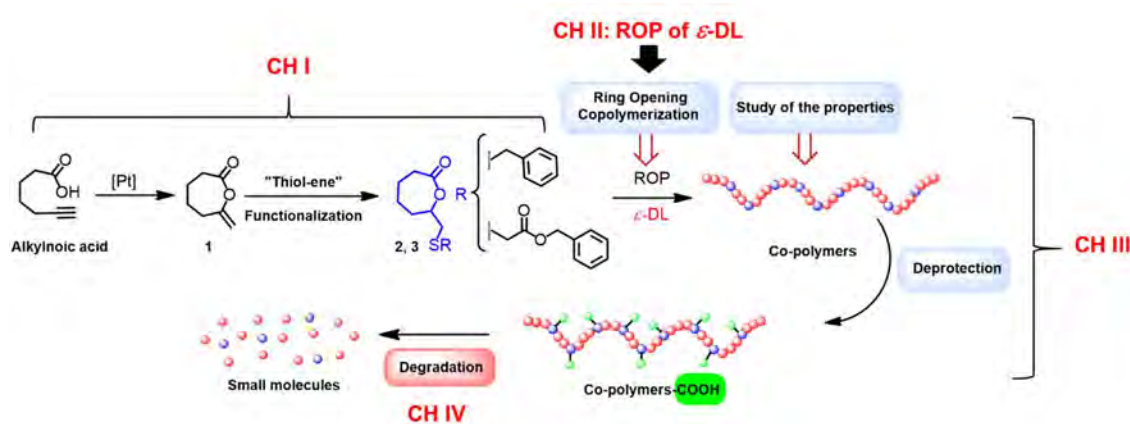

Schéma 3. Aperçu du projet illustrant les différents chapitres: préparation des monomères fonctionnalisés, développement d'un système catalytique de ROP adapté, copolymérisation et étude de dégradation des copolymères fonctionnalisés.

Chapitre I : Préparation de ε-CL ε-fonctionnalisées par une séquence cycloisomérisation-thiol-ène.

Préparation du précurseur par cycloisomérisation catalysée par un complexe pince indènediide de Pt

Sur la base de la stratégie proposée, le précurseur de lactone fonctionnalisée, l'ε-alkylidène-ε-lactone, est facilement préparé par cycloisomérisation de l'acide alcynoïque correspondant. La réaction est complète après 21 heures à 90 °C avec l'absence d'additif ou de base. Le brut réactionnel a été purifié par sublimation pour donner une forme pure de **1** avec un bon rendement (79% pour une échelle de 2,5 grammes). La structure a été confirmée par RMN ^{1}H avec les signaux caractéristiques du groupe fonctionnel oléfinique (=CH2) à 4,79 et 4,66 ppm correspondant à ceux rapportés par notre groupe.[17] Comme mentionné précédemment, le

composé **1** est un précurseur possible pour la préparation de l'ε-caprolactone fonctionnalisée. De plus, la réaction peut être réalisée correctement à grande échelle, jusqu'à une échelle de 5 grammes avec un bon rendement (72%). Ce précurseur sera ensuite modifié par une fonctionnalisation simple et sélective, la réaction de thiol-ène, avant la copolymérisation avec l'ε-DL conduisant à des copolymères fonctionnalisés. Notons que la cycloisomérisation et la fonctionnalisation thiol-ène sont des réactions à total économie d'atomes.

Réaction thio-lène sur 1.

L'étape suivante consiste à la réaction de thiol-ène qui implique l'addition sélective d'un thiol sur la position la moins substituée de l'alcène (position β) (schéma 1.1).
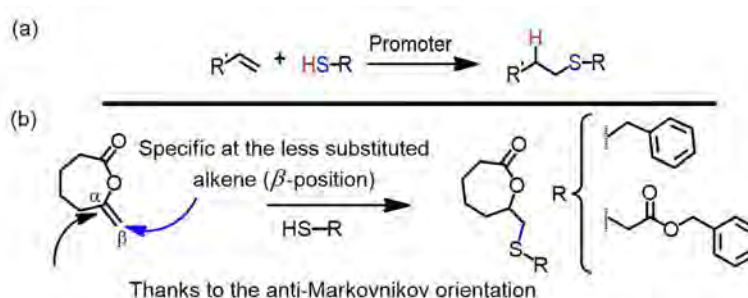

Schéma 1.1. (a) Réaction générale thiol-ène avec le produit anti-Markovnikov (b) La position β du composé **1** visée à être fonctionnalisé par réaction thiol-ène.

Dans un premier temps, le couplage du composé **1** avec le benzylthiol a été étudié pour définir les conditions de réaction comme étude modèle. Différentes conditions de réaction ont été étudiées afin de trouver un bon protocole, dans lequel le couplage thiol-ène serait favorisé par rapport à l'ouverture de cycle de **1**. La première partie de l'étude était basée sur le criblage du promoteur: I_2, peroxyde de benzoyle (BPO), et 2,2-diméthoxy-2-phénylacétophénone (DMPA). Elle a permis d'écarter le diiode, puisque qu'il conduit à l'ouverture de la lactone. Ensuite, nous sommes passés à la voie d'addition des radicaux libres en utilisant BPO ou DMPA comme amorceur radicalaire. Deux essais de réaction thiol-ène du composé **1** (0,5 M dans CDCl$_3$) et du benzyl thiol (1,2 équiv.) ont été initialement effectués en utilisant 2% en poids de l'amorceur radicalaire, BPO ou DMPA, sous irradiation UV (365 nm) à 40 °C. Après 4 jours d'irradiation UV, la réaction initiée par BPO montrait la consommation totale de **1** observée par RMN [1]H. En revanche, la tentative avec le DMPA a donné de meilleurs résultats: **1** a été complètement consommé après seulement 24 heures, plus rapidement que l'utilisation de BPO. Cependant, l'essai initial avec le DMPA a montré non seulement la formation du produit cible **2**, mais également l'isomérisation de **1** et d'autres réactions secondaires (par exemple, la formation de dimère de thiol et l'ouverture du cycle de **1**). L'isomérisation est

évidemment une des principales réactions concurrentielles de cette réaction thiol-ène, car le rendement RMN de 40%pour l'isomère a été détecté contre un rendement de 55% en monomère **2**. Pour augmenter l'efficacité du couplage thiol-ène, l'optimisation des conditions de réaction a été entrepris: (i) source lumineuse, (ii) solvant (type / concentration), (iii) quantité de composé thiol, et (iv) quantité d'amorceur. Les résultats obtenus ont permis d'identifier que l'efficacité du couplage thiol-ène sera accrue si la réaction est envisagée (1) en abaissant la concentration initiale de 1 à 0,25 M, (2) en utilisant un solvant polaire (CDCl$_3$ plutôt que C$_6$D$_6$), (3) en présence initialement de 2% en poids de DMPA (et d'en rajouter jusqu'à 6% en cours de réaction), et (4) avec une concentration supérieure de benzyl thiol supérieure à 3,0 équiv. L'optimisation des conditions de réaction thiol-ène en utilisant ces conditions a permis d'améliorer de manière notable l'efficacité de la réaction et, de plus, ce protocole peut être appliqué jusqu'à une échelle de 1 gramme avec un excellent rendement (80%) (schéma 1.2).
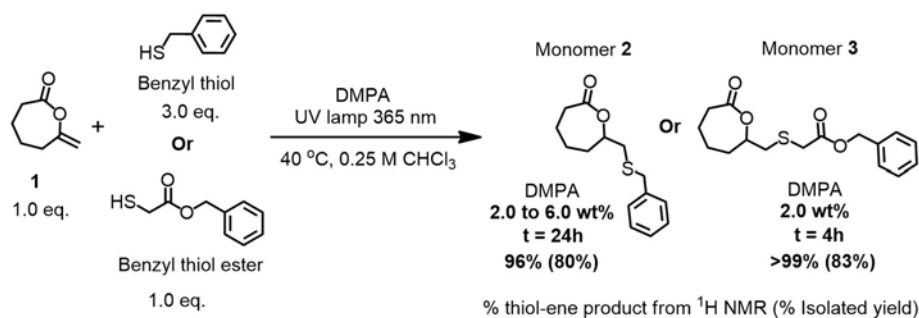

Schéma 1.2. Synthèse de nouveaux monomères fonctionnels par fonctionnalisation thiol-ène

Les conditions optimales de réaction thiol-ène pour la synthèse du monomère **2** ont ensuite été appliquées pour la préparation du produit cible **3**, comportant une fonction acide carboxylique protégée, par couplage du composé **1** avec le 2-mercaptoacétate de benzyle (ester de benzyle thiol). De manière surprenante, cette réaction thiol-ène est complètement finie après seulement 4 heures sans addition séquentielle de DMPA. De plus, aucun des produits secondaires n'a été observé. Avec son efficacité de couplage thiol-ène élevée, la synthèse du monomère ciblé a ensuite été planifiée avec une quantité inférieure d'ester benzylique thiol. Comme mentionné précédemment, une quantité inférieure de thiol peut affecter le taux de couplage thiol-ène ainsi que l'efficacité de couplage. Plusieurs expériences ont été étudiées en diminuant la quantité d'ester benzylique thiol de 3,0 équivalents à 2,5, 2, 1,5 et 1 équiv. Fait intéressant, toutes les études ont montré un résultat équivalent à celui utilisant 3 équiv. d'ester benzylique de thiol. Aucun des produits secondaires n'a été observé et les réactions ont été réalisées dans les délais (4 heures). De plus, cette réaction thiol-ène peut être portée à 3 grammes avec un excellent rendement (83%).

Le monomère ciblé, composé **3**, sera utilisé comme co-monomère pour la copolymérisation avec l'ε-DL, ce qui permettra de moduler les propriétés de la PDL. Mais avant cela, la polymérisation par ouverture de cycle (POR) de l'ε-DL avait encore des problèmes à résoudre, dûs au fait que peu d'études avaient été réalisées à l'époque. Par exemple, il fallait trouver un bon catalyseur fonctionnant dans des conditions douces et permettant une polymérisation vivante et contrôlée. Ce travail sera discuté dans le prochain chapitre.

Chapitre II : Développement d'un catalyseur alternatif pour la ROP de ε-DL

Au début de notre étude, l'octanoate d'étain $Sn(Oct)_2$ et la TBD étaient les catalyseurs les plus utilisés pour polymériser l'ε-DL.[20,21] Les polymérisations étaient principalement effectuées en masse à haute température (110 °C à 150 °C) et permettent un contrôle relativement bon des M_n et des Đ. Même si des polymérisations avec des rapports monomères / catalyseurs élevés pouvaient être effectuées, le problème majeur résidait dans les conditions dures de réaction et dans les traces de catalyseur restant dans le polymère en fin de réaction. Notre objectif était donc de trouver un catalyseur alternatif qui pourrait promouvoir la ROP de l'ε-DL dans des conditions plus douces et qui pourrait être retiré facilement en fin de réaction.

Seuls quelques exemples de catalyseurs favorisant la ROP de l'ε-DL en solution ont été rapportés, et pour la plupart d'entre eux (complexes d'aryloxiamine $La(OAr)_3$,[22] complexes de Ca et de Zn,[23] et le système dual MgI_2/isothiourée cyclique[24]), un exemple unique de ROP de l'ε-DL est décrit. Ce n'est que dans les travaux de C. C. Lin sur les complexes NNO tridentate ketimines Zn que le contrôle de la polymérisation a été brièvement exploré,[25] bien que les avantages et les limites du catalyseur n'aient pas été examinés. Néanmoins, des PDL de Mn > 15 000 et des distributions moléculaires étroites (Đ < 1,15) peuvent être préparées dans des conditions douces (50 °C, 3-5h), ce qui est également le cas du seul exemple rapporté utilisant le double système catalytique combinant MgI_2 et une isothiourée cyclique.[24]

La catalyse duale, basée sur la coopération entre un acide de Lewis métallique et une base de Lewis organique, est un concept largement utilisé en synthèse organique.[26] Il n'a été étendu qu'au cours de la dernière décennie au domaine de la chimie des polymères, et plus particulièrement à la ROP des lactones et des carbonates cycliques.[27,28] La force de la catalyse duale est l'association d'un acide de Lewis avec une base de Lewis (pour activer le monomère et l'amorceur protique, respectivement), qui sont inactifs séparément tandis que leur combinaison et leur coopération permettent une polymérisation dans des conditions douces. Ceci constitue une approche intéressante pour augmenter l'activité, tout en maintenant une bonne sélectivité vis-à-vis des réactions de transfert en chaîne (transestérifications). En outre,

M. Hillmyer a présenté en 2010 une étude détaillée sur la capacité de l'association InCl$_3$/NEt$_3$ à agir comme catalyseur pour la ROP contrôlée du lactide.[29] Dans le même article, des résultats préliminaires ont été décrits sur la ROP de plusieurs lactones dont un exemple avec l'ε-Me-ε-CL, suggérant que ce système catalytique dual est capable de propager la ROP via des motifs In-alkoxide secondaires. Les bons résultats de l'association InCl$_3$/NEt$_3$ avec ε-Me-ε-CL nous ont incités à étudier le comportement de ce double catalyseur très simple envers l'ε-DL, qui est un analogue plus lourd de l'ε-Me-ε-CL. Comme indiqué ci-après, l'association InCl$_3$/Et$_3$N promeut en effet la ROP de manière contrôlée et vivante, avec une absence de catalyseur résiduel dans les PDL. Différents types d'initiateurs peuvent être utilisés (alcools, amines) conduisant à des PDL à terminaisons ester et amide. Les copolymères blocs et aléatoires avec PCL peuvent également être facilement préparés.
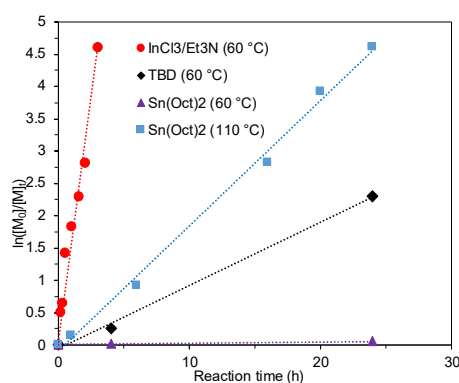

Figure 2.1. ROP de ε-DL (toluène, [ε-DL]0 = 3 mol/L, DP50) catalysée par InCl$_3$/NEt$_3$/BnOH 1:2:1 à 60 °C (ligne rouge et points), TBD/BnOH 1:1 à 60 °C (ligne noire et losange), Sn(Oct)$_2$/BnOH 1:1 à 60 °C (ligne violette et triangles), Sn(Oct)$_2$/BnOH 1:1 à 110 °C (ligne bleue et carrés).

La ROP de l'ε-DL promue par l'association InCl$_3$/Et$_3$N (rapport 1/2) et amorcée par l'alcool benzylique avec un rapport ε-DL/BnOH de 50 a d'abord été réalisée dans une solution à 3 mol/L de toluène à 60 °C. Le système dual a ensuite été comparé avec SnOct$_2$ et TBD dans des conditions de réaction similaires. Comme le montre la figure 2.1, la réaction est nettement plus rapide pour l'association InCl$_3$/Et$_3$N. Seulement 4 h sont nécessaires pour obtenir une conversion complète, alors qu'après 24 h de réaction, 90 % et 5 % de conversion sont atteints avec TBD et SnOct$_2$, respectivement. En raison des très faibles conversions observées pour le SnOct$_2$ à 60 °C, la réaction a également été réalisée à 110 °C, mais même à cette température, la conversion est plus lente qu'avec l'association InCl$_3$/Et$_3$N (~24 h pour obtenir une conversion complète). L'association d'InCl$_3$ et Et$_3$N est donc un catalyseur rare pour promouvoir la ROP de l'ε-DL en solution dans des conditions douces. L'échantillon PDL obtenu avec InCl$_3$/Et$_3$N

(après trempe de la polymérisation avec un excès de PhCO$_2$H et précipitation) présente un poids moléculaire de 9800 g/mol ($M_{n\ th}$ 8600 g/mol) et une faible distribution molaire ($Đ$ = 1,13), ce qui suggère un assez bon contrôle de la polymérisation comme dans le cas du ROP de l'ε-DL avec SnOct$_2$ à 110 °C (M_n = 6 116 g/mol, vs $M_{n\ th}$ = 6978 g/mol et $Đ$ = 1,19).

En utilisant les mêmes conditions de réaction et de l'alcool benzylique ou de l'alcool 3,5-diméthoxybenzylique (DMBA) comme initiateur (selon le rapport M/I, de sorte que l'intégration précise des spectres RMN ^{1}H puisse être effectuée), le contrôle de la polymérisation a été étudié pour des rapports monomère/ initiateur de 20 à 175. Pour ces rapports M/I, toutes les caractéristiques typiques d'une polymérisation contrôlée et vivante ont été observées (Figure 2.2). Comme le montre la figure 2.2a,b, le poids moléculaires des PDL résultantes augmentent linéairement avec les rapports M$_0$/I$_0$, tout en restant à faibles $Đ$ (1,08-1,13). De plus, le nombre de chaînes à croissance active reste constant tout au long du processus de polymérisation, comme le montre la courbe cinétique semi-logarithmique, cohérente avec un premier ordre cinétique partiel pour le monomère, et par l'évolution linéaire du poids moléculaire du polymère avec conversion du monomère (figures 2.2c et 2.2d, respectivement).
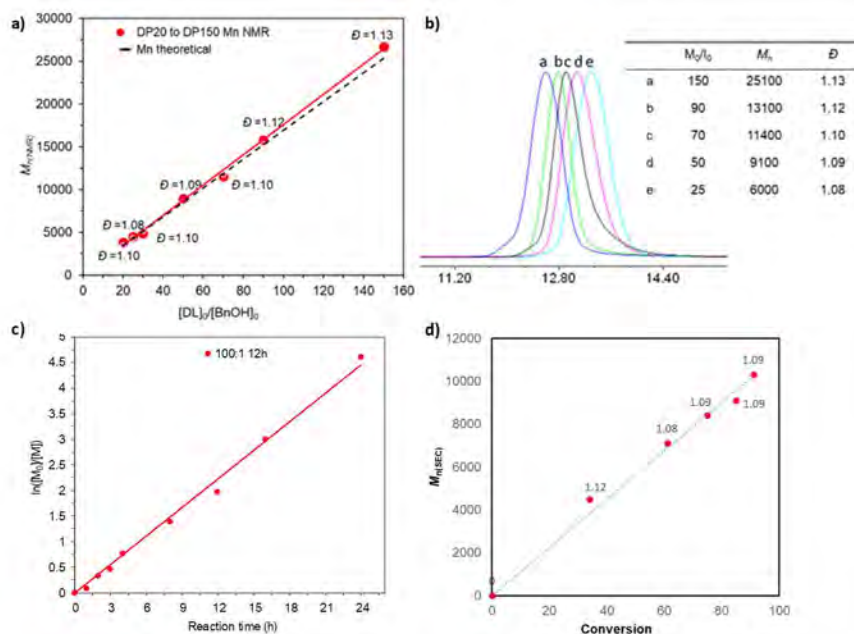
Figure 2. Caractère contrôlé de la ROP de l'ε-DL catalysée par InCl$_3$/Et$_3$N/BnOH 1:2:1 dans le toluène ([ε-DL]0 = 3 mol/L) à 60 °C pour DP20 à DP175: a) Tracé de M_n vs[ε-DL]$_0$/[BnOH]$_0$. b) Empilement des traces SEC des PDL obtenus. c) Tracé semi-logarithmique pour [ε-DL]$_0$/[BnOH]$_0$ = 100. d) Evolution de M_n avec conversion pour [ε-DL]$_0$/[BnOH]$_0$/[BnOH]$_0$ = 50, $Đ$ valeurs sur le graphique.

L'efficacité de l'amorçage et la fidélité des bouts de chaîne ont été démontrées par spectroscopie RMN ^{1}H et MALDI-TOF MS. Toutes ces données indiquent que des PDL de structures bien définies avec M_n jusqu'à ~30 000 g/mol et des distributions molaires étroites ($Đ$ < 1,13) peuvent être préparées de manière contrôlée en fixant le rapport M/I. Un autre point à remarquer est que l'analyse ICP-OES des polymères, obtenue après précipitation par addition d'une solution concentrée de DCM sur du méthanol froid, a montré une teneur en In d'environ 10 ppm, ce qui signifie que plus de 99 % du catalyseur In introduit a été enlevé. Cette faible teneur en résidus de catalyseur devrait limiter le risque d'altération des polymères lors de traitements thermiques à haute température.

Nous avons aussi exploré l'impact des conditions de réaction sur le processus de polymérisation et les propriétés du polymère. La réalisation de la réaction à 30 °C a entraîné une conversion très lente (moins de 12 % après 12 h), tandis que l'augmentation de la température de réaction à 80 °C a permis une conversion rapide et a donné des PDL à poids moléculaire élevé (M_n = 26 300 g/mol). Cependant, un contrôle plus faible de la polymérisation est indiqué par les distributions molaires plus élevées observées ($Đ$ de 1,39 vs 1,13 à 60 °C). Conformément à ce résultat, la polymérisation en masse à 100 °C a conduit à des valeurs plus élevées de $Đ$ (1,50 contre 1,15 à 60 °C, en utilisant DMBA comme initiateur et M/I = 50). Le chloroforme peut être utilisé comme solvant au lieu du toluène sans que cela n'ait d'impact sur le caractère cinétique ou contrôlé de la polymérisation. Le toluène a été préféré pour le reste de l'étude. Pour pousser plus loin le système en termes de DP, une polymérisation a été réalisée avec deux alimentations consécutives de 175 et 150 équivalents de l'ε-DL. Un PDL avec M_n = 57 490 g/mol et $Đ$ = 1,35 a ainsi été obtenu. Bien que la valeur de $Đ$ augmente légèrement, la valeur de M_n se situe dans la fourchette de la valeur cible ($M_{n\ th}$ 55 500 g/mol).

La présence des deux partenaires InCl$_3$ et Et$_3$N est nécessaire pour que la polymérisation se déroule efficacement. L'élimination de l'un ou l'autre d'entre eux entraîne une conversion faible ou nulle. Cette observation est cohérente avec le double caractère du système catalytique. Dans le cas du lactide,[26] Hillmyer a proposé que l'InCl$_3$ et l'Et$_3$N forment des composés dinucléaires d'In à pont alcoxy comme espèces clés pour une polymérisation de coordination-insertion. Un autre scénario consiste en l'activation concomitante du monomère et de l'alcool par InCl$_3$ et Et$_3$N, respectivement. Les deux mécanismes sont concevables avec ε-DL. La capacité d'InCl$_3$ à s'associer et à activer l'ε-DL a été démontrée par spectroscopie RMN. Les analyses RMN ^{1}H et ^{13}C des mélanges 1:1 et 1:2 de ε-DL:InCl$_3$ dans le CDCl$_3$ ont révélé des déplacements vers les champs inférieurs des signaux correspondant aux fragments C(=O)O-CH et C(=O)O-CH.

La possibilité de faire varier l'initiateur, de sorte que l'une des extrémités de la chaîne polymère puisse être modifiée, a également été évaluée (figure 2.3). En plus des alcools primaires, comme le BnOH, le DMBA et le 1-pentanol, des alcools secondaires peuvent être utilisés. Dans tous les cas, l'incorporation de l'initiateur est complète et la valeur M_n de la PDL obtenue correspond bien à celle attendue. Notamment, l'initiation avec du 1,4-benzènediméthanol permet la préparation d'un PDL dihydroxylé téléchélique (la spectroscopie RMN ^{1}H indique une initiation à partir des deux fractions alcool).
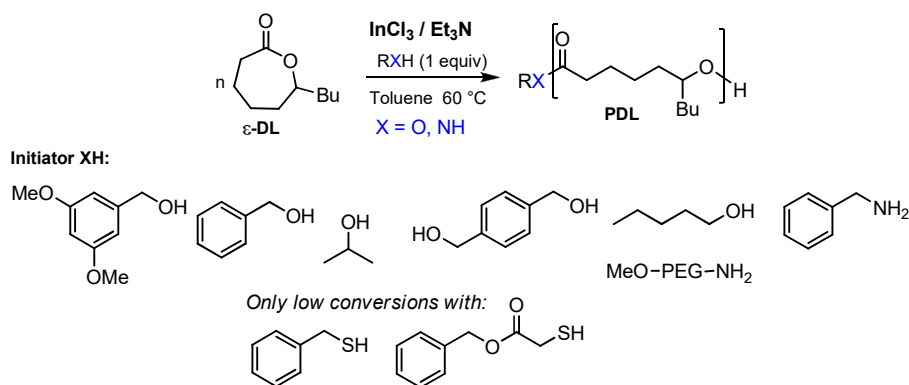

Figure 2.3. ROP de DL promue par InCl$_3$ / 2Et$_3$N et amorcé par différents amorceurs protiques (alcools et amines)

Il est intéressant de noter que les amines primaires peuvent également être utilisées comme amorceurs, ce qui permet de préparer des PDL à extrémité amides qui sont sensiblement plus forts que les groupements ester.[30,31] L'incorporation de la benzyl amine comme extrémité de chaîne amide a été soigneusement analysée par RMN ^{1}H pour déterminer si une ou deux liaisons N-H étaient impliquées dans l'initiation. Le spectre affiche un multiplet et un doublet à 7,25 et 4,45 ppm (intégrant respectivement 5 et 2 H) qui peuvent être attribués aux groupes Ph et CH$_2$-N du fragment benzyle. Un signal large supplémentaire qui disparaît lorsque l'analyse RMN est effectuée en présence de D$_2$O est observé à 6,00 ppm, ce qui correspond à la présence d'un groupe NH et suggère l'initiation d'une seule chaîne polymère. Nous avons ensuite profité de la capacité des amines à agir comme initiateurs pour préparer des copolymères séquencés amphiphiles présentant un lien robuste entre les deux blocs en utilisant un PEG-NH$_2$ (M_n SEC = 2100, Đ = 1,03) comme macro-initiateur.[30,31] Comme observé avec les alcools amorceurs, la modification du rapport monomère sur amine permet d'ajuster finement le poids moléculaire des polymères.

La possibilité de préparer des copolymères blocs et statistiques avec l'ε-CL a aussi été explorée (tableau 2.1). Les résultats obtenus montrent qu'avec le catalyseur dual InCl$_3$/NEt$_3$, il est possible de préparer des copolymères PCL/PDL à blocs ou aléatoires de structures contrôlées

dans des conditions douces. Grâce à l'efficacité d'amorçage élevée et au faible impact des réactions secondaires de redistribution de la chaîne, la nature des extrémités de la chaîne peut également être réglée avec précision. L'analyse DSC illustre l'impact de la structure bloc ou aléatoire des copolymères sur leurs propriétés thermiques. Les deux copolymères à blocs présentent une transition vitreuse aux valeurs T_g (-54,8 et -57,8 °C pour PDL-*b*-PCL et PCL-*b*-PDL, respectivement) dans la gamme de celles des deux homopolymères (-53 et -60 °C, respectivement pour PDL et PCL), et une température de fusion à T_m = 55,5 °C associée au bloc PCL semi cristallin. En revanche, le copolymère statistique est totalement amorphe et ne présente qu'une transition vitreuse à -60 °C. Bien que la CL soit convertie à une vitesse légèrement plus élevée, les séquences CL ne sont pas assez longues pour apporter la cristallinité, ce qui est cohérent avec le caractère aléatoire du copolymère.

Tableau 2.1. Preparation of PCL/PDL block and copolymers by ROP with InCl$_3$/Et$_3$N[a]

test	polymer	CL$_0$/DL$_0$	t (h)	$M_{n\,Th}$	M_n[b]$_{NMR}$	M_n[c]$_{SEC}$	$\DJ$[c]	DP[d]$_{NMR}$ CL/DL	T_g[e] (ºC)	T_m[e] (ºC)	T_d[e] (ºC)	χ[f]
1	PDL	0:50	3	8700	8800	11200	1.11	-/52	-53	-	356	-
2	PCL	60:0	0.5	7000	6900	7200	1.18	59/-	-61[g]	55[g]	330	55[g]
3	PCL-*b*-PDL	50:50	5.5	14400	14400	22000	1.24	50/50	-57.8	55.2	337	27
4	PDL-*b*-PCL	50:50	10	14400	15000	16300	1.25	56/50	-54.8	55.2	362	30
5	P(CL-*r*-DL)	50:50	2.5	14400	15500	19400	1.17	55/53	-60	-	351	-
6	P(CL-*r*-DL)	40:40	3.2	11500	11000	11700	1.13	40/37	-60.2	-	339	-

[a]Polymérisations effectuées dans du toluène,[monomère]$_0$ = 3M, à 60 °C, en utilisant du DMBA = 3,5-diméthoxybenzyl alcool comme initiateur, et InCl$_3$/Et$_3$N/DMBA = 1:2:1. [b]Calculé par RMN ^{1}H, {[(DP$_{NMR}$ de DL)*170,25, M$_w$ de ε-DL] + [(DP$_{NMR}$ de CL)*114,14, M$_w$ de ε-CL }] + M$_w$ de DMBA. [c]M$_{nSEC}$ déterminé sur polymère après purification à l'aide d'étalons de polystyrène. [d]DP$_{NMR}$ = Intégration du signal CH-O (PDL) ou CH$_2$-O (PCL) dans ^{1}H NMR divisé par l'intégration du signal de référence de l'initiateur (DMBA = 6H, référence à -(OCH$_3$)$_2$). [e]Déterminé par DSC. [f]Déterminé par DSC, en utilisant une valeur de chaleur de fusion pour une PCL cristalline à 100 % de 136,0 J g-1. [g]Données de la réf 24. n.d. = non déterminé.

En conclusion sur cette partie, l'utilisation de l'association InCl$_3$ / Et$_3$N permet ainsi des progrès significatifs pour la polymérisation de l'ε-DL en conditions douces, et est complémentaire du SnOct$_2$, ce dernier étant plus adapté à la ROP en masse à haute température. Il donne accès à une variété de polymères et de copolymères dérivés de ce monomère renouvelable. Ce travail souligne également l'intérêt de la catalyse duale et élargit son champ d'application à l'ε-DL, une lactone se propageant via un alcool secondaire à encombrement stérique et donc assez difficile à polymériser.

Chapitre III : Copolymérisation de l'ε-CL ε-fonctionnalisée avec l'ε-DL

L'étape suivante du projet consiste en la copolymérisation statistique des nouveaux monomères **2** et **3** avec l'ε-DL en utilisant le système catalytique dual étudié au chapitre II. Les nouveaux monomères fonctionnels (**2** et **3**) ont un substituant en position ε, de sorte que l'étude de l'homo- et de la copolymérisation avec un monomère de structure proche comme l'ε-DL a été planifiée pour assurer un comportement similaire en ROP et pour étudier leurs conditions de polymérisation contrôlée. L'homo- et la copolymérisation des nouveaux monomères, **2** et **3**, avec l'ε-DL utilisant un système catalytique similaire seront donc présentées. Leur modification post-polymérisation pour obtenir le polymère ciblé à base de PCL à fonction carboxyle sera également discutée.

Dans un premier temps, l'homopolymérisation de chaque nouveau monomère a été étudiée. Malheureusement, les résultats obtenus montrent des conversions faibles et la formation de polymères à SEC multimodale. Il semble donc que l'homopolymérisation de **2** et **3** est non seulement très lente, mais se produit aussi avec un faible contrôle. Comme décrit au chapitre II pour la copolymérisation simultanée de l'ε-DL avec l'ε-CL, un copolymère PCL-*r*-PDL aléatoire a été obtenu avec une distribution régulière des monomères le long de la chaîne polymère, malgré la réactivité différente de ces monomères en homopolymérisation qui aurait pu favoriser la formation de copolymères à structure de type bloc plutôt que de véritables copolymères aléatoires. Fait intéressant, le suivi de la conversion du monomère a révélé que les deux monomères étaient consommés à des vitesse de réaction proches. Ces résultats ont révélé que le monomère le plus réactif peut en fait favoriser des vitesses plus élevés de ROP du monomère le moins réactif. Cela nous a incités à étudier directement la copolymérisation d'un nouveau monomère (**2** et **3**) avec l'ε-DL.

Profitant du caractère vivant et contrôlé de la ROP de l'ε-DL promue par $InCl_3/NEt_3$, la copolymérisation de l'ε-DL avec **2** a été initialement réalisée à 60 °C avec différents rapports ε-DL/**2** de 45:5, 40:10, 35:15 et 25:25 pendant respectivement 18 h, 24 h et 48 h (schéma 3.1).
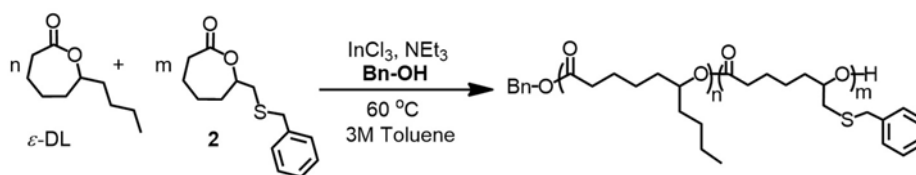

Schéma 3.1. Copolymérisation de l'ε-DL avec **2** catalysée par $InCl_3/NEt_3$ en utilisant BnOH comme amorceur.

Les réactions ont été effectuées en ajoutant un mélange de l'ε-DL et de **2** dans une suspension agitée de BnOH (1 équivalent), NEt$_3$ (2 équivalents) et InCl$_3$ (1 équivalent) dans du toluène ($[2]_0 = [DL]_0 = 3$ mol/L). La consommation des deux monomères a été suivie par spectroscopie RMN ^{1}H (voir Figure 3.15 pour un exemple). Si l'on examine les résultats du tableau 3.1 (entrée 1) pour la ROcoP avec le rapport ε-DL/2 de 45:5, l'ε-DL et **2** ont été complètement consommés après 18 heures. Le brut de copolymères contenant 10 % en moles de 2 a d'abord été trempé avec un excès d'acide benzoïque, puis le solvant a été évaporé sous vide. Le brut a ensuite été dissout dans un volume minimum de DCM suivi de précipitations dans du méthanol froid (deux fois consécutives), puis filtré et séché sous vide pour donner des pâtes collantes jaunâtres avec un excellent rendement (90%). Tout d'abord, on peut noter que bien que la conversion complète des deux monomères soit atteinte, elle s'effectue dans des temps significativement plus longs que celle de l'homoROP de l'ε-DL (3 h vs 18 h pour homoROP-DL et copolymérisation de l'ε-DL avec **2**, respectivement). Un copolymère avec un poids moléculaire de 9200 g/mole et de faibles distributions moléculaires ($Đ = 1,17$) a été obtenu selon l'analyse SEC. Le spectre RMN ^{1}H montre la disparition des signaux des protons des deux monomères (à 4,22 ppm et à 4,04 ppm, correspondant respectivement au proton -CHO- de l'ε-DL et de **2**), donnant lieu aux signaux multiplets (a) à 4,88 - 4,80 ppm pour le -CHO-PDL et (b) à 4,97 - 4,90 ppm pour le -CHO-P2. De plus, le spectre affiche également deux signaux singulets à 5,09 (d) et à 3,71 (c) ppm correspondant aux deux protons du groupe ester benzylique résultant de l'initiation de la ROP par BnOH et aux deux protons du groupe méthylène du -S-CH$_2$Ar (figure 3.1). Le groupe en bout de chaîne a également été étudié par spectroscopie RMN ^{1}H, comme le montre un signal large à 3,59 (a'+ b') ppm correspondant au groupe CHOH terminal. La valeur relative de 2 pour 1 de l'intégration des signaux d et (a'+ b') est cohérente avec la plupart des chaînes portant le même ester/alcool à l'extrémité de la chaîne, confirmant l'efficacité de l'initiation. En outre, la valeur d'intégration relative entre les signaux de protons de PDL et P2 (a et b) et de BnOH (d) proche de 46:5 (ε-DL : 2) qui indique une composition et DP$_{RMN}$ selon le M$_0$/I$_0$ (voir spectre RMN 1H de la figure 3.16)
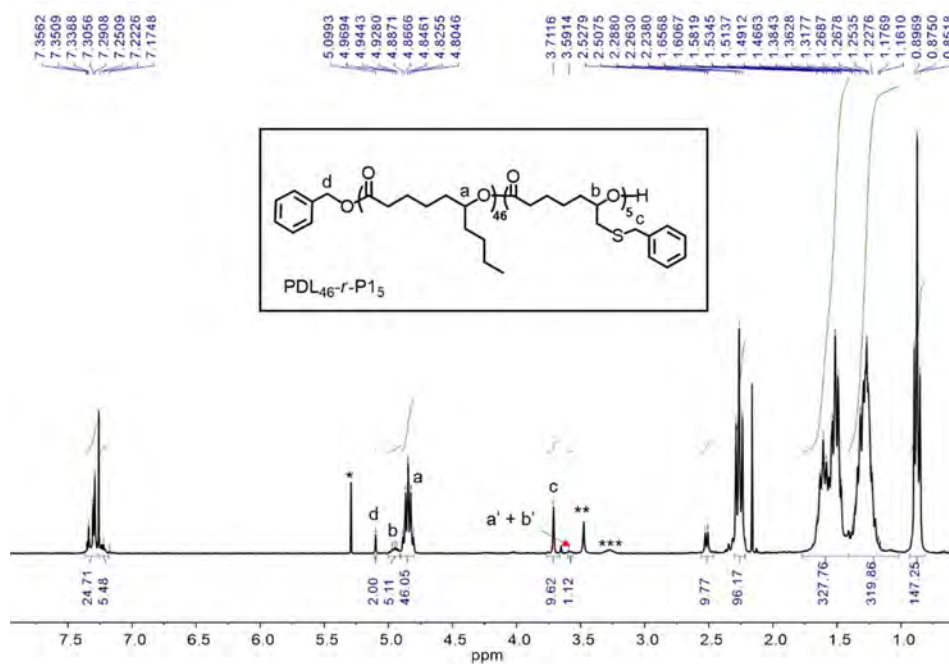
Figure 3.1. Spectre RMN ^{1}H (CDCl$_3$, 300 MHz) du copolymère de l'ε-DL et de **2** PDL$_{46}$-*co*-P**2**$_5$ (residu de *DCM, **MeOH, et ***sel d'ammonium).

Nous avons alors décidé d'augmenter la quantité de **2** dans la ROcoP avec le rapport ε-DL/**2** de 40:10 (Tableau 3.1, entrée 2), cette copolymérisation a pris plus de temps que la première, et elle n'était pas complète. Une conversion de 98 % et de 87 % pour l'ε-DL et **2**, respectivement, a été détectée après 24 heures, et la conversion des deux monomères n'a pas changé même après 24 heures supplémentaires. Un M_n faible (SEC) qui diffèrent significativement de la valeur théoriquement attendue et aussi de la valeur M_n calculée à partir de DP$_{NMR}$ a été obtenu (5300 g/mol), bien que $Đ$ soit étroite (1,10). Avec l'augmentation de la quantité de monomère **2** jusqu'à 30 % en moles et 50 % en moles (tableau 3.1, entrée 3 et 4), aucune copolymérisation n'a été observée après 48 heures (aucun des monomères n'ayant été consommé).

Tableau 3.1 Copolymérisation de l'ε-DL avec **2** promue par InCl$_3$:NEt$_3$ en utilisant BnOH comme amorceur.

Entry	ε-DL:**2**:Initiator	Amount of **2** (mol%)	Reaction time (h)	Conv. of ε-DL (%)	Conv. of **2** (%)	Mn^a (Theo.)	M_n (g/mol)^b	$Đ^b$	DP^a DL/**2**
1	45:5:1	10	18	>99	>99	8900	9200	1.17	46/5
2	40:10:1	20	24	98	87	9100	5300	1.10	32/8
3	35:15:1	30	48	No reaction					
4	25:25:1	50	48	No Reaction					

^{a}Déterminé par ^{1}H NMR, ^{b}Déterminé par SEC .

La copolymérisation de l'ε-DL avec **3** a ensuite été étudiée en utilisant les mêmes conditions de polymérisation et l'alcool 3,5-diméthoxybenzylique (DMBA) comme amorceur, avec différents rapports ε -DL/3 de 49:1, 47,5:2,5, 45:5, 42,5:2,5, 40:10 et 35:15 (schéma 3.2).
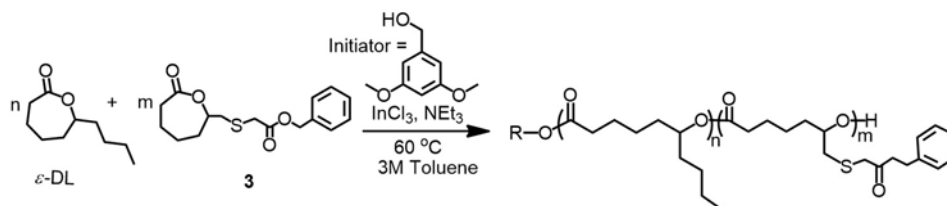

Schéma 3.2. Copolymérisation de ε-DL avec **3** catalysée par InCl$_3$/NEt$_3$ en utilisant DMBA comme initiateur.

Si l'on examine les résultats du tableau 3.2 (entrée 1-5), on observe une conversion complète après 4, 8, 12, 18 heures. Des copolymères contenant de 2 à 20 % de **3** avec de M_ns allant de 5700 à 11700 g/mol ont été obtenus après trempe de la polymérisation avec un excès d'acide benzoïque et précipitation dans du méthanol froid. Les M_ns obtenus (SEC) diffèrent légèrement de la valeur théorique attendue, en particulier pour les copolymères contenant des quantités élevées de **3** (Tableau 3.2, entrée 4 et 5) et des distributions moléculaires relativement larges (Đ) ont été observées (1.33-1.38). Notez que ces valeurs de M_n sont relatives, puisque nous travaillons avec la détection de l'indice de réfraction (RI° et l'étalonnage avec des étalons de polystyrène. Actuellement, nous ne disposons pas d'informations sur le comportement de ces copolymères ou sur l'impact des groupes latéraux sur le rayon hydrodynamique des chaînes polymères.

Tableau 3.2. Copolymérisation de l'ε-DL avec **3** promue par InCl3:NEt3 en utilisant du DMBA comme initiateur

Entry	ε-DL:3:Initiator	Amount of 3 (mol%)	Reaction time (h)	Conv. of ε-DL (%)	Conv. of 3 (%)	Mn[a] (Theo.)	M_n (g/mol)[b]	Đ[b]	DP[a] DL/3
1	49:1:1	2	4	>99	>99	8800	11700	1.33	49/1
2	47.5:2.5:1	5	8	>99	>99	9000	11100	1.34	47/3
3	45:5:1	10	12	>99	>99	9300	9100	1.36	45/5
4	42.5:7.5:1	15	18	>99	>99	9700	7900	1.46	43/7
5	40:10:1	20	18	>99	>99	10000	5700	1.38	40/10
6	35:15:1	30	48	**No Reaction**					

[a]Déterminé à partir des spectres RMN de ^{1}H, [b]Calculé à partir des traces SEC.

Comme dans le cas de **2**, les réactions ont duré plus longtemps que celles de l'homoROP de l'ε-DL (3 heures), et les Mns/Đs se sont révélées différentes des PDL (par exemple, PDL DP50 avec M_n/Đ = 11200/1.11 vs copolymère contenant 10 mol% de **3** avec M_n/Đ = 9100/1.36). Pour les quantités plus élevées de **3**, les groupes latéraux d'ester benzylique thiol ont un impact non

seulement sur les vitesses de ROP mais aussi sur le volume hydrodynamique des PDL. Pour confirmer la limitation du rapport -DL/**3** qui peut être utilisé pour cette copolymérisation, des quantités plus élevées de monomère **3** ont été utilisées (30 % en moles, voir tableau 2, entrée 6). Encore une fois, aucune copolymérisation n'a eu lieu après 48 heures, puisqu'aucun des monomères n'a été consommé.

La figure 3.2 montre le spectre de RMN ^{1}H du copolymère contenant 10 % en moles de **3** (rapport -DL/**3** de 45:5). Il représente les signaux typiques attendus pour une chaîne polymère PDL à (a) 4,85 ppm correspondant au proton -CHO-, à 1,64 - 1,20 ppm pour les groupes -CH$_2$-, et à 0,87 ppm pour le groupe méthyle. En outre, les signaux multiplets (b) à 5,03 - 4,98 ppm pour le -CHO-P3, un signal (d) à 3,29 - 3,15 ppm pour le S-CH$_2$-COOBn, et (c) à 2,86 - 2,67 pour le -OCH-CH$_2$-S- sont détectés. Le spectre montre également un signal singulet à 5,09 (e) correspondant aux deux protons du groupe ester benzylique du monomère **3** (figure 3.2). Le DP$_{RMN}$ a été déterminé avec précision à l'aide de six protons (f) de groupes (-OCH$_3$)$_2$ de la DMBA. La fidélité du groupe en bout de chaîne a également été étudiée par spectroscopie RMN ^{1}H. Un signal large à 3,58 ppm (a'+ b') correspondant au groupe CHOH terminal est observé en accord étroit avec la valeur relative 6 à 1 de l'intégration des signaux f et (a'+b').
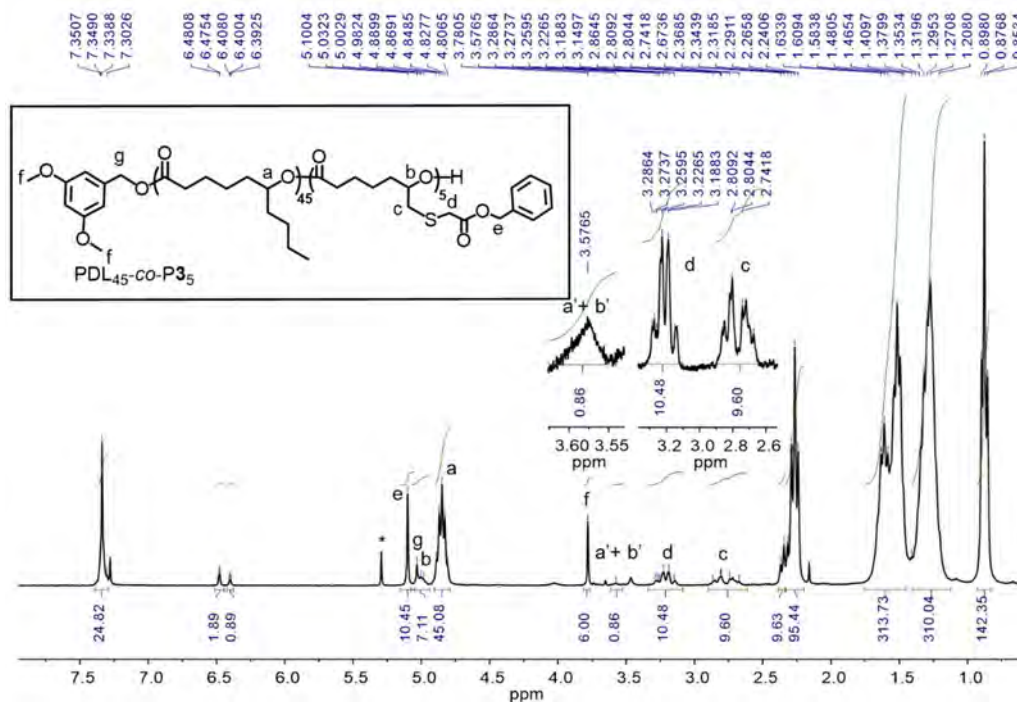

Figure 3.2. Spectre RMN 1H (CDCl$_3$, 300 MHz) du copolymère de l'ε-DL / **2** en PDL46-co-P25 (*DCM).

Comme les deux monomères (ε-DL et **3**) présentent une réactivité très différente en homopolymérisation, un copolymère à blocs plutôt qu'aléatoire pourrait être formé. Pour

explorer l'architecture du copolymère, le suivi des conversions des monomères par spectroscopie RMN ^{1}H a été réalisé en utilisant le rapport ε-DL/**3** de 80:20. Les résultats ont montré une conversion de plus de 80 % des deux monomères en 72 heures. Un ralentissement de la consommation de ε-DL a été observé (moins de 40 % de conversion en 12 heures), tandis que la consommation plus rapide du monomère **3** a également été constaté (plus de 45 % de conversion en 12 heures). Ces résultats révèlent une conversion simultanée des deux monomères et, par conséquent, l'obtention d'une structure aléatoire serait envisageable. De plus, la spectroscopie RMN ^{13}C est diagnostique pour la formation du copolymère aléatoire (Figure 3.3). Les spectres RMN ^{13}C de ces copolymères révèlent des signaux larges ou multiples à ~173,54 et 170,05 ppm pour les groupes C=O de PDL et P3, indiquant la présence d'environnements différents pour les groupes CO de chaque monomère en raison d'une distribution statistique. Notamment, des caractéristiques spectrales similaires sont observées dans la région -CHO-, comme en témoignent les signaux multiples à 73,85 ppm (PDL) et 66,12 ppm (P3) dans le spectre ^{13}C NMR.
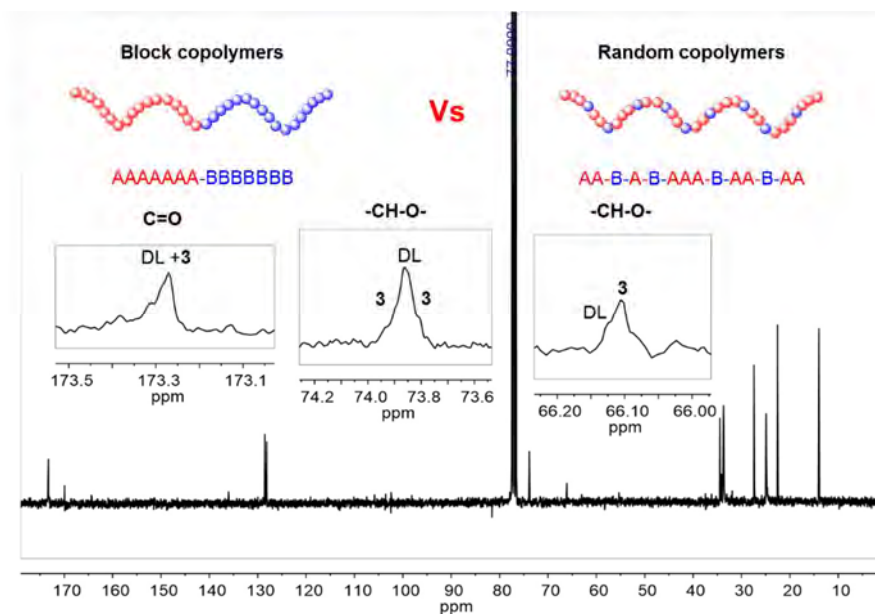
Figure 3.3 Spectre de RMN ^{13}C (CDCl$_3$, 300 MHz) du copolymère aléatoire PDL-*r*-P3 (40:10).

En conséquence, un copolymère aléatoire PDL-*r*-P3 avec une distribution régulière des monomères le long de la chaîne polymère a été obtenu, comme le suggère le suivi de la conversion des monomères et la spectroscopie RMN ^{13}C.

Pour obtenir les copolymères à base de PDL à fonction latérale carboxyle, la modification post-polymérisation de copolymères contenant 2% et 5% d'ester benzylique thiol a été réalisée en deux étapes: (1) acétylation et (2) hydrogénolyse. Premièrement, les groupes hydroxyle

terminaux ont été acétylés avec de l'anhydride acétique pour éviter les réactions compétitives. Ensuite, les groupes latéraux acides carboxyliques dans les copolymères sont obtenus en utilisant un protocole simple et fiable pour l'hydrogénolyse du groupe O-benzyle. Les conditions de réactions ont dû être mises au point et finalement, la préparation *in situ* d'un catalyseur Pd^0/C actif sous atmosphère H_2 a permis de mener à bien la déprotection. L'élimination complète des groupes protecteurs benzyliques est démontrée par la disparition de tous les signaux aromatiques du spectre RMN ^1H (figure 3.4). De plus, ce protocole respecte également l'intégrité du squelette du polymère, car aucune des étapes de post-polymérisation n'affecte le squelette du polymère, un M_n assez constant est maintenu avec une $Đ$ plus étroitedémontrée par une analyse SEC (tableau 3.3).
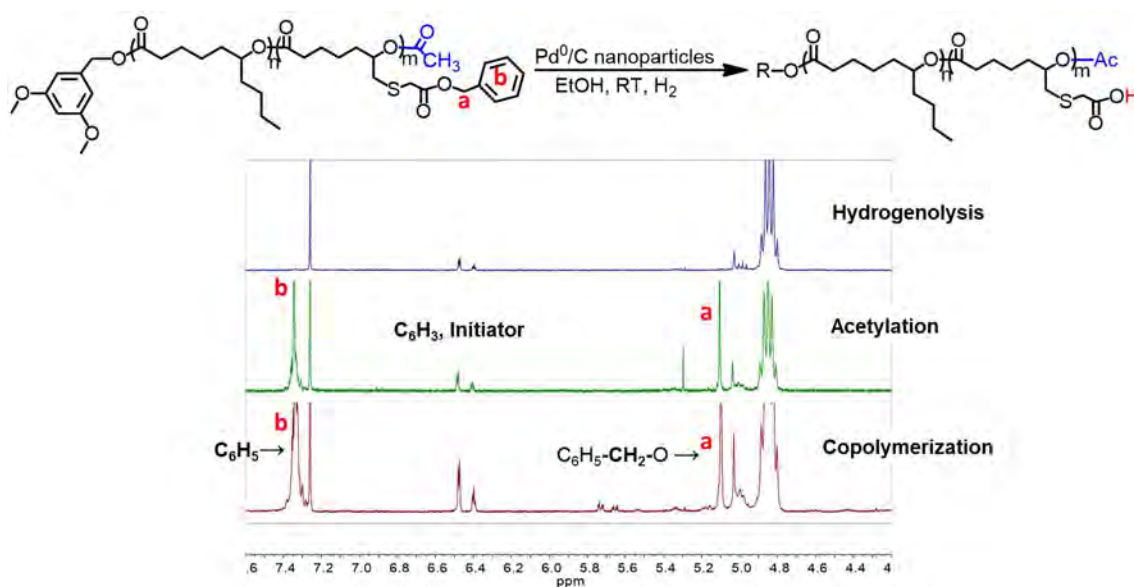
Figure 3.4. Spectres RMN ^1H empilés (CDCl$_3$, 300 MHz) de copolymères contenant 2% d'ester benzylique thiol (copolymérisation), de copolymères acétylés (acétylation) et de copolymère déprotégé (Hydrogénolyse).

Tableau 3.3. SEC et analyse thermique des copolymères de l'ε-DL et **3**, des copolymères acétylés et des copolymères à fonction carboxyle.

PDL$_{47.5}$-r-P3$_{2.5}$	M_n (g/mol)	Đ	T_g (°C)	PDL$_{49}$-r-P3$_1$	M_n (g/mol)	Đ	T_g (°C)
Polymerization	11000	1,32	-51.8	Polymerization	10400	1,23	-54
Acetylation	9000	1,27	-53.8	Acetylation	11000	1,19	-54.3
Hydrogenolysis	8200	1,19	-58.5	Hydrogenolysis	10300	1,17	-55.9

Chapitre IV: Etude comparative de dégradation hydrolytique et enzymatique d'un PDL et de deux copolymères

L'impact des groupes latéraux acide carboxylique sur les vitesses de dégradation des copolymères, par rapport au PDL a ensuite été étudiée. Dans ce chapitre, nous présenterons la préparation des films polymères ainsi que les résultats des tests de dégradation hydrolytique et enzymatique. Comme décrit au chapitre III, la déprotection des groupes carboxyle pendants a été réalisée dans des conditions douces, en respectant l'intégrité du squelette du polymère, selon l'analyse RMN ^{1}H et SEC. Des copolymères fonctionnalisés avec de fonctions carboxyle (PDL-*r*-P3-COOH) avec des teneurs en groupes fonctionnels contrôlés ont ainsi été obtenus, et leur dégradabilité sera comparée à celle des PDL purs. Trois polymères différents seront ensuite soumis à l'étude de dégradation: PDL DP50, CP-2%-COOH et CP-5%-COOH; M_n/ $Đ$ = 11800/1.16, 10300/1.17 et 8200/1.19, respectivement).

La stratégie choisie pour les études de dégradation est la suivante: nous avons choisi de travailler avec des films des polymères en conditions hydrolytiques et enzymatiques. Nous avons choisi une lipase comme enzyme à pH 7,4. Pour les conditions hydrolytiques, nous travaillerons à pH 7,4 (pour comparer avec la dégradation enzymatique) et à pH 9 (conditions basiques). Les essais de dégradation se déroulent en quatre étapes (figure 4.1): (1) préparation des films polymères, (2) addition des milieux d'hydrolyse (solution tamponnée pH 9, pH 7,4 et la solution enzymatique), (3) essais de dégradation in vitro à température contrôlée constante (40 °C), sans agitation, et (4) analyse après dégradation d'échantillons (le pourcentage de perte de poids, les compositions du polymère restant et des produits de dégradation (3 échantillons chacun).

Figure 4.1. Illustration des essais de dégradation.

   a) Préparation des films polymères

Tout d'abord, nous avons étudié la préparation de films polymères à partir de PDL, DP50 et DP100 non fonctionnalisés, comme matériaux modèles. Deux solutions de PDL, DP 50 et DP

100, dans du DCM (300 mg dans 6 mL) ont été placées dans une boîte de Pétri en verre borosilicaté, et le solvant s'est évaporé lentement à température ambiante pendant 2 jours. Ensuite, les boites contenant un film polymère collant sur le fond ont été séchées sous vide à 40 °C pendant 1, 3 ou 5 jours, et à 55 °C pendant 3 et 5 jours. Ce traitement a permis l'élimination totale du solvant sans affecter les propriétés du polymère, mais malheureusement, tous les échantillons étaient trop mous et collants pour être prélevés en film.

Nous avons alors décidé de préparer le film du polymère collant directement dans un flacon de verre à fond plat, bien que cela signifie que seule la surface supérieure serait initialement en contact avec le milieu de dégradation. Les premières tentatives ont été faites avec PDL DP50. Le polymère a été dissout dans du DCM (30 mg/mL) et placé (1 mL) dans des piluliers de verre à fond plat. On a laissé le solvant s'évaporer lentement à température ambiante pendant la nuit, obtenant ainsi une phase homogène pour l'ensemble de l'échantillon (en surface et en masse). Par la suite, les flacons ont été séchés dans un four sous vide poussé à 60 °C pendant 2 jours. Des couches minces d'un diamètre de 13 mm et d'une épaisseur de $\approx 0,5$ mm, correspondant à un poids d'environ 30 mg, ont été obtenues. Pour s'assurer que la température élevée n'affecte pas le squelette du polymère, les films obtenus (après 2 jours de séchage à 100 °C) ont été analysés par SEC et ^{1}H NMR, révélant des propriétés similaires à celles de la matière première. Par la suite, ce procédé a été appliqué à la préparation de films de copolymères contenant 5% et 2% de groupes latéraux d'acides carboxyliques avec des résultats similaires.

b) Profils de dégradation

Comme le montrent les profils de perte de masse du PDL DP50 de la figure 4.2, après 30 jours d'hydrolyse, très peu de dégradation (moins de 10 % de la perte de poids) de la chaîne du PDL a été observée dans les conditions hydrolytiques et enzymatiques. Cela correspond à la dégradation assez lente de la PDL hydrophobe non fonctionnalisée.[32]

Pour le CP-2 %-COOH, une perte de poids notable a été observée dès le premier jour dans toutes les conditions de dégradation (figure 4.2). Au cours des 6 premiers jours, une perte de masse exponentielle a été constatée, de 17% à 41% de la perte de poids. Cependant, on a observé qu'une perte de masse mineure entre le 6e et le 15e jour, atteignant un plateau de 44 % de poids. Dans la solution tampon de pH 7,4, seulement 5 % de perte de poids a été observée après 1 jour. Entre les jours 3 à 12, les pourcentages de perte de poids ont affiché une tendance similaire à celle du jour 1, n'observant que 6 à 10 % de perte de poids. Enfin, 25 % de la perte de poids a été détectée après 30 jours. Après 1 jour, la dégradation enzymatique et le milieu tampon pH 7,4 ont donné des résultats similaires (environ 7 % de perte de masse). Il est

intéressant de noter qu'une augmentation significative de la perte de masse a été observée les jours suivants pour la dégradation enzymatique, avec une perte de masse atteignant 25% et 43%, après 6 et 15 jours, respectivement. Une diminution marquée de la masse de 47 % de la perte de poids a été observée après 30 jours. Ce résultat est différent de celui obtenu dans un milieu tampon de pH 7,4 en l'absence d'enzymes, mais proche de ce qui a été observé dans le pH 9.
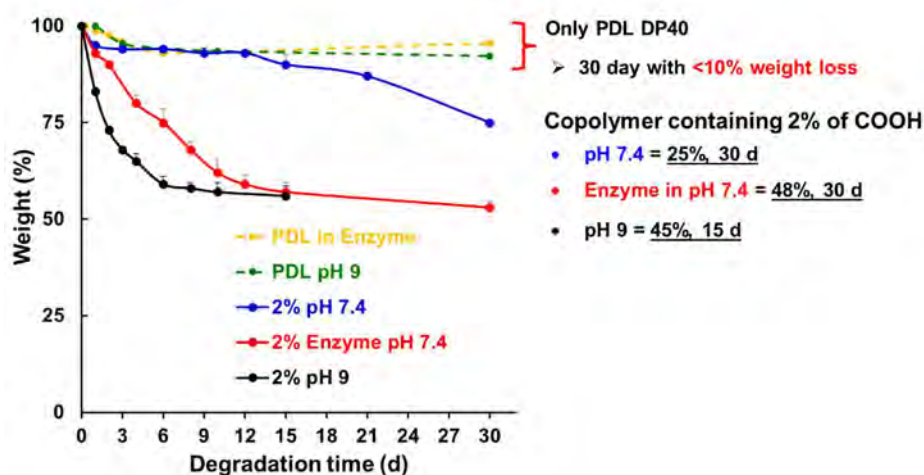

Figure 4.2 Profils de perte de masse pour la dégradation du CP-2%-COOH dans trois conditions différentes et du PDL DP50 dans une solution tampon pH 9 et une solution enzymatique.

Les résultats obtenus avec les polymères PDL et CP-2%-COOH confirment le fait que la présence de groupes latéraux acides carboxyliques affecte significativement le processus de dégradation du polymère. De plus, les enzymes à pH 7,4 favorisent la dégradation à des vitesses deux fois supérieures à celles en conditions neutres (tampon pH 7,4), prouvant l'efficacité des milieux enzymatiques dans la dégradation du polymère. Il est à noter que le profil de perte de masse du CP-2%-COOH en solution enzymatique a atteint un plateau de dégradation après 10 jours, similaire à celui du tampon pH 9 après 6 jours. La dégradation dans les deux conditions a atteint près de 50 % de la perte de poids, probablement parce que les chaînes PDL non fonctionnalisées pourraient être les principaux constituants du polymère restant.

La dégradation de copolymères contenant 5% de groupes pendants carboxyle (CP-5%-COOH) a également été étudiée dans les trois conditions différentes à 40 °C: (1) Solution tampon pH 9 (pendant 15 jours), (2) Solution tampon pH 7,4 (pendant 21 jours) et enzymes dans une solution tampon pH 7,4 (pendant 12 jours). Après seulement 12 heures, une perte en poids de 9 % a été observée dans le tampon pH 9 (Figure 4.3). Ensuite, une augmentation significative de la perte de masse jusqu'à 20% a été mesurée après 1 jour, et jusqu'à 42% après 8 jours. Enfin, la perte

de masse a atteint ≈ 52 % après 15 jours. Malheureusement, à ce stade, il n'y avait plus d'échantillons pour continuer l'étude.
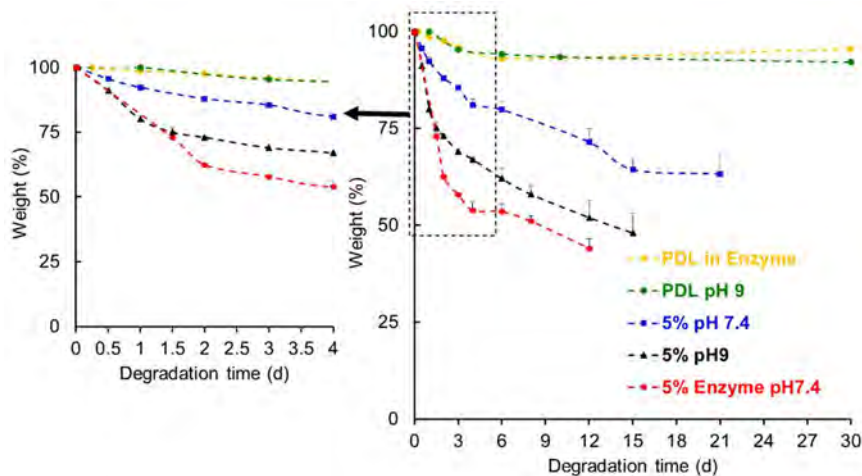

Figure 4.3. Profils de perte de masse résultant de la dégradation du PDL DP50 et du CP-5%-COOH dans différentes conditions d'hydrolyse.

Dans le tampon pH 7,4, 4 % et 8 % de perte en poids ont été observés après 12 heures et 1 jour, respectivement. Entre le deuxième et le sixième jour, un léger changement dans la perte de masse a été constaté, atteignant 20% de la perte en poids. Après 12 jours, les profils de perte de masse ont montré une diminution significative de la masse, puisque 29 % des copolymères ont été libérés dans le milieu de dégradation. Enfin, les résultats après 15 à 21 jours ont révélé un plateau de ≈ 36 % de perte en poids. Pour la dégradation enzymatique, les résultats sont différents de ceux des dégradations hydrolytiques. Au début, une perte en masse de 27 % et 38 % a été observée après un jour et demi et deux jours, respectivement. A 8 jours, une légère augmentation de la perte en poids a été observée, atteignant 49%. Enfin, le dernier échantillonnage a révélé une perte en poids de 56 % après 15 jours.

En comparant les profils de perte de masse entre la dégradation du CP-2%-COOH et du CP-5%-COOH (Tableau 4.2 et Figure 4.3), la dégradation du CP-5%-COOH a montré des pourcentages de perte en poids supérieurs à ceux du CP-2%-COOH dans toutes les conditions, bien qu'ils étaient assez proches pour un pH 9. En comparant les profils de perte de masse du PDL et du CP-2%-ou-5%-COOH, la très faible perte de poids due à la dégradation du PDL est compatible avec une hydrophobie plus élevée, causée par les groupements latéraux butyles le long du squelette du PDL. Par conséquent, le taux de diffusion de l'eau dans la matrice polymère est très lent, ce qui réduit le risque de clivage de la chaîne causé par les ions

hydroxyde. En revanche, les groupements latéraux carboxyle des chaînes de copolymère favorisent la diffusion de l'eau dans le polymère, car ils devraient augmenter l'hydrophilie des chaînes PDL. Ceci conduit à une diminution significative de la masse du copolymère, qui peut résulter de l'augmentation de l'affinité de l'eau et de l'augmentation subséquente du taux de clivage de la chaîne polymère.

Les profils de perte en masse ont montré une grande différence dans les vitesses d'hydrolyse entre PDL DP50, CP-2%-COOH, et CP-5%-COOH (Figures 4.2 et 3). Avec une charge de 2 % ou de 5 % de fonction carboxyle à l'intérieur des chaines PDL, les taux de dégradation sont 2,5 à 5 fois et 4 à 6 fois plus rapides (pour une charge de 2 % et 5 %, respectivement) que ceux de l'homo-PDL. La dégradation du CP-2%-COOH dans des conditions hydrolytiques a montré très peu de changement dans le M_n et le $Đ$ observé par la SEC. Le polymère restant a révélé que le M_n n'est inférieur que de 100-300 Da et le $Đ$ est plus large (jusqu'à 1,4) que la matière première. Cependant, les spectres RMN ^{1}H des produits libérés par la dégradation n'ont montré aucun signal correspondant aux produits dégradés tels que les formes hydrolysées de ε-DL et le monomère **3**.

En revanche, l'analyse par spectroscopie RMN ^{1}H des produits libérés dans les phases aqueuses (milieux de dégradation) a confirmé la présence de monomère ε-DL hydrolysé dans le cas de la dégradation enzymatique. Des oligomères hydrophiles finement dispersés dans une solution tampon ont été observés pour toutes les études de dégradation par analyse SEC (après extraction du produit libéré en phase organique). De plus, les produits de dégradation libérés en phase organique ont été aussi détéctés par MALDI-TOF, et des oligomères à 12 unités DL et une unité de monomère **3** sous forme d'acide carboxylique ont été détectés dans le spectre de masse. Il est à noter que les oligomères sont en fait solubles dans les milieux de dégradation (pH 7,4 et 9 solutions tampons).

Les processus de dégradation hydrolytique et enzymatique du CP-5%-COOH ont montré non seulement une perte de masse significative et une différence marquée de M_n et $Đ$ observées par SEC, mais aussi la forme hydrolysée de l'ε-DL et du monomère 3 sous forme déprotégée ont été détectées par spectroscopie RMN [1]H. Les copolymères restants présentaient une forte diminution en M_n (3000-5000 g/mol) par rapport à la matière première, et un plus large $Đ$, de 1,19 à 1,52. De plus, aucun signe d'oligomères n'a été observé par la SEC, dans lequel ces résultats sont totalement différents de ceux du CP-2%-COOH. Cela confirme que non seulement la présence des unités carboxyliques le long des chaînes polymères favorise la

dégradation, mais aussi que le nombre de groupes fonctionnels a un impact sur les vitesses de dégradation.

Tous ces résultats révèlent que l'introduction de faibles quantités (2-5 %) de groupes carboxyle le long des chaînes polymères du PDL, grâce au nouveau monomère **3**, a un impact marqué sur son hydrophilie et les vitesses de dégradation, tant en conditions hydrolytiques qu'enzymatiques. De plus, le comportement différent du CP-2%-COOH et du CP-5%-COOH montre également qu'il est possible d'ajuster la vitesse de dégradation en ajustant la quantité du groupe fonctionnel. Les matériaux étudiés ici sont donc des candidats prometteurs comme alternatives renouvelables et biodégradables aux matériaux à base de pétrole disponibles sur le marché.

Conclusion

L'objet de ce travail était de développer des polyesters biodégradables à base d'un monomère renouvelable (ε-DL) aux propriétés modulables, en particulier la vitesse de dégradation. Pour se faire, l'introduction de groupements fonctionnels latéraux le long des chaînes de polymères a été envisagée par la copolymérisation de l'ε-DL avec des monomères fonctionnalisés de structure apparentée. Nous avons développé une nouvelle stratégie pour la préparation d'ε-caprolactones ε-fonctionnalisées, dont la structure est proche de celle de l'ε-DL. Une séquence de réaction consistant en une cycloisomérisation catalysée par un métal de transition suivie d'un processus de couplage thiol-ène radicalaire conduit sélectivement aux lactones ciblées. Cette stratégie permet notamment de surmonter le problème de régiosélectivité associé à l'oxydation de Baeyer-Villiger des cétones dissymétriques fonctionnalisées, ce qui constitue le principal inconvénient. L'alkylidène-lactone (**1**) a été facilement préparée à grande échelle (5 grammes) avec un bon rendement (72%) grâce à la cycloisomérisation catalytique de l'acide 6-heptynoïque avec un complexe pince de platine. Ensuite, la fonctionnalisation du composé **1** avec du benzyl thiol et de l'ester de benzyle thiol a été réalisée, donnant les monomères **2** et **3**, respectivement. Il faut remarquer que les deux monomères fonctionnalisés **2** et **3** peuvent être synthétisés à échelle multigramme avec de bons rendements (> 80%).

Au chapitre II, nous avons décrit un autre catalyseur dual associant $InCl_3$ et NEt_3 afin de promouvoir une ROP contrôlée de l'ε-DL dans des conditions douces (toluène, 3 M, 60 ° C, 1 à 20 h). Des PDL de structures bien définies avec M_n jusqu'à 30 000 g / mol ($Ð \sim$ 1,2) et dépourvues de résidus catalytiques ont été obtenues. Outre les PDL à terminaison ester

typiques, des groupes terminaux amide ont été installés grâce à la capacité du catalyseur double à fonctionner avec des amines primaires en tant qu'amorceurs. En conséquence, des copolymères séquences amphiphiles PEG-NH-PDL, avec une forte liaison peptidique entre les deux séquences pourraient être préparés. Des copolymères du bloc PDL-*b*-PCL / PCL-*b*-PDL) et aléatoires P(DL-*r*-CL) ont également été préparés par ROP séquentielle et simultanée avec l'ε-CL, respectivement. L'utilisation de l'association InCl$_3$ / NEt$_3$ permet donc des progrès significatifs dans la polymérisation de l'ε-DL. Ce catalyseur est donc complémentaire de ceux rapportés précédemment en termes de conditions de réaction, de fonctionnalité en bout de chaîne et de qualité de pureté du polymère.

Au chapitre III, la préparation dans des conditions douces (toluène, 3M, 60 ° C) de copolymères de l'ε-DL et le monomère **3** en utilisant le catalyseur dual (InCl$_3$ / NEt$_3$) a été décrite. Sur la base du contrôle des conversions de monomères par spectroscopie RMN, il a été confirmé que les copolymères obtenus étaient des copolymères statistiques. Pour obtenir le copolymère à base de PDL à fonctionnalité carboxyle, la modification après polymérisation de copolymères contenant 2% et 5% d'ester benzylique a été réalisée par acétylation de l'hydroxyde terminal suivie d'une hydrogénolyse catalysée au Pd. L'élimination complète des groupes protecteurs du groupe benzyle en respectant l'intégrité du squelette du polymère a été confirmée par spectroscopie RMN ^{1}H et par SEC.

Dans le dernier chapitre, la dégradation de CP-2% -COOH et de 5% de CP-5% -COOH a été étudiée dans des conditions hydrolytiques et enzymatiques, et les résultats ont été comparés à l'homo-PDL. Les profils de perte de masse de PDL, CP-2% -COOH et CP-5% -COOH ont montré que les taux de dégradation sont 2,5 à 5 fois et 4 à 6 fois (pour une charge de 2% et une charge de 5%, respectivement) plus rapidement que l'homo-PDL. L'analyse des produits libérés a révélé la formation d'oligomères hydrophiles, de petites quantités de 6-hydroxydécanoate (produit d'hydrolyse de l'ε-DL) et le produit d'hydrolyse du monomère **3**. Toutes ces données révèlent l'impact des groupes carboxyle latéraux sur le caractère hydrophile et les vitesses de dégradation des chaînes de PDL. Les matériaux étudiés ici sont des candidats prometteurs comme solutions de remplacement renouvelables et biodégradables aux matériaux à base de pétrole disponibles dans le commerce.

Ce travail est également une preuve de concept de l'impact des groupements fonctionnalisés polaires sur les propriétés de la PDL. Il ouvre la voie à d'autres modifications structurelles sur mesure susceptibles d'ouvrir de nouvelles possibilités d'application pour ces polymères. Dans une perspective à moyen terme, nous proposons une application de la lactone **2** en tant que

monomère pour la préparation de produits biodégradables sensibles aux espèces réactives de l'oxygène (ROS), en tirant parti de la présence du groupe thioéther. Pour ce faire, les copolymères amphiphiles à blocs sensibles aux ROS pourraient être préparés par ROP du monomère **2** en utilisant le PEG-NH$_2$ comme macro-amorceur, de sorte que la structure dibloc puisse résister au cours de l'application grâce à la forte liaison amide entre les deux blocs. L'aptitude de ces copolymères à former des nanoparticules micellaires dans l'eau doit ensuite être étudiée. Ensuite, leur capacité à piéger les espèces oxydantes doit être sondée par la réaction avec H$_2$O$_2$. De plus, il peut être intéressant d'étudier l'hydrophilie et la dégradabilité de ces copolymères contenant des motifs soufrés de polarité différente (par exemple thioéther, sulfoxyde et sulfone).
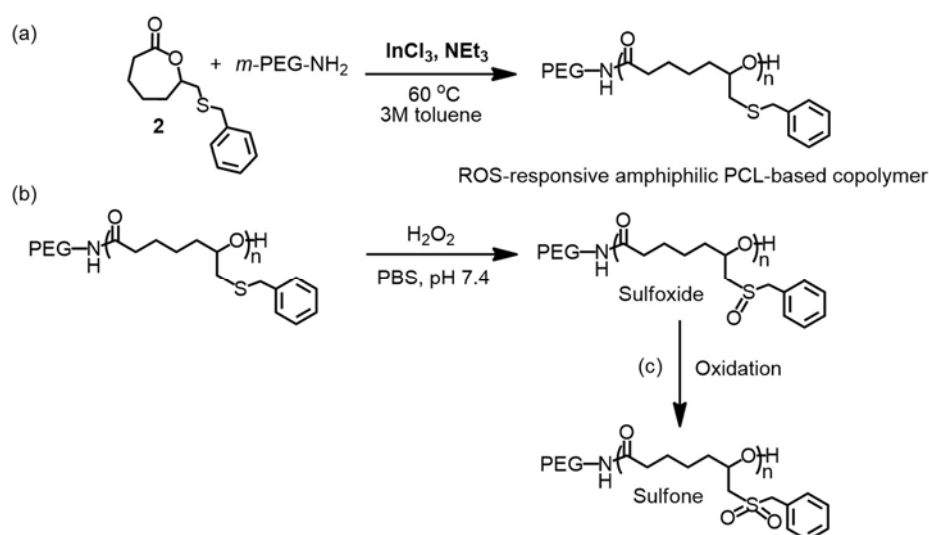

Schéma 1. Stratégie proposée pour la préparation de copolymères blocs amphiphiles à base de PCL fonctionalisé sensibles aux ROS (a), l'étude de leur réponse aux oxydants H$_2$O$_2$ (b)(c).

Références:

1. (a) Williams, C. K. *Chem. Soc. Rev.* **2007**, *36*, 1573. (b) Bednarek, M. *Prog. Polym. Sci.* **2016**, *58*, 27. (c) Vert, M. *Biomacromolecules*, **2005**, *6*, 538.

2. Laycock, B.; Nikolić, M.; Colwell, J. M.; Gauthier, E.; Halley, P.; Bottle, S.; George, G. *Prog. Polym. Sci.* **2017**, *71*, 144.

3. Bioplastics market data 2017, European Bioplastics, https://www.european-bioplastics.org/market/. 21.06.2018.

4. Schneiderman, D. K.; Hillmyer, M. A. *Macromolecules*, **2017**, *50*, 3733.

5. Ragauskas, A. J.; Williams, C. K.; Davison, B. H.; Britovsek, G.; Cairney, J.; Eckert, C. A.; Fredrick Jr., W. J.; Hallett, J. P.; Leak, D. J.; Liotta, C. L.; Mielenz, J. R.; Murphy, R.; Templer, R.; Tschaplinski, T. *Science*, **2006**, *311*, 484.

6. Albertsson, A.-C.; Varma, I. K. *Biomacromolecules*, **2003**, *4*, 1466.

7. (a) Abedalwafa, M.; Wang, F.; Wang, L.; Li, C. *Rev. Adv. Mater. Sci.* **2013**, **34**, 123. (b) Buntara, T.; Noel, S.; Phua, P. H.; Melián-Cabrera, I.; de Vries, J. G.; Heeres, H. J. *Angew. Chem. Int. Ed.* **2011**, *50*, 7083

8. Almeida, B. C.; Figueiredo, P.; Carvalho, A. T. P. *ACS Omega* **2019**, *4*, 6769.

9. Parenty, A.; Moreau, X.; Campagne, J. M. *Chem. Rev.* **2006**, *106*, 911.

10. Galli, C.; Mandolini, L. J. *Chem. Soc., Chem. Commun. 1982*, 251.

11. (a) Herrmann, J. L.; Schlessinger, R. H. J. *Chem. Soc., Chem. Commun.* **1973**, 711. (b) Habnouni, S. E.; Darcos, V.; Coudane, J. *Macromol. Rapid Commun.* **2009**, *30*, 165.

12. Darcos, V.; El Habnouni, S.; Nottelet, B.; El Ghzaoui, A.; Coudane, J. *Polym. Chem.* **2010**, *1*, 280.

13. ten Brink, G. J.; Arends, I. W. C. E.; Sheldon, R. A. *Chem. Rev.* **2004**, *104*, 4105.

14. Oulié, P.; Nebra, N.; Saffon, N.; Maron, L.; Martin-Vaca, B.; Bourissou, D. *J. Am. Chem. Soc.* **2009**, *131*, 3493.

15. Oulié, P.; Nebra, N.; Ladeira, S.; Martin-Vaca, B.; Bourissou, D. *Organometallics* **2011**, 30, 6416.

16. (a) Nebra, N.; Monot, J.; Shaw, R.; Martin-Vaca, B.; Bourissou, D. *ACS Catal.* **2013**, *3*, 2930. (b) Espinosa-Jalapa, N. Á.; Ke, D.; Nebra, N.; Le Goanvic, L.; Mallet-Ladeira, S.; Monot, J.; Martin-Vaca, B.; Bourissou, D. *ACS Catal.* **2014**, *4*, 3605. (c) Monot, J; Brunel, P; Kefalidis, C. E.; Espinosa-Jalapa, N. Á; Maron, L; Martin-Vaca, B; Bourissou, D. *Chem. Sci.* **2016**, *7*, 2179.

17. Ke, D.; Espinosa-Jalapa, N. Á; Mallet-Ladeira, S.; Monot, J.; Martin-Vaca, B.; Bourissou, D. *Adv. Synth. Catal.* **2016**, *358*, 2324.

18. Long, T. R.; Wongrakpanich, A.; Do, A.-V.; Salem, A. K.; Bowden, N. B. *Polym. Chem.* **2015**, *6*, 7188.

19. Thillaye du Boullay, O.; Saffon, N.; Diehl, J.-P.; Martín-Vaca, B.; Bourissou, D. *Biomacromolecules* **2010**, *11*, 1921.

20. Olsén, P.; Borke, T.; Odelius, K.; Albertsson, A. C. *Biomacromolecules* **2013**, *14*, 2883.

21. Kakde, D.; Taresco, V.; Bansal, K. K.; Magennis, E. P.; Howdle, S. M.; Mantovani, G.; Irvine, D. J.; Alexander, C. *J. Mater. Chem. B* **2016**, *4*, 7119.

22. Lin, J. O.; Chen, W.; Shen, Z.; Ling, J. *Macromolecules* **2013**, *46*, 7769.

23. Jasinska-Walc, L.; Bouyahyi, M.; Rozanski, A.; Graf, R.; Hansen, M. R.; Duchateau, R. *Macromolecules* **2015**, *48*, 502.

24. Bai, J.; Wang, J.; Wang, Y.; Zhang, L. *Polym. Chem.* **2018**, *9*, 4875.

25. Chuang, H. J.; Chen, H. L.; Huang, B. H.; Tsai, T. E.; Huang, P. L.; Liao, T. T.; Lin, C. C. *J. Polym. Sci. A Polym. Chem.* **2013**, *51*, 1185.

26. Peters, R. *Cooperative Catalysis*. Wiley, New York. **2015**.

27. Piedra-Arroni, E.; Amgoune, A.; Bourissou, D. *Dalton Trans.* **2013**, *42*, 9024.

28. Hong, M.; Chen, J.; Chen, E. Y. X. *Chem. Rev.* **2018**, *118*, 10551.

29. Pietrangelo, A.; Knight, S. C.; Gupta, A. K.; Yao, L. J.; Hillmyer, M. A.; Tolman, W. B. *J. Am. Chem. Soc.* **2010**, *132*, 11649.

30. Buwalda, S. J.; Dijkstra, P. J.; Feijen, J. *J. Control. Rel.* **2010**, *148*, e23.

31. Alba, A.; Thillaye du Boullay, O.; Martin-Vaca, B.; Bourissou, D. *Polym. Chem.* **2015**, *6*, 989.

32. Arias, V.; Olsén, P.; Odelius, K.; Höglund, A.; Albertsson, A.-C. *Polym. Chem.* **2015**, *6*, 3271.

Abstract

The development of new sustainable polymers endowed with improved performances but minimal environmental impact has become a major concern. In this context, aliphatic polyesters are attracting increasing attention in the medical field and packaging applications, due to their biodegradable character and suitable physical properties. Ring-opening polymerization (ROP) is a method that has been used in these areas to access a broad range of polyesters with different and well-controlled structures. One of the well-known lactone monomers for ROP is ε-caprolactone (ε-CL), a compound derived from petrochemical source. An alternative lactone monomer derived from biomass is ε-decalactone (ε-DL). Being a 7-membered ring as ε-CL, ε-DL is thus a renewable monomer that is attracting increasing attention. However, the pendant butyl group at ε-position has a large impact on mechanical and thermal properties as well as degradation rates. To modulate these properties, we have been working with the functionalized monomers of close structure to ensure similar behavior in ROP. First, the ε-functionalized-ε-CL monomers were prepared from 6-heptynoic acid by a sequential transition metal catalyzed cycloisomerization and subsequent thiol-ene reaction. Afterwards, their copolymerization with ε-DL has been explored including the identification of controlled/living polymerization using $InCl_3$-based bicomponent catalyst and the confirmation of their random architecture. In addition, the preparation of copolymers featuring pendant carboxyl groups by post-modification steps have also been completely achieved. Finally, the hydrolytic and enzymatic degradation of these functionalized copolymers has been thoroughly investigated, proving the influence of our new functionalized monomer (in deprotected form) on degradation rates of PDL.

Keywords: Biodegradable Polymers, Thiol-ene Reaction, Ring-opening Polymerization, Functionnalized lactones, Functionnalized Polyesters

Résumé

Le développement de nouveaux polymères durables dotés de performances améliorées avec un impact environnemental minimal est devenu une préoccupation majeure. Dans ce contexte, les polyesters aliphatiques attirent de plus en plus l'attention dans le domaine médical et les applications d'emballage, en raison de leur caractère biodégradable et de leurs propriétés physiques appropriées. La polymérisation par ouverture de cycle (ROP) est une méthode qui a été utilisée dans ces domaines pour accéder à une vaste gamme de polyesters ayant des structures différentes et bien contrôlées. L'un des monomères de type lactone bien connus pour la ROP est l'ε-caprolactone (ε-CL), un composé dérivé du pétrole. Une autre lactone dérivée de la biomasse est l'ε-décalactone (ε-DL). Cycle à 7 chaînons comme l'ε-CL, l'ε-DL est un monomère renouvelable qui attire de plus en plus d'attention. Le groupe butyle pendant en position ε a un impact important sur les propriétés mécaniques et thermiques ainsi que sur la vitesse de dégradation. Pour moduler encore plus ces propriétés, nous avons travaillé avec des monomères fonctionnalisés de structure proche pour assurer un comportement similaire en ROP. Premièrement, les monomères d'ε-CL- ε-fonctionnalisés ont été préparés à partir de l'acide 6-heptynoïque par une stratégie séquentielle à grande économie d'atome : une cycloisomérisation catalysée par un métal de transition suivie d'une réaction thiol-ène. Ensuite, leur copolymérisation avec l'ε-DL a été réalisée en utilisant un catalyseur bicomposant à base d'InCl$_3$, un comportement de polymérisation contrôlée/vivante a été identifié et des copolymères à caractère aléatoire ont été obtenus. Grâce à cette stratégie, la préparation de copolymères présentant des groupes acides carboxyliques pendants a été développée. Enfin, la dégradation en conditions hydrolytiques et enzymatiques de ces copolymères fonctionnalisés a fait l'objet d'études approfondies, prouvant l'influence de notre nouveau monomère fonctionnalisé (sous forme déprotégé) sur la vitesse de dégradation du PDL.

Mots-clés: Polymères Biodégradables, Réaction Thiol-ène, Polymérisation par ouverture de cycle, Lactones fonctionnalisées, Polyesters fonctionnalisés